BELL AEROSYSTEMS COMPANY

DIVISION OF BELL AEROSPACE CORPORATION - A textron COMPANY

3 600

REPORT NO. 7129-933003

FINAL REPORT
RESEARCH ON ZERO-GRAVITY
EXPULSION TECHNIQUES

MARCH 1962

Alexander Krivetsky
William H. Bauer
Harvey L. Loucks
Joseph Padlog
John V. Robinson
William H. Walters

FOREWORD

This final report has been prepared by the Bell Aerosystems Company under NASA Contract No. NASr-44, Research on Zero-Gravity Expulsion Techniques. Mr. Alexander Krivetsky was Technical Director in charge of the study.

The Project Manager of this Expulsion Techniques contract was Mr. Henry Burlage, Chief, Analysis and Experimental Development, ᴨid Rockets for NASA. Mr. Richard N. Porter of the Jet Pᴉ ᴉsion Laboratory, California, was the Technical Manager on this program.

ABSTRACT

This report presents design concepts of zero-gravity expulsion devices on an extremely broad basis and forms a compendium of such device configurations as an aid to system designers in the selection of expulsion systems to particular applications. As a supplement to the concept presentations, the report also presents some of the more important data necessary for design with emphasis on information not readily available in current literature.

TABLE OF CONTENTS

TABLE OF CONTENTS (CONTINUED)

TABLE OF CONTENTS (CONTINUED)

TABLE OF CONTENTS (CONTINUED)

TABLE OF CONTENTS (CONTINUED)

LIST OF TABLES

LIST OF ILLUSTRATIONS

LIST OF ILLUSTRATIONS (CONTINUED)

LIST OF ILLUSTRATIONS (CONTINUED)

LIST OF ILLUSTRATIONS (CONTINUED)

LIST OF ILLUSTRATIONS (CONTINUED)

LIST OF ILLUSTRATIONS (CONTINUED)

LIST-OF ILLUSTRATIONS (CONTINUED)

I. INTRODUCTION

GENERAL

As we probe deeper and deeper into space, new requirements become essential for the design of space vehicles. A technological area of major importance is the design of positive expulsion devices for transfer of propellants under zero-g environment. A re-examination of the classical propellant expulsion methods has become necessary due to the increase in severity of the operational environment and the continued growth, duration, and complexity of operational requirements. The principal changes which result when considering these new missions, which penetrate deeper and deeper in space and also perform more difficult space maneuvers are principally a result of (1) the design criteria resulting from the necessity for operation within the space environment, (2) the long times that are required, and (3) the versatility of the use of the propulsion system (start and restart).

In carrying out space missions such as earth satellites, lunar or interplanetary flights, a so-called zero-gravity environment is produced on the vehicle during certain portions of its flight trajectory. The term zero-gravity is actually a misnomer since the effect is caused by the vehicle and its contents both experiencing the same gravitational force which varies with the locale or position, but which is never zero. It is the acceleration of the contained matter relative to the vehicle which is zero. The principal effect of zero gravity is the absence of body forces. Every body retains its mass but does not exert any weight forces on its environment.

There are numerous space missions or space maneuvers that require positive expulsion or restarts in a zero gravity environment. These are indicated below:

Orbital Rendezvous and Correction

This maneuver is generally used to change position of the vehicle. These changes may be necessary to accomplish intercept or rendezvous with a second space ship in orbit, or to change the vehicle position in anticipation of a more extended mission in space.

Orbital Maintenance

Drag, magnetic fields, solar winds, and other associated forces may cause a space vehicle to deviate from its desired position. A correction maneuver is employed to correct the effects of these perturbing forces.

Attitude Control

For space orientation of the vehicle, control may be
necessary for tracking of various objects such as sun, earth,
or to provide specific vehicle orientation for main thrust
application for trajectory control in orbit.

Planetary Orbit and Transfer Establishment

In order to accomplish some space missions, velocity vari-
ations of the space vehicle are required. A transfer between
the earth's heliocentric orbit and Mars' heliocentric orbit,
for example, requires changes in the vehicle heliocentric
velocity at departure and arrival. In addition, upon arrival
in the vicinity of the moon or other planets, it may be
required to enter a satellite orbit. A propulsive maneuver
is necessary to change the vehicle velocity to the local
orbit velocity.

Abort

A delay or cancellation of a flight due to technical dif-
ficulties while on the launch pad could necessitate propel-
lant drainage to minimize hazardous working conditions. In
such a situation, the expulsion device could be activated
to fully expel the propellants. The abort condition, although
it is not associated with a space mission and its associated
environment, is somewhat of a unique criteria for an expulsion
device. The abort condition, as far as the expulsion device
is concerned, is not serious. In this situation the gravita-
tional field is present and with the associated pressure head,
drainage can be readily accomplished.

BASIC APPROACH

The traditional approaches to the solution of the positive
expulsion problem have included the use of plastic or elastomeric
bladders, conventional pistons and bellows. A flexible bag tech-
nique, however, is the predominant method is use today for positive
expulsion of propellants. This traditional approach to positive
expulsion systems has consisted of the utilization of suitable
plastic or pliable materials, specifically Teflon, as bladders to
contain and expel the propellants. During the course of recent
development programs, it has become apparent that plastic bladders
possess characteristics which tend to restrict their usage in
growth versions of the propulsion system. Prime among these is
the degradation of the physical properties with accumulated
radiation dosage experienced during deep space flight. In addi-
tion, currently available bladders exhibit an undesirable degree

of permeability to the propellants and show some degradation of properties on becoming saturated with the propellant. Less permeable polymer type bladders can only be obtained with a sacrifice in bladder flexibility and an increase in the tendency to crease and tear on collapse in the expulsion cycle. Cryogenic temperatures also tend to decrease flexibility characteristics of polymers.

As a result, strong emphasis is being placed on other types of expulsion devices. This study was conducted to present design concepts of positive expulsion on an extremely broad basis and to form a compendium of such configurations as an aid to system designers in the selection of expulsion systems to particular applications.

As a supplement to the concept selection assistance, the study also presents some of the more important data necessary for design of the expulsion devices with emphasis on information not readily available in current literature. This report,which summarizes the study results,is divided into the following main sections.

Literature Survey

This section includes a rather extensive search of the litera-ture dealing with positive expulsion and its associated problems in a zero-gravity environment. Abstracts of a great many reported and printed material are presented.

Morphological Approach

The morphological technique is employed to ascertain the various possibilities that do or can exist for expelling a fluid. It represents a catalog of expulsion and orientation devices.

Characteristics of Devices

Some of the simple and complicated expulsion devices obtained by means of a morphological matrix are described and the numerous advantages and disadvantages of these devices are enumerated. In many instances, selected structural design information is pre-sented that is applicable to that design concept.

Space Environment

The space environment can introduce deleterious effects into a device that can shorten its operational life and/or actually induce failures. The various aspects of the space environment are summarized so that integration with other conditions or materials can be realized.

Material Considerations

The existence of the space environment on materials and total expulsion device system, propellant compatibility, radiation damage, permeability, etc., affect the choice and selection of materials that can be incorporated in these devices. Test data is presented on specific candidate materials to insure a more realistic choice and provide a more reliable operational configuration.

Slosh and Vibration Considerations

Fuel sloshing, tank modes of vibration and acoustic excitation possibilities are discussed to clarify mode characteristics, assemble information on frequency determination, and other procedures and observations which will be useful during design and/or test of positive expulsion devices.

DATA PRESENTATION

In the preparation of the report and the presentation of the associated data, the arrangement of the contents had to be modified according to its applicability to either a specific expulsion configuration or to many different configurations.

The scope of the data presentation takes into account selected information on design for some of the configurations and thus gives a picture of the knowledge to date on specific design features. Analysis data applicable to a specific design is presented within the text of that configuration whereas design information that is more general and applicable to several configurations is presented as an Appendix to this report.

II. LITERATURE SURVEY

This section presents a survey of the available literature on positive expulsion devices and techniques. The survey is directed towards a determination and evaluation of the "state-of-the-art" in order to avoid duplication of past efforts. The test procedures, results and achievements of similar projects are investigated as permitted by available communications or reports. The scope of the survey includes the fields of materials, fabrication techniques, criteria and environment, testing and weightlessness simulators, as well as pressurization systems.

Well over 250 papers, reports, pamphlets, magazine and newspaper articles were screened and are represented in this literature survey.

The plastic bladder configuration is quite popular as a positive expulsion device and is mentioned in many references. Squeeze-type tubes, another positive expulsion configuration, is mentioned in some articles with particular application as food containers for astronauts in the zero-g environment. Pistons and spinning tanks are briefly discussed and in many cases only a short sentence presents or describes these concepts. Articles on behavior of liquids in a zero-g environment including gas and vapor intermix, liquid wettability and capillary action are also included in this survey.

With the exception of the plastic bladder positive expulsion device wherein testing procedures, tests, material selections, etc. are mentioned. Very little information is presented on other types of expulsion techniques for the zero-gravity environment.

In the study of electric and magnetic expulsion devices, it was considered advantageous to incorporate the literature survey with the description and performance of the devices. The references quoted for these various and selected expulsion techniques constitute a considerable literature search and represent a preliminary effort toward the possible application of such devices for a zero-g environment.

L1. Rose, C. C. and Young, R. B.: The Design of Tanks for Liquid Propellant Rocket Power Plants. Journal of the American Rocket Society, No. 75, September-December 1948, pp 107-118.

A paragraph on some schematic diagrams of methods of insuring continuous flow are depicted. The five methods mentioned include the external bag, internal bag, diaphragm, piston, and swinging pipe. The authors favor the piston diaphragm as the installation is both simple and the servicing is not complicated.

The bag installations have difficulties related to bleeding during propellant feeding and bag failures resulting from excessive wrinkling in the loaded condition. The swinging or rotating pipe (scoop) is not suitable for extreme fore-and-aft accelerations and has the disadvantage of the packed joint.

L2. Biondolillo, S.: Aluminum Foil Bladders. Report BTR-49-1, Bell Aircraft Corporation. January 6, 1949.

This investigation was undertaken to evaluate the feasibility of developing a collapsing metal bladder (1100-0 aluminum). Foils of various thicknesses were evaluated and subsequently bladders were fabricated and tested. Water and liquid N_2 were the test fluids used. Excellent results were obtained with both fluids. This program, though limited in scope, did however prove the feasibility of positive expulsion with a metal bladder.

L3. Turansky, C. J. and Rinehart, R. D.: Creation of High-Pressure Gas Source for Rocket-Motor-Propellant Supply Systems. Journal of the American Rocket Society, No. 78, September 1949.

Here, again, some early work on bladders as performed by Bell Aerosystems is shown. A unit employing an accumulator (a bladder and oil) is utilized to boost helium gas from 500 psi to 5000 psi. The result was an oil-free dry-gas helium pressure booster.

L4. Sheridan, W. R.: Expellant Bags for Rocket Propellant Tanks, Journal of the American Rocket Society, No. 85, June 1951, pp 80-82.

This short paper shows the early work performed on expulsion at the Bell Aerosystems Company. Bladder material and fluid compatibility are briefly discussed.

L5. Biondolillo, S.: Storageability and Handling of Liquid Rocket Propellants, Bell Aircraft Corporation Report No. 02-989-014, March 1, 1956.

This report covers an experimental investigation of liquid rocket propellants for use aboard ship under conditions of sealed storage and packaged missile units. IRFNA and hydrazine were stored in bladder type positive expulsion tanks under conditions simulating shipboard storage. A gas expanded teflon bladder was used in the IRFNA tank and a neoprene compound bladder was used in the hydrazine tank. Loaded tanks were subjected to a one-year storage program during which time periodic slosh and vibration tests were conducted.

L6. Anon: Combined Monthly Summary #54, for the Period June 1,
        1956 to August 1, 1956, CIT/JPL, Pasadena, California.

     The R&D section of this report dealt with the design of an
auxiliary power unit. A spherical bladder tank was used to supply
hydrazine to a gas generator. A butyl rubber bladder was used in
a series of tests for over a one-month period with no deleterious
results being noted. A piston-type propellant tank was built
that weighed approximately 14 pounds. A spherical tank of spun
aluminum having equivalent capacity of the piston tank and employ-
ing a butyl-rubber bladder to separate gas and liquid was also
designed and fabricated. The spherical bladder tank has the
advantage of simplicity and light weight (approximately 3.3 pounds).

L7. Love, J. and Stillwell, W.: Hydrogen Peroxide Reaction
        Control System for the X-1B Research Airplane, NASA TN
        D-185, December 1959.

     This report encompasses the design and development of a
hydrogen peroxide reaction control system for the X-1B rocket
research airplane. In this system a piston type tank was used
for positive expulsion. Hydrogen peroxide was expelled from the
vessel by pressurizing one side of a moving piston. A tube
through the center of the tank was used for piston alignment
and as the outlet line. The piston was guided on the outlet
tube by a Teflon bushing which is sealed from the tube and
vessel wall by two Viton "O"-rings. This tank operated reli-
ably during the entire flight test program.

L8. Neiner, J. J.: The Effects of Zero Gravity on Fluid
        Behavior and System Design. WADC TN 59-149, April 1959.

     Tests, employing a modified C-131B aircraft, were conducted
to simulate the zero-g condition to study fluid behavior, the
behavior of gas released in fluids and the effect of surface
tension on this behavior. The test results indicated that loca-
tion of the fluid in a container cannot be predicted and the con-
ventional methods of fluid transfer by pressurization and/or pump-
ing cannot be successfully utilized at zero-g. Fluid transfer by
means of (a) installation of ullage rockets, (b) a piston-
expulsion tank, (c) a positive expulsion bladder, and (e) a
rotating chamber pump are suggested as other methods of fluid
transfer. Test areas which are contemplated for future evalua-
tion are to include surface tension and capillary action.

L9. Gerathewohl, S. J. and Steinkamp, G. R.: Human-Factors
        Requirements for Putting a Man in Orbit. Astronautica
        Acta, Vol. V/Fasc. 1, 1959, pp 73-81.

     Under the heading of Weightlessness, it is stated that liquids
must be squeezed from bottles instead of being handled in open

containers and this also holds for solids which float about at
touch if not properly stored. This special hardware is mentioned
under the areas of eating and drinking.

L10. Anon: Proceedings of the Manned Space Stations Symposium.
        Sponsored by the Institute of the Aeronautical Sciences
        with the cooperation of NASA and the Rand Corporation;
        Los Angeles, California, April 20-22, 1960.

    The numerous papers presented at the symposium dealt mainly
with space environment, aeromedical results and problems, ecology
requirements, space power requirements and space station struc-
tural design concepts. Although zero-g and artificial gravity
was mentioned by some authors, the review did not disclose any
information of immediate value.

L11. Hise, E. C.: Design, Development, and Operation of Metal-
        Diaphragm Reactor-Service Pumps. Oak Ridge National
        Laboratory, ORNL - 2841, May 10, 1960.

    A summary of the development of, and experience with high
pressure liquid pumps which employ a hydraulically deflected
circular metallic diaphragm is presented. The diaphragm is
clamped between two contoured plates which control the maximum
deflections and stresses in the diaphragm as it is hydraulically
pushed from one contoured plate to the other. Contour and
diaphragm configurations such as the so-called "free-deflection"
and two-radii contour are considered. Methods for the design of
a diaphragm configuration which will give the maximum volumetric
displacement based on an allowable fatigue stress is presented.

L12. Clarke, R. M.: Positive Expulsion Systems - Design Data
        and Performance Characteristics. The Joclin Manufacturing
        Company, Wallingford, Connecticut. Technical Report No.
        2-B-1, June 1, 1960.

    A review of the positive expulsion system is presented
based on a flexible bladder concept. Seamless Teflon or Kel-F
expulsion cells (now called Fluorocells) was the principal
material in the investigation. It should be noted that the
Joclin Manufacturing Company is a manufacturer of bladders and
much of the report represents recorded work accomplished through
mutual efforts of the Joclin Manufacturing Company and its
customers.

L13. Snyder, N. W.: Power Supplies for Space Vehicles,
        Astronautica Acta, Vol. VI/Fasc. 6, 1960, pp 271-310.

    The gravitationless field problems are mentioned under a
chapter heading of "Special Problems and Special Components".
The transfer of heat by condensation of a vapor on the internal
radiator surfaces while under this field is discussed to a limited

degree. In order to remove liquid from these surfaces one can
think of using a sweep gas (the vapor to be condensed) to provide
a frictional force on the liquid (collecting as a film). The
removal of the liquid can be accomplished by the introduction of
an artificial gravitational field wherein the fluid or whole
system spins. Spinning makes it more difficult to control the
satellite or space ship attitude because of the gyroscopic forces,
and the vibrational perturbations caused by uneven flow of the
liquid (water-hammer or slug-flow effects). Using a sweep gas
effect to remove the liquid film, however, presents the unattractive-
ness of high pressure drops occurring in two phase flow.

L14.   Hugo, A. J.: Development of a 5.0 Inch Liquid Propellant
           Target Motor, U. S. Naval Ordnance Test Station, Report
           No. IDP862, 25 July 1960.

       This report covered the design development and testing of
a complete propulsion system for a target missile. Included in
this system were positive expulsion tanks which utilized 1100-0
aluminum bladders. Both propellants were contained within the
same tank. Gas was introduced between the two bladders which
collapsed the inner one and expanded the outer one. Tank opera-
tion was outstanding in all respects during the course of the
flight test program. Propellants were IRFNA and UDMH.

L15.   Anon: Research Summary #36-5. Vol. II, For the Period
           August 1, 1960 to October 1, 1960, CIT/JPL, Pasadena,
           California.

       Section IV.D of this report deals with the investigation
of liquid behavior in a zero "g" environment. It is anticipated
that results, relative to the characteristics of a weightless
liquid with a free surface, will be obtained which may be applic-
able to liquid systems of future space vehicles. Emphasis has
been directed toward the wetting or concave liquid gas inter-
face. Tests have been conducted for both static and dynamic
conditions.

       Section VIII.D of this report was devoted to Teflon expul-
sion bladders. Tests were conducted on both spherical bags and
hemispherical diaphragms. Tests were conducted with water at
7 psig in a 41" diameter clear "see-through" plastic tank.

L16.   Brown, E. L.: Human and System Performance During Zero G.
           Vistas in Aeronautics - 1960, Vol. III, Proceedings of
           the Third AFOSR Astronautic Symposium, October 1960.

       The problem of fluid transfer during zero g was dramatically
brought to attention during the early flights of the C-131B air-
craft by the propellers overspeeding. To provide the necessary
oil pressure to prevent this propeller overspeeding, the installa-
tion of a rather complicated system that used nitrogen pressure

operating against a flexible diaphragm that forced oil into the lines was employed. While the system was considered a bother to use, it did solve the problem of overspeeding propellers. Another system mentioned for transferring fluid at zero g involves the use of a cylinder-type container and a device for causing the fluid mass to rotate rapidly in such a manner that it forces itself against the inner circumference of the cylinder. The fluid can then be picked off from any point on the circumference and air bled into the center of the tank.

L17.   Skopp, G. H.: Basic Investigation of the Operation of
       Propellant Actuated Devices in Space Environment.
       Phase I. - A Literature Survey. WADD TR 60-346.
       November 1960.

       The report presents a brief description of natural and induced environments. A short dissertation on zero gravity lists the following effects to its presence:

   (a) Mixture of liquid and gases.

   (b) No preferred orientation.

   (c) Gas bubbles may fail to rise in batteries interrupt-
        ing their action.

   (d) Direction sensitive devices may not operate properly.

   (e) Pumps may behave differently because of lack of
        hydraulic head.

   (f) Marginal equipment which will not operate upside down
        on earth may not work.

   (g) Clearances in spring-mounted equipment will change.

   (h) Devices working on fluid levels will fail.

L18.   Skopp, G. H.: Basic Investigation of the Operation of
       Propellant Actuated Devices in Space Environment.
       Phase II-A Theoretical Study. WADC TR 60-347,
       November 1960.

       The work in this report was prepared by the Frankford Arsenal which was assigned the project of investigating the operation of propellant actuated devices in space environment. During this phase, the standard propellant actuated devices (PAD) were examined with respect to natural and induced environments. Zero gravity was considered an induced environment. It is mentioned that during the operation of a propellant actuated device, the loss of 1 g may result in excessive force imparted to moving parts which may cause mechanical failure and/or malfunction. The effect of the

zero gravity on the performance of a catapult would result in at
least 1 g increase in acceleration. This would be undesirable
where a catapult's acceleration under standard conditions is at
its maximum limit.

L19.   Pohl, H. A.:   Nonuniform Electric Fields.   Scientific
           American.   Vol. 203, No. 6, December 1960.

        The long-neglected effects of nonuniform electric fields
on charged and uncharged particles which are being investigated
in the laboratory are briefly discussed in this popular scientific
journal. Dielectrophoretic forces are mentioned and photographs
of a laboratory experiment that employs this force phenomena to
precipitate fine powders from liquid suspension. A photograph
is also presented of a test showing a pump with no moving parts.
Here, a spray of carbon tetrachloride is thrown upward by a non-
uniform electric field which is set up by electrodes that are
connected to a Van deGraff generator. Some sketches are also
shown how liquid can be stirred by a nonuniform electric field,
how it can be "pumped" from a dish and how a liquid can be
attracted to a wire. Some of these effects are laboratory
curiosities, but some may be well worth exploiting.

L20.   Van Der Wal, L.:   Semiannual Report on Liquid - Gas Interface
           in Zero-G.   1 July - 31 December 1960.   Space Technology
           Laboratories, Inc.

        In September 1960 an Atlas re-entry nose cone test vehicle
was flown which housed an experimental unit consisting of a camera,
placed so as to observe and record the interaction of gas and water
contained in a plastic cube during the 25-minute near-zero-g
conditions present on an ICBM flight. The nose cone was not
recovered from the ocean as planned so that film data from zero-g
experiment were lost, and only telemetered data were available
for analysis. Schematic as well as external and internal con-
figurations of the zero-g experiment unit are shown in the report.

L21.   Anon: Research Summary #36-6, Vol. II, For the Period
           October 1, 1960 to December 1, 1960, CIT/JPL, Pasadena,
           California.

        This report covered the continuation of work reported in
L15 of this literature survey. Configurations were extended to
include a single reversing diaphragm, a double diaphragm, a
collapsing bladder and an expanding bladder. As previously
reported all tests were conducted with water as the working
fluid in a 41" diameter plastic tank.

L22.   Anon: Twelve Tank Pressurization Study, Rocketdyne -
           NAA Report No. AFFTC-60-64, R 2656.

        This study was conducted to determine the optimum method of
pressurization for a small ICBM. Systems studied included:

(a) Cold stored gas
(b) Heated helium
(c) Solid gas generation
(d) Liquid gas generation
(e) Tank injection of propellants
(f) Vapor pressure pressurization

Systems were evaluated for reliability, weight and cost in that order of importance. This evaluation revealed that the heated helium system was actually the most reliable, lightest and least costly of all the systems evaluated for this particular application.

L23. Bitten, J.: Liquid Oxygen Converter, WADD TR 60-669

Development of a liquid oxygen converter for life support systems is described. The converter is expected to work under zero-g gravity conditions. The liquid oxygen is contained and separated from bubbles by a permanent magnet inserted into the "bottom" of the converter. The liquid oxygen is transported by a capillary to the converter valve. A method is given for the computation of the forces acting on a para-magnetic droplet in an inhomogenous magnetic field. Semi-empirical equations have been established and tested for the transport of various liquids through wetted horizontal capillaries. The tests showed that bubbles in the liquid oxygen will not interrupt the flow through the capillary. The flow rate of interest is 5.5 liters per minute gaseous oxygen. It is indicated that the phenomenon of wetting can be used for transporting a liquid.

L24. Li, T.: Hydrostatics in Various Gravitational Fields, General Dynamics/Astronautics.

A closed axisymmetric container placed in a gravitational field is partially filled with a liquid and the stable configuration of the liquid-vapor interface is determined by minimizing the sum of the potential energy and the surface energies. The paper is of a mathematical nature. It is stated that in a zero-g field the test results of a liquid in a small tank can be applied to the same liquid in a larger but geometrically similar tank, provided that the vapor-to-container volume ratio remains the same. However, the scaling becomes complicated when the gravity is different from zero.

L25. Li, T.: Liquid Behavior in a Zero-G Field, Convair (Astronautic) Division, General Dynamics Corporation Report No. AE60-0682, Revised September 1960.

A solution, based on the principal of minimum surface energy, indicates that if the liquid wets the tank wall, it will cling to it and leave a vapor bubble in the tank. The surface of the bubble is a surface of revolution and the exact shape depends upon the ratio of the volume of the liquid to that of the vapor.

Small rotational disturbances are found to have a stabiliz-
ing effect and will cause bubbles to coalesce along the center of
rotation. Some of the analysis has been verified by tests. Some
of the conclusions obtained during this study are:

(a) Liquid behavior in a zero-g field is dominated by
surface tension.

(b) Instruments containing mercury or other liquid may
not give accurate information in a zero-g field.

(c) The vapor bubble can be kept at the top of this tank
by erecting uprights from the floor of the tank.

(d) A simple venting pipe leading to the vapor bubble
may be used to replace complicated liquid and vapor
separator.

L26. Bauer, W. and Fleming, W.: Metallic Propellant Tank Expul-
sion Techniques and Studies. Internal Report No. 253,
Bell Aerosystems Company, January 1961.

This report was formulated as a result of a study to deter-
mine the state-of-the-art in positive propellant expulsion and to
delineate design concepts which might be applicable to future
space vehicle propulsion system requirements. Both plastic and
metallic expulsion devices were analyzed to determine their
suitability and operating limits for both short term and extended
space mission requirements. At the completion of this study it
was concluded that the ultimate positive expulsion device would
have to be metallic. This was based upon the assumption that the
ultimate design will be one that is not affected by radiation, has
zero permeability and is compatible with all rocket propellants.

L27. Spieth, C. W., et al: Development of Positive Expulsion
Systems for Cryogenic Fluids - Phase I. Beech Aircraft
Corporation Report No. 9501, January 1961.

This document describes work performed pertaining to tanks
capable of expelling cryogenic liquids under a zero "g" environ-
ment. The areas of effort included the analysis of various
capacity tank systems and the methods of expelling the fluids.
A test program was conducted with a mylar bladder in a 24" glass
dewar. Liquid hydrogen was the expulsion fluid used. The mylar
test bladder underwent 75 complete expulsions without failure.
This program was the first phase of a two-phase effort which is
to culminate in the design and test of a 1000 gallon liquid
hydrogen tank using a bladder for positive expulsion.

L28.   Ginwala, K.:   Engineering Study of Vapor Cycle Cooling
       Equipment for Zero-Gravity Environment. WADC Technical
       Report 60-755, January 1961.

       This report discusses the results of some analytical and
experimental studies on wicks and capillary tubes. Wick materials
are considered well-suited to zero-gravity evaporators. It is
stated that the experimental work conducted must be extended
before any reliable design and construction of a wick evaporator
is possible. The liquid rise in wick materials is similar to
that in a capillary tube but is a far more complicated case.
The wick material can be considered to be composed of a group
of randomly orientated capillaries.

       Sections of the report discuss flow in capillary tubes
and in wick materials. Laboratory test results are also given
for flow through capillary tubes and for liquid rise in wick
materials as a function of time.

L29.   Anon: Operations Research Analysis of Gas Pressurization
       System, Aero-Jet General Corporation Final Report No.
       8160-01Q-6F, Vol. 5, January 12, 1961.

       The purpose of this study was to make an analytical
comparison of various pressure fed systems and pump fed systems
for various upper stage missions. An important by-product of this
study was the establishment of a comparison method which leads to
the optimum system for a particular mission. The following systems
were analyzed for the lower velocity increment systems considered:

       (a)   Helium stored gas
       (b)   Solid gas generation (sodium ozide)
       (c)   Liquid gas generation
       (d)   Dual liquid vaporization self pressurization

       Of the systems studied the solid ozide gas generation system
proved to be the best system with the broadest application.

L30.   Li, Ta: Liquid Behavior in a Zero-G Field, IAS Paper No.
       61-20, Presented at the IAS 29th Annual Meeting, New York,
       New York, January 23-25, 1961.

       A theory is developed mathematically for a closed non-
repellant metal tank which is filled with a wall wetting liquid
and its vapor to investigate the stable configuration of the liquid
in a zero-g field. It is found that the liquid will cling to the
wall and leave a vapor bubble in the tank. The surface of the
bubble is a surface of revolution. In the case of a non-wetting
liquid like mercury, it is found that the liquid will detach
itself from the wall and form a sphere in the "center" of the
tank. The mathematical theory is confirmed by tests carried
out by various institutions.

L31. Anon: Space Zero "G" Fuel Studies to Aid Centaur, Rover,
          and Saturn Propulsion Programs. Western Aviation,
          Missiles and Space, February 1961, Pages 12 and 13.

This article describes the forthcoming firings of the
Aerobee 150-A whose payload will include a partially filled
liquid hydrogen Dewar and instrumentation to record heat trans-
fer coefficients for the liquid hydrogen in the absence of
gravity. The flight trajectory will undergo five minutes of
zero gravity. A sequence camera is focused on the Dewar to
record the liquid behavior during the flight.

L32. Sirocky, P. J.: Transfer of Cryogenic Fluids by an
          Expulsion-Bag Technique. NASA TN D-849, April 1961.

This report covers a test program that was conducted to
demonstrate the feasibility of transferring cryogenic fluids by
the expulsion bag technique. Mylar coated dacron bags, used as
fluid containers, were found to be flexible enough to collapse at
temperatures of approximately -424°F and thereby expel the fluid.
No damage was evident even after repeated cycling with liquid
nitrogen. Attempts to fill the bladder with liquid helium failed
however, rendering these tests results inconclusive. This program
was extremely limited in scope and seemed to be a duplication of
effort of the Beech Program previously mentioned.

L33. Abramson, H. N.: Liquid Dynamic Behavior in Rocket Propel-
          lant Tanks. Symposium Proceedings - Structural Dynamics
          of High Speed Flight. Vol. I, ACR-62, Los Angeles,
          California, April 24-26, 1961. Pages 287-318.

Various types of liquid dynamic behavior occurring in
propellant tanks such as normal sloshing, vortexing, liquid
impact, bubble and spray formation and low gravity phenomena
are described and discussed. A short discussion is given on
restart of engines in space or orbital flight and the movement
of liquid to the proper location for pumping into the engine.
Mention is made of applying low-level thrust by compressed gas
or solid propellants, or such devices as expulsion pistons and
bladders.

L34. Williams, H. E.: Liquid Surface Shapes-Research Summary
          No. 36-8 for the Period February 1, 1961 to April 1,
          1961, Jet Propulsion Laboratory, May 1, 1961, pp 98-99.

This summary presents the effect of surface tension forces
in hydrodynamics, the hydrostatic free surface of a fluid in
contact with a vertical wall. For walls that are parallel flat
plates, the solution for the shape of the free surface can be
obtained exactly. For a circular cylindrical wall, an approxi-
mate value for the free surface shape inside the tube is obtained.

L35.   Swann, W. F. G.: "Can There Be a Shield for Gravitation."
       Journal of the Franklin Institute, Vol. 271, No. 5,
       May 1961. Pages 355-360.

       This communication represents an amplification of an essay
of the same title submitted to the Gravity Research Foundation.
A theory of gravitation put forward by LeSage many years ago
postulated that all space was filled with small particles travel-
ing in all directions with high speeds. Bombardment by these
particles on two bodies some distance apart would cause relative
attraction because fewer particles reach the space between the
bodies. This region would be a "shield" for gravitation. This
speculation is considered unreasonable today. The article con-
cludes that if gravitational forces could be explained in terms
of waves, one might be able to realize a shield of gravitation
in the same way that one can shield electrical apparatus from the
effects of external electrical disturbances.

L36.   Baggs, R., Conrad, K., et al: Ultra-Low-Chamber-Pressure
       Systems. Aerojet-General Corporation, Azusa, California.
       Aerojet Report No. 0406-01-3, May 1961 (Confidential).

       A section of the report presents an analysis of a zero-g
start system that employs a variation of the "settling rocket"
principle and a gas separator. In addition, a test capsule for
proving out the start system in a zero-g environment is described.

L37.   Anon: Propulsion Requirement for Space Missions Rocketdyne
       Report R-3208, Vol. III, May 1961.

       The difficulty of separation of gas and liquid in propellant
tanks is mentioned as one of the problems brought about by zero
gravity. Buoyancy and natural convection do not exist. Two
methods of gas and liquid separation are mentioned:

       (1) Accelerating the tank with an auxiliary rocket so that
            the liquid gas interface will be perpendicular to the
            acceleration.

       (2) Permanent separation of the liquid and gases with a
            diaphragm or bladder.

       A method is also mentioned using the wetting properties of
the cryogenics. Poles are planted in the lower surface of the
tank and because of the wetting properties of the cryogenic liquid,
these poles will not readily penetrate the liquid-gas interface.
The gas bubble will be kept in the upper part of the tank and
liquid at bottom. These wetting properties can also be used to
design an entrance to the propellant feed line that will tend to
admit only liquid.

L38. Siegel, Robert: Transient Capillary Rise in Reduced and
Zero-Gravity Fields. Transactions of the ASME, Vol. 28,
Series E, No. 2, June 1961, pp 165-170.

Experimental information is given on the transient "capillary"
rise of water into vertical tubes subjected to reduced and zero-
gravity fields. The tubes ranged in internal diameter from 0.075
to 1.295 inches. An approximate analysis is presented to aid in
the interpretation of the data and predict the transient rise.
Photographs are given which illustrate the behavior in short tubes
where the water is able to move beyond the top of the tube during
part of the zero-gravity period.

L39. McGinness, H. D.: Capillary Pumping for Closed Cycle Gas
System, Research Summary No. 36-9, V.I. JPL, July 1961,
pp 23-26.

A design of the closed-cycle gas supply systems for gas
bearing instruments is illustrated of a model consisting of the
following parts: (1) an ice cooled well, partially filled with
one end of a wick of 5×10^{-4} in. glass fibers; (2) a 3/4 inch
I.D., 12 inches long glass tube filled with the extension of the
wick; (3) an electrically heated cavity, partially filled by the
other end of the wick; (4) a glass tube originating in the heated
cavity and ending in the bottom of a wick tube partially filled
with Hg (the height of the Hg column representing the head across
the gas bearing); (5) a return line from the top of the tube to
the cooled well. Freon-114 fills the cavities and saturates the
wick. When the heater is turned on, Freon evaporates on the heated
end and a free surface develops. The capillary force drives the
liquid from the cooled well to the hot-end. The vapor travels
from the latter against the head of Hg back into the cooled well.
Circulation stops when the driving pressure, generated by the
capillary force is exceeded by the head of mercury. It was found
that the estimated driving pressure greatly suppressed the limit-
ing velocity head (3.5 versus 0.6 psi). Uneven packing in the wick
is the suspected cause of the discrepancy.

L40. Bowring, J. I. R. and Ebert, B. P.: A Hypothetical Mission
to Space in a Three-Man Sealed Cabin. Planetary and Space
Sciences, Vol. 7, July 1961, Pergamon Press, pp 309-323.

This paper deals with a hypothetical flight into orbit in
a sealed cabin with three persons constituting the crew. One of
the problems concerns feeding devices which are positive expul-
sion devices. A roller type and a pressure operated flexible
diaphragm food container is discussed to a limited degree.

L41. Van Der Wal, L.: Package Experiments for Bioastronautics
Research. Planetary and Space Sciences, Vol. 7, July
1961, Pergamon Press, pp 356-369.

A brief discussion on liquid-gas mixtures at zero-g is presented. An artificial gravity field by rotation of the vehicle, provides the necessary force to establish control on the liquid and gaseous state. The alternate method of rotating only the subsystem having the liquid-gas interface problem is considered to require excessive power but no justification is presented for this latter statement.

L42. Barker, Jr., C. L.: Space Flight Acceleration Simulator. Planetary and Space Sciences, Vol. 7, July 1961, Pergamon Press, pp 335-344.

A study that outlines the concepts of a simulator which produces the acceleration-time history of rocket flight and the "g" fields of the Moon and Planets is presented. The proposed system is a track captured capsule that can carry several trainers or hundreds of pounds of equipment through programmed flight trajectories, including zero-g environment. Zero-g conditions for periods of 15 seconds are indicated in the study.

L43. Unterberg, W. and Congelliere, J. T.: Zero Gravity Problems in Space Powerplants - A Status Survey. American Rocket Society Paper No. 2133-61. Space Flight Report to the Nation, New York, October 9-15, 1961.

The paper mentions some tests performed by other investigators on the transient capillary rise of a liquid into a tube during reduced and zero g. For long zero g durations, the tube with the largest diameter will show the highest rise. A mere statement is made that a positive expulsion bladder provides a means for supplying liquids at a controlled rate, and independent of the gravitational forces.

An artificial force field could be utilized for fluid phase separation and rotation of the entire vehicle could provide such a force curving the flow path of the fluid by using a helical tube or by inserting twisted strips in the tube can also supply the necessary centrifugal force to separate the phases of a two-phase fluid.

L44. Barger, J. N. and Hanson, D. L.: Research and Development on Components for Pressure-Fed Liquid Oxygen-Liquid Hydrogen, Upper-Stage Propulsion Systems. Pressurization-System-Feasibility Expulsion Tests. Aerojet-General Corporation Report No. 1953, Vol. II (AFFTC-TR-61-7, II) (Confidential).

Test, analysis, and design data for a recommended LO_2/LH_2 rocket gas pressurization concept are reported. Two-part testing demonstrated the concept and determined the hydrogen gas requirements; expulsion tests were made with a 30 ft^3 aluminum (6061-T6) tank using LH_2/GH_2, LN_2/GN_2 and LO_2/He at 90 psia. Two-part

analyses correlated the tank thermal-energy model with LH^2 test data and the dynamic-response model with limited LH_2 slosh-test data. The design work applied the test results to a minimum-weight pressurization system.

L45. Li, T.: Cryogenic Liquids in the Absence of Gravity, General Dynamics/Astronautics, 1961.

In above reference it is stated that venting devices utilizing pressure difference, may be used to solve the venting problem. A pipe leading from the inside of the tank to the outside may be equipped with a moving lip, which has the shape of a truncated cone, so that the surface of the minimum area cannot be tangent to the lip. The lip rotates because of the differential pressure. When it rotates a centrifugal force is created which produces a small gravitational field to throw the liquid against the tank wall and to draw the vapor bubble towards the axis. This device will eliminate at least partly the escape of the liquid. It may adequately solve the venting problem.

L46. Gerathewohl, S. J.: Zero-G Devices and Weightlessness Simulators. National Academy of Sciences - National Research Council, Publication 781, 1961.

The report concerns devices, methods and techniques which have been employed for the investigation of the effects of zero-g and weightlessness by many investigators. Descriptions of research equipment and techniques are included. The zero-g devices mentioned include vertical motion devices, aircraft flying a parabolic path and ballistic missiles. Weightlessness simulators that are described include water immersion and frictionless devices and platforms.

L47. Hunder, B. J., Bell, J. E., and Penner, J. E.: Expulsion Bladders for Cryogenic Fluids, Cryogenic Engineering Conference, Ann Arbor, Michigan, 1961.

The test work performed at the Beech Aircraft Corporation in Boulder, Colorado on Mylar bladders with liquid hydrogen as the fluid is summarized. A spherical container was utilized and the laboratory tests indicated that the construction of Mylar bladders in a series of gores is feasible. This paper and that of L48 of this literature survey are similar except that the test procedure is explained more fully in the subject paper.

L48. Bell, J. E. and Reid, W. H.: Cryogenic Tankage for Chemical Space Power Systems. Progress in Astronautics and Rocketry - Vol. 4, Space Power Systems. Academic Press, New York 1961, pp 595-611.

A bladder-type expulsion system for cryogenic fluids is mentioned in the paper. A spherical bladder is considered the

optimum shape. For a liquid hydrogen expulsion system, a bladder
of three unbonded plys of 1/2 mil aluminized Mylar withstood 79
full cycles of liquid hydrogen filling and expulsion with no
leaks.

L49.   Anon: Final Report - Study and Design of Unfurlable
          Antennas, WADD TR 61-26, Vol. II (Lockheed LMSD 704036,
          Pt. II).

     The goal of this study was to design unfurlable antennas
for satellites and other space vehicles. Areas of study covered
were (1) space environment effects on antenna materials, and (2)
the effects of folding and unfolding on antenna materials. As a
result several large laminated Mylar and aluminum foil antennas
were constructed and tested. Although these designs were
specifically antennas, their operation is directly related to
bladders for positive expulsion.

L50.   Anon: Design Manual - Rolling Diaphragms, BF400-A,
          October 1960. Bellofram Corporation, Burlington, Mass.

     The subject manufacturers literature presents descriptions,
operation, advantages, applications, installation suggestions and
design data on rolling diaphragms. The concern provides rolling
diaphragms in a wide variety of elastomers for use in numerous
environmental gases or fluids. The numerous installation sugges-
tions provide a wealth of information on these configurations. It
seems possible to extend the aforementioned data and principles
to metallic configurations, especially in the larger sizes, wherein
the thin gage metal will tend to behave in a membrane fashion.

L51.   Anon: The Seals Book, Machine Design, A Penton Publication,
          1961 Edition.

     This handbook contains basic design facts about seals,
packings and gaskets to aid in proper selection and application
as well as detailed information on types and manufacturers of
seals, packings and gaskets as a guide to specification. The
section on the bellows-type axial mechanical seals and the chapter
on diaphragm seals contain information that is directly applic-
able to certain positive expulsion systems. Design precautions
are enumerated and the advantages of several types of systems are
listed.

L52.   Hesse, Mary B.: Forces and Fields. Thomas Nelson and Sons
          Ltd., New York, 1961.

     This 318-page book was acquired too late in the program to
perform an adequate review of its contents. The subtitle of the
book is given as "A Study of Action at a Distance in the History
of Physics."

III. SYNTHESIS OF EXPULSION DEVICES

MORPHOLOGICAL APPROACH

Introduction

The continued growth in the duration and complexity of operational requirements and in the severity of the operational environment has necessitated an evaluation of the various possible propellant expulsion methods. A morphological technique has been employed to ascertain the classification and types of expulsion devices that can accrue from such a study. References 1, 2 and 3, which have been employed in other fields, were utilized in order to disclose systems that could perhaps be overlooked by the conventional inventive approach of design. The inventive approach is a time consuming process and very much dependent upon the capability of the individual.

Actually two major macroscopic categories of forces, (forces that move the fluid) are involved in positive expulsion devices. These two categories of forces are:

      I.   Contact-Force Movement
     II. Field-Force Movement

Contact-Force Movement is attributed to a displacement device wherein contact with the fluid is provided to insure movement. A piston-cylinder combination is a typical example.

In the Field-Force Movement, a force field is involved that may not have any mutual or mechanical contact with the fluid to be displaced. The forces may be attraction or repulsion. A magnetic field is one such example.

Table I represents a morphological listing or matrix of expulsion devices. The totality of expulsion devices may be analyzed schematically as follows:

Expulsion Forces

Expulsion forces may be accomplished through the use of contact forces or long-distance or field forces. The former usually requires a mechanical system of the following types.

    A. Contact-Force

        a. Bladder
        b. Diaphragm
        c. Mechanical
        d. Surface Forces
        e. Chemical
        f. Inertia

TABLE I.   MORPHOLOGICAL APPROACH TO POSITIVE EXPULSION SYSTEMS

1	Expulsion Forces	
A	Contact-Force	a Bladder
		b Diaphragm
		c Mechanical
		d Surface Forces
		e Chemical
		f Inertia
B	Field-Force	a Magnetic
		b Electric
		c Electromagnetic

2	Propellant
A	Gaseous
B	Liquid
C	Solid

3	Material	
A	Metallic	a Homogeneous
		b Non-Homogeneous
B	Non-Metallic	a Homogeneous
		b Non-Homogeneous
C	Composites	

4	Operation
A	Continuous
B	Intermittent

5	Motion
A	No Motion
B	Translatory
C	Rotary
D	Oscillatory
E	Random or Complex

6	Shape	
A	Surface of Revolution	a Sphere
		b Torus
		c Ellipsoid
		d Cylinder
		e Cone
B	Complex	

7	Pressure
A	Low
B	High

8	Control
A	Controlled
B	Uncontrolled

9	Driving Medium
A	Chemical
B	Thermo-Chemical
C	Electrical
D	Stores Energy
E	Nuclear
F	Mechanical

Bladders, diaphragms and mechanical concepts are self-explanatory. Surface forces constitute capillary action encountered in capillary tubes, wicks and grids or screens.

The chemical category includes forces generated by chemical reactions.

Inertia implies that an acceleration is produced in some manner that results in settlement of the fluid in the desired location in the container.

The field force can be divided into three main classes:

B. Field-Force

a. Magnetic
b. Electric
c. Electromagnetic

The characteristics of these field forces and their application to expulsion devices is explained more fully under the title of Field-Force Devices.

The Physical State of the Propellants

Three different physical states of the propellants may be distinguished, namely,

A. The Gaseous State
B. The Liquid State
C. The Solid State

There are, however, some additional states of propellant that can be considered composites that have characteristics that are attributable to combination of the above-mentioned states. These are defined below.

Gel - A gel is an apparently solid, often jelly-like material. Some gels may contain as much as 90% liquid yet in their properties are more like solids than liquids.

Slurry - This state can be considered as a thin paste. It is a solid phase suspended in a liquid phase.

Aerosol - An aerosol is a colloidal system such as a mist or a fog in which the dispersion medium is a gas.

Another characteristic or descriptive term of propellants, although it does not necessarily pertain to physical state, is that of storability.

Storable propellants are those fuels and oxidizers which can be continuously stored in the missile or space vehicle in a state of instant readiness for relatively long periods of time without evaporating or changing state or corroding the containing structure.

Cryogenic propellants are fluids which require refrigeration to maintain it as a stable liquid in an environment of normal atmospheric pressure and temperature.

This descriptive characteristic of storability affects choice of material, type of construction, and thermal studies for the expulsion device.

The reactivity or combustion of the propellants is another characteristic. Here two pure cases may be distinguished:

    a. The propellants may be self-igniting,

    b. The propellants are not self-igniting, and an artificial ignition is necessary. System complexity is introduced with the latter characteristic which can influence the expulsion device choice.

Structural Material

The materials of construction can be classified by three broad categories such as:

A. Metallic

    a. Homogeneous
    b. Non-Homogeneous

B. Non-Metallic

    a. Homogeneous
    b. Non-Homogeneous

C. Composites

The homogeneous materials need no further clarification.

The non-homogeneous materials, in the metallic classification, constitute cladding, coatings and/or plated layers not of the same material.

In the non-metallic group, rovings, fibres, strands, filaments, etc., bonded with a resin are included within this category.

The composite group encompasses combinations of metals and non-metals. A metal weave (metallic cloth) with a plastic coating is one such product. Multiple layers or multiwall construction such as metallic coated plastic is another example.

Mode of Operation

Two modes of operation are possible; namely,

A. Continuous
B. Intermittent

Continuous mode of operation is self-explanatory, Intermittent motion can be pulsating or periodic or cyclic.

Motion Incorporated in an Expulsion Device

In the operation of an expulsion device there are five possible modes of motion of the principal activating parts.

A. No Motion
B. Translatory
C. Rotary
D. Oscillatory
E. Random

The above motions are self-explanatory with the possible exception of random motion. Random motion cannot be defined by a kinematic analysis approach. For example, in the complete collapse of a circular cylinder under external pressure, the buckling pattern, the resulting creases, single and multiple folds, wave pattern shift, etc., are not amenable to analytical prediction, location or magnitude of deformation. The formation of these buckles is considered a random motion. Bladders are a typical example that incorporate such a motion characteristic.

The Character of Shape

The configuration or shape of the fluid container is a rather broad category because of the numerous possibilities of shapes that can be evolved. Surfaces of revolution are a common structural configuration for a container although space limitations could introduce shapes that are of complex contour. Thus two main categories can be included in the shape characteristic of the fluid container:

A. Surface of Revolution
B. Complex Shape

The surfaces of revolution are:

a. Sphere
b. Torus
c. Ellipsoid
d. Cylinder

    1. Flat Ends
    2. Spherical Ends
    3. Alliptical Ends
    4. Torispherical Ends
    5. Conical Ends

e. .Cone

    1. Flat Ends
    2. Spherical Caps
    3. Elliptical Caps
    4. Torispherical Caps

The position of the ends or caps, that is, concave or convex outward on the cylinder or cone introduces other combinations of configuration shape for the surface of revolution. It should be noted that two different types of heads or caps can also be employed on the same cylinder or cone.

The complex shape container is self-explanatory and needs no further clarification.

Pressure

The positive expulsion devices must be capable of producing a desired and/or required pressure head. The magnitude of the generated pressures in many cases is an inherent characteristic of the system employed. The following two classes of pressure regimes are considered sufficient for the present study.

A. Low
B. High

Control

In the control of any system or device, two definite and broad possibilities present themselves. They are:

A. Controlled
B. Uncontrolled

The important variables to be controlled in expulsion devices include:

    a. Mass Flow
    b. Volume Flow
    c. Pressure

The characteristics of such control for the devices can include:

    1. Holding at a constant force in any position
    2. Holding at a constant position rather than with constant force
    3. Locking-in at any given position
    4. Broad adjustment in force
    5. Variation in speed
    6. Initial response

Driving Medium

The driving medium, the energy required to motivate the device to expel the fluid, is a study within itself and will not be considered in great detail in the subject work. It should be borne in mind, however, that the choice or availability of the necessary energy can or will dictate the choice of a particular expulsion device. For example, the integration of a gas generator with an expulsion device or the power potential with a nuclear reactor on board can even alter the type of expulsion forces, (contact-force or field-force) that can be considered.

Table I can be employed to exploit various combinations of characteristics that result in numerous and specific devices. To obtain an expulsion device by this procedure, we choose one of each numbered variable for each lettered parameter. The combination of such identifications makes available an expulsion device from the characteristics selected. As an example, the combination 1Ab, 2B, 3Aa, 4B, 5B, 6Aa, 7B, 8A and 9D, represents a diaphragm construction for a liquid propellant state whose container material is a homogeneous metal. The device can operate intermittently with a translatory motion of the diaphragm within a spherical tank and can expel the fluid at a high pressure. The device can be controlled at all times and the power to operate the diaphragm device is by means of stored energy (pressurized gas).

EXPULSION DEVICE METHODS

The morphological classification that has been presented thus far must now be examined from a more specialized point of view. Many of the possibilities presented must be excluded

from serious consideration because of their obvious impracticality or self-contradictions. A large number of feasible designs still remain, many of which are untested. Many other designs are derived from a few basic ones, usually by attempts to obtain better efficiency and reliability, the results of advancement in new materials and fabrication techniques, etc. In practice, certain expulsion devices may be strictly circumscribed by various dimensional, and material limitations.

Figure 1 presents an array of expulsion devices that have been grouped and expanded into certain fundamental classes. An expansion of this type of presentation gives the designer an opportunity to exercise his ingenuity and judgment in various combinations of the morphological matrix.

FORM BLOCKS

FRAMES

LONGITUDINAL

WIPER

ACCORDION

ROTATING   GUIDED   RESTRAINED

ROLLING   MULTIPLE   CORRUGATED

CIRCUMFERENTIAL BELLOWS   SINGLE   FLUTED   GUIDED

TELESCOPIC   DISHED   EXPANDED

CONVOLUTED

DIAPHRAGM

BLADDER

JAPANESE L

UMBRELLA

SPOKE & MEMBRANE

ACCORDION

UNFURLABLE

BELLOWS   SQU

COLLAPSED

MECHANICAL

EXPULSION METHODS

ORIENTATION

TRAP TANK

ULLAGE ROCKET

ENCLOSED SQUIB

SOLID

SURFACE FO

SCREENS

FORCE FIELDS

CHEMICAL

FOAM DISPLACEMENT

GELLED

CONDUCTIVE FLUID   PRESSURE

SLURRY

HYDROMAGNETIC

COATING

SUPERCRITICAL

SUBCRITICAL

INJECTION

HYBRID

CONCENTRIC BLADDERS

ROLL & PEEL DIAPHRA

ELECTRO

DI

Figure 1. Positive Expulsion Methods

IV. EXPULSION DEVICE CONFIGURATIONS

INTRODUCTION

An investigation and study of positive expulsion devices disclose numerous types of concepts and principles some of which have been categorized in Figure 1. These various categories are enumerated below. Examples of some of the devices in each category are examined in greater detail in the ensuing text.

    a. Diaphragm-Type Configurations
    b. Bladder-Type Configurations
    c. Controlled Deformation or Folding Configurations
    d. Mechanical Systems
    e. Orientation Systems
    f. Surface Forces
    g. Hybrid or Miscellaneous Systems
    h. Chemical
    i. Field Forces

An effort is made to list the advantages and disadvantages of the numerous configurations depicted in the sketches and to present some analytical design data that is applicable to a specific configuration. In some instances, only qualitative data could be presented and it was considered advantageous to do so.

DIAPHRAGM-TYPE CONFIGURATIONS

Diaphragm-type configurations are dividing membranes installed within an enclosed shape in such a manner that two fluid-tight areas are formed. The cross-sectional shape of the diaphragm, however, can be established during fabrication to meet specific requirements. As a consequence, some of the resulting shapes are defined below.

    1. Convoluted Diaphragms

Convoluted diaphragms have one or more concentric convolutions which are either pressed, formed or spun. Convolutions increase the working stroke of a diaphragm and allows the diaphragm to operate with material flexing rather than material elongation.

    2. Dished Diaphragms

Dished diaphragms are either spun or formed in the shape of a dish. The dish shape increases the allowable stroke which can be almost twice the dish height without material stretching.

3. Flat Diaphragms

Flat diaphragms are flat circles, usually made of a thin
flexible and stretchable material. These types of diaphragms
have limited stroke capabilities compared with convoluted or
dished diaphragms.

4. Rolling Diaphragms

A rolling diaphragm is a long stroke, deep convolution,
constant area diaphragm which is free positioning with complete
relaxation at any point in its stroke. The diaphragm is attached
to the piston head and as the diaphragm and piston are moved in
an axial direction, due to an applied pressure, the diaphragm
will roll off the piston side wall, and onto the cylinder
side wall, (or in a reverse process), with a smooth and continuous
frictionless motion.

5. Spherical Diaphragms

Spherical diaphragms are shaped in the form of a hemis-
phere and are essentially a reversing-type configuration during
operation. A snap-through type of buckling or instability is
introduced during the expulsion process when the diaphragm
reverses itself and deforms from one portion of the hemisphere
into the other.

Several typical illustrations of diaphragms are shown in
Figures 2 and 3.

Some experimental tests were performed by the Bell Aerosystems
Company on a bathtub-type reversing diaphragm made from .016 in.
aluminum alloy (1100-0) to note its behavior and the folding and
unfolding of the wrinkles and buckles during the expulsion cycle.
Figure 4 is a photographic history of the metal diaphragm defor-
mation under the stimulus of a negative pressure being introduced
within the container. This is equivalent to the pressuring
gas inducing an external pressure under an actual service condition.

DOUBLE CONVOLUTED DIAPHRAGMS

The double convoluted diaphragm configuration, which is
illustrated in Figure 5 for a spherical container possesses the
following advantages and disadvantages:

Characteristics of Double Convoluted Diaphragms

Advantages

1. The hemispherical head or tank is the optimum shape
for employing a convoluted diaphragm.
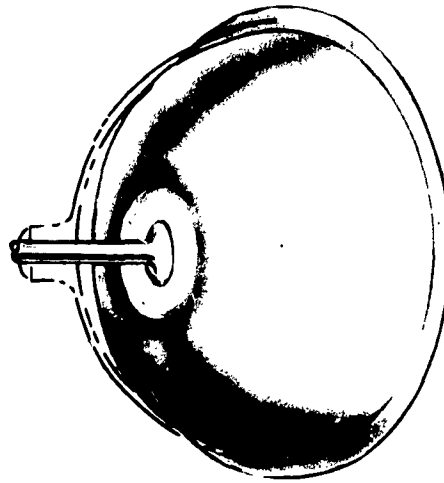
Guided
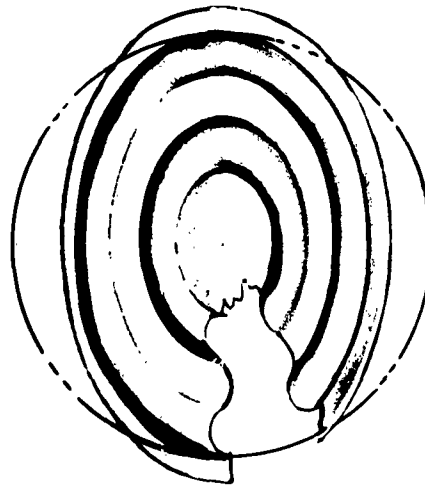
Convoluted
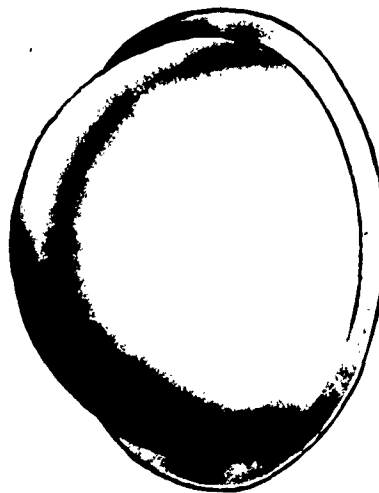
Spherical

Figure 2.   Typical Diaphragm Configuration
For Spherical Containers

After Expansion

As Installed

(2 Diaphragms Welded
Together)

Gas
Inlet
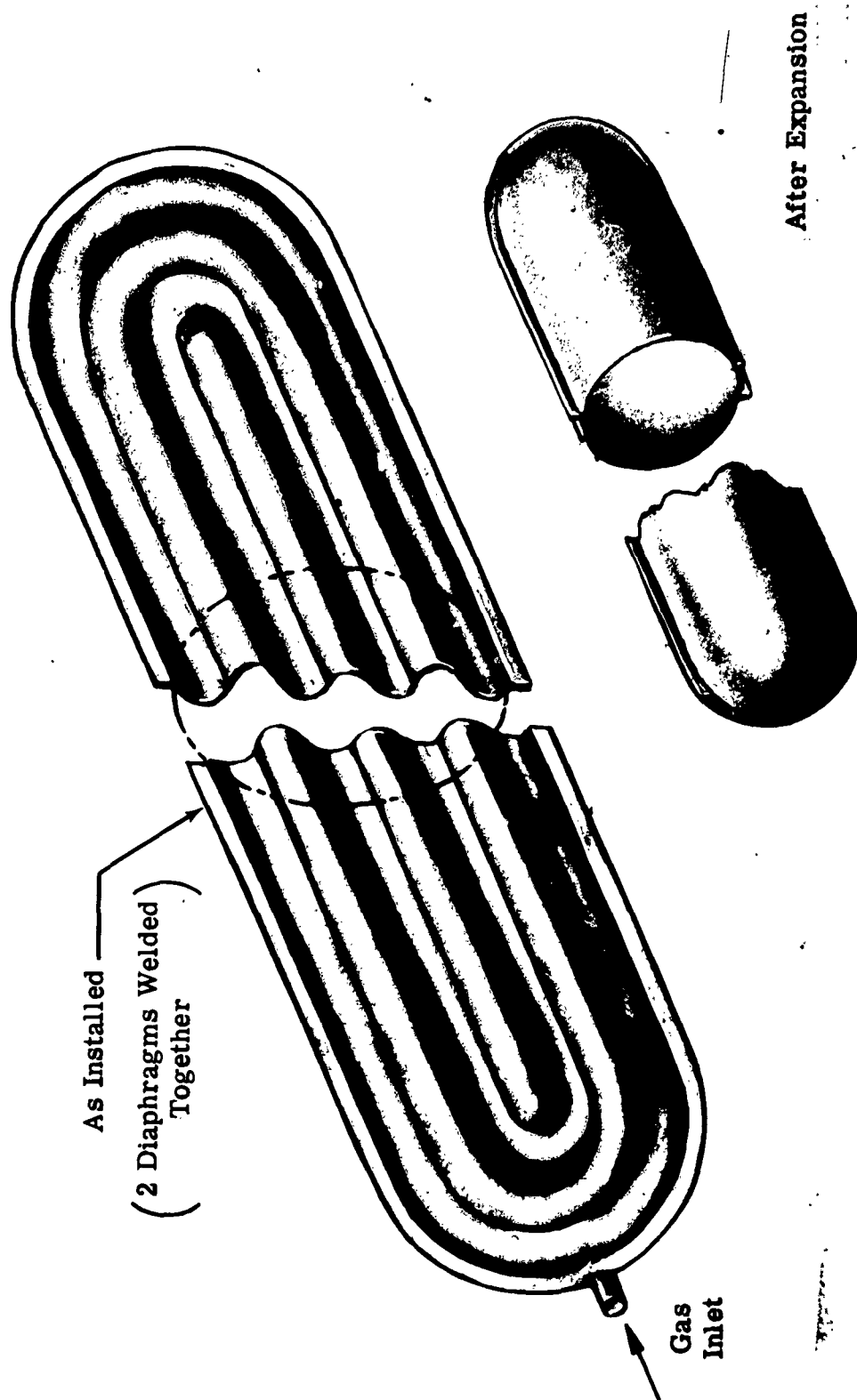
Figure 3.   Double Longitudinal Diaphragm

(a) 100% Full

(b) 75% Full

(c) 50% Full

(d) 25% Full

Figure 4. Aluminum Alloy Bathtub-Type Reversing Diaphragm Configuration and Deformations During Expulsion
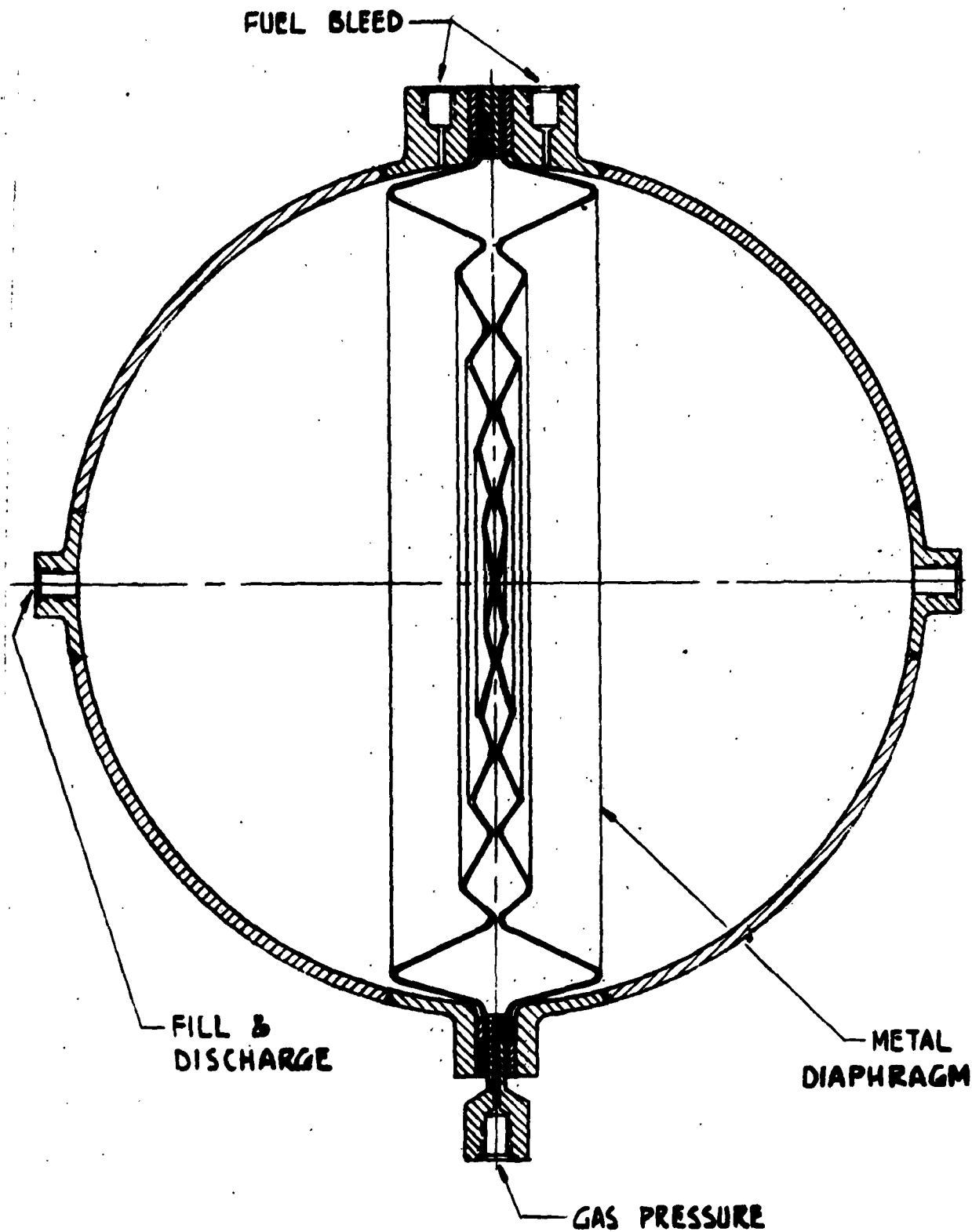
Figure 5.   Double Convoluted Diaphragm

2.   The circumferential corrugations or convolutes can be designed so that the equivalent length fits the inside contour of the outer shell.   Stretching or elongation of the diaphragm is thus minimized.

3.   The diaphragm is merely a flat orthotropic plate which is relatively easy to make and handle.

4.   Rectangular tanks employing surface of revolution heads can employ these diaphragms.   Convolutes within the head area are analytically computed in a manner to produce an equivalent length or surface equal to the internal surface area in the deformed state.

5.   Pressurizing gas is introduced between the diaphragms and the resulting deflection does not induce any creases, folds or rolling of the surfaces.

6.   The two halves of the convoluted diaphragms can be welded and assembled as a unit and thus constitute a preformed or prefolded bladder in the flat.

7.   Each of the two halves or volumes of the configuration can be used for a bi-propellant system within a single tank geometry.

Disadvantages

1.   Installation will require circumferential or longitudinal bolted-type flanges about the equator of the tank.   This induces a weight penalty.

2.   Sealing of the diaphragm between the tank halves may present a problem.

3.   The diaphragms produce two tank volumes that must be interconnected by a collector tube to insure expulsion from both halves of tanks.

4.   When a bi-propellant combination is employed, a 50-50 fuel and oxidizer combination is desirable but may not be so. Equal volume separation by the diaphragm is thus not possible and design difficulties are introduced; such as, tank is no longer a symmetrical surface of revolution, one diaphragm must deflect more than the other, pressure and mass ratios for propellants must be regulated in desired proportions.

5.   The device is orientation sensitive with respect to acceleration forces.

Analysis Data

Design Concepts

A qualitative approach for establishing the pattern or shape of the corrugations for a convoluted diaphragm is presented on the following pages. A circular convoluted diaphragm is used as an illustrative example although the same philosophy of approach can be readily applied to other shapes that constitute a surface of revolution.

A corrugated or convoluted circular diaphragm supported at its periphery and subjected to a pressure differential across its surface will initially deflect primarily as a consequence of bending strains. For small deflections, the influence of membrane strains on the deflections are negligible. As the deflection increases with increase in differential pressure and become relatively large with respect to the diaphragm thickness, significant membrane strains are introduced. For thin gaged corrugation diaphragms, the resistance to deformation in the meridional direction will be much less than in the circumferential direction as a result of meridional bending strains. In addition, as the membrane is deflected and the corrugation waves are flattened, resistance to meridional rotational deformations will be governed by the early introduction of plastic "hinges" at the crowns and crests of the corrugations where meridional bending moments are greatest. As the diaphragm convolutions are stretched and flattened further and the diaphragm approaches the general shape of the inside contour of the container, both meridional and circumferential membrane strains will primarily govern further deformations, depending on the initial configuration of the corrugated diaphragm.

Based on this general simplified discussion of the behavior of a corrugated diaphragm, it appears that the best design procedure is to determine the general diaphragm configuration in such a manner that the final shape (a sphere, for illustrative purposes) is approached primarily as a consequence of the relatively low resistance to meridional bending. Consequently, the design of a corrugated diaphragm is initiated by assuming the diaphragm to be a pure membrane, i.e. there is no resistance to meridional bending moments. Such a diaphragm would be stress-free if it were shaped in such a manner that all circumferential fibers do not grow or contract when the diaphragm is deflected from its initial position to the final spherical position.

Consider two circumferential fibers of the diaphragm in the expanded spherical form, as indicated in Figure 6, by the points a and b. These fibers will not experience any membrane strains if they were originally located at the same relative
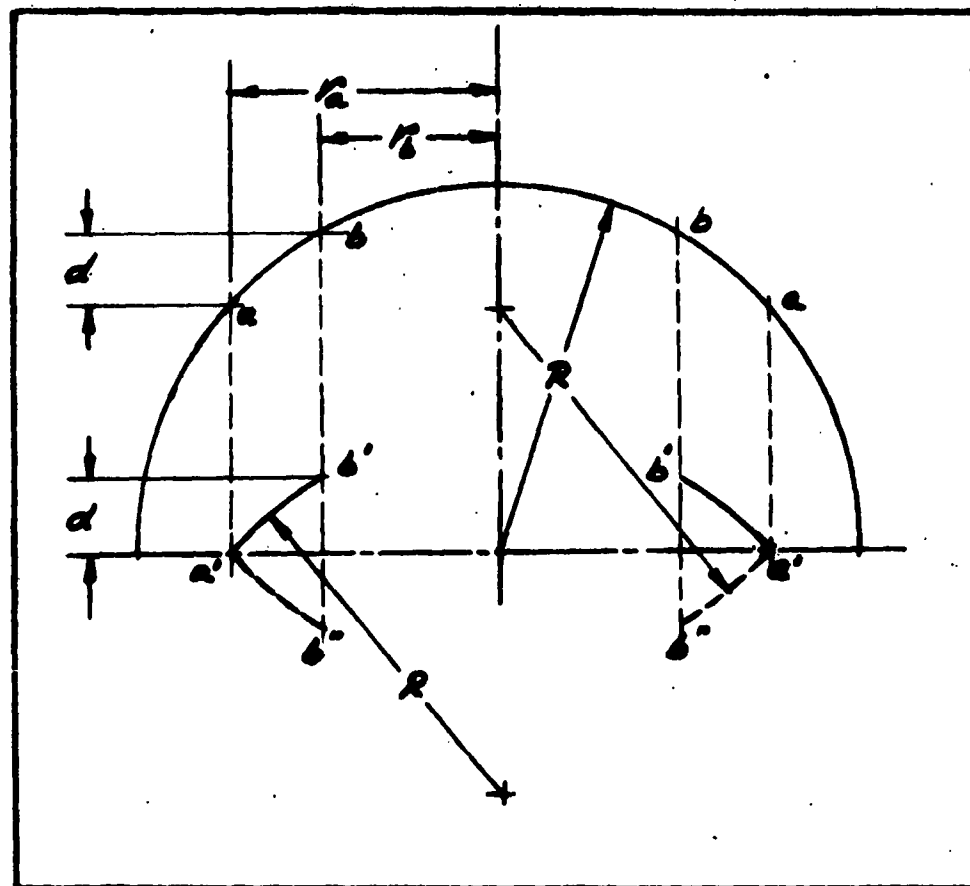
Figure 6. Strain-Free Deflection of Membrane

positions on the vertical dashed line and also if all other con-
nected circumferential fibers were similarly originally oriented
so as to be geometrically compatible. If, for example, circum-
ferential fiber, a, was initially located at point a', then, to
ensure a stress-free expanded condition, the fiber, b, must be
originally located at point b' and all intermediate fibers must
form a segment of the sphere, i.e. the curve a'-b'. It should
be noted that a membrane stress-free condition will also be
attained if the circumferential fiber at point b were initially
located at point b" and the correspondingly intermediate fibers
were to form the circular arc a'-b". Consequently, an ideal
initial shape for the membrane would be to shape it as segments
of the inside contour of the container, which for the case under
consideration, is a sphere.

From the above considerations, it is obvious that there
are an infinite number of stress-free ideal membrane shapes that
may be formed. The procedure suggested for the design of a
diaphragm is to first shape the diaphragm based on the above con-
cept of a pure membrane and then to introduce the necessary modi-
fications if they are required. Such modifications may be based
on fabrication limitations, ullage requirements, differential
pressure limitations, expulsion efficiency, mechanical properties
of the material and undesirable buckling.

Ideal Diaphragm Configurations

The cross section of various ideal diaphragm configura-
tions composed of spherical segments are shown in Figures 7
through 9, together with the details that were used in their con-
struction. A three convolution diaphragm was chosen for illus-
trative purposes. To restrict the many possible configurations,
the diaphragm configurations shown were devised such that they
rest on a diametral plane of the sphere. The diaphragm con-
figurations illustrated were devised by either (1) assuming
constant depth for the convolutions, Figure 7; (2) assuming
constant pitch for the convolutions, Figure 8; or (3) assuming
constant developed length of convolution, Figure 9. It will be
noted that the developed surface area of each ideal diaphragm
configuration is equal to the surface area of the corresponding
half sphere. In addition, each portion or section of the convo-
lution is coincident with the sphere in the extended configura-
tion. It should be noted that the selection of the magnitude
of one of the design parameters (depth, pitch or constant
developed length), dictates the magnitude of the other two param-
eters. If the magnitude of each of these design parameters is
decreased, the ullage volume decreases and in the limit it will,
for a pure membrane, approach zero as the membrane approached a
flat plate. This limiting configuration is of course only pos-
sible if the diaphragm was fabricated from sheet material
approaching zero thickness.
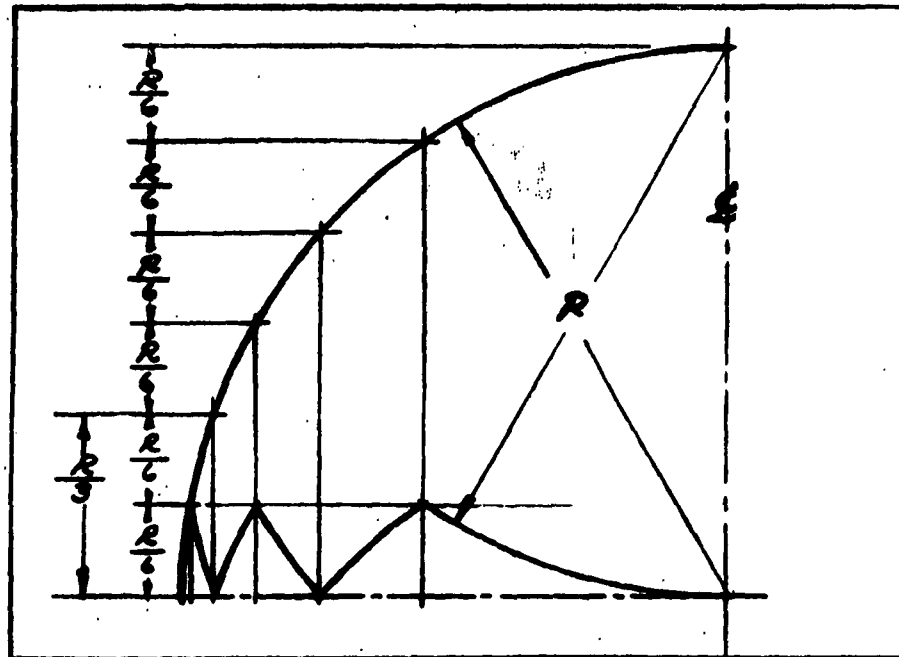
Figure 7.   Constant Depth Convolutions
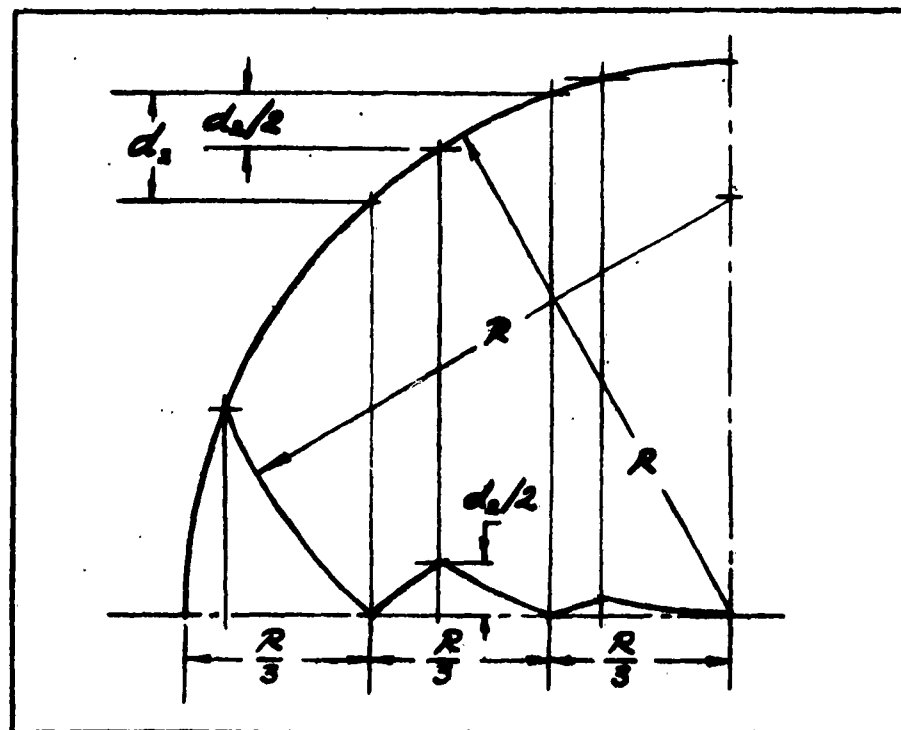
Figure 8.   Constant Pitch Convolutions
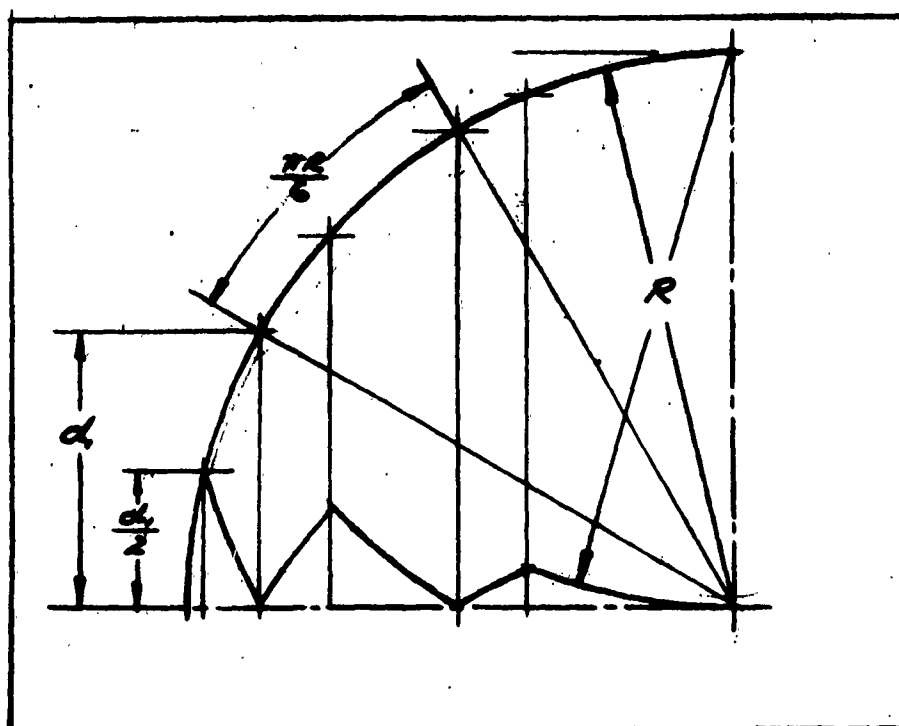
Figure 9.   Constant Developed Length Convolutions
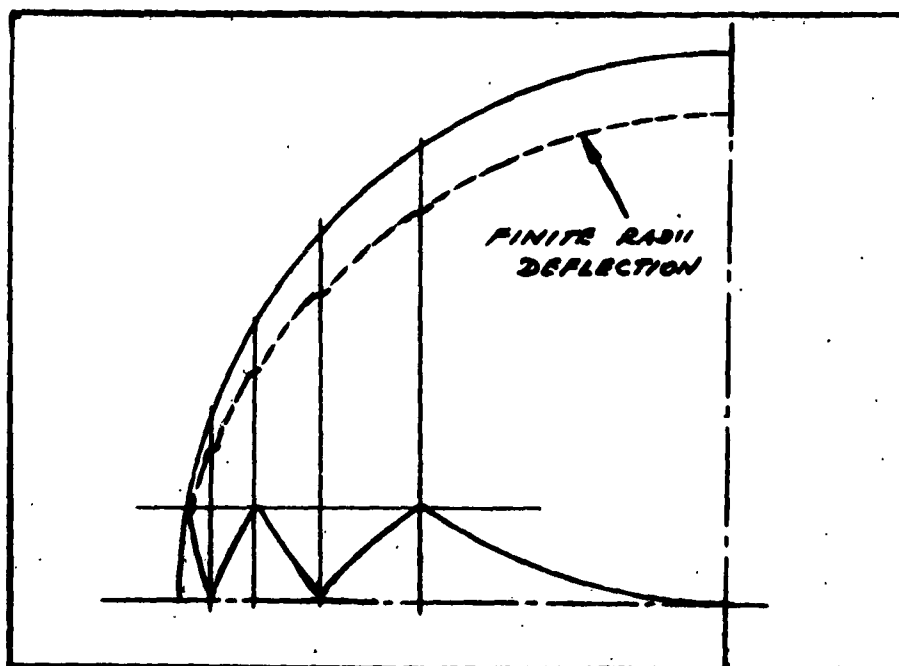
Figure 10.   Stress-Free Deflection of Diaphragm With
Finite Radii at Crowns

Practical Design Considerations

All the ideal diaphragm configuration designs devised
on the concept of a pure membrane will experience no strains and
thus will require very low Δp (pressure differential) when
deflected to the desired spherical form. However, these ideal
configurations have cusps at the crests of the waves which are
difficult to fabricate with finite thickness material. In addi-
tion sharp folds are to be avoided because they will introduce
relatively large local plastic strains when fabricated and also
when the diaphragm is extended to the inside contour of the
container. Employing a convolution with finite radii at the
crests of the waves will circumvent this difficulty. However,
with the presence of finite radii at the crests of the waves,
it is not possible to attain a strain-free condition as the
diaphragm is deflected from the original to the final spherical
position. This is due, in part, to the original horizontal slope
at the crests of the convolutions or corrugations which cannot
conform to the spherical shell form without introducing circum-
ferential strains.

To illustrate the effect of finite curvatures at the
crests of the waves, the diaphragm of Figure 7 was redrawn with
small radii at the crests of the waves and the result presented
in Figure 10. Also shown by the dashed curve in Figure 10 is
the membrane stress-free deflection condition of the diaphragm
considered as a pure membrane. It will be noticed that as a
consequence of the finite radii at the crowns of the waves the
deflected membrane stress-free shape is not smooth but rather
contains points of zero slope corresponding to the crests of the
waves. In addition, the deflected shape is not in the desired
spherical form because of the reduction in developed length of
the corrugations when the radii at the crowns were introduced.
Consequently, for this corrugated membrane configuration and for
all other configurations which are in variance with the ideal
configuration, meridional and circumferential strains will be
introduced if the final internal container shell form is to be
attained. The space between the shell and the deflected form
can obviously be reduced by increasing the developed length of
the convolutions. When altering the ideal diaphragms by incor-
porating finite curvature at the crowns of the convolutions,
the radii should be kept as small as practicable so as to mini-
mize the membrane strains.

Dynamic Effects

Diaphragms Perpendicular to Vehicle Acceleration

After some fuel has been expelled, it is possible for
the diaphragms to twist out of their planes so that lateral slosh

type mode can be excited. The natural frequency of the mode will depend on diaphragm stiffness as well as tank steady acceleration. Pressurization will not be significant to the mode. Fuel in upper and lower compartments will be moving in the same direction at the same time except for a phase shift due to the fact that the upper and lower tanks will not have the same natural frequency except at zero g. The upper and lower diaphragms will then have corresponding points always moving toward and away from each other approximately simultaneously. The two diaphragms could pound together when the tanks are almost full. The diaphragm stiffness will allow the mode to exist at zero g.

The difference in the upper and lower frequency is due to the fact that tank acceleration will add to the total elastic restraining stiffness for the bottom tank and subtract from it in the case of the upper volume.

Diaphragms Parallel to Vehicle Acceleration

If the tank is oriented so that the tank acceleration lies in a plane parallel to the planes of the diaphragms then the mode described in I.b will again be possible except that tank acceleration will not have any effect on the natural frequency of the mode, the modal stiffness coming entirely from the diaphragm.

Steady acceleration will make the pressure against the bottom of the diaphragm larger than that at the top of the diaphragm thus causing the center parts of the diaphragm to deflect unevenly out of its normal plane. This probably would not cause any difficulty.

REVERSING DIAPHRAGM

The reversing diaphragm shown schematically in Figure 11 has the following characteristics:

Characteristics of Reversing Diaphragms

Advantages

1. Complete dispensing of material in the container is possible.

2. The metal cup folded within itself is readily fabricated on the principles of reverse drawing and the metallurgical properties of alloys which permit the manufacture of long cans of small diameter.
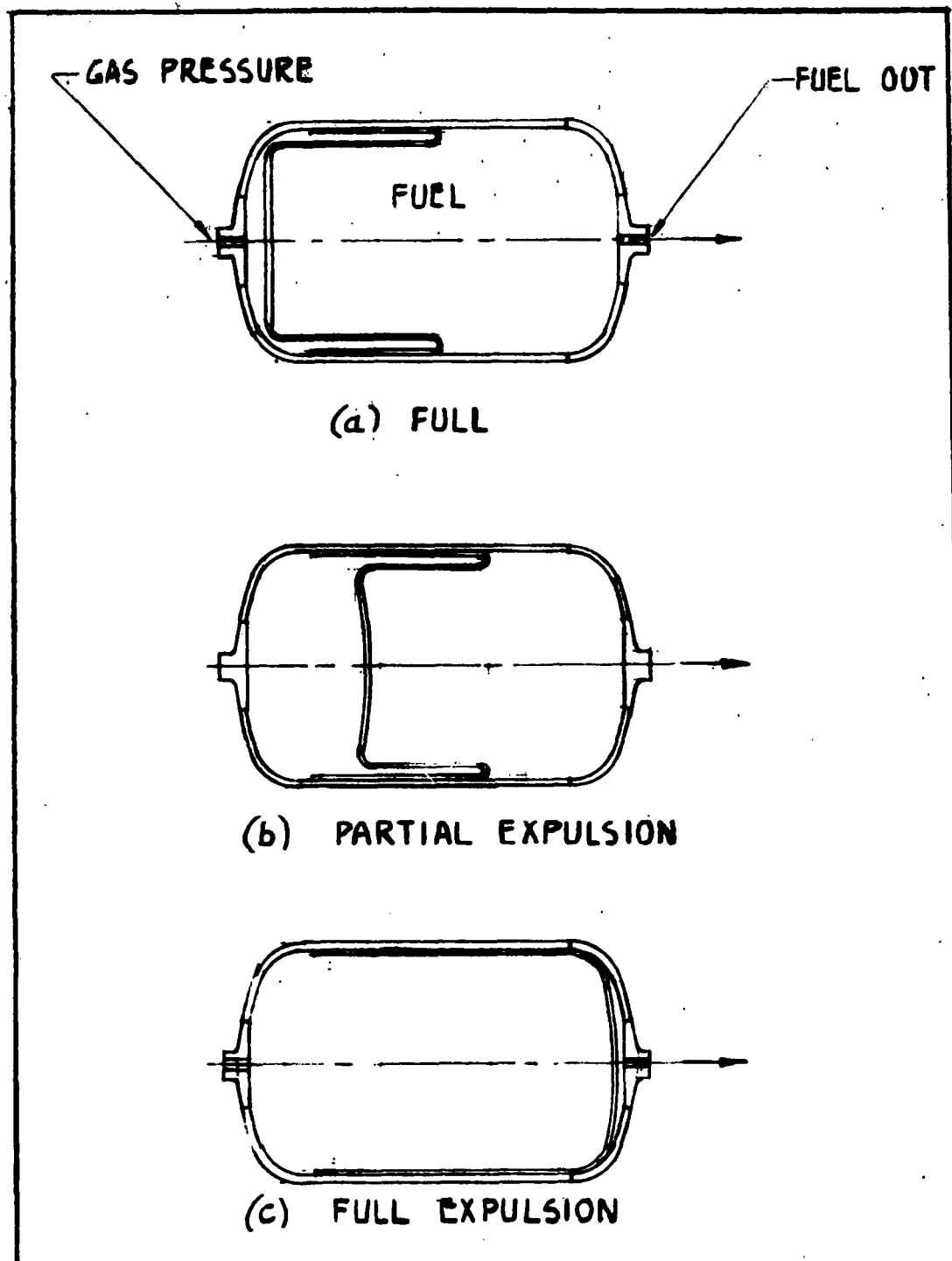
Figure 11.   Reversing Diaphragm

3.   The reversing diaphragm principle has been proven in ejectors, separation bolts and actuators.

Disadvantages

1.   Process is not readily reversible and only one cycle of operation is reliable.

2.   The principle has been employed as a fast action device.   Extremely slow operation may induce local buckling rather than the desired rolling.

3.   The possibility exists of buckling of the shell that could restrict further motion.   Buckling would induce increased stiffness and an increase in gas pressure to provide additional expulsion.

DUAL REVERSING DIAPHRAGMS

An extension of the reversing diaphragm to a dual reversing diaphragm is shown in Figure 12.   Some advantages and disadvantages of such a device are listed below.   These characteristics are in addition to those listed for the single reversing configuration.

Characteristics of Dual Reversing Diaphragms

Advantages

1.   Required volumes of each bi-propellant can be readily established.

Disadvantages

1.   Control of mass ratio flow could be difficult because buckling and rolling of the diaphragms may not produce the required proportional collapse between the diaphragms.

BICONVEX DIAPHRAGM

The biconvex diaphragm configuration shown in Figure 13 is representative of the common and conventional fuel pumps employed in automotive power plants.   The Literature Survey L11 presents the design and construction of such a stainless steel diaphragm reactor service pump actually put into service by the Oak Ridge National Laboratory.

Although such devices have been employed as continuous operating pumps with flat diaphragms, the diaphragm oscillating
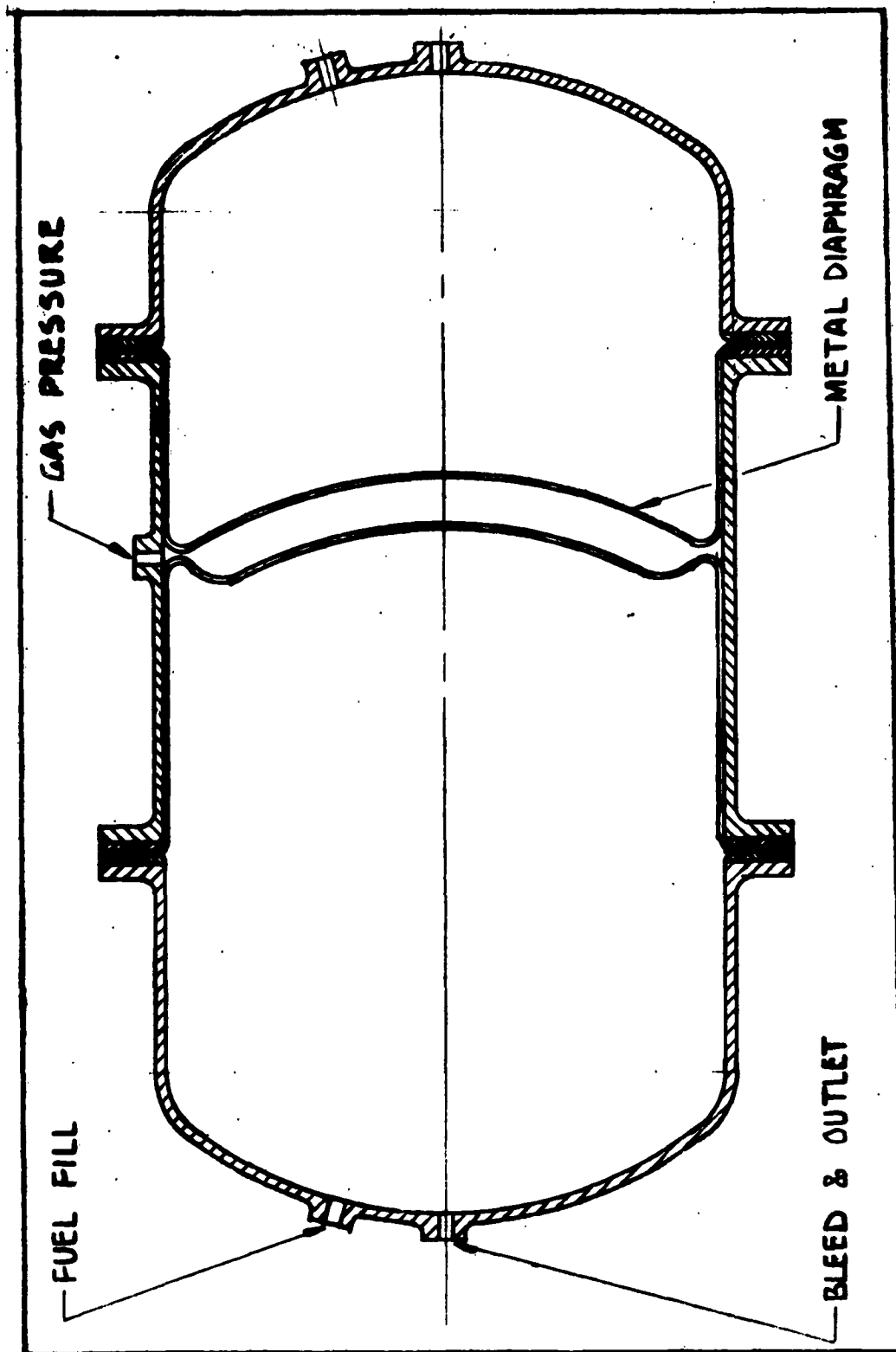
Figure 12.   Dual Reversing Diaphragm
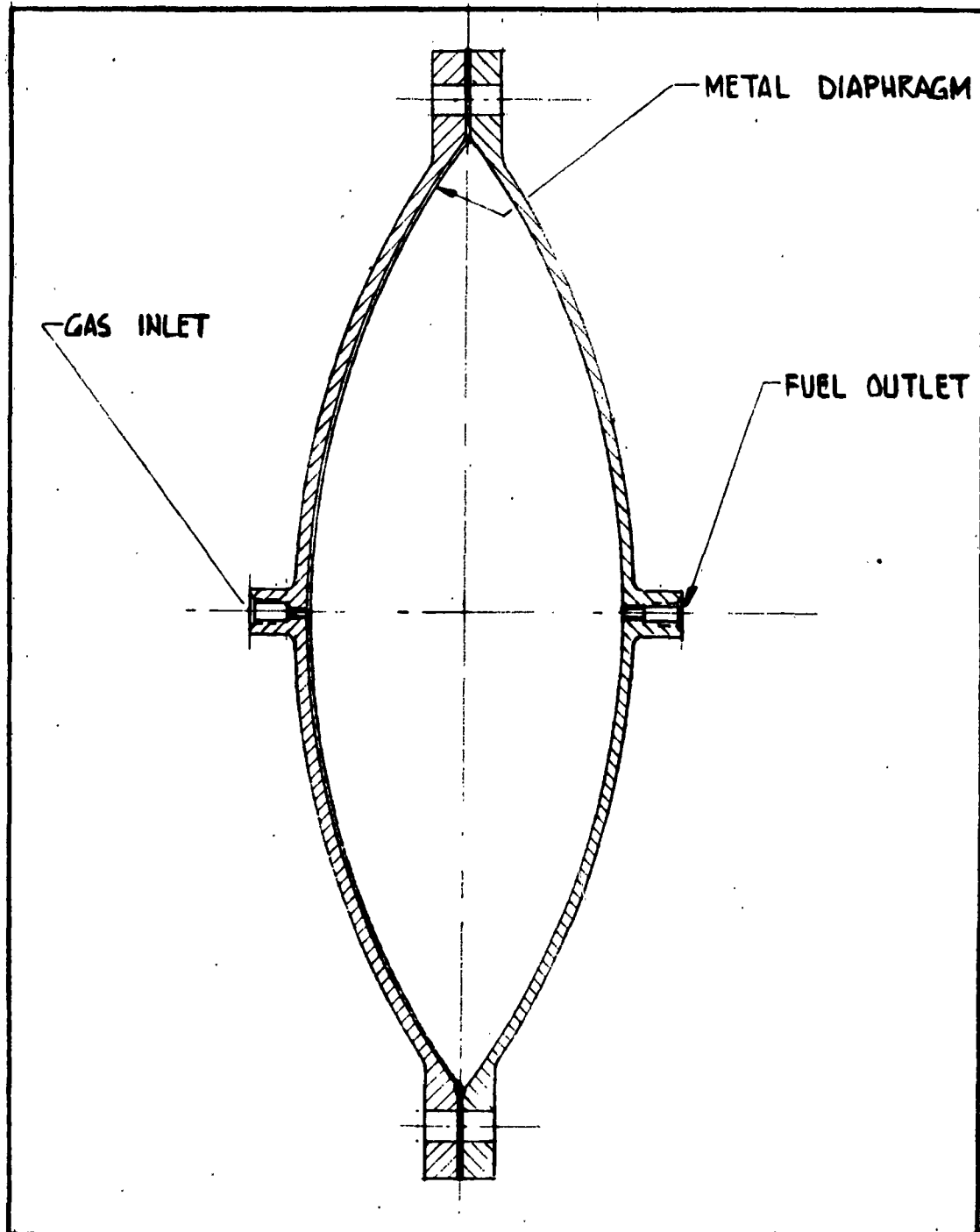
Figure 13.   Biconvex Diaphragm

between the two halves of the biconvex heads, the incorporation
of a spherical cap diaphragm converts the unit into a single
cycle expulsion device.

Characteristics of Biconvex Diaphragms

Advantages

1. Can be used for repeated cycles when depth of
diaphragm deformation to reverse position is small. (This is
principally employed in conventional diaphragm pumps.)

Disadvantages

1. The biconvex cross-section requires an equatorial
ring and local shell thickness increase to take care of dis-
continuity stresses.

2. Volume of device is relatively small.

CONTROLLED ROLLING DIAPHRAGM

A schematic of a controlled rolling diaphragm configuration
is shown in Figure 14. The one indicated has a full 180-degree
convolution. In this configuration, when the piston moves down,
the diaphragm rolls off the cylinder wall and onto the piston
side wall. Almost the entire pressure load is supported by the
piston head and only a small increment of pressure is felt by
the diaphragm. Contained pressure holds the rolling diaphragm
against the walls of the cylinder and piston.

In a controlled rolling diaphragm, as it operates, it is
subjected to a change in circumference. When it rolls from the
smaller or inner diameter to the larger or outer diameter, its
circumference must increase. Thus a diaphragm with numerous
convolutions that behaves like a toroidal inversion configura-
tion must be designed to give low elongations. Thin gage
materials and relatively large diameters tend to alleviate the
severity of such elongations and associated stresses due to
roll-over.

Characteristics of Controlled Rolling Diaphragm

Advantages

1. The piston provides controlled rolling of the
diaphragm.

2. Piston sealing is not required.

(b) PARTIAL EXPULSION

FUEL OUTLET

FUEL

(a) FULL
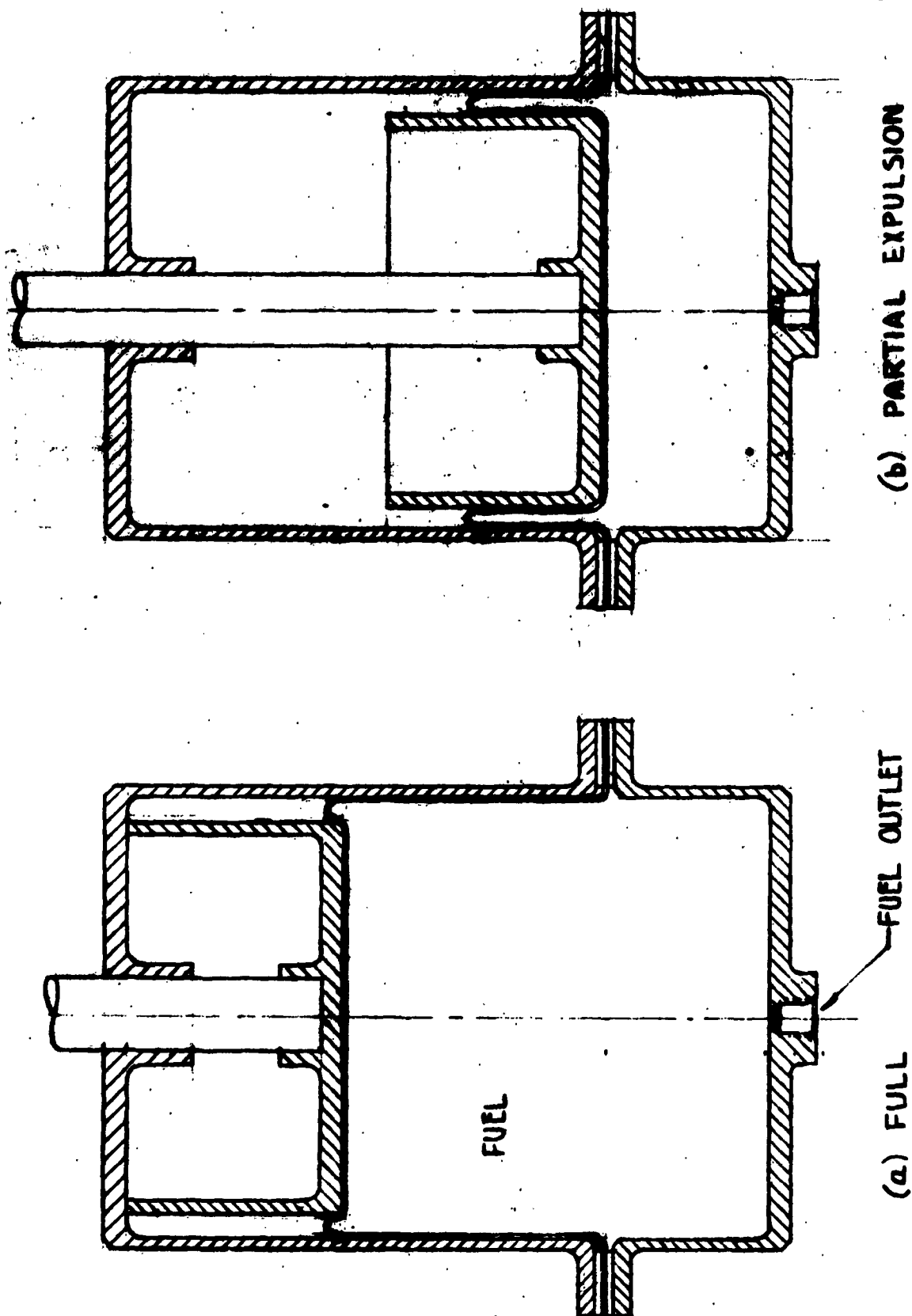
Figure 14.   Controlled Rolling Diaphragm

3.   Device may operate for more than one cycle. The limit would be the fatigue involved in the rolling of the diaphragm.

4.   A larger diameter of the cylinder reduces the circumferential stresses.

5.   Very little pressure load is felt by the diaphragm. Almost the entire pressure load is supported by the piston.

6.   Contained pressure holds the rolling diaphragm against the walls of the cylinder and piston.

7.   Close machine tolerances on pistons and cylinders are not required.

8.   The rolling diaphragm can tolerate minor accentricities and cocking of the piston rod and cylinder without affecting the operation of the unit.

9.   The rolling diaphragm is a free positioning device during normal operation.

10.   Vibratory problems are not a major consideration.

Disadvantages

1.   The long skirt on piston produces a "dead" volume.

2.   Piston rod increases over-all length of device.

3.   A homogeneous metallic material is not as advantageous as a pliable or plastic material.

4.   The use of a metallic diaphragm would require a larger force input to the piston.

Feasibility Tests

Rolling diaphragms are commercially available in pliable fabrics impregnated with an elastometric sealant of synthetic rubber. This type of material, however, is somewhat limited for space vehicle applications. The use of a metal for the diaphragm, however, would have numerous advantages, provided the metal can be made to behave like an elastomer or other pliable material.

A small feasibility test program was initiated to study the behavior of a metal under a rolling action similar to that

experienced in a rolling diaphragm. The 1100-0 aluminum material was chosen for these tests. This material is also ideally suited for an end-item because of its many favorable characteristics such as propellant compatibility, radiation, ductility, etc.

A simple parallel wood face slide was constructed with one end of the 1100-0 material attached to the base of the jig and the other end attached to the slide. The aluminum strip was 1 inch wide and .031 inch thick. The U-bend in the strip, shown in Figure 15 together with the simple wooden jig, was made to roll on itself, that is bend and unbend when a force was applied in the direction of the arrow. The total depth of the U-bend for this test was restricted to 0.25 inch, which is the distance between the parallel slide faces.

At the completion of this simple demonstration, circular cylindrical containers were fabricated to ascertain, by test, the behavior of the rolling action along the circumference and height of the cylinder. The container was spun from 1100-0 aluminum to the shape shown at the left in Figure 16. The availability of the spinning form dictated the use of the head enclosure on the cylinder. This head does not influence the results of the rolling action, once a steady rolling is achieved. The center two cylinders in Figure 16 show the inversion of the shell that was accomplished by means of applying a load to a circular bar, which is equivalent to a piston, to the head of the aluminum shell. The cylinder was not restrained when the load for inversion was applied.

The view at the left in Figure 16 represents a cut cross-section of a metallic rolling diaphragm after the rolling process. This simple test demonstrated the feasibility of the application of metal to a rolling diaphragm.

Analysis Data

In the incorporation of a metallic rolling diaphragm as an expulsion device, it is necessary to establish the forces and stresses on the piston and on the diaphragm during the rolling process to insure its operational success. The rolling diaphragm concept is a deep convolution with a long stroke and is free positioning along its stroke.

The operation of the homogeneous metallic rolling diaphragm is dependent on the ability of the metal to decrease circumferentially without excessively elongating the material fibers as the diaphragm rolls off the cylinder walls and piston. Premature failure will result if the circumferential elongation cannot be provided by the material.
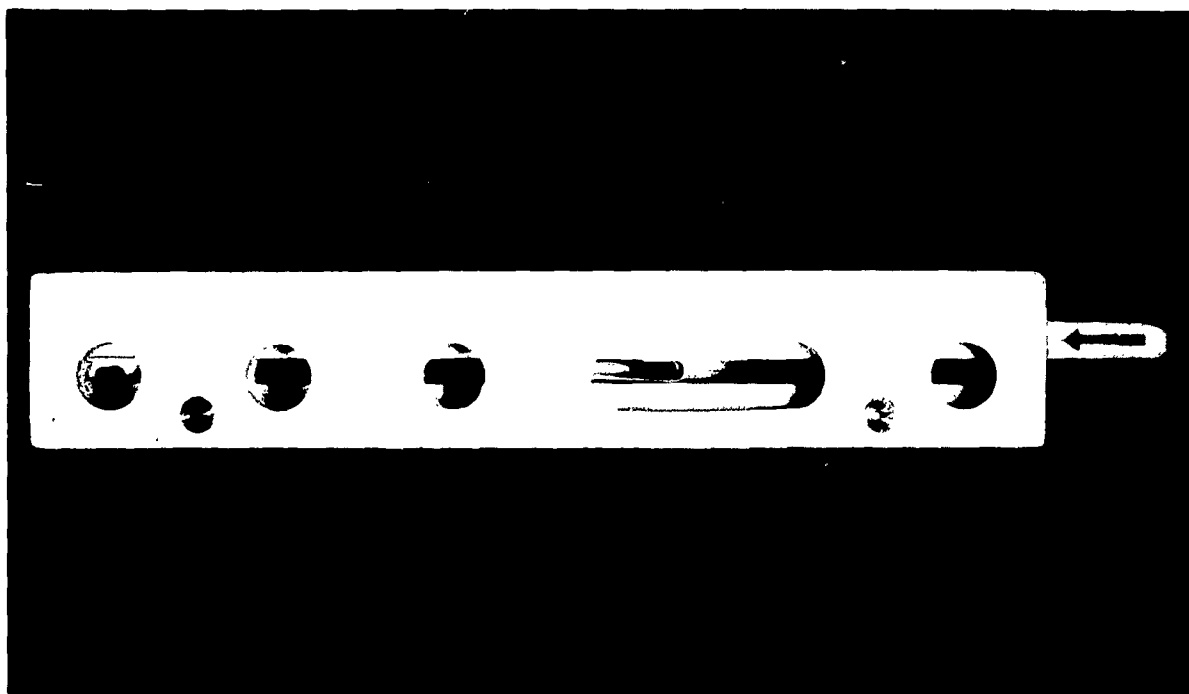
Figure 15.   Sheet Roll-and-Unroll Bending Jig

Figure 16.   Metallic Rolling Diaphragm Deformation

The work on the following pages presents preliminary studies to determine the force required to move a rolling diaphragm and the associated stresses encountered during the operation, also, some preliminary test results are shown and compared with the calculations. In the derivation of the required equations, the following assumptions were employed:

    1. The piston and cylinder are concentric throughout the stroke.

    2. The diaphragm comes into contact with the piston walls during the operation.

    3. The buckling stability of the diaphragm shell (against cylinder wall) has not been considered.

    4. The neutral axis is also the centerline of the sheet material and is a constant.

    5. Strain energy due to axial forces is neglected.

    6. Strain energy of bending and unbending during the rolling process are assumed to be equal.

    7. During rolling the material is assumed to bend through a full angle of 180 degrees.

The basic approach used herein to obtain the piston force required to roll the diaphragm into a deep convolution is based on equating the work done by the external forces to the internal (strain) energy of the system. The energies considered are the strain energy of bending as the diaphragm rolls on the piston wall and the strain energy of hoop compression which results from the shortening of the circumference.

The two methods of analysis are presented on the following pages. The essential differences between these two methods lies wholly with the shape of the stress-strain curve chosen. The first case estimates the strain energy of bending and hoop compression assuming the stress-strain curve to have ideal plastic behavior. The second method is based on the use of the nominal stress-strain curve of the material. The former approach is considered to yield more conservative results.

Analysis Based on Ideal Plastic Material

    The bending moment per unit width for a wide beam can be represented by (See Reference 89, page 269)

$$M = \frac{2}{\sqrt{3}} \, \sigma_o \, \frac{t^2}{4} = 0.29 \, \sigma_o \, t^2 \tag{1}$$

The strain energy of bending with a constant bending moment is equal to the product of the moment and the total bend angle ϕ, radians. However, since the beam is straight as it rolls on the piston, the total strain energy of bending is twice this value. Therefore, for a full bend angle of 180 degrees the energy is:

$$U_b = 2\pi M \tag{2}$$

so that with the aid of Equation (1), for unit length,

$$U_b = 1.82 \, \sigma_o t \tag{3}$$

With the established relationship, (on the basis of the neutral axis location at the center of the sheet thickness),

$$\frac{r}{t} = \frac{1}{2}\left(\frac{1}{\epsilon_1} - 1\right) \tag{4}$$

and with

$$\epsilon_1 = \epsilon_2 = \frac{1}{2\left(\frac{r}{t}\right) + 1} \tag{5}$$

and, from the notation indicated on Figure 17

$$\mathcal{P}_a = \mathcal{P} + \frac{t}{2} \tag{6}$$

or

$$\mathcal{P}_N = \frac{t}{2\epsilon_1} \tag{7}$$

For a 180° bend in the sheet, the affected straight length of beam is, employing Equation (7)

$$L_o = \pi\left(\frac{t}{2\epsilon_1}\right) \tag{8}$$

However, noting that in the expression for U_b as represented by Equation (3), bending and unbending takes place, the effective straight length is $2L_o$ or $\pi t/\epsilon_1$. In computing the strain energy of hoop compression this same length will be employed.

The radial displacement is illustrated in Figure 18 and is represented by

$$\Delta = 2(r + t) \tag{9}$$
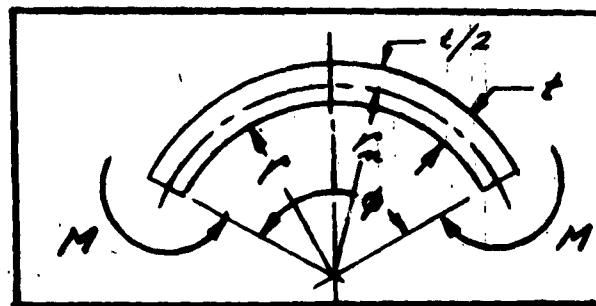
Figure 17. Wide Plate in Bending
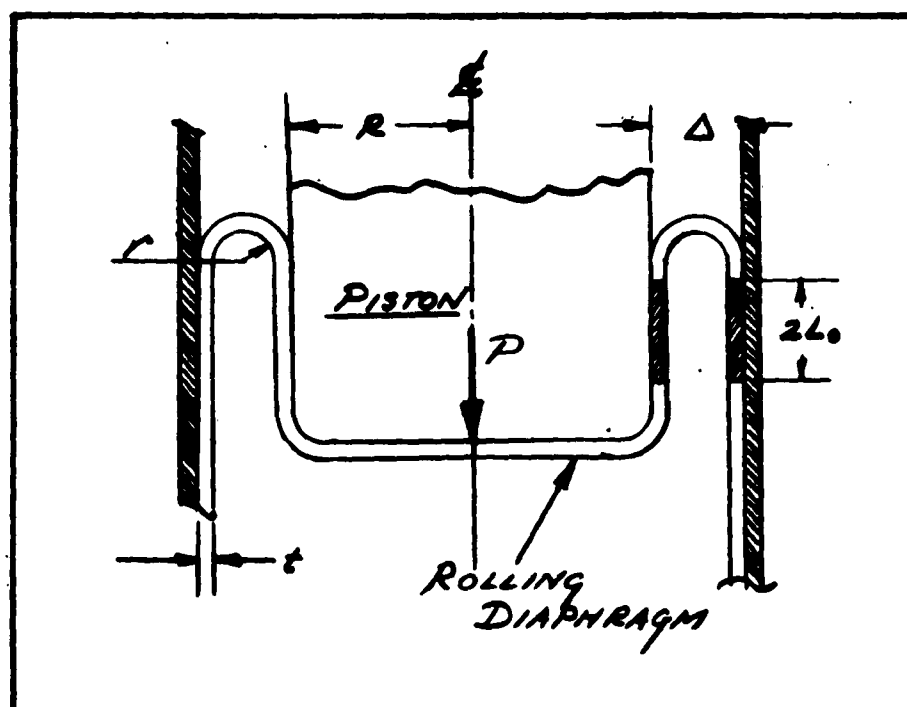
Figure 18. Schematic and Notation of a Controlled
Rolling Diaphragm

and hoop strain is

$$\epsilon_h = \frac{2 \, r+t}{R + 2(r+t)} = \frac{2}{2 + \left[\frac{\left(\frac{R}{r}\right)\left(\frac{r}{t}\right)}{\left(\frac{r}{t}\right)+1}\right]} \tag{10}$$

The unit strain energy of hoop compression is $\sigma_o \epsilon_h$, and for the element of length $2L_o$ the strain energy becomes:

$$U_h = (\sigma_o \epsilon_h)(2 \, L_o t) \tag{11}$$

Employing Equation (8) for L_o ,

$$U_h = 2t \, \sigma_o \left(\frac{\pi t}{2\epsilon_1}\right)\epsilon_h \tag{12}$$

$$U_h = \frac{\pi t^2}{\epsilon_1} \, \sigma_o \, \epsilon_1 \quad (\textit{IN.LB./IN.}) \tag{13}$$

The piston vertical movement is also $2L_o$ and the external work done, assuming motion is imparted by a uniform pressure, p, is

$$W_{piston} = \pi \rho \, R^2 (2L_o) \tag{14}$$

Equating the external work to total strain energy, Equations (3), (13) and (14)

$$\pi \rho \, R^2 (2L_o) = 2\pi R (U_b + U_h) \tag{15}$$

and substituting Equations (3), (5), (8) and (13) one obtains the general expression:

$$\frac{\rho R}{\sigma_o t} = 1.16 \left\{\frac{1}{2 + \left(\frac{r}{t}\right)+1}\right\} 2\epsilon_h \tag{16}$$

It is to be noted that this expression is independent of material. A more generalized expression can be obtained if one employs the relationship for ϵ_h given by Equation (10).

Thus,

$$\frac{pR}{\sigma_0 t} = \frac{1.16}{2\left(\frac{r}{t}\right)+1} + \frac{4}{2+\left[\frac{\left(\frac{R}{r}\right)\left(\frac{r}{t}\right)}{\left(\frac{r}{t}\right)+1}\right]} \tag{17}$$

Now the stress ratio $(pR/t)/\sigma_0$ is merely a function of the geometry of the rolling diaphragm, R/r and r/t .

Utilizing a value of $\sigma_0 \approx$ 13,000 psi for 1100-0 aluminum (typical ultimate strength value for this material), Equation (17) becomes

$$\frac{pR}{t} = \frac{15100}{2\left(\frac{r}{t}\right)+1} + \frac{52000}{2+\left[\frac{\left(\frac{R}{r}\right)\left(\frac{r}{t}\right)}{\left(\frac{r}{t}\right)+1}\right]} \tag{18}$$

This Equation (18) is represented graphically in Figure 19.

Analysis Based on Nominal Stress-Strain Curve

For pure bending of a bar with a rectangular cross section of unit width, the bending moment can be expressed as: (see Reference 107, page

$$M = \frac{t^2}{(\epsilon_1 + \epsilon_2)^2} \int_{-\epsilon_1}^{\epsilon_2} f(\sigma, \epsilon)\,\epsilon\,d\epsilon \tag{19}$$

and with the use of Equation (5) the moment expression becomes:

$$M = \frac{t^2}{\left[\frac{2}{2\left(\frac{r}{t}\right)+1}\right]^2} \int_{-\epsilon_1}^{\epsilon_2} f(\sigma, \epsilon)\,\epsilon\,d\epsilon \tag{20}$$

Equation (3) is now modified to include Equation (20) so that
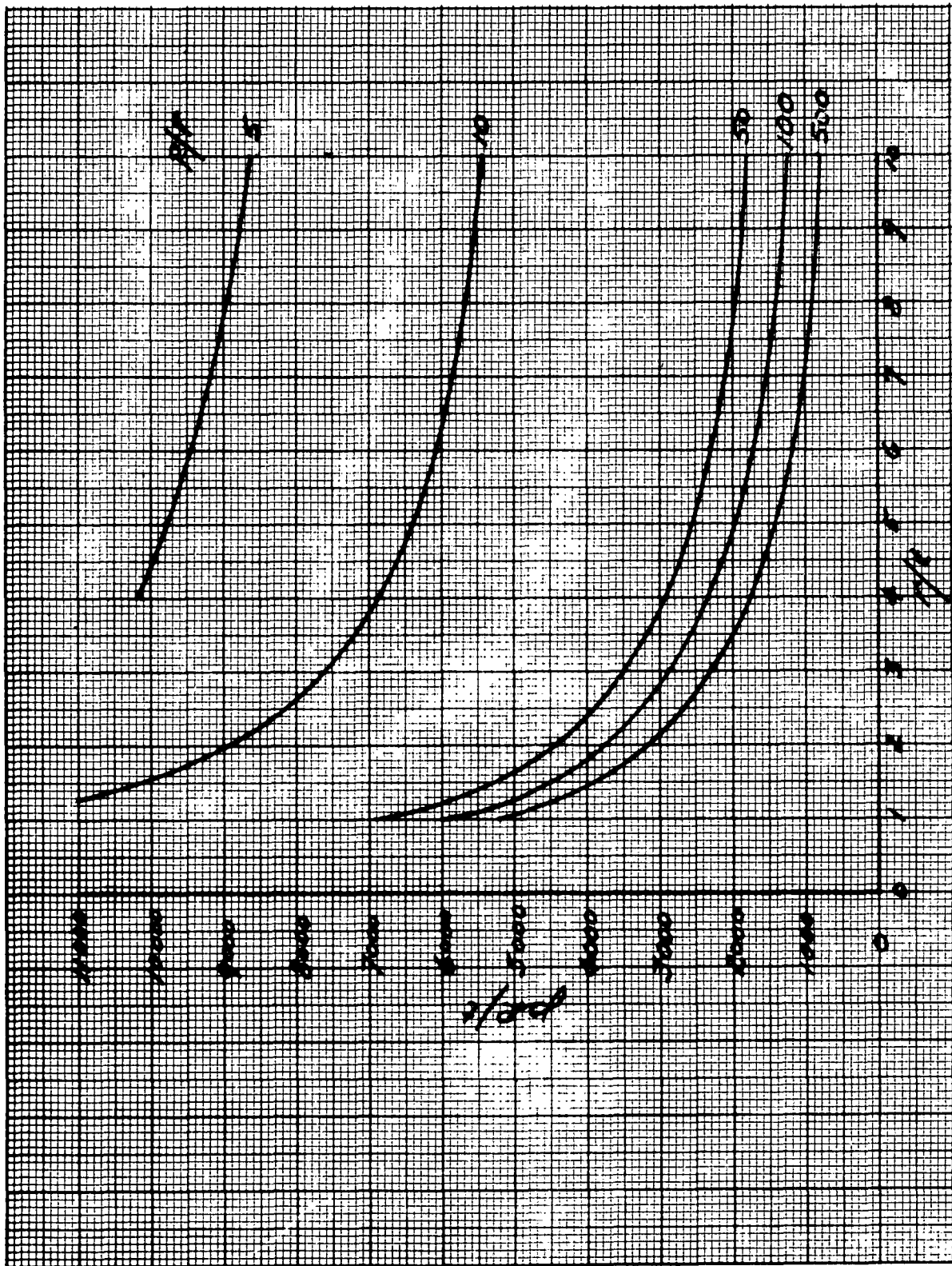
Figure 19. Pressure on Piston During Rolling of Diaphragm
Based on Ideal Plastic Material

$$U_b = \frac{\pi t^2}{2} \left[2\left(\frac{r}{t}\right) + 1 \right]^2 \int f(\sigma, \epsilon) \, \epsilon \, d\epsilon \tag{21}$$

The strain energy of hoop compression is similar to that previously derived for the ideal plastic case, Equation (13), with the exception that actual (nominal) stress-strain function is used,

$$U_h = 2 L_o t \int_0^{} f(\sigma, \epsilon) \, d\epsilon \tag{22}$$

Incorporating the values of Equation (8) and Equation (20) the strain energy of hoop compression becomes

$$U_h = \pi t^2 \left[2\left(\frac{r}{t}\right) + 1 \right] \int f(\sigma, \epsilon) \, d\epsilon \tag{23}$$

Equating the work done by the piston to the strain energy quantities just derived one obtains, with the use of Equations (14)

$$\pi_\rho R^2 (2 L_o) = 2 \pi R (U_b + U_h) \tag{24}$$

With the aid of Equations (5), (8), (21) and (23) and some algebraic manipulations,

$$\frac{\rho R}{t} = \left[2\frac{r}{t} + 1 \right] \int f(\sigma, \epsilon) \, \epsilon \, d\epsilon + 2 \int f(\sigma, \epsilon) \, d\epsilon \tag{25}$$

The integral expressions in Equation (25) are evaluated grapho-analytically for 1100-0 aluminum material and the results are depicted in Figures 20 and 21. The material stress-strain that was employed in the evaluation of the integrand is depicted in Figure 22.
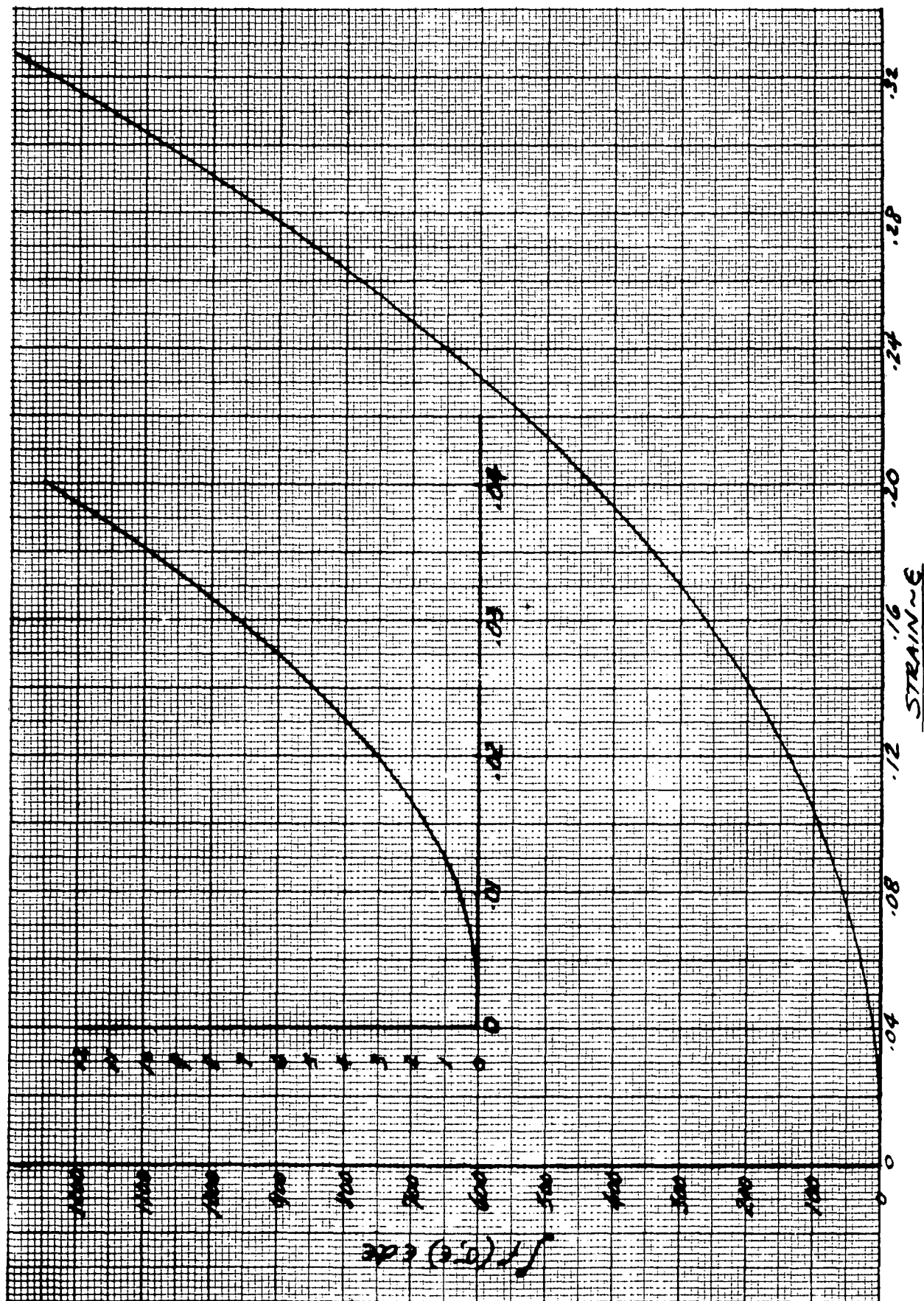
Figure 20. Evaluation of $\int f(\sigma, \epsilon) \epsilon \, d\epsilon$, (1100-O Aluminum)

Figure 21. Evaluation of $\int f\,(\sigma,\epsilon)\,d\epsilon$, (1100-0 Aluminum)
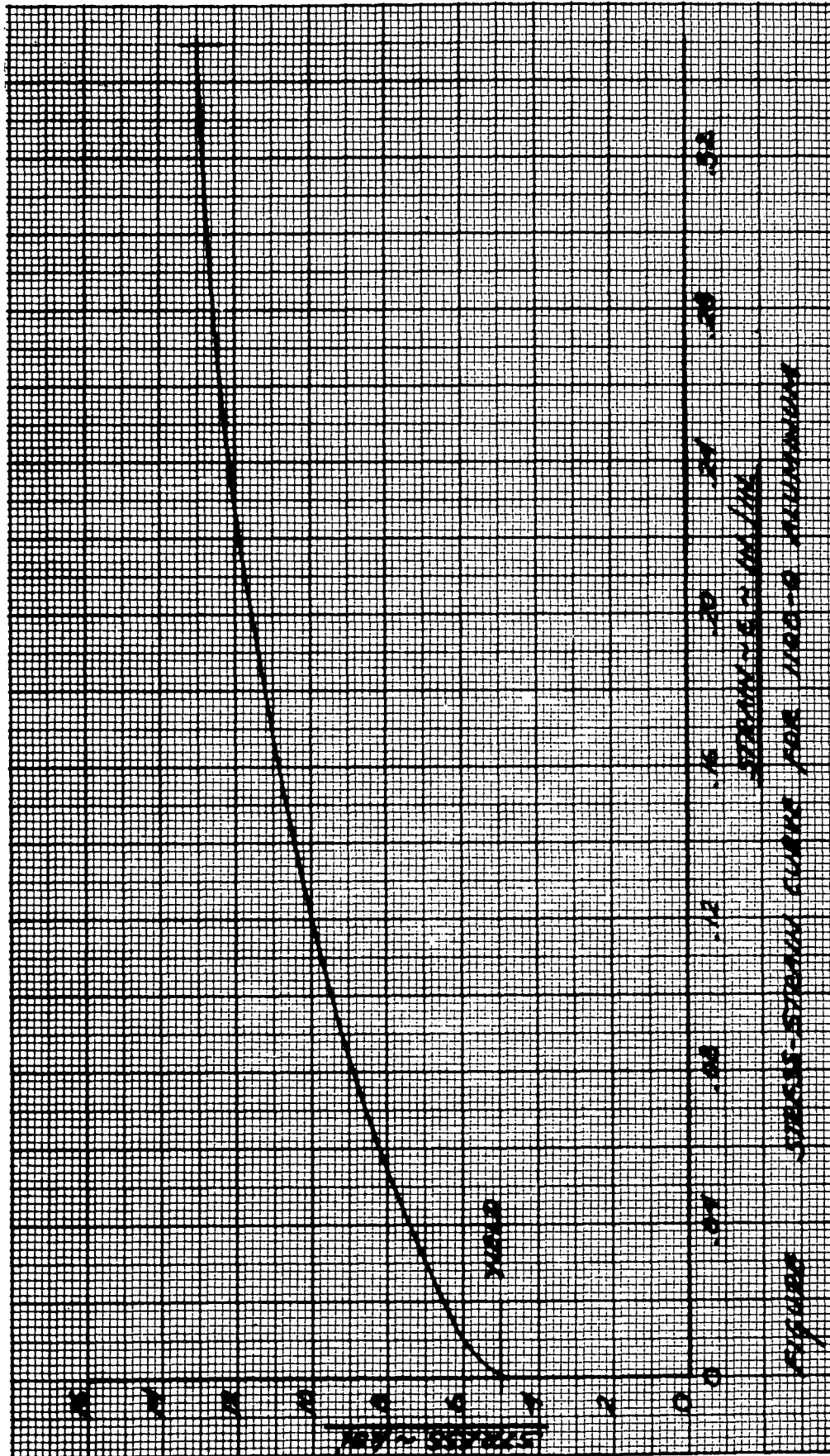
Figure 22.   Stress-Strain Curve for 1100-O Aluminum

The total solution of Equation (25) is depicted in Figure 23. This Figure 23 is analogous to Figure 19 and indicates the variation in $\mathscr{P}\mathcal{R}/t$ associated with the two approaches employed. Figure 19 yields higher values throughout the entire range of the geometric values of $\mathcal{R}/r$ and r/t .

Preliminary Test Results

Two specimens with dimensions as indicated in Table II were tested in a standard tensile test machine and the load P, (lbs) recorded.

In view of the limited tests performed it is not possible to arrive at a definite conclusion. Also the analytical approach presented herein represents a preliminary attempt, and as such, the curves are intended to be useful only in obtaining initial estimates for design. With respect to Test 2 it is worth noting that the piston diameter used was smaller than in Test 1. Consequently, the diaphragm rolled to a conical shape which is a function of depth of piston displacement forming a loose fit with the piston wall. This situation did not permit a full rolling bend of 180 degrees to take place so that one might conclude from this observation that the diaphragm can indeed roll without hoop collapse even though the piston diameter is insufficient to enforce the full bend radii assumed in the analysis. The additional problem area resulting from the above preliminary test indicates that a rolling radius stability problem is present. Although two different piston diameters were employed in the test, the final r/t of the rolling diaphragm was practically identical for both test specimens. It seems that a specific minimum value of r/t is attained that may vary only with material and the displacement of the piston.

TWO-SECTION CONTROLLED ROLLING DIAPHRAGM

The incorporation of a controlled rolling diaphragm for a bi-propellant system is shown in Figure 24. This is merely a modification of the controlled rolling diaphragm device indicated in Figure 11. The characteristics mentioned for the latter device are also applicable to this two-section unit. An inherent characteristic or disadvantage of the two-section device is the large "dead volume" that is present within the piston volume. This diminishes the fuel volume capacity for the larger size configurations, and makes it difficult to provide the required mass and/or volume ratios for the bi-propellants.
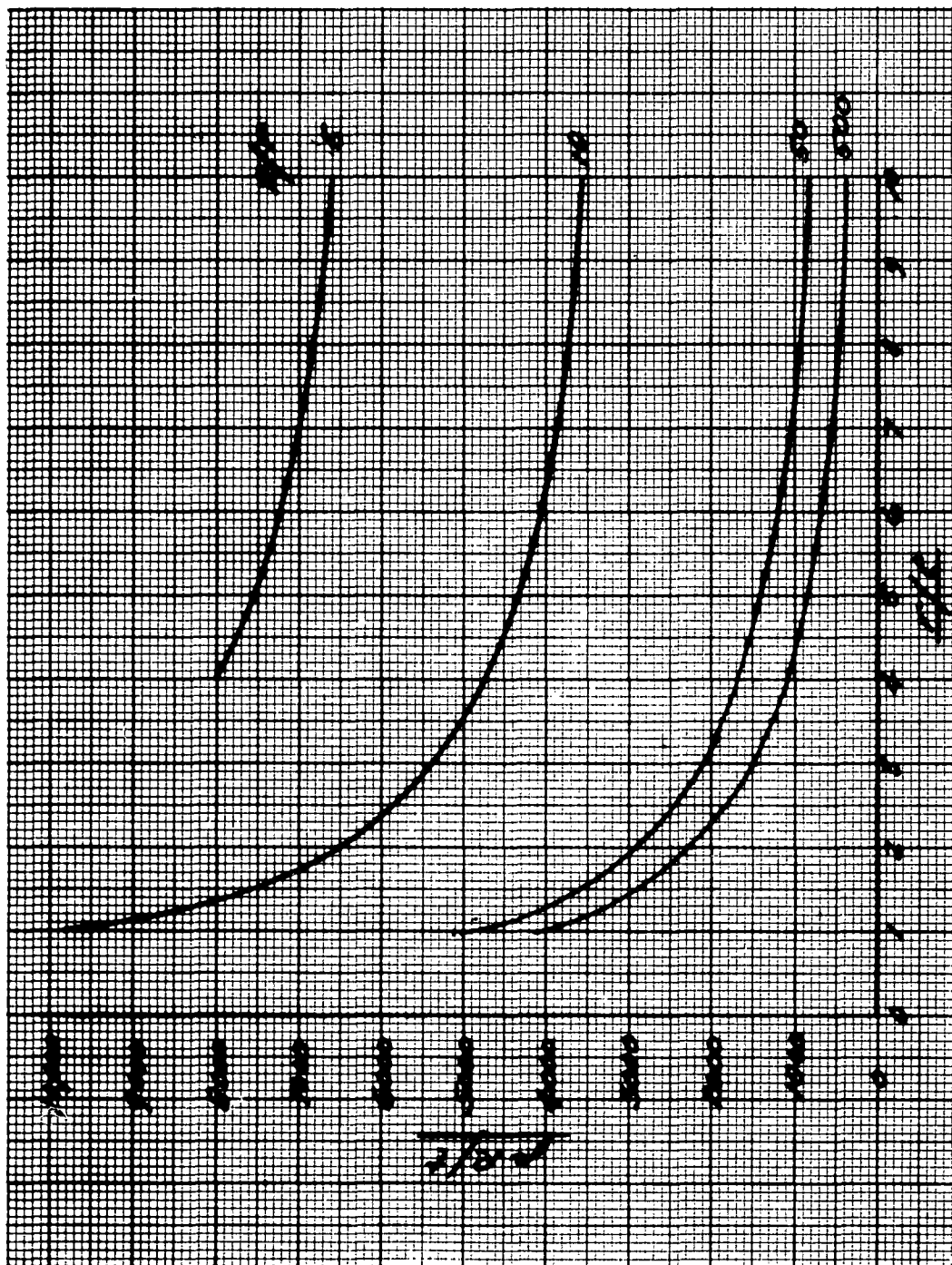
Figure 23.   Pressure on Piston During Rolling of Diaphragm Based on Nominal Stress-Strain Curve

FUEL OUTLET

OXIDIZER OUTLET

OXIDIZER

FUEL OUTLET

METAL DIAPHRAGM

FUEL

GAS
PRESSURE
INLET

R
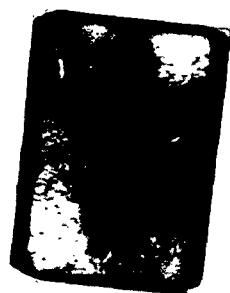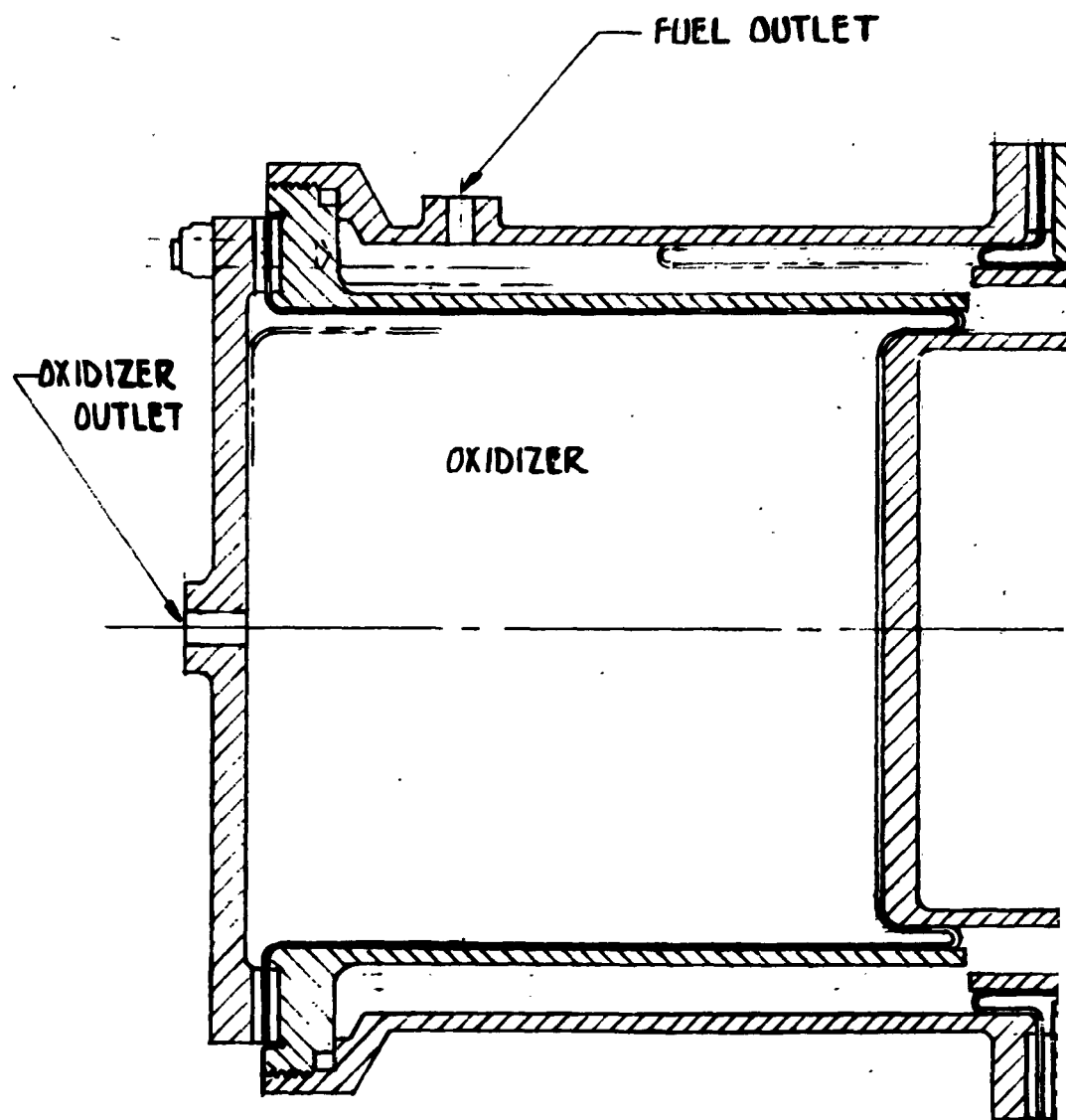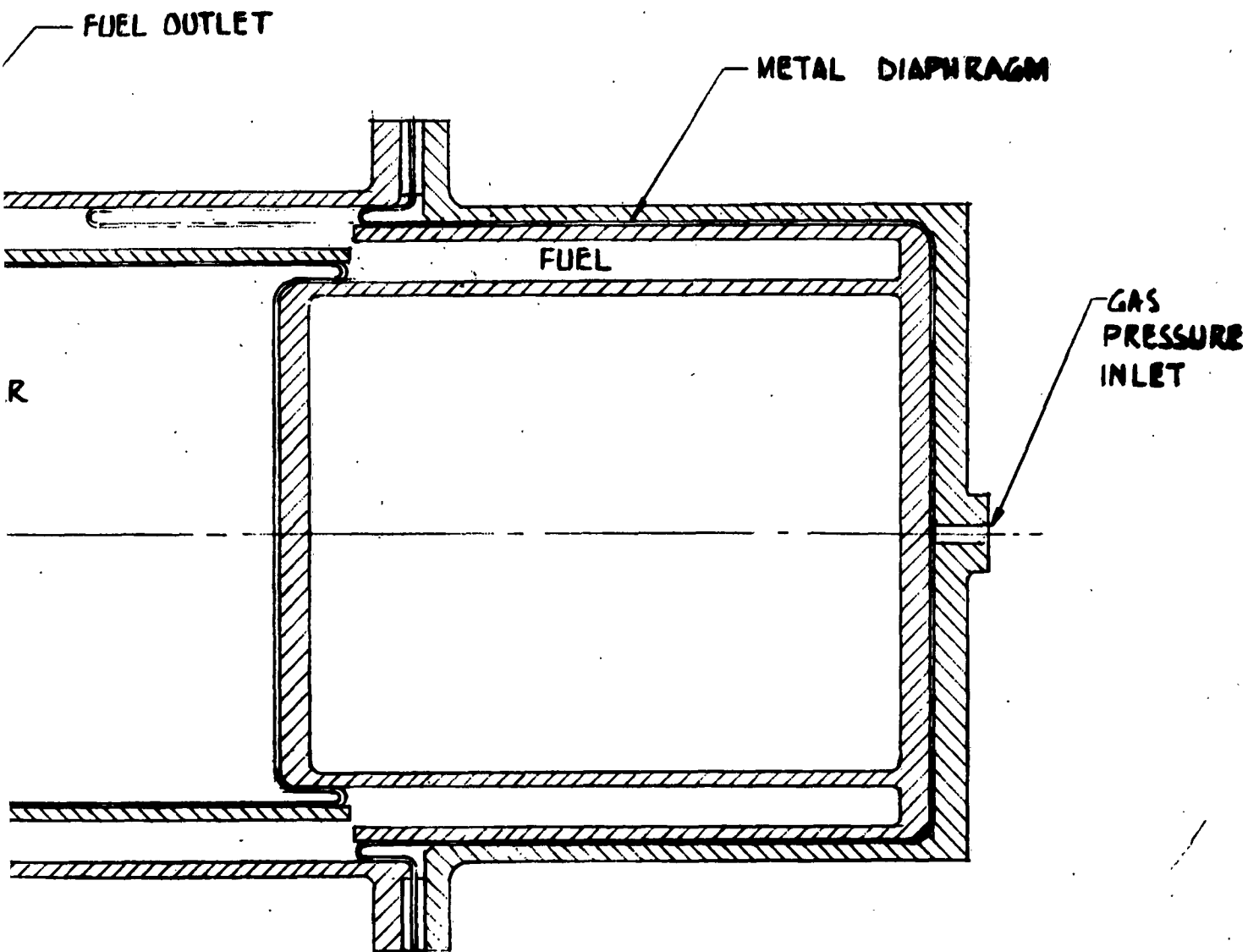
Figure 24. Two Section Controlled Rolling Diaphragm

TABLE II.   TEST DATA ON A ROLLING DIAPHRAGM

Geometry and Test Data

Spec.	R	D	r	t	$\frac{r}{t}$	$\frac{R}{r}$	P Test
1	1.188	2.376	.0302	.026	1.16	39.2	500
2	1.125	2.25	.025	.021	1.38	38.8	475

Theoretical Data

Spec.	Ideal Strain		Nominal Strain	
	$\frac{pR}{t}$	$P_{calc.}$	$\frac{pR}{t}$	$P_{calc.}$
1	6810	658	4880	474
2	6140	455	4400	326

MULTI-CELL DIAPHRAGM CONFIGURATION

The multi-cell diaphragm configuration illustrated in Figure 25 is similar to the biconvex diaphragm design of Figure 13. The advantages and disadvantages of the device are given below.

Characteristics of Multi-Cell Diaphragm Configuration

Advantages

1. The multiplicity of the cells insures the reliability of the unit.

2. The small motion or displacement of the diaphragm minimizes the bending and stretching of the bladder material.

Disadvantages

1. Excessive welding length is required thus requiring greater quality control to insure against leakage.

2. Diaphragms are not replaceable once the device is assembled by welding.

FUEL TO ENGINE

BLADDER WHEN
FUEL IS
EXPELLED

SEPARATOR
(PERFORATED)
3 REQD

— BLADDER WHEN
TANK IS FULL

— GAS PRESSURE IN
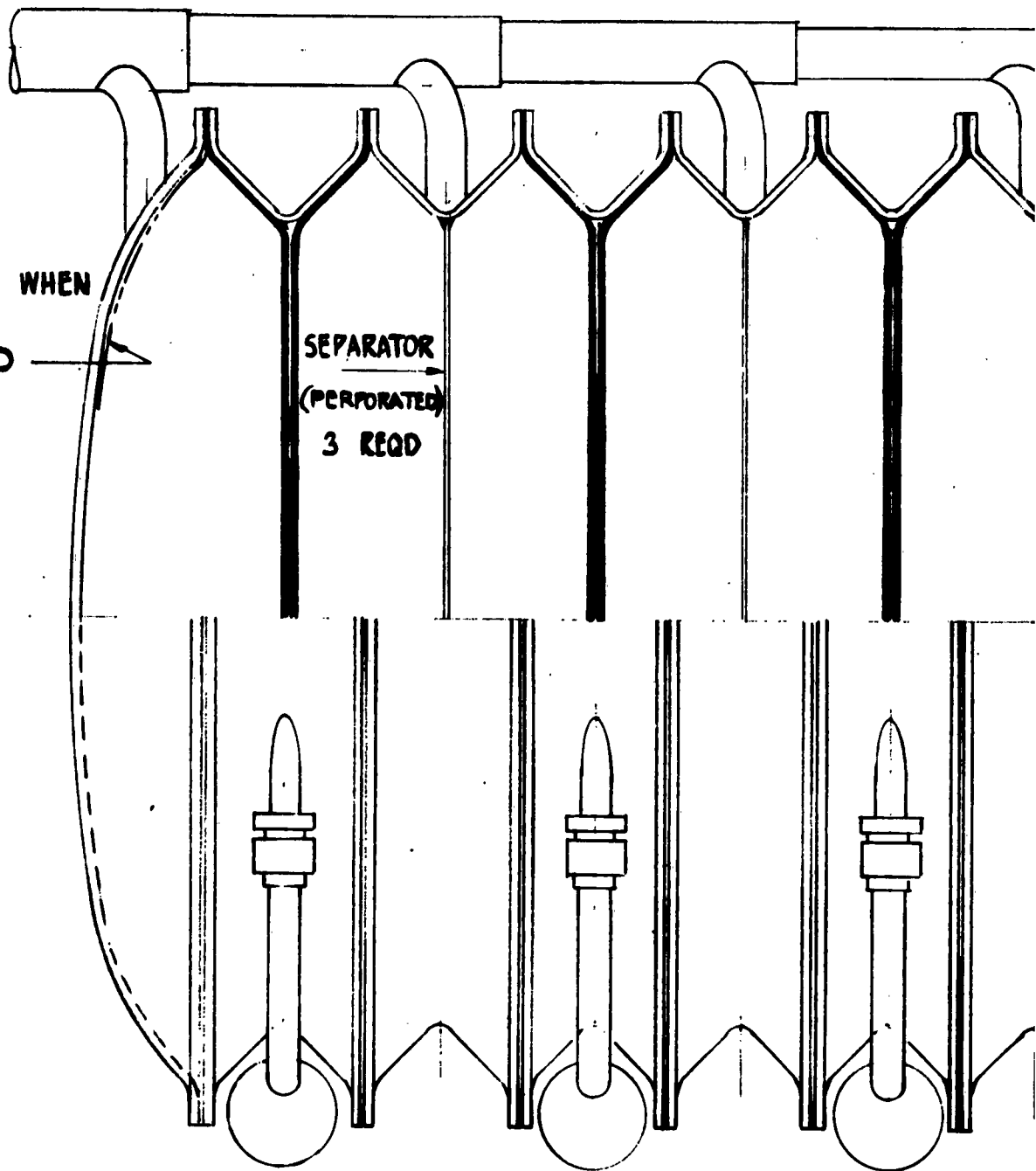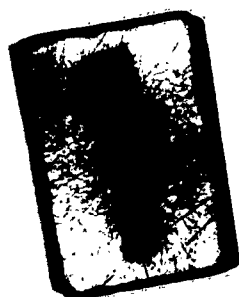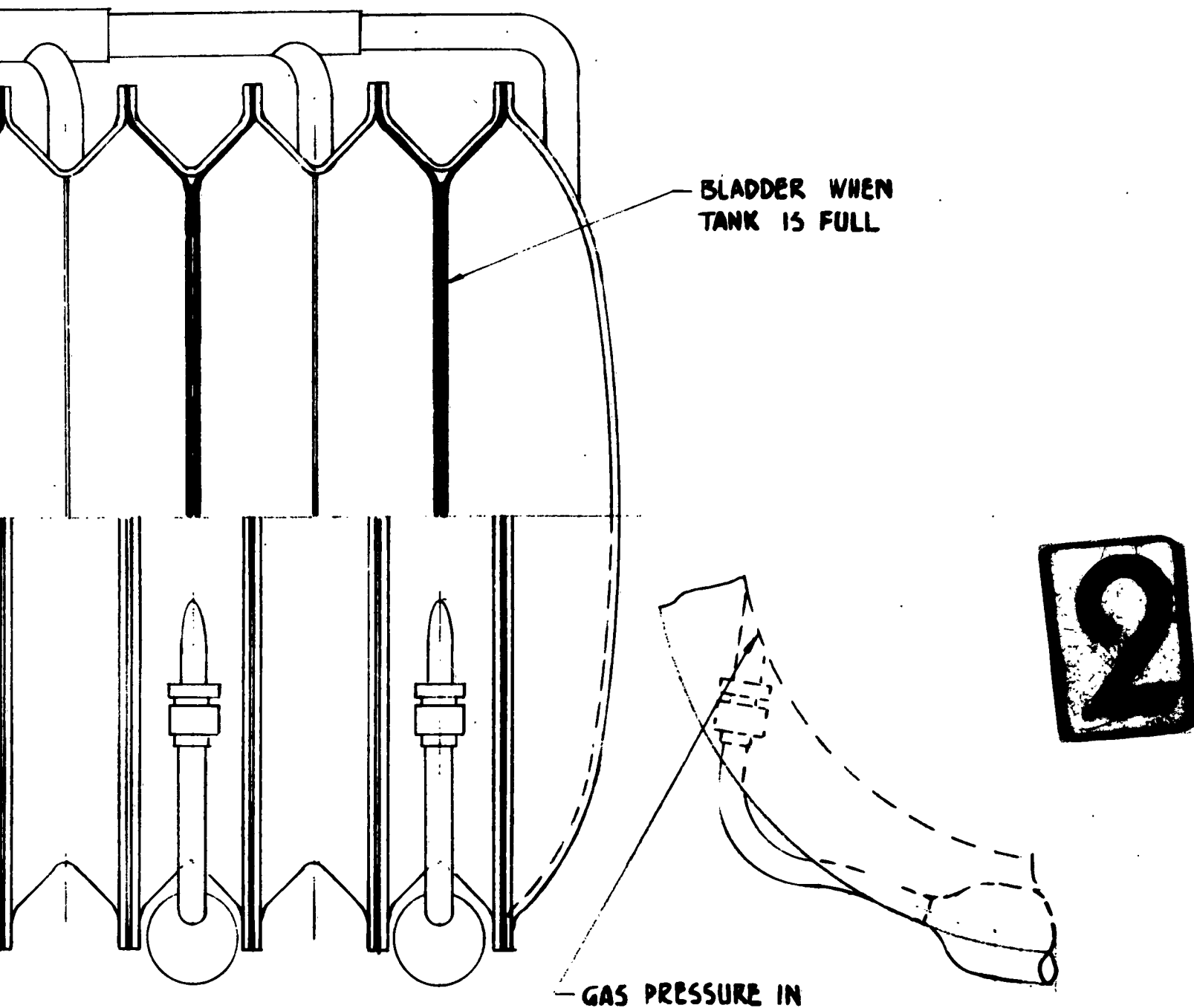
Figure 25.   Multi-Cell Diaphragm Configuration

BLADDER-TYPE CONFIGURATIONS

A bladder can be defined as a relatively thin flexible container or tank enclosed within a structural shell. Two types of bladders become apparent: a collapsing bladder and an expanding bladder, the designation referring to its geometric configuration during operation.

1. Expanding Bladder

An expanding or pre-folded bladder is mounted within a rigid container through an opening provided for its installation. The fluid to be expelled is contained outside the collapsed diaphragm. Positive expulsion is achieved by the introduction of a pressurizing gas into the collapsed bladder causing the bladder to expand and forcing the fluid outside the bladder to flow out by means of a withdrawal line system.

2. Collapsing Bladder

The collapsing bladder is generally made to fit the inside smooth contour of a rigid container or tank. In this configuration the pressurizing gas is applied external to the bladder causing the bladder to deflect and collapse and at the same time forcing the fluid within the bladder to flow out.

INTRODUCTION

A relatively simple approach for a positive expulsion device is the use of bladders. In this system, the operational characteristics of the device are dependent upon the initial bladder shape and the associated deformations, extensions, buckles, structural collapse, etc., due to a pressure source that produces the necessary collapse or extension of the device to expel the desired fluid. An illustration of a typical collapsing and expanding bladder is presented in Figure **26.**

A traditional approach to a short-lived positive expulsion system has been the use of plastic materials as bladders to contain and expel the fluid. Such positive expulsion bladders were designed and developed by the Bell Aerosystems Company for the GAM-63 (Rascal) air-to-ground missile. Experiments were conducted on a teflon bladder in the oxidizer tank (IRFNA) and a Buna-N rubber over nylon cloth bladder in the fuel tank (JP-4). Figures **27** and **28** are photographs of the prototype bladders employed in the propellant tanks. The size of these bladders is clearly depicted in these photographs when compared with the man. Plastics, however,

Discharge Tube

Collapsing Bladder (Metal)

Expanding Bladder (Metal)
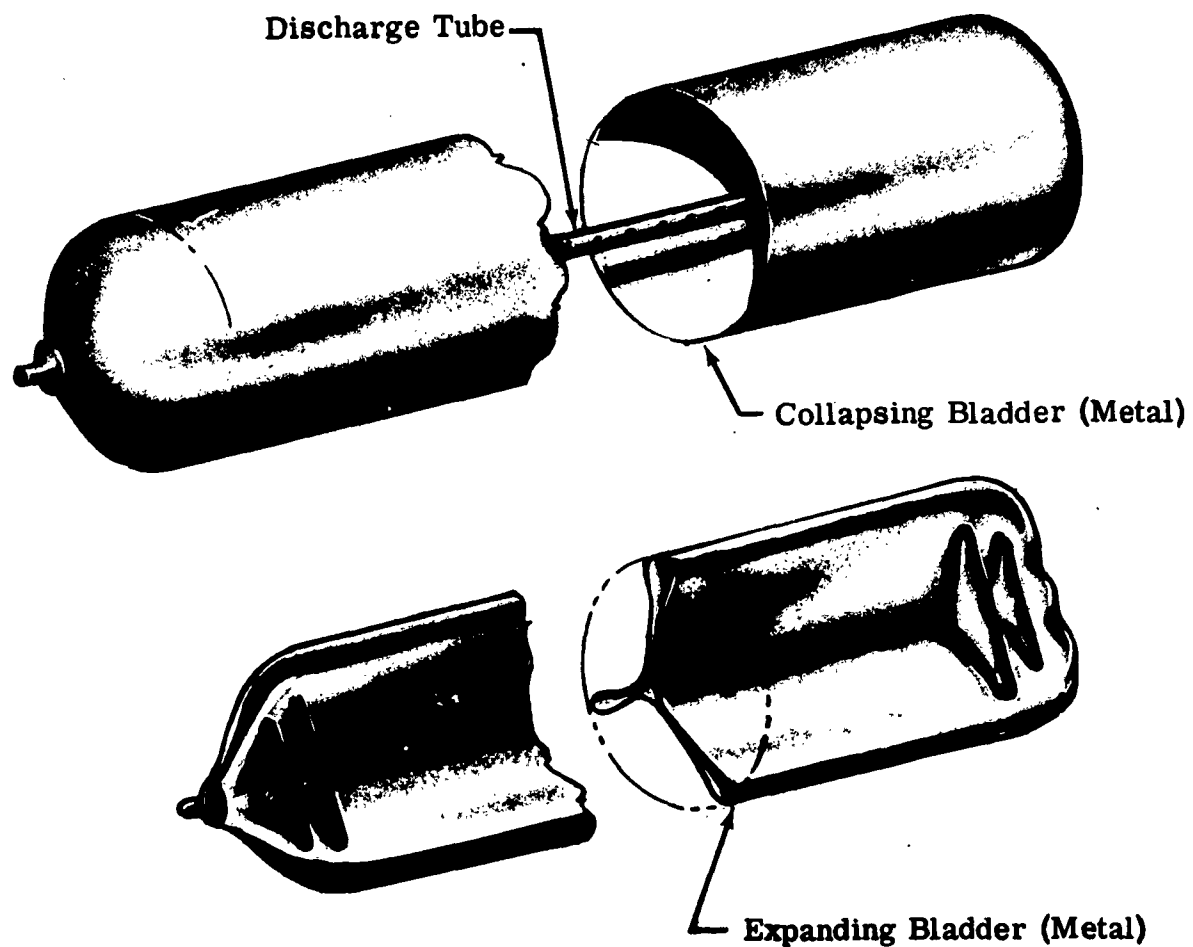
Figure 26. Typical Bladders

Figure 27.   Teflon Bladder for IRFNA Oxidizer

Figure 28.   Buna-N Rubber Over Nylon Cloth
Bladder for JP-4 Fuel

have limitations that restrict their use such as: degradation
of physical properties due to radiation, permeability to some
of the propellants or fluids, degradation of physical properties
on becoming saturated with the operating fluid and also due to
temperature environment.

The incorporation of metals for the construction of the
bladder can alleviate many of the aforementioned limitations
or disadvantages. The concept of the metal diaphragm or bladder
is not new. The feasibility of a collapsing aluminum cylinder
for expulsion has been demonstrated in the past by the Bell
Aerosystems Company (Literature Survey L2).

BLADDER AND TANK GEOMETRY CONSIDERATIONS

Many analyses have been undertaken for the purpose of pre-
dicting the material and geometric behavior of metal bladders
and diaphragms during the expulsion cycle. The numerous attempts
and results of these studies clearly indicate the difficulty
encountered in trying to synthesize the deflection and ultimate
or complete collapse of shells where local yielding not only
occurs but is greatly exceeded. Unpredictable wrinkles and their
locations, creases, cambers and folds offer resistance to further
deformations and collapse and thus add additional complexities
to analytical design solutions. It should be borne in mind that
for conventional shell design as applied to airframe vehicles
initial buckling is considered as a failure. For an expulsion
bladder configuration, however, the initial buckling with its
associated deformations must be extended to include complete
collapse if the expulsion cycle is based on such a configuration.

In a general sense, the initial configuration or geometry
of the bladder establishes the pattern of collapse or expulsion.
Whether this deformation continues progressively until the
required expulsion efficiency is attained depends on the surface
contours that are initially constructed into the component. As
an example, a flat or single curvature surface will deflect or
deform more readily under normal pressure than a panel having
a compound curvature and of similar dimensions.

With metal expulsion bladder configurations, the required
excessive buckling with the associated local plastic deformations
must be further investigated before establishing a design.
General quantitative results for such extreme buckling phenomena
are nonexistent and design criteria may be established only
through testing of several configurations. There are, however,
certain qualitative deductions that can be made to establish
some "figure-of-merit" among various designs. As an example, a
long cylinder under external pressure will collapse at a lower
pressure than a short cylinder. A sphere will require greater
pressure than either one of the cylinders for a comparable size,
to buckle inward or collapse.

The various buckle and deformation patterns introduce undesirable increasing stiffness with a resulting possible reduction in expulsion efficiency. Sharp creases or folds during the collapse of the bladder can induce tears and actual rupture of the component. The formation and distribution of the irregularity and the magnitude of the deformations does not seem amenable to an exact solution. However, there are means that can diminish some of these undesirable characteristics of bladder collapse.

In many cases, scoring is beneficial. Scoring metal consists of permanently deforming the metal by stressing it beyond its yield point in a localized and restricted region. Some plastic flow of the metal occurs, but the reduction in the thickness of the foil or sheet is generally negligible. Scoring will result in smooth bends and minimizes tearing of the foil or sheet material. Scoring provides controlled bending and deformations that may make its employment beneficial to the system.

Chemical milling of the material to vary thickness of the expulsion bladder can be used to obtain certain advantages. Initial buckling can thus be controlled in local areas, stresses can be made more uniform, for example, head and cylinder portions of tank, and required stiffening can be introduced in local areas so that a fold or bend can be initiated.

The possibility of controlling a homogeneous material bladder or diaphragm movement appears more promising when the unit is fabricated in the folded or collapsed configuration. This technique insures a prescribed manufactured fold or crease rather than a random form experienced during actual collapse. In addition, the operational cycle involves an inflation or expansion of the prefolded device which is a desirable feature and eliminates the possibilities of pin-hole leaks due to corner or handkerchief-type folds. The final shape is more predictable for an inflated shell than that of a collapsed structure as a result of an external pressure. Although the final expanded shape is determined by the enveloping or external structure, this limiting shape is always approached by the inner container during the operational expulsion cycle. On the other hand, the final shape of a shell under external pressure, when complete collapse is attained, does not necessarily result in a reproducible deformed configuration due to variations and random dispersal of initial buckle patterns and the resulting progressive resistance of the folds and creases during deformation.

The single and multiple folds and their random patterns and formation are an inherent characteristic of a collapsing bladder configuration. These various and random type of folds or excessively deep buckles are clearly illustrated in Figure 29, for a nickel electroformed bladder configuration.
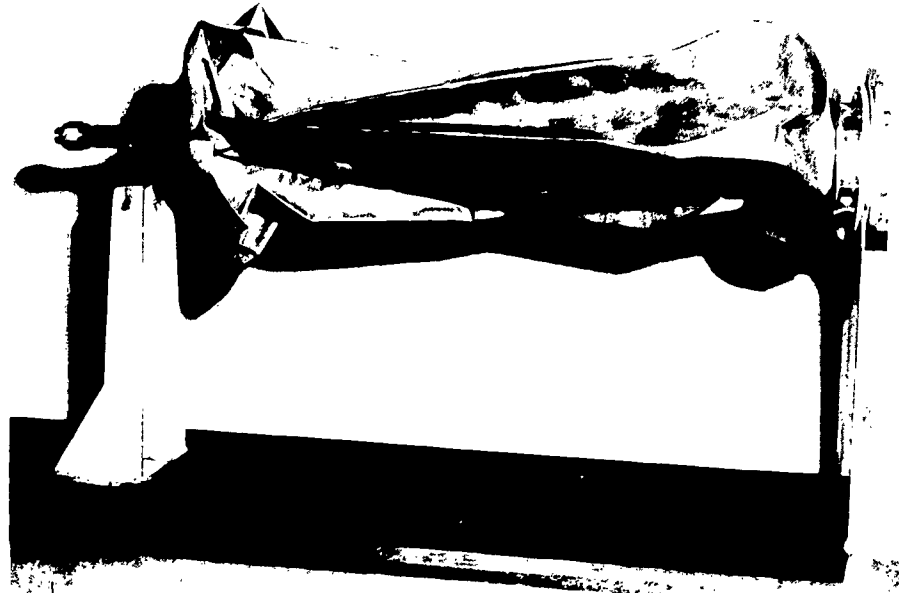
Figure 29. Collapse of a Nickel Bladder After
Expulsion Test

Figure 30. Local Double-Fold Type Failure in
Nickel Bladder
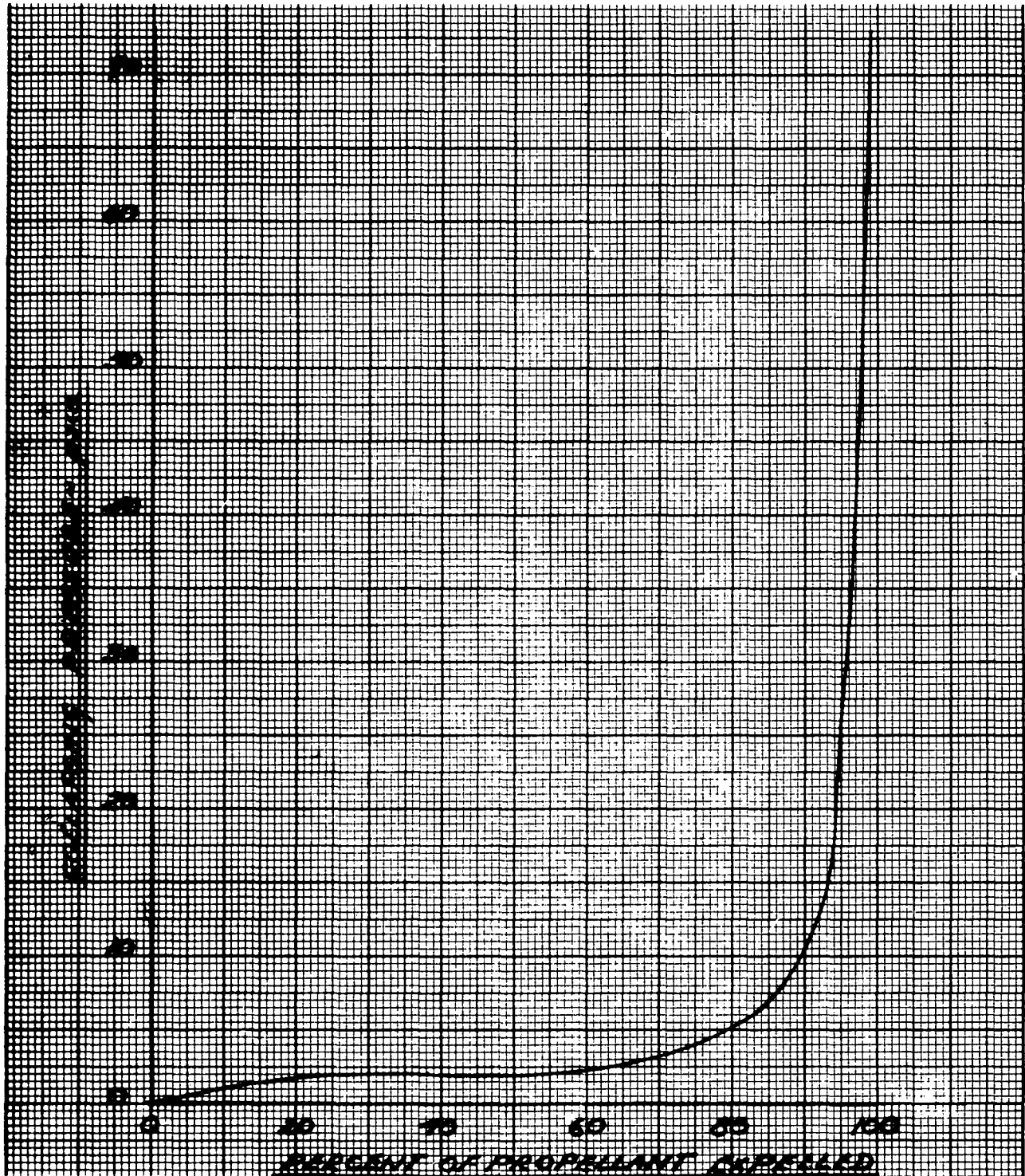
Figure 31.   Collapse Pressure Vs Expulsion Efficiency
            for a Collapsing Bladder

This metallic configuration is one of the studies conducted at Bell Aerosystems Corporation to investigate and improve bladder performance. The photograph in Figure 30 shows the failure in the metal as a result of a random double fold that was developed during the first expulsion test. It should be noted that this type of fold is not a characteristic of metal configurations but can and does occur in pliable or non-mettalic materials.

Similar tests were performed on an aluminum configuration (1100-0 material) and although this device sustained more than one expulsion cycle, similar pin-hole leaks due to double folds developed in the repeated fill and expel cycle tests. In the aluminum bladder test, the pressure differential, Δ p, between the pressurization gas and the expelled fluid was measured and is depicted in Figure 31. The low flexibility and stiffness of this aluminum bladder indicates the small Δ p value attained during the greater portion of the expulsion. This is a desirable characteristic because it dictates the energy requirements for the expulsion device. The contribution to the buckled configuration stiffness by the creases, single and double folds is apparent in the rise in Δ p to overcome this situation by further collapse of the bladder. It should be noted that a rather good expulsion efficiency was attained in this aluminum bladder test.

ANALYSIS DATA

Effects of Creases & Bends in Bladders

Introduction

The walls of bladders employed in the positive expulsion of liquids from containers are relatively thin and consequently will buckle under very small external pressure. It is most desirable to keep the external buckling pressure as small as possible to minimize the pressure differential across the bladder. During the initial stages of collapse the buckle waves or bends are large and sheet bending is no problem. However, as the bladder is collapsed further to smaller volumes, bend radii decrease and a double fold analogous to that which occurs in a handkerchief occurs. The folding condition can be also likened to the post buckling crippling that occurs in thin cylinders and short formed columns under compressive loads. It should however be noted that the wrinkles in the bladder will occur at a rate in conformance with the rate of expulsion of the contained incompressible fluid.

The double fold essentially occurs at localized points in the bladder. When the bladder is fully collapsed the inside radius of the first and second folds are very small. This folded

configuration introduces large bending strains at the outer fibers
of the sheet which, for metallic sheet material will be in the
plastic range. Repeated folding and unfolding of the sheet to the
double bend configuration results in fracture by fatigue at the
point of the double fold and the creation of an intolerable pin
hole there. The object of this study is to determine the number
of bladder collapse cycles that can be sustained before this type
of failure occurs and to examine design features which may increase
the number of cycles.

The manner in which the double fold is developed and its
severity depends on the geometry of the bladder contour and the
mechanics of its formulation will not be treater here. For
analysis purposes, the double fold condition will be assumed to
be similar to that which occurs to a flat wide sheet when folded,
by bending moments only, 180° on itself and then folded a second
time such that the second fold is perpendicular to the first fold.
The first and second fold configurations are depicted diagrammat-
ically in Figure 32.

Experimental observations reveal that the magnitude of
the inside radius which occurs after the first fold, is finite, i.e.
the inside bend radius cannot be reduced by mechanical means to
zero by the application of pure bending moments. However, during
the application of bending moments at right angles to the first
fold, a second fold occurs by local instability or flattening
which is analogous to the flattening which very long cylinders
experience at bending instability. Hence, the second fold is
seen to be accompanied by compressive pressures which tend to
reduce the inside radius of the first fold to zero. The inside
crease at the second fold appears to be sharp and as the second
fold is closed the inside radius of the second fold definitely
approaches zero.

In this discussion, the plastic strains which occur at the
bends are approximated and then used in conjunction with the low
cycle fatigue characteristics of matallic materials to predict the
number of folding and unfolding cycles that can be sustained.

Plastic Analysis of Sheet Bending

The mode of failure precipitated as a consequence of the
folding of wide sheets is that of local cracking at the surfaces.
Cracking or local material fracture may occur during the folding
operation or unfolding operation and depends on the state of stress
and plastic strains that are induced. A method for predicting
failure by fatigue is presented in the next section. To do this,
however, it is necessary to determine the magnitude of the plastic
strains that are induced during the folding and unfolding operation.

(a) SINGLE 180° FOLD

(b) DOUBLE FOLD
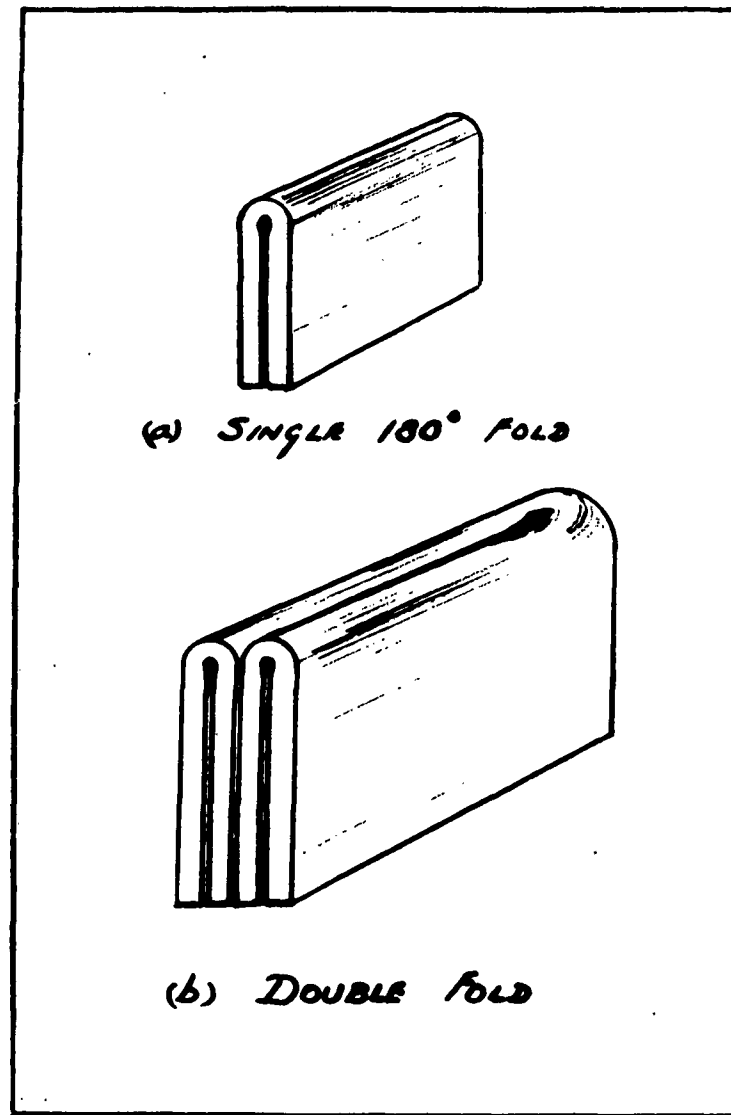
Figure 32. Sheet in Folded Configuration

The bending of wide plates has been treated in References 89 through 96. A theoretical analysis of a wide sheet in pure bending has been presented in References 89 and 90, and was based on the following assumptions:

1. The elastic region is small.

2. The material is ideally plastic, i.e. it does not strain harden.

3. A condition of plane strain exists.

4. The plate is deformed by equal and opposite couples into a hollow circular cylinder.

5. The deflections are large.

6. The distortion-energy condition of plastic flow is valid.

7. The compression and tension flow stresses are equal, i.e. the yield strength in tension and compression are equal.

From the results of the analysis in the references cited it was found that the neutral axis location is given by the expression

$$r_n = \sqrt{a_o \cdot b}$$ (26)

where a_o = inside bend radius and b = outside bend radius. It is of interest to note that the neutral axis location approaches the concave surface of the bend as the inside radius decreases. The stress distribution changes with the severity of the bend but the plastic bending moment is a constant and given by (Reference 88),

$$M = \frac{2\sigma_y t_o^2}{\sqrt{3}}$$ (27)

On the basis of plane strain, it is found that a two to one biaxial state of stress is present at both inner and outer surfaces. In addition, due to the small bend radii, compressive stresses are induced through the thickness of the plate with the maximum compressive stress located at the neutral axis. For very small values of inside radius, a_o, this maximum compressive stress is relatively large and fibers near the inside surface experience a triaxial state of compressive stresses.

The magnitude of the plastic strains are governed by the severity of the bend as measured by the inside bend radius and sheet thickness. Since for the case of pure bending planes originally plane always remain plane and sheet thickness remains constant (Reference 89), the strains can be determined by purely geometric considerations together with the assumption of an incompressible material. Such considerations result in the following expression for equal, but of opposite sign, nominal circumferential strains in the inner and outer surface fibers.

$$e_{a_0} = - e_b = \frac{1}{1 + 2(a_0/t_0)}$$

(28)

The variation with a_0/t_0 of the plastic inner and outer strains as given by Equation (28) is shown in Figure 33.

Prediction of Failure

Failure occurs in a bladder when a pin hole develops in the sheet as a consequence of local fracture or cracking when the cohesive strength of the material is exceeded. A crack may develop on the outside surface of the sheet during bending or on the inside surface during unfolding depending on the ductility and strain hardening characteristics of the material under the existing state of stress. For a ductile but strain hardenable material local fractures will occur after a certain number of repeated folding and unfolding cycles as a consequence of the depletion of the material ductility due to plastic strain cycling. Since the initial and final geometric configurations of the sheet are essentially predetermined, failure by repeated folding cycles will occur by the low cycle fatigue process. Consequently the prediction of failure can be accomplished with the use of data obtained from constant amplitude plastic strain cycling tests.

An empirical relationship which satisfactorily expresses the low cycle fatigue characteristics of metallic materials is given by (See References 97 through 100)

$$N^n \Delta \epsilon_p = k$$

(29)

where N is the number of cycles to failure, $\Delta \epsilon_p$ is the true plastic strain reversal that occurs during each cycle and n and k are material constants. For many metallic materials it has been shown that the exponent, n, which can be considered as a measure of the strain hardening characteristics of the material,
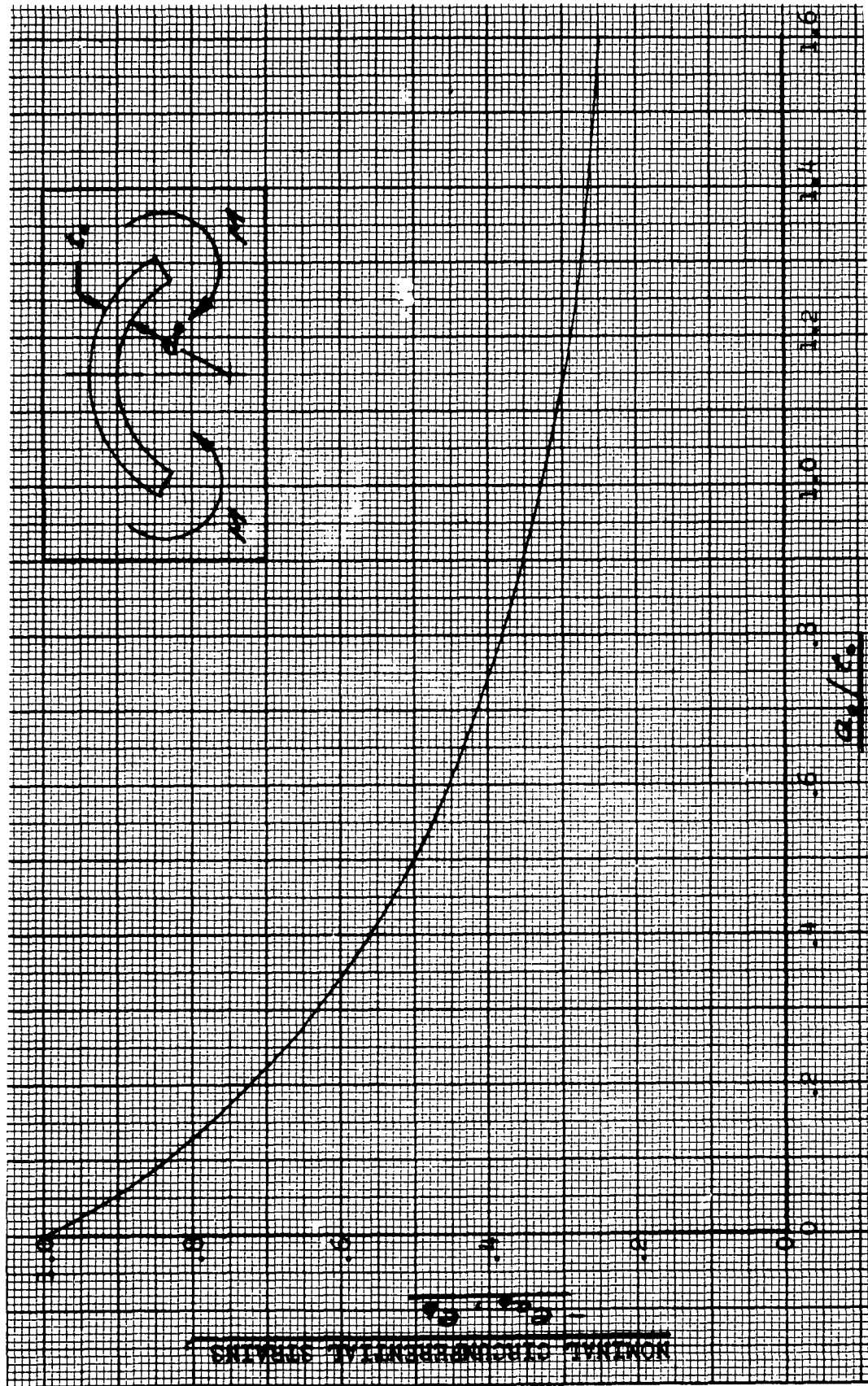
Figure 33.   Variation of Nominal Plastic Strain at Surfaces of Bent Sheet

is approximately equal to .5. The constant k is related to the ductility of the material and will be approximated here as follows.

The ductility of a material is measured quantitatively by the true elongation at fracture, say ϵ_{puw} which is obtained from a uniaxial stress test sheet or bar specimen, and can be considered to occur at N = 1/2. Substituting N = 1/2 and $\Delta\epsilon_p = \epsilon_{puw}$ into Equation (29) gives

$$k = .707\ \epsilon_{puw} \tag{30}$$

Thus Equation (29) reduces to

$$N^{.5}\Delta\epsilon_p = .707\ \epsilon_{puw} \tag{31}$$

The true strain can be expressed in terms of the reduction in area obtained from a uniaxial stress tensile test by noting that

$$\epsilon_{puw} = \ln\frac{L}{L_0} = \ln\frac{A_0}{A} = \ln\frac{1}{1-A_R} \tag{32}$$

where A_R = reduction in area and is given by $A_R = (A_0-A)/A_0$ Hence Equation (31) with the aid of Equation (32) becomes:

$$N^{.5}\Delta\epsilon_p = .707\ \ln\frac{1}{1-A_R} \tag{33}$$

It is now assumed that $\Delta\epsilon_p$ equals the true inner or outer strain ϵ_{a_0} or ϵ_b, developed in the sheet during the folding or bending process. Hence from Equation (28) and the definition of true strain we have

$$\Delta\epsilon_p = \epsilon_b = \ln(\epsilon_b+1) = \ln\frac{2(1+a_0/t_0)}{1+(2a_0/t_0)} \tag{34}$$

Substituting $\Delta\epsilon_p$ as given by Equation (34) into Equation (33) results in the expression:

$$\left[\frac{2(1+a_0/t_0)}{1+(2a_0/t_0)}\right]^{N^{.5}} = \frac{1}{(1-A_R)^{.707}} \tag{35}$$

Equation (35) essentially gives the minimum ductility, as measured by reduction in area, A_R, required to sustain N folding and unfolding cycles to a bend geometry defined by the ratio a_0/t_0. The variation of minimum required ductility with N and a_0/t_0 is given in Figure 34.

These results are valid for the single fold but can be used to approximate the life for a double fold if the ratio a_0/t_0 is set equal to $a_0/2t_0$.

The ductility of various metallic materials suitable for bladder applications is compiled in Table III. A comparison between the minimum ductility required to sustain N folding and unfolding cycles for a_0/t_0 = 0 and 0.4 and the room temperature ductility of several of the listed materials is shown in Figure 35. Comparisons of this type, i.e. between required and available material ductility, indicate that with the exception of pure tin most materials will fail after the application of relatively few cycles when a_0/t_0 = 0 (which is of prime interest here). For example, the results of Figure 35 show that nickel with ductilities in the range of from 60 to 75% area reduction will sustain from 1/2 to 2 cycles, respectively. From a required ductility standpoint, pure tin appears to be an excellent material for bladder repeatedly subject to the double fold condition. However, it can be demonstrated that pure tin in thin sheet form has a very low tear (or tensile) strength and consequently from this standpoint is very restricted as a bladder material.

In an effort to increase the number of folding and unfolding cycles, multi-layered sheet is considered in the next section.

Multilayer Sheet Construction

From an examination of the results presented thus far, it is quite conclusive that the number of folding and unfolding cycles to failure depends primarily on the ductility of the material and the ratio of inside bend radius to sheet thickness. Based on these conclusions, a bonded multilayered metallic sheet appears desirable for several reasons. Such a sheet would presumably sustain more cycles than a corresponding single sheet material if the outer layers were of a very ductile material with little or some strength and if the inside or core material were ductile but of sufficient strength to hold the composite sheet together as well as sustain imposed loads. For example, a promising multilayer construction would be to use pure tin, which has a very high ductility but relatively low strength, for the outer or face layers and such materials as pure nickel or aluminum for the core. For this type of configuration, the core
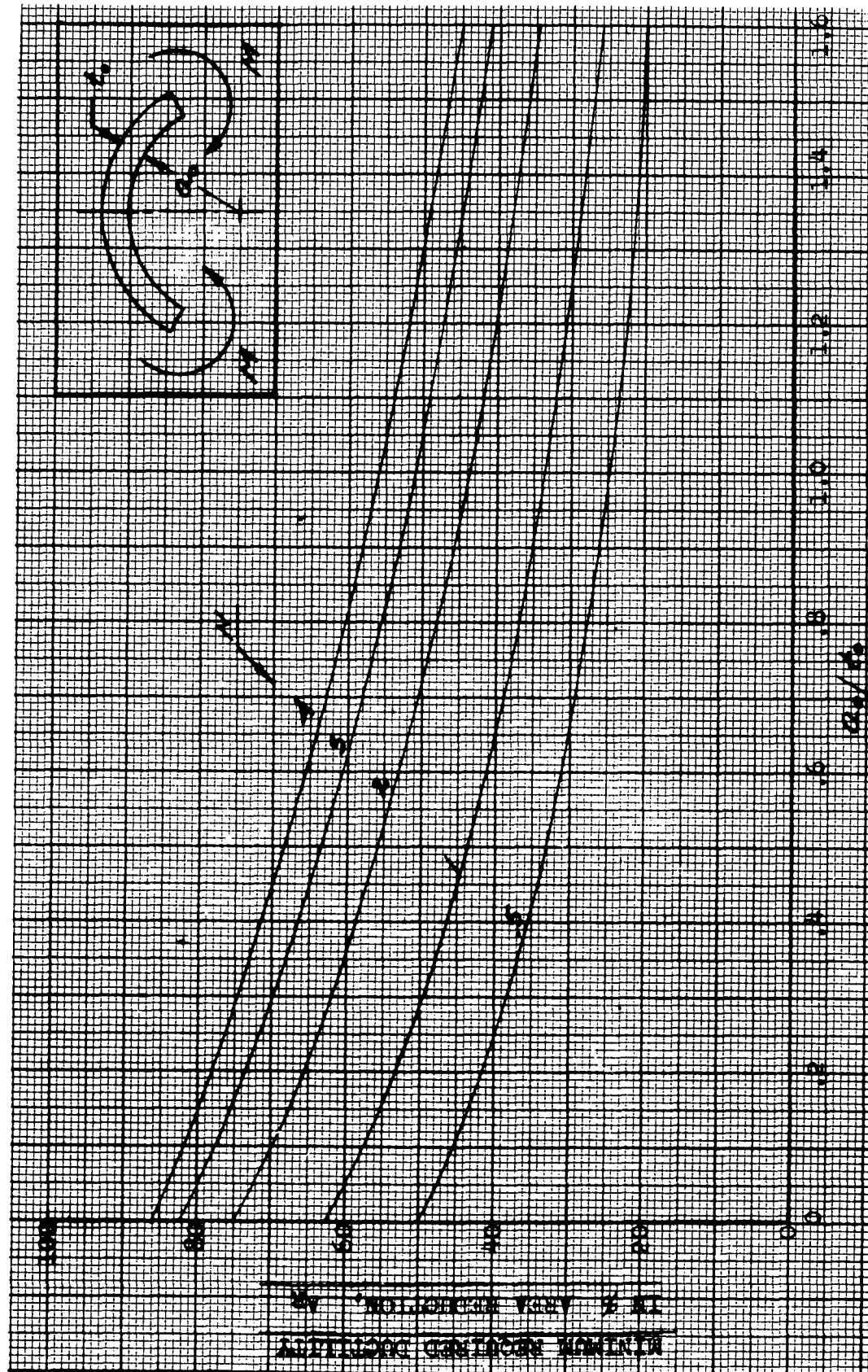
Figure 34. Number of Cycles to Failure for Single Folding and Unfolding of Sheet
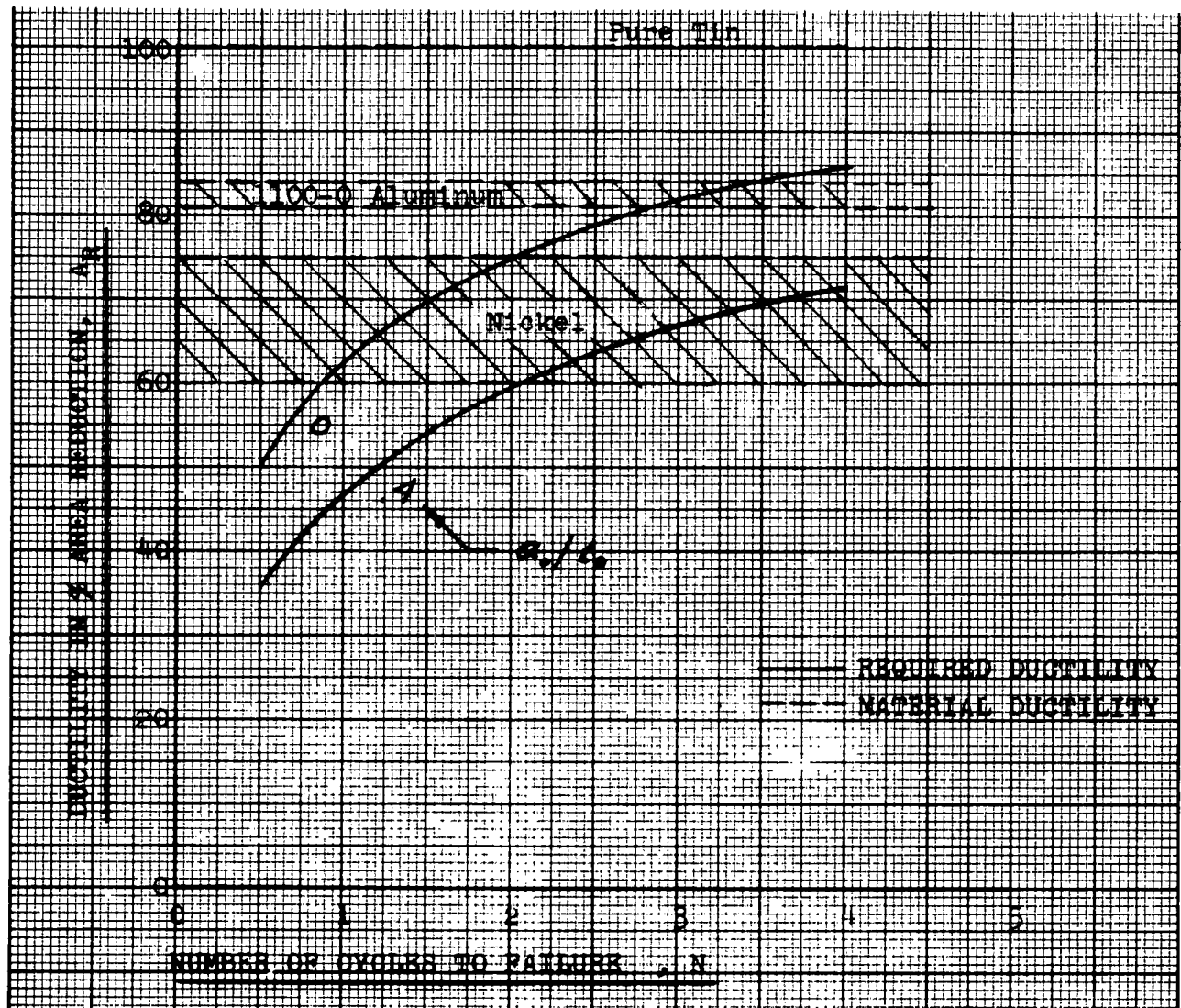
Figure 35.   Comparison of Ductility of Various
Materials with Required Ductility

TABLE III

DUCTILITY OF VARIOUS MATERIALS

Material	Temperature $^\circ F$	% Reduction in Area	Reference
Annealed Tantalum	-318	75	101
Annealed Tantalum	Room	86	102
1100 Aluminum	Room	81-84	103
Niobium	-320	1.91-2.86	101
Niobium	Room	90	101
Nickel (99.4 Ni + Co)	Room	60-75	102
Pure Tin	-260	10	102
Pure Tin	-200	85	102
Pure Tin	Room	100	103

material can be envisioned as the structural material, i.e.
failure occurs when the core material fractures regardless of
the condition of the face material.

From another point of view the purpose of the face
material can be considered as providing a limit on the bend
radius that can be imposed on the structural core layers. By
limiting the bend radius of the core material, a decrease in the
magnitude of the induced plastic strains is effected with an
accompanying increase in fatigue life. With regard to improv-
ing fatigue life by limiting the bend radius of the structural
core material, various outer layer or face configurations may
prove desirable. For example, it may prove beneficial to in-
corporate an orthotropic groove or slit pattern in the outer
layers or to utilize faces of fibrous material such as a wire
mesh.

To ascertain the benefits that may be derived from the
use of multilayered sheet for bladder purposes, an analysis is
presented on the following pages for the single bending of a
three layered sheet with both faces of the same material.

Stress Distribution

A section of a bent three layer sheet as shown in
Figure 36 is considered. All the assumptions previously listed
for the homogeneous sheet are retained. From the distortion-
energy condition of plasticity and equilibrium conditions for a
volume element, it is found (Reference 89) that the radial stress
distribution for each layer of material considered separately is
given by

$$\frac{\sqrt{3}}{2}\left(\frac{\sigma_r}{\sigma_y}\right) = \pm \ln r + C_1 \tag{36}$$

and the tangential stress distribution by

$$\sigma_\theta = \sigma_r \mp \frac{2}{\sqrt{3}}\sigma_y \tag{37}$$

where C_1 is a constant of integration. The constants of integra-
tion are determined from the known conditions of radial stress
at the surfaces of each layer. Thus, at the external surfaces
$r = a$ and $r = b$ the radial stresses, σ_r, are zero and at
the internal core to face contact surfaces, $r = c$ and $r = d$,
the radial stresses must be continuous. After the determination

(a) BEFORE DEFORMATION

(b) AFTER DEFORMATION
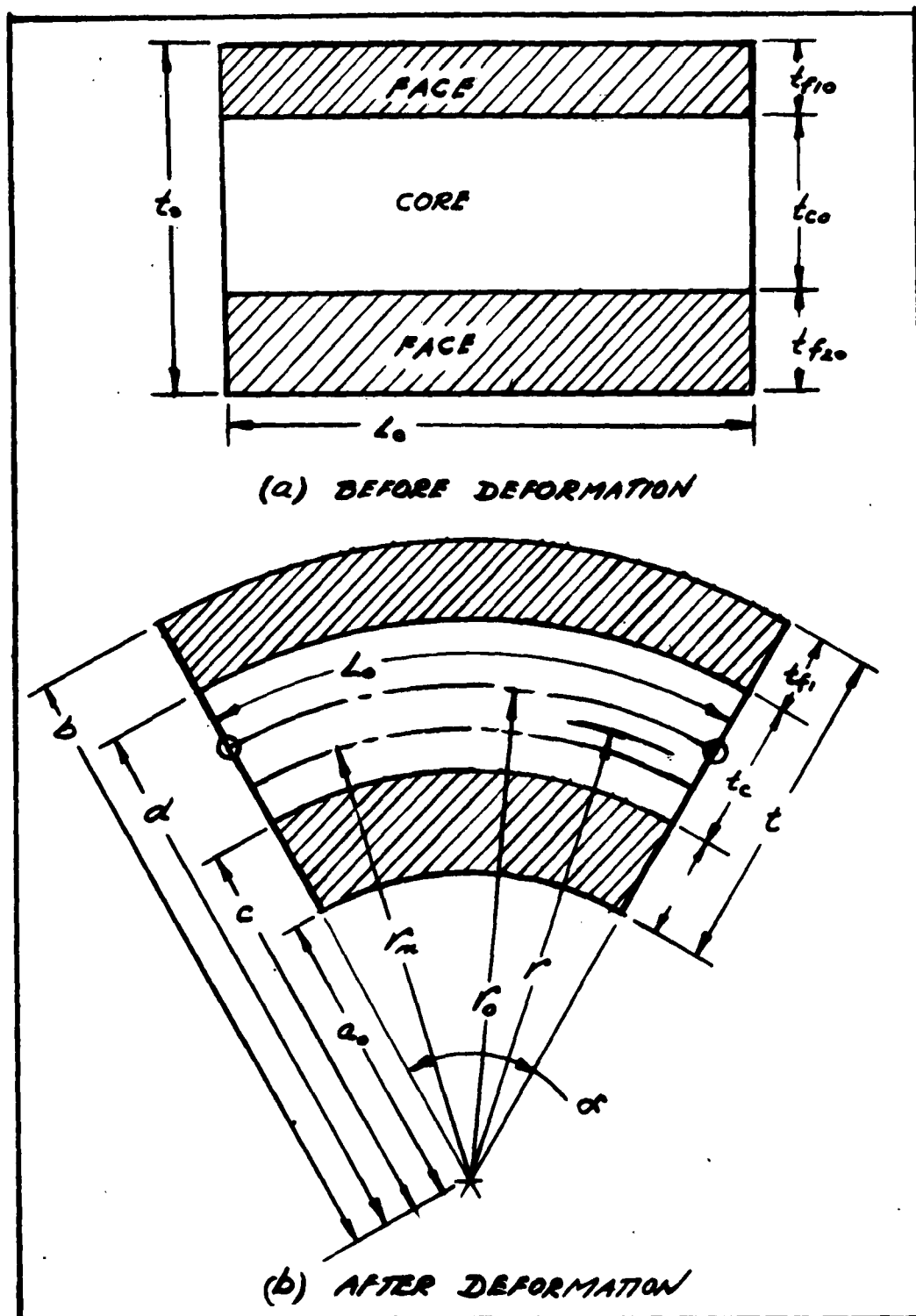
Figure 36.   Dimensions of an Element of a Bent
Multi-Layer Sheet

of the constants of integration by application of the boundary
conditions to Equation (36), the following equations were obtained
for the radial and tangential stress distributions.

For neutral axis location in the range $c < r_n < d$:

$$\frac{\sqrt{3}}{2}\left(\frac{\sigma_r}{\sigma_{yf}}\right) = \ln\left(\frac{r}{b}\right) \qquad\qquad d < r < b \qquad (38)$$

$$\frac{\sqrt{3}}{2}\left(\frac{\sigma_\theta}{\sigma_{yf}}\right) = \ln\left(\frac{r}{b}\right) + 1 \qquad\qquad\qquad\qquad (39)$$

$$\frac{\sqrt{3}}{2}\left(\frac{\sigma_r}{\sigma_{yc}}\right) = \ln\left(\frac{r}{d}\right) + \beta \ln\left(\frac{d}{b}\right) \qquad r_n < r < d \qquad (40)$$

$$\frac{\sqrt{3}}{2}\left(\frac{\sigma_\theta}{\sigma_{yc}}\right) = \ln\left(\frac{r}{d}\right) + \beta \ln\left(\frac{d}{b}\right) + 1 \qquad\qquad (41)$$

$$\frac{\sqrt{3}}{2}\left(\frac{\sigma_r}{\sigma_{yc}}\right) = \ln\left(\frac{c}{r}\right) + \beta \ln\left(\frac{a_o}{c}\right) \qquad c < r < r_n \qquad (42)$$

$$\frac{\sqrt{3}}{2}\left(\frac{\sigma_\theta}{\sigma_{yc}}\right) = \ln\left(\frac{c}{r}\right) + \beta \ln\left(\frac{a_o}{c}\right) - 1 \qquad\qquad (43)$$

$$\frac{\sqrt{3}}{2}\left(\frac{\sigma_r}{\sigma_{yf}}\right) = \ln\left(\frac{a_o}{r}\right) \qquad\qquad a_o < r < c \qquad (44)$$

$$\frac{\sqrt{3}}{2}\left(\frac{\sigma_\theta}{\sigma_{yf}}\right) = \ln\left(\frac{a_o}{r}\right) - 1 \qquad\qquad\qquad (45)$$

For neutral axis location in the range $a_o < r_n < c$:

$$\frac{\sqrt{3}}{2}\left(\frac{\sigma_r}{\sigma_{yf}}\right) = \ln\left(\frac{r}{b}\right) \qquad\qquad d < r < b \qquad (46)$$

$$\frac{\sqrt{3}}{2}\left(\frac{\sigma_\theta}{\sigma_{yf}}\right) = \ln\left(\frac{r}{b}\right) + 1 \qquad\qquad\qquad\qquad (47)$$

$$\frac{\sqrt{3}}{2}\left(\frac{\sigma_r}{\sigma_{yc}}\right) = \ln\left(\frac{r}{d}\right) + \beta \ln\left(\frac{d}{b}\right), \qquad c < r < d \qquad (48)$$

$$\frac{\sqrt{3}}{2}\left(\frac{\sigma_\theta}{\sigma_{yc}}\right) = \ln\left(\frac{r}{d}\right) + \beta \ln\left(\frac{d}{b}\right) + 1 \qquad\qquad (49)$$

$$\frac{\sqrt{3}}{2}\left(\frac{\sigma_r}{\sigma_{yf}}\right) = ln\left(\frac{r}{c}\right) + \frac{1}{\beta} ln\left(\frac{c}{d}\right) + ln\left(\frac{d}{b}\right) \quad \Bigg] \tag{50}$$

$$r_n < r < c$$

$$\frac{\sqrt{3}}{2}\left(\frac{\sigma_\phi}{\sigma_{yf}}\right) = ln\left(\frac{r}{c}\right) + \frac{1}{\beta} ln\left(\frac{c}{d}\right) + ln\left(\frac{d}{b}\right) + 1 \quad \Bigg] \tag{51}$$

$$\frac{\sqrt{3}}{2}\left(\frac{\sigma_r}{\sigma_{yf}}\right) = ln\left(\frac{a_o}{r}\right) \tag{52}$$

$$a_o < r < r_n$$

$$\frac{\sqrt{3}}{2}\frac{\sigma_\phi}{\sigma_{yf}} = ln\left(\frac{a_o}{r}\right) - 1 \tag{53}$$

The symbols σ_{yf} and σ_{yc} are the yield strengths of the face and core materials respectively and the parameter β defines the ratio

$$\beta = \frac{\sigma_{yf}}{\sigma_{yc}} \tag{54}$$

The longitudinal stresses, σ_z , as determined directly from the assumed condition of plane strain is given by the expression

$$\sigma_z = \frac{\sigma_r + \sigma_\phi}{2} \tag{55}$$

Neutral Axis Location

With the establishment of the stresses in the sandwich or multilayer sheet, the neutral axis position is a necessary prerequisite for the determination of the plastic strains which are required to predict failure.

The location of the neutral axis, $r = r_n$, for multi-layer sheet construction is determined from the condition that the derived equations for the radial stresses on either side of the neutral axis must yield identical radial stresses at the neutral axis. Application of this condition to Equations (40) and (42), the neutral axis location when in the region $c < r_n < d$ is found to be given by the expression

$$r_n = \left(\frac{a_o b}{c d}\right)^{\beta/2} \sqrt{c d} \tag{56}$$

Similarly, from Equations (50) and (52) the neutral axis location
when located in the region $a_o < r_m < d$ is given by the expression

$$r_m = \left[\left(\frac{d}{c} \right)^{\frac{1-\beta}{2\beta}} \right] \sqrt{a_o b} \tag{57}$$

By taking note of the fact that

$$
\begin{aligned}
b &= a_o + t \\
c &= a_o + t_{f_2} \\
d &= a_o + t - t_{f_1}
\end{aligned}
\tag{58}
$$

Equations (56) and (57) were nondimensionalized into the follow-
ing expressions, respectively

$$\frac{r_m - a_o}{t} = \left[\frac{\frac{a_o}{t}\left(\frac{a_o}{t}+1\right)}{\left(\frac{a_o}{t}+\frac{t_{f_2}}{t}\right)\left(1+\frac{a_o}{t}-\frac{t_{f_1}}{t}\right)} \right]^{\beta/2} \sqrt{\left(\frac{a_o}{t}-\frac{t_{f_2}}{t}\right)\left(1+\frac{a_o}{t}-\frac{t_{f_1}}{t}\right)} - \frac{a_o}{t} \; ; \tag{59}$$

$$c < r_m < d$$

$$\frac{r_m - a_o}{t} = \left[\frac{1+\frac{a_o}{t}-\frac{t_{f_1}}{t}}{\frac{a_o}{t}+\frac{t_{f_2}}{t}} \right]^{\frac{1-\beta}{2\beta}} \sqrt{\frac{a_o}{t}\left(\frac{a_o}{t}+1\right)} - \frac{a_o}{t} \; ; \quad a_o < r_m < c \tag{60}$$

It should be noted that the parameter $(r_m - a)/t$ is the non-
dimensional instantaneous distance from the inside surface of the
bend to the neutral surface. In addition this parameter is given
in terms of the instantaneous values of t, t_{f_1} and t_{f_2} which
are as yet not known. However, the ratios of (t_{f_1}/t) and (t_{f_2}/t)
can be determined as a function of the ratio (a_o/t) by considera-
tion of the condition of plastic incompressibility. It is shown
in Reference 90 that if $m t_o/2$ locates the distance of a fibre
from the center plane in the unbent sheet, the fibre location
in the deformed sheet bent to an inside radius $r = a_o$ is given by

$$r_m^2 = \frac{1}{2}(a_o^2 + b^2) + \frac{1}{2}(b^2 - a_o^2)m \tag{61}$$

For the case of initially equal thickness faces, $t_{f1_o} = t_{f2_o}$ the initial locations of the fibres at the core to face bonded surfaces of the unbent sheet are given by $m = t(t_{c_o}/t_o)$. Hence for the unbent sheet, the location of the bonded surfaces after bending are given by

$$c^2 = \frac{1}{2}(a_o^2 + b^2) - \frac{1}{2}(b^2 - a_o^2)\left(\frac{t_{c_o}}{t_o}\right) \tag{62}$$

$$d^2 = \frac{1}{2}(a_o^2 - b^2) + \frac{1}{2}(b^2 - a_o^2)\left(\frac{t_{c_o}}{t_o}\right) \tag{63}$$

The instantaneous laminate thickness ratios as obtained from Equations (62) and (63), are given by the following expressions:

$$\frac{t_{f_1}}{t} = \frac{b-d}{t} = \frac{a_o}{t} - 1 - \sqrt{\left(\frac{a_o}{t}\right)^2 + \frac{a_o}{t}\left(1 + \frac{t_{c_o}}{t_o}\right) + \frac{1}{2}\left(1 + \frac{t_{c_o}}{t}\right)} \tag{64}$$

$$\frac{t_{f_2}}{t} = \frac{c - a_o}{t} = -\frac{a_o}{t} + \sqrt{\left(\frac{a_o}{t}\right)^2 + \frac{a_o}{t}\left(1 - \frac{t_{c_o}}{t_o}\right) + \frac{1}{2}\left(1 - \frac{t_{c_o}}{t_o}\right)} \tag{65}$$

$$\frac{t_c}{t} = 1 - \frac{t_{f_1}}{t} - \frac{t_{f_2}}{t} \tag{66}$$

The variation of the instantaneous thickness ratios for both faces and core laminas with inside bend radius, as obtained from Equations (64) through (66) are shown in Figure 37 for an arbitrary $(t_{f1_o}/t) = (t_{f2_o}/t_o) = .2$ or $(t_{c_o}/t_o) = .6$. It will be noticed that relative to the instantaneous sheet thickness, t, the outside face and core thicknesses decrease and the inside face thickness increases with decrease in the inside bend radius. However, the magnitude of the instantaneous thickness of each layer depends on the instantaneous total sheet thickness.

The location of the neutral axis as obtained from Equations (59), (60), (64), and (65) for the dimensionless ratio $(t_{f1_o}/t) = (t_{f2_o}/t_o) = .2$ and various values of β is shown
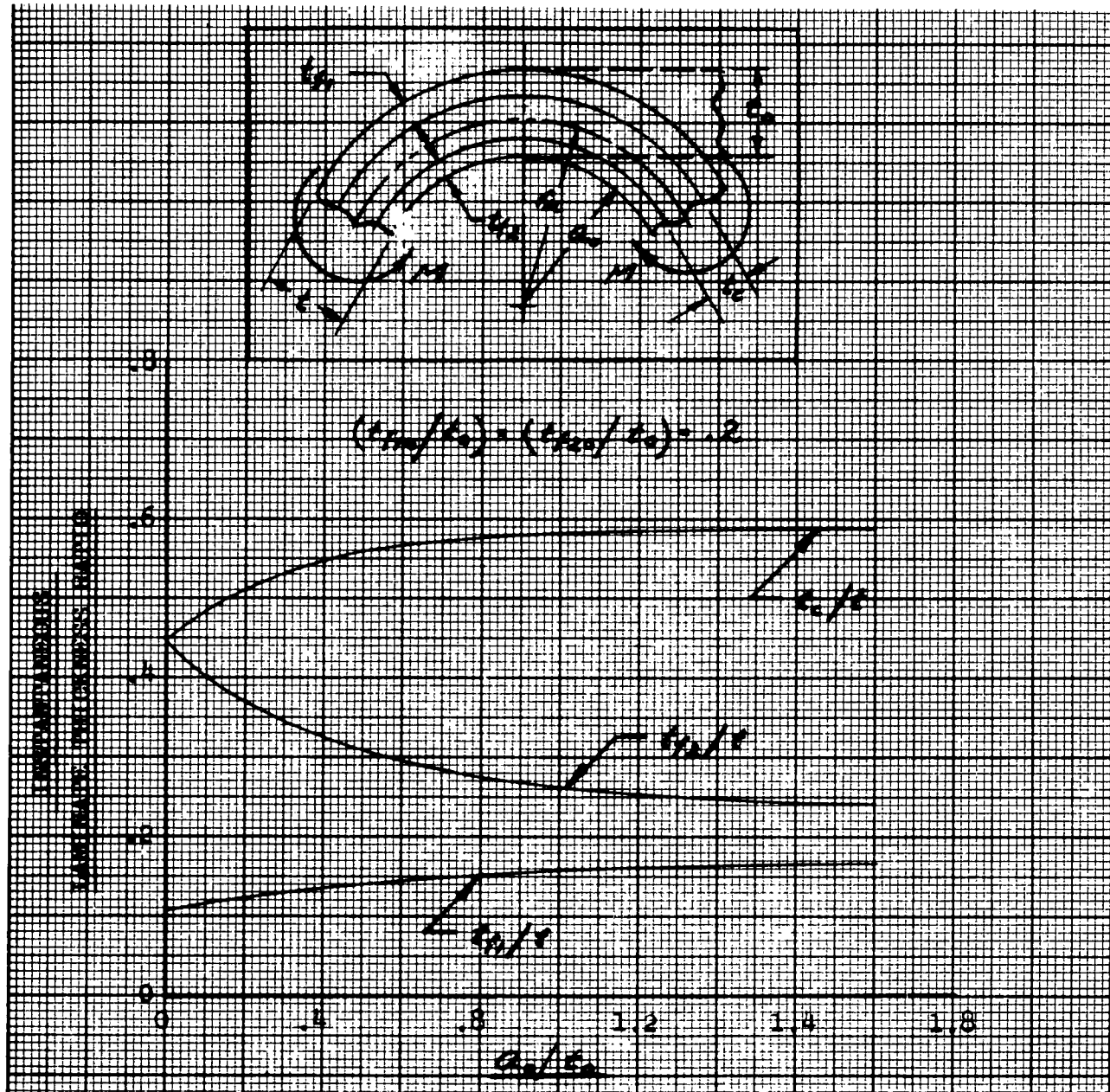
Figure 37. Variation of Laminate Thickness Ratio
with a_0/t

in Figure 38 as a function of the ratio of inside bend radius to instantaneous total sheet thickness.

Plastic Strains

As mentioned previously, plastic strains are associated with failure prediction. The determination of these strains for a sandwich or three-layer bonded sheet construction is presented below.

The method of prediction of the plastic strains which are induced in the sheet during bending follows from the assumption that planes before bending remain plane during the bending processes. However, the determination of the plastic strains is not a simple straightforward matter because, as shown in Figure 37, the neutral axis location is a function of the ratio of inside radius to instantaneous total thickness, a_o/t. Therefore during each incremental change in the ratio, a_o/t, the axis of rotation of a plane section through the sheet shifts. Consequently, the total strain that a fibre possesses at a particular value of a_o/t depends on the shift in the neutral axis as the sheet is bent (See Reference 90). Because of the shift in the neutral axis, for example, a circumferential fibre initially on the concave side of the neutral surface will at first experience compressive strains but as a_o/t is decreased the fibre may experience tensile strains if, due to neutral axis shift, it is now located on the convex side of the neutral surface. It follows, therefore, that for a particular value of a_o/t, there will be a fibre which has experienced equal amounts of compressive and tensile circumferential strains, i.e. the length of this curved fibre in the bent sheet is equal to the initial unstrained length, say L_o. If the location of this particular fibre is at the radial coordinate $r = r_o$, as indicated in Figure 36, the nominal circumferential plastic strain, e_θ, for all other fibres will be given by the following relation.

$$e_\theta = \frac{L - L_o}{L_o} = \frac{r - r_o}{r_o} \tag{67}$$

The symbol L refers to the length of a fibre located at the radial distance r from the center of curvature. The expression on the right hand side of Equation (67) was obtained by noting that $L = r\alpha$ and $L_o = r_o\alpha$, where α is the angle of bend.

The magnitude of r_o can be determined in terms of t and a_o by application of the assumption of incompressibility to an element such as that shown in Figure 36. By equating the
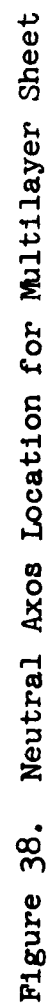
Figure 38. Neutral Axos Location for Multilayer Sheet

volumes before and after bending deformation and noting that $\angle_o = r_o \alpha$, we obtain

$$r_o = \frac{2a_o + t}{2} \left(\frac{t}{t_o} \right) \tag{68}$$

Eliminating r_o from Equation (67) gives

$$e_\theta = \frac{2 \frac{a_o}{t} \left(\frac{r}{a_o} \frac{t_o}{t} - 1 \right) - 1}{1 + 2 \left(\frac{a_o}{t} \right)} \tag{69}$$

Since a state of plane strain was assumed in the analysis, the nominal radial strain is given by $e_r = -e_\theta$.

      Evaluation of the plastic strains from Equation (69) requires a knowledge of the instantaneous thickness t. However, in general, when $r = a_o = 0$ Equation (20) gives $e_{a_o} = -1$, which indicates that the maximum compressive strain at the inside surface is identical for the laminated and solid sheets. On the other hand for $a_o = 0$ and $r = b$, Equation (20) yields $e_b = 2(t_o/t) - 1$. Hence the maximum strain appears to depend on whether the multi-layer sheet thins or thickens. Evidently it is better that the sheet thicken.

      From the relationships derived in References 89 and 90 it can be shown that the change in total sheet thickness corres-ponding to a change in inside bend radius is given by the follow-ing equation:

$$\frac{dt}{da_o} = \frac{1 + \left(\frac{r_o}{t} \right)^2 \left(1 - \frac{a_o}{t} \right)^2}{\frac{a_o}{b} + \left(\frac{r_o}{t} \right)^2 \left(\frac{b}{a_o} - 1 \right) \left(1 - \frac{a_o}{b} \right)} - 1 \tag{70}$$

A closed form solution to this first order nonlinear differential equation could not be obtained. Consequently, an approximate solution was obtained by means of a method discussed in Reference 104. The variation of dt/da_o with a_o/b as obtained from Equation (70) for an arbitrary value of $\beta = .5$ and $(t_{f_{1o}}/t) = (t_{f_{2o}}/t) = .2$ is shown in Figure 39. An inspection of this curve reveals that the sheet thickness does not change for values of a_o/b approxi-mately greater than 0.7. The initial condition necessary to solve Equation (70) was therefore taken as $(a_o/b) = .7$ and $(t/t_o) = 1$.
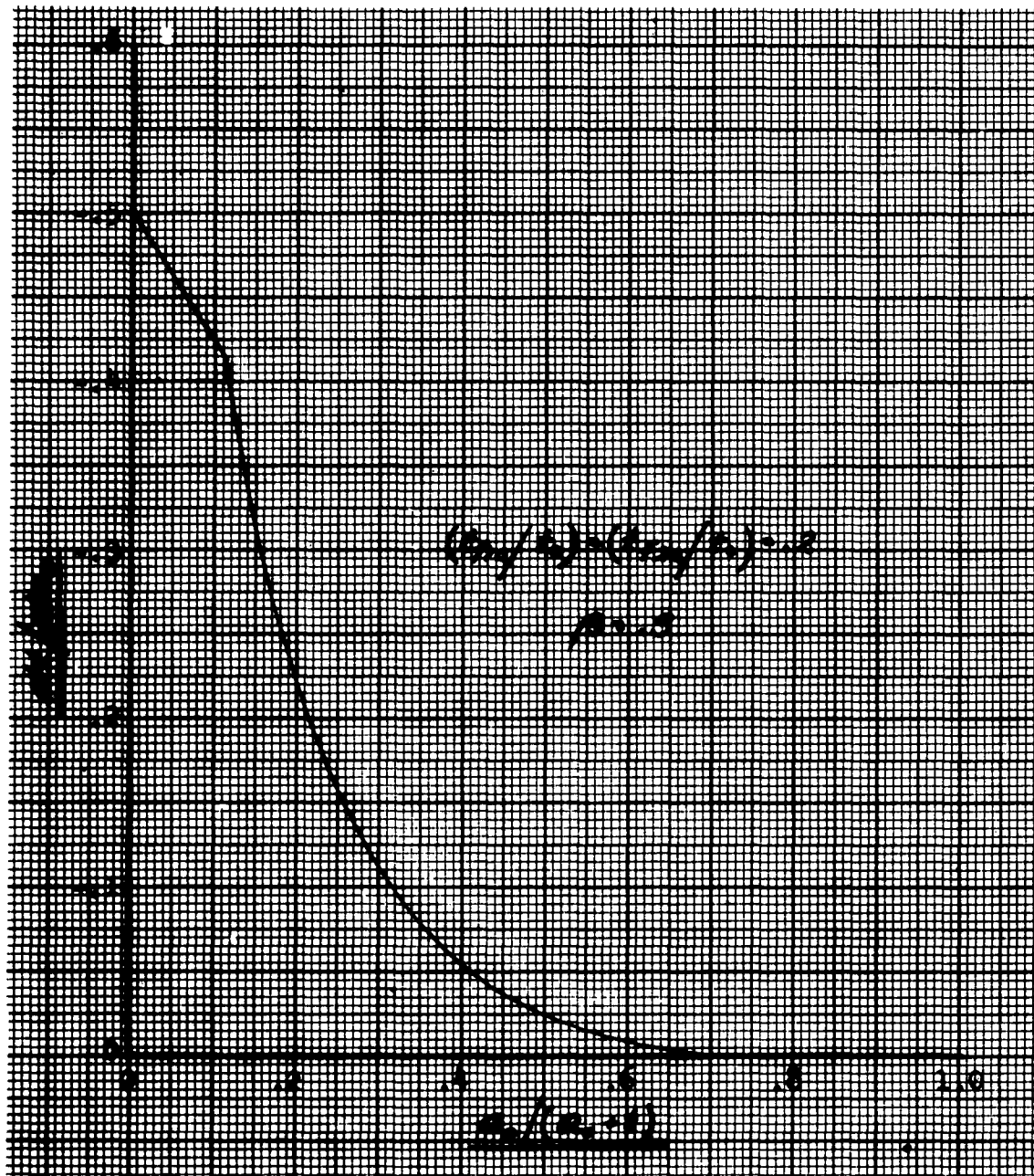
Figure 39.   Variation of the Change in Multilayer
             Sheet Thickness During Bending

The approximate solution obtained for the instantaneous thickness is shown in Figure 40. Relatively large increments of a_o/t were used in the determination of (t/t_o) from Equation (70) and therefore the instantaneous thicknesses shown are underestimated.

The variation of the plastic strains with (a_o/t_o) as obtained from Equation (69) is shown in Figure 41 for a three-layer laminate at four locations in the sheet corresponding to points a_o, b, c and d . As shown in Figure 41, the maximum plastic strain of $e_{a_o} = -1$ occurs at $r = a$ when $a_o/t_o = 0$, and is identical to the maximum plastic strain induced in the homogeneous sheet. Since the maximum induced plastic strains are equal for the homogeneous and laminate sheets, it may be concluded that the multilayer sheet will fracture at the same number of cycles given by the curve in Figure 35 for $(a_o/t_o) = 0$. However, since a multilayer sheet permits the use of a very ductile material at the faces, a significant increase in life is possible. It should be emphasized at this point that the life of the multilayered sheet may be controlled by the maximum plastic strain reversals in the core. Thus, referring to Figure 41 a maximum tensile plastic strain of $e_d = .56$ in/in occurs in the core at $r = d$ for $(a_o/t_o) = 0$ and a maximum compressive plastic strain of $e_c = -.344$ in/in occurs at $r = c$ for $(a_o/t_o) = .275$.

The number of cycles to failure, N, by fatigue of the core can now be readily approximated from the expression (see Equations (33) and (34)

$$N^{.5} \ln (e+1) = .707 \ln \frac{1}{1-A_R} \tag{71}$$

where e_o equals the maximum nominal circumferential plastic strain determined from Figure 41.

It should be noted that the results presented are for the single fold configuration and an extension of the analysis to the more complex double fold configuration is necessary. However, it is believed that the general results found for the single fold are indicative of double fold behavior.

Design Procedure

A summary of the approximate procedure developed for predicting the number of folding and unfolding cycles to failure by fatigue of sheet materials is outlined below. Two illustrative sample problems are included.

7129-933003
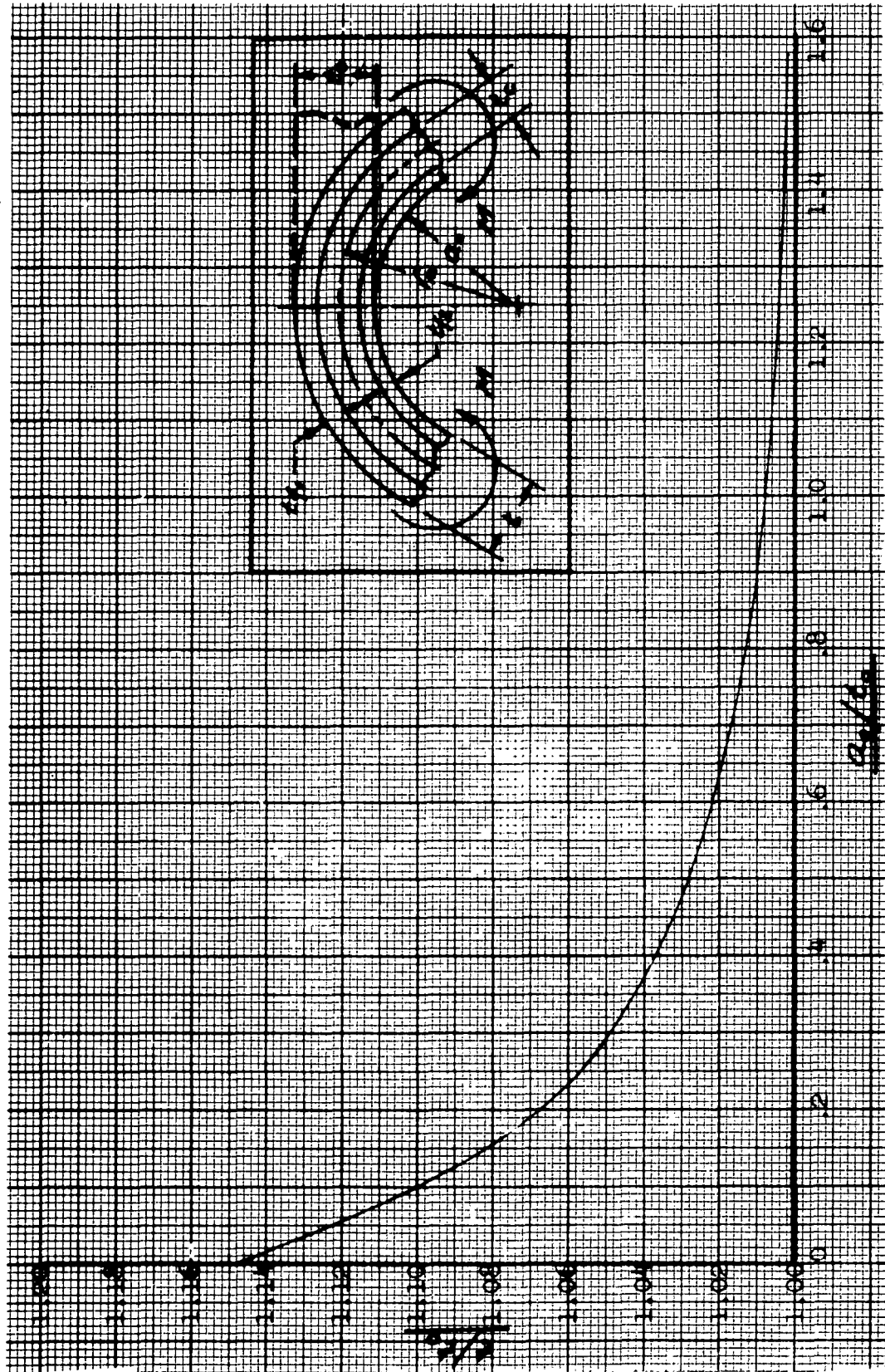
Figure 40. Variation of Multilayer Sheet Thickness with Bend Radius

Figure 41. Nominal Plastic Strains in Multilayer Sheet
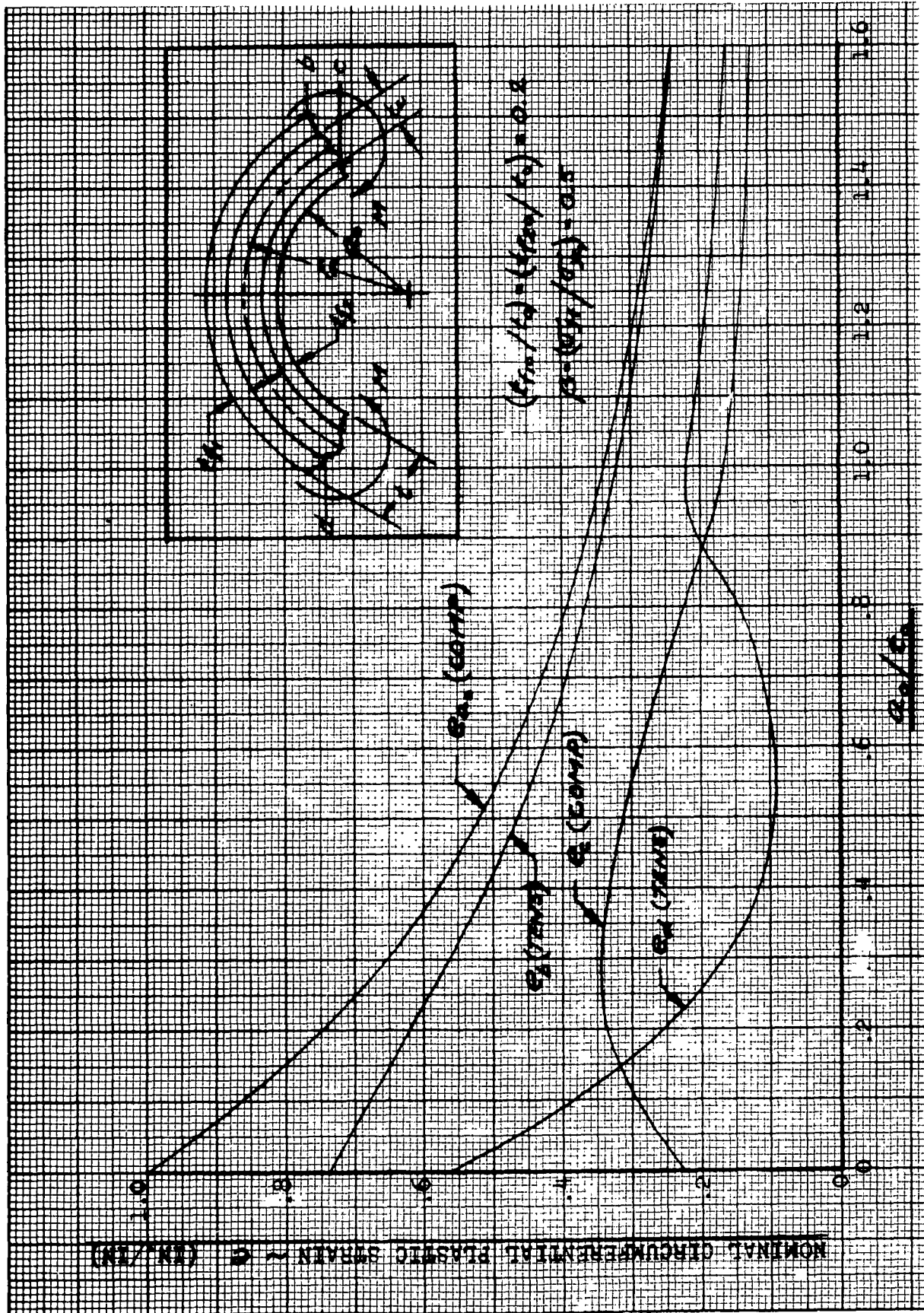
A.   Single Thickness Homogeneous Sheet

     1.   Select a material and determine its ductility.

     2.   For an inside bend radius of a_0 and sheet thickness t_0 , compute the ratio a_0/t_0 for repeated single bending of the sheet or compute the ratio $a_0/2t_0$ for repeated double bending of the sheet. However, for repeated single bending the inside bend radius is generally not known and for repeated double bending it is approximately equal to zero. Therefore, it is suggested that for either type of repeated bending assume $a_0 = 0$.

     3.   With $(a_0/t_0) = 0$ and known material ductility, determine the number of cycles to failure, N, by fatigue from Figure 34.

Illustrative Problem No. 1

     Determine the number of cycles a bladder can be folded and unfolded when the ductility of this bladder material is 80% reduction in area.

     A metallic bladder will experience a double fold condition with an inside bend radius approximately equal to zero. Therefore, for an assumed ratio of $a_0/t_0 = 0$ and a ductility of 80%, the number of cycles to failure by fatigue at the double fold is obtained from Figure 34 and is found equal to $N \approx 2.5$ cycles.

B.   Three Layer Bonded Sandwich Sheet - Single Bending Only

     1.   Select face and core materials and thicknesses. Determine the yield strengths and ductilities of the face and core materials selected.

     2.   Determine the maximum plastic strains in the faces and core as the sheet is bent from the flat configuration to a final inside radius a_0 . Since the final inside bend radius is not known it is suggested that it be conservatively assumed equal to zero.

     To find the maximum plastic strains, which may occur at values of $(a_0/t_0) \geqslant 0$ we must first determine the variation of the circumferential plastic strains with (a_0/t_0) as follows.

     a.   Determine the instantaneous laminate thicknesses, (t_{f_1}/t) and (t_{f_2}/t) as a function of (a_0/t) from Equations (64) and (65).

b. Next determine the neutral axis location as a function of (a_o/t) from Equations (59) and (60) and the results of the previous step.

c. Determine the instantaneous thickness of the sandwich sheet as a function of (a_o/t) by integrating Equation (70).

d. The plastic circumferential strains as a function of (a_o/t) can now be obtained from Equation (69) and the information obtained in the previous step.

3. The maximum plastic strains in the core and faces, determined in the preceding step, are now used to approximate the number of cycles to failure. This determination can be accomplished by use of Equation (71), or from Figures 33 and 34 in the following manner. From Figure 33 determine a ratio (a_o/t_o) corresponding to the maximum plastic strain. With this ratio of (a_o/t_o) and the ductility of the material, determine the number of cycles to failure from Figure 34.

4. To obtain a multilayer configuration which will yield the largest number of cycles to failure, repeat the above computational steps for different core and face materials and dimensions.

Illustrative Problem No. 2

A bonded sandwich sheet having the following characteristic is to be used for a bladder.

$$\beta = \frac{\sigma_{xy}}{\sigma_{cy}} = .5$$

$$(t_{f_{1o}}/t_o) = (t_{f_{2o}}/t_o) = .2$$

ductility of face material = 85%
ductility of core material = 65%

It is desired to determine the number of fold and unfold cycles this bladder will sustain.

During each folding cycle, the sandwich sheet will experience local single folds. The inside bend radius at the fold is not known, however, it will be conservatively assumed that the minimum inside bend radius is zero.

a. For $(a_o/t_o) = 0$, maximum plastic strains are obtained from Figure 41. These strains are $e_{a_o} = 1.0$ in/in for the face and $e_d = .56$ for the core.

b. For this value of e_{a_0} = 1.0 and with the aid of Figure 33, a value of (a_0/t_0) = 0 is obtained and with e_α = 0.560, (a_0/t_0) is 0.4.

c. For (a_0/t_0) = 0 and a ductility of 85% for the face material, and for (a_0/t_0) = .4 and a ductility of 65% for the core material, the number of cycles to failure, N, by fatigue are obtained from Figure 34. The number of cycles are N ≈ 3.5 for the face and N ≈ 2.5 for the core.

SIMPLE BLADDER CONFIGURATION

The more common bladder configurations employed to date have the following characteristics.

Characteristics of Simple Bladder Configuration

Advantages

1. The bladder's low inertia and its large surface area is especially good for absorbing line shops.

2. It possesses the necessary fast action to take a high rate of flow.

3. It is an extremely simple device and long employed by other industries.

Disadvantages

1. The bladder material, during collapse, is susceptible to single and multiple folding or flexing with a resultant pin-hole or fracture development.

2. Compatibility requirements for the propellant and the bladder materials imposes a restriction on material selection, especially in the plastic and polymer class.

3. A diffuser or collector tube must be employed to eliminate bladder extrusion through a large exit port and to prevent fuel entrapment within folds of bladder.

4. The bladder device is direction sensitive and port opening or exit should be in the direction of the acceleration for maximum efficiency.

5. Inside surfaces of the structural container must be very smooth and free of any protuberances to insure extended life of this bladder during operation. Smooth contours will prevent chafing, tears, etc.

Analysis Data

External Collapse Pressures on Shells.

In the application of an expanded bladder as a positive expulsion device, the buckling or collapse of the bladder under and external pressure initiates expulsion of the fluid within the bladder. The external collapsing pressure of a bladder represents the initial pressure differential between the pressurizing gas medium and the start of the fluid expulsion flow.

The external pressure required to collapse a thin walled circular cylinder with hemispherical heads is shown in the Figure 42. This figure gives the buckling or collapse pressure as a function of diameter-to-thickness ratio, D/t, and length-to-radius ratio, ℓ/a, for any material. As ℓ/a approaches zero, a spherical container is approached which is the upper limit for the data presented.

For values of $\ell/a > 1$ the curves presented in Figure 42 were obtained from relationships derived in References 112 and 113 for the buckling of circular cylinders with simply supported edge conditions. Since, for the configuration under consideration, the hoop stress in the cylinder is greater than the stress in the sphere by a factor of two for the same material thickness, it is reasonable to assume that the spherical shell ends will provide sufficient elastic support to the cylinder so that it can be considered as simply supported.

For very short cylinders, $\ell/a < 1$, it is substantiated in Reference 114 that the cylinder buckles essentially as a plate. A comparison of the results given for very short shells in Reference 114 and for spherical shells in Reference 115 reveals that there is a range of ℓ/a values for which very short cylinders will buckle at an external pressure which is greater than that for the sphere. From these observations it can be concluded that in the range of $0 \leq \ell/a \leq 1$ there is a buckling interaction between the sphere and the cylinder. The external collapse pressure in this range of ℓ/a was approximated by interpolation between the collapse pressure derived for a spherical shell in Reference 115 and that for cylinders with $\ell/a > 1$. The results presented in Reference 114 for very short cylinders were employed as a guide in the interpolation process.

SPHERICAL REVERSING BLADDER

A pliable bladder-tank configuration with some unique features is shown in Figure 43. In this approach, an internal ring is provided that is installed inside the bladder, approximately at the tank equator and perpendicular to the direction of the outlet
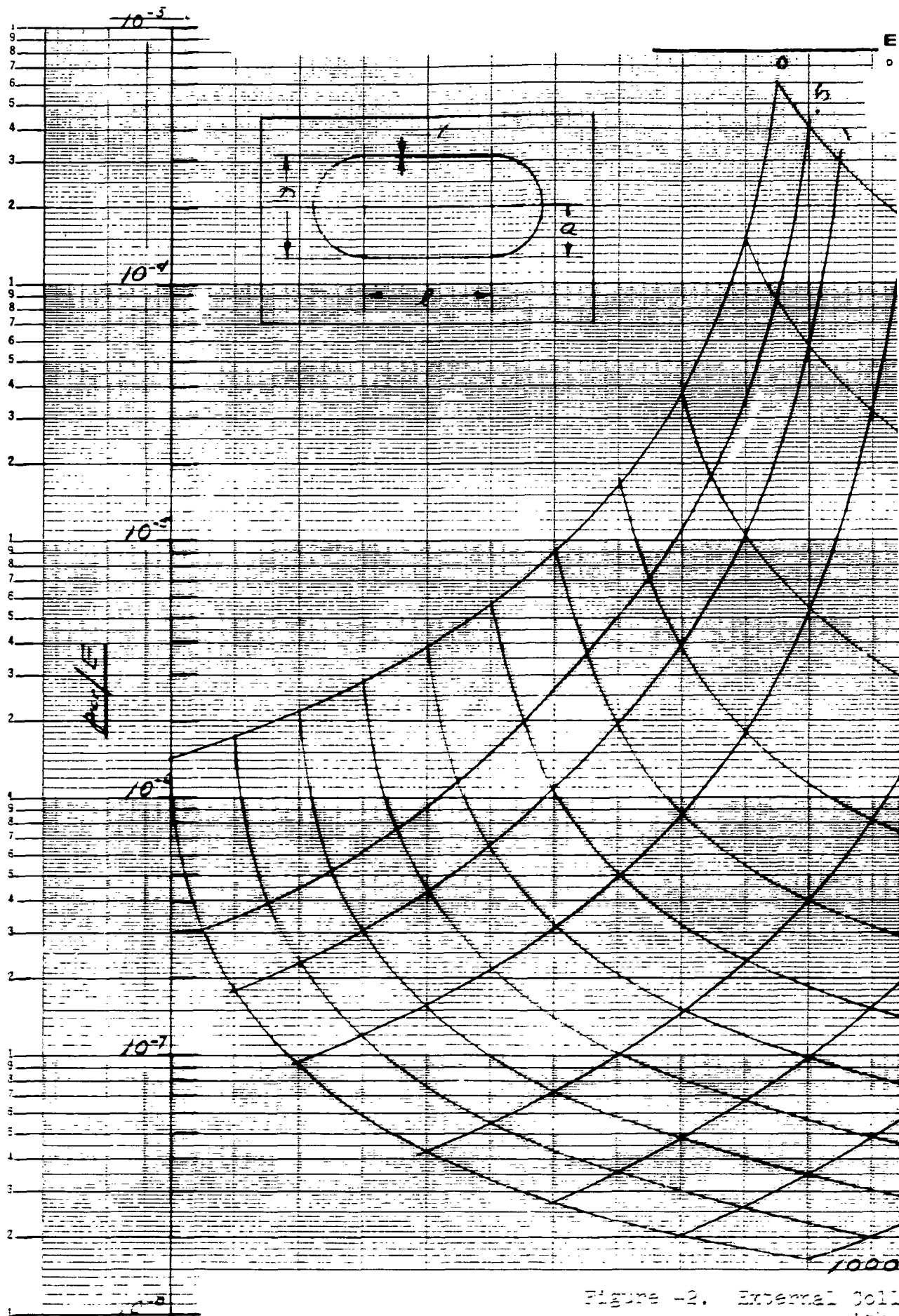
Figure -2. External Coil
with
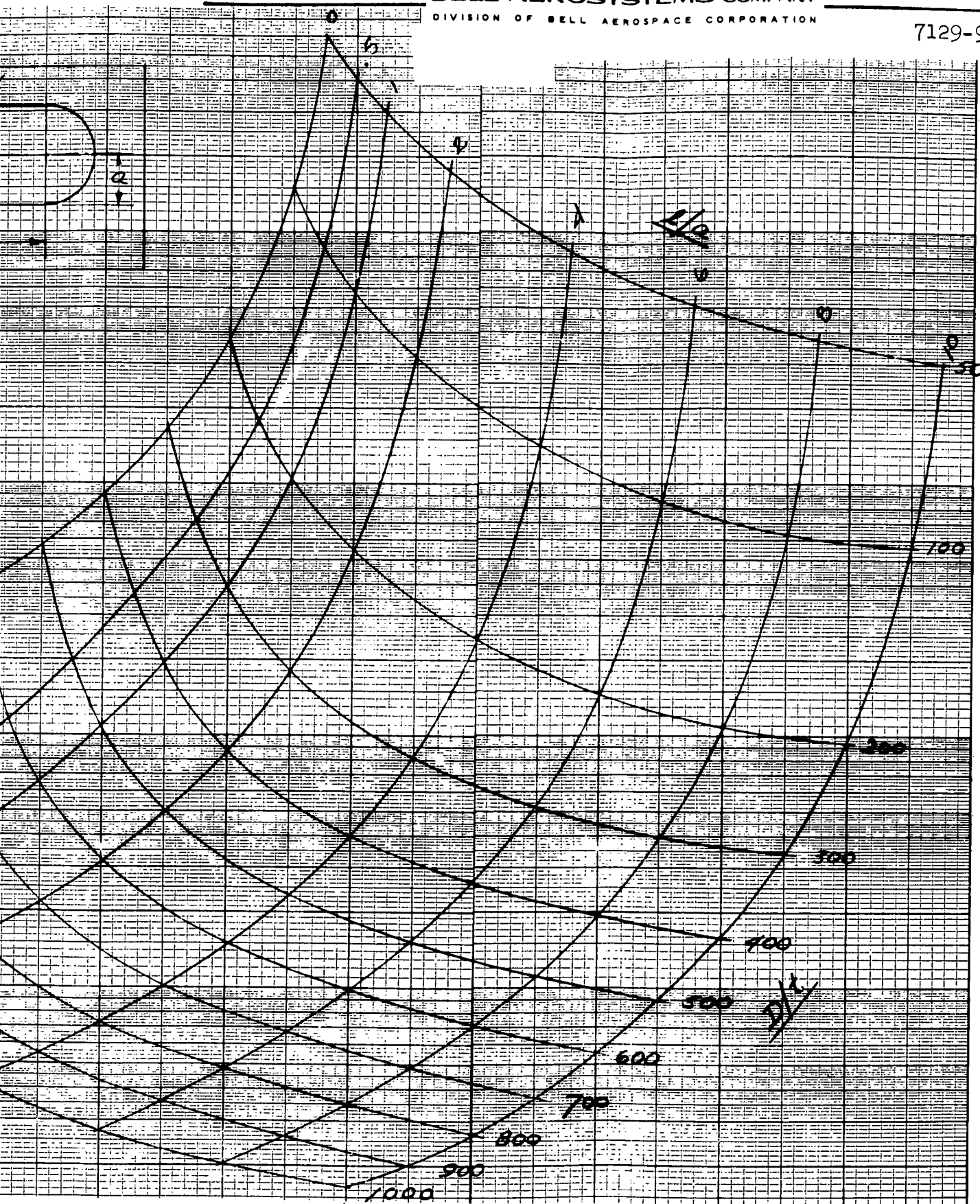
Figure 42. External Collapse Pressure for Circular Cylinders
with Spherical Ends

flow. An access port is provided to install the bladder and the
ring. The ring, which is a segmented unit capable of being folded
so that it can be inserted through the access port opening, is
sized and adjusted to hold the bladder against the tank. The ring
is installed after the bladder has been inserted into the tank.

During the expulsion cycle, the bladder acts in a manner similar
to a diaphragm. As the expulsion cycle progresses, one-half of the
bladder will collapse and traverse through the tank center and
towards the propellant outlet port. At the end of the expulsion
cycle the bladder will then be folded within itself in a manner
concentric hemispheres jointed at their common base.

For the sperical reversing bladder device depicted in Figure 43,
the following characteristics are apparent.

Characteristics of Spherical Reversing Bladder

Advantages

1. Only one-half the bladder is completely collapsed and
flexed, thus reducing the number of folds and creases.

2. A heavy external equatorial flange is not required
to join the two tank halves.

3. A diffuser outlet tube is not required thus reducing
folds of the bladder around the tube.

4. With the incorporation of a pliable bladder material,
numerous expulsion cycles are possible.

Disadvantages

1. Installation of the segmented ring could produce
installation difficulties for the smaller tank capacities.

2. The inherent features of the device restrict the
bladder to a very pliable material and their associated environ-
mental limitations.

3-CELL COLLAPSING BLADDER

An illustration of the 3-cell collapsing bladder is shown in
Figure 44.
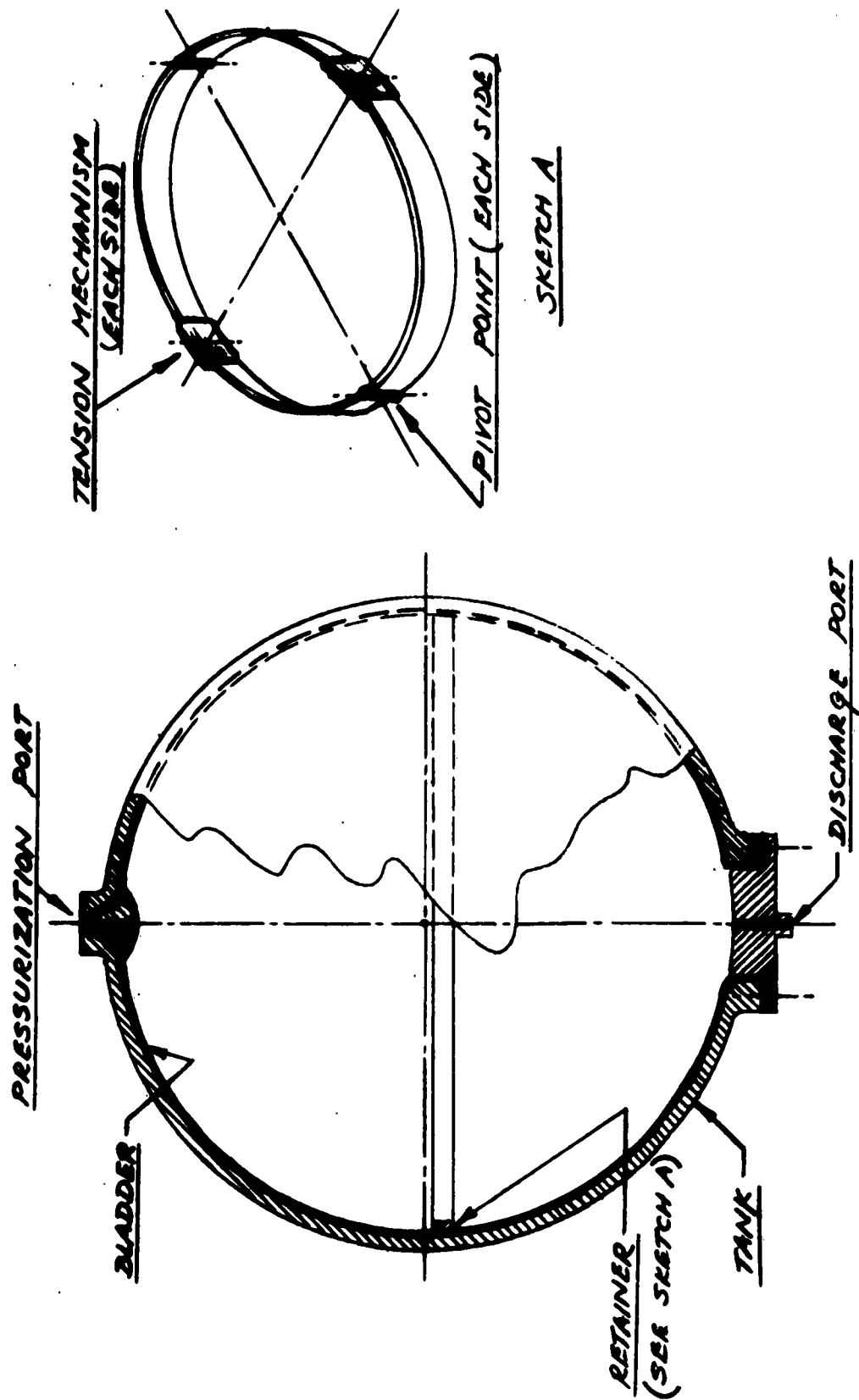
Figure 43.   Spherical Reversing Bladder
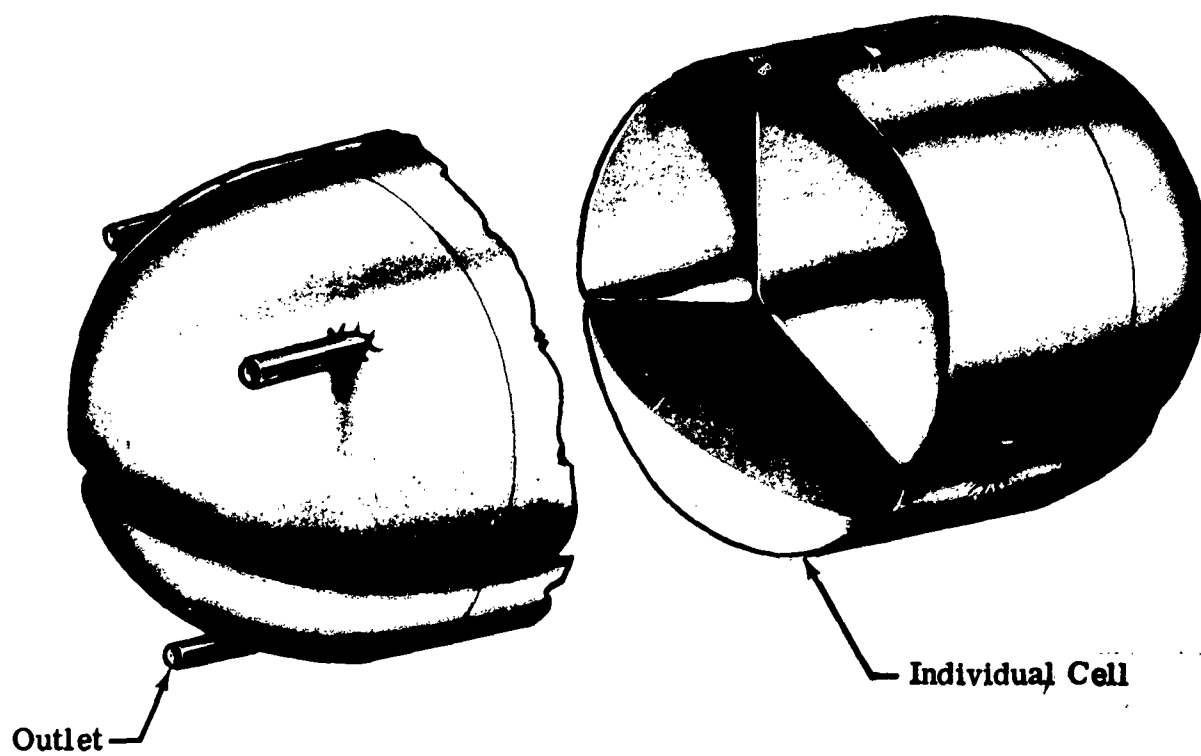
Figure 44. Three-Cell Collapsing Bladder

Characteristics of 3-Cell Collapsing Bladder

Advantages

1. Creases or folds produced in the three metal bladders during explusion are not likely to be detrimental to the operation as in one large unit.

2. The collapse procedure of the bladder is favorable because an elongated collapsed length around the inside tank periphery is formed.

Disadvantages

1. A weight penalty is incurred due to three separate tank or bladder installations.

2. The three units increase welding lengths required and require unit assembly prior to installation within main tank.

3. Outlet manifold must be welded to bladders and main tank head which may produce some manufacturing and fitting difficulties.

PREFORMED 3-LOBE EXPANDING BLADDER

A representative 3-lobe expanding bladder is shown in the lower portion of Figure 26.

Characteristics of Performed 3-Lobe Expanding Bladder

Advantages

1. The initial buckles occur to the point of instability or snap-through for the lobes and thence bladder tends to act like a membrane.

2. The prefold or flute has a material length equivalent to the inside circumference of tank so that no material stretching is produced.

3. The shape of the manufactured lobes provides stiffness in handling during assembly.

Disadvantages

1. Fabrication is not a simple procedure.

2. Propellant outlet may become blocked during the expansion process of the bladder and a collector tube may be required.

3. Ullage volume may be excessive depending on tank size and head shape.

DUAL CONCENTRIC BLADDER

A sketch of the dual concentric bladder configuration is shown in Figure 45. The unit incorporates an expanding and collapsing bladder within one structural container.

Characteristics of a Dual Concentric Bladder

Advantages

1. Oxidizer and fuel are within one tank envelope so that the minimum volume or space is used. An additional tank, with its heads, is thus eliminated.

2. The use of longitudinal corrugations or convolutions for the fuel expulsion system makes the unit reliable and efficient because little internal pressure is required for the corrugated cylinder to expand and attain a circular shape.

3. The oxidizer bladder is a long circular cylinder and does not require high external pressures to buckle and collapse.

Disadvantages

1. The drawing or forming of the convolutions or corrugations that blend into a circular cylinder at the ends will require special study, tooling or dies.

2. The collapsing bladder, due to its smaller diameter at the ends, may have to be of multiple construction; a rolled-sheet tube section and formed of spun ends. This will require an appreciable amount of welding.

3. The attachment of the bladders to the tank heads produce "dead-volume" that may produce an ullage greater than required.

4. Tank assembly with the bladders inserted is not a simple process.

5. Control of the system (fluid mass ratios) may be a problem because the collapsing and expanding bladders could require differing and varying expelling pressures.

6. If both bladders failed during an expulsion cycle an explosion would undoubtedly result if hypergolic propellants were employed.

Center Outlet

(Expanding) Outer Bladder

Inner Bladder (Collapsing)
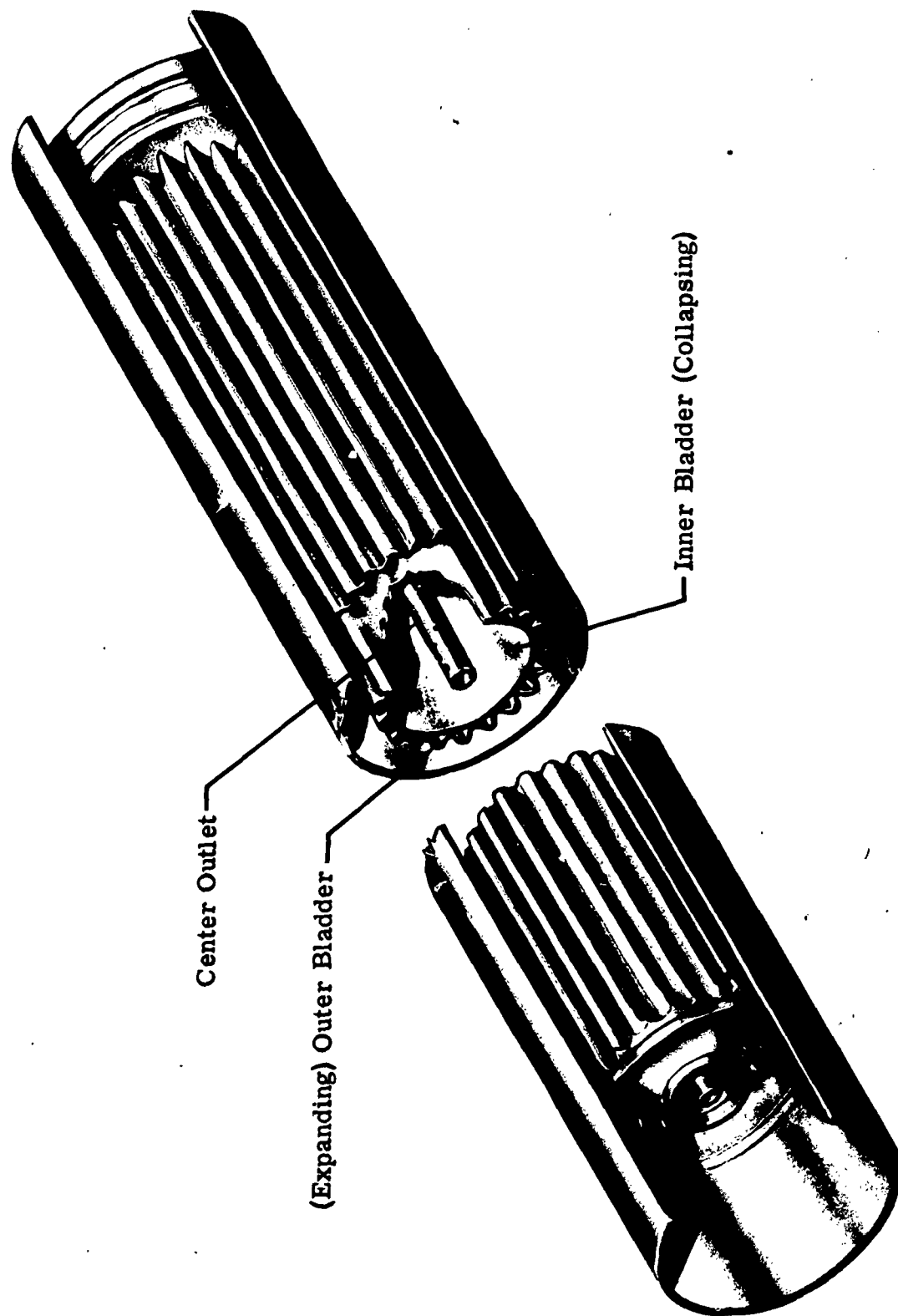
Figure 45. Dual Concentric Bladder

MECHANICAL SYSTEMS

A mechanical system can be considered as a unit governed by kinematic principles amenable to direct quantitative calculations. This category would include:

1. Piston

A piston is a sliding member, usually a short cylinder moving within a cylindrical vessel. The motion is imparted to the piston by a piston rod (axial slide shaft) or by a screw thread shaft. A free floating piston is considered to be shaftless and under a fluid pressure on each face.

2. Squeeze Tube

This design constitutes a tube that is squeezed between a roller and plate or between two rollers. In a sense it is equivalent to a toothpaste tube that is squeezed to expel the contents within the tube.

3. Twisting Tube

In this conception, the colapse of the tube is initiated and continued by imparting a rotary or twisting motion at its ends. The twist induces a wrinkling in the tube and a consequent decrease in diameter. The twisting configuration resembles the appearance of the wringing or twisting of clothes to eliminate the water.

4. Rotating Tank and/or Fluid

The application of the centrifugal force principles is another means of obtaining a positive expulsion feed device. One such system is basically an inverted centrifugal pump. Here it is meant that the impeller is stationary and the pump body, in this case the propellant tank, is revolving.

PISTON DEVICES

The sketch of the piston tank device shown in Figure 46 possesses the following features.

Characteristics of Piston Devices

Advantages

1. It is an extremely simple device that does not require a great deal of research and development time.
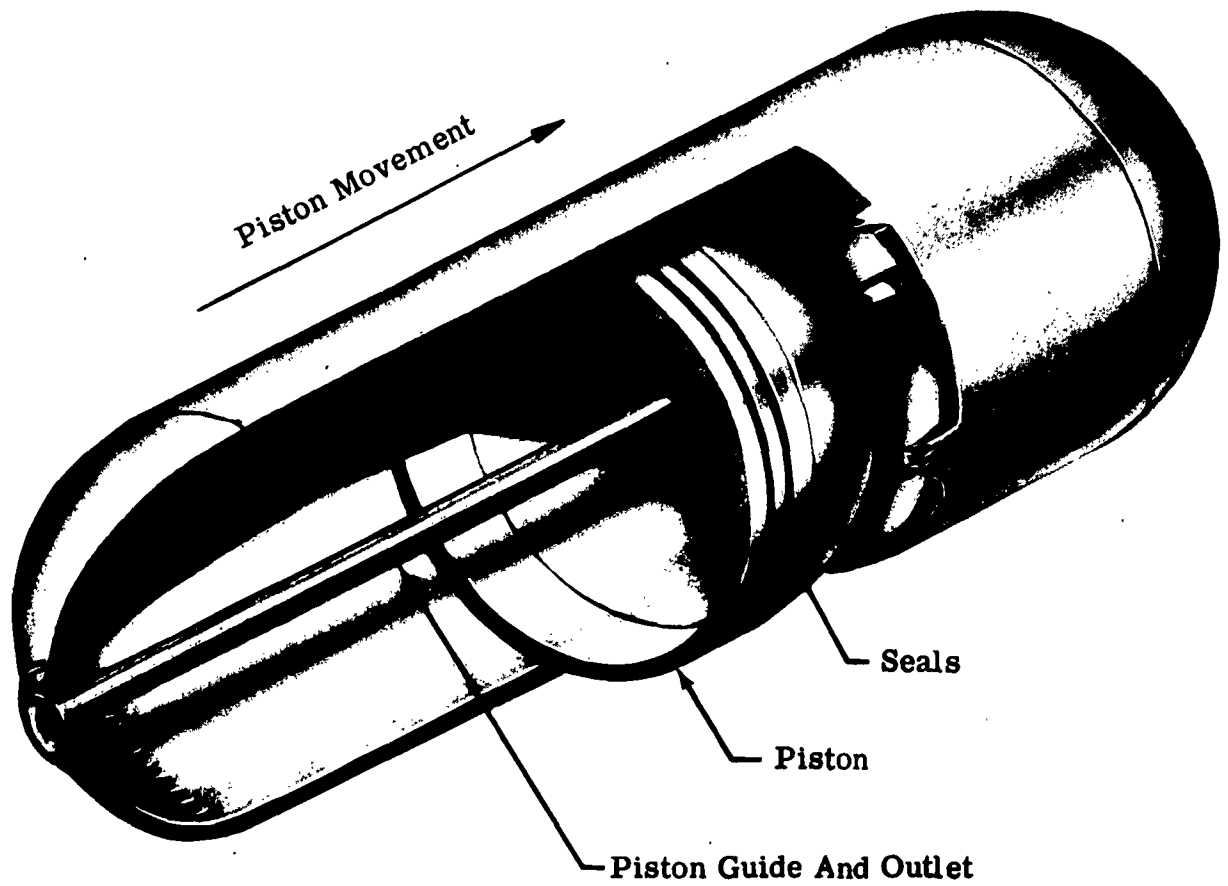
Figure 46. Piston Tank Device

2. The system is reliable and capable of cyclic operation, including full expulsion cycles.

3. It is possible to predetermine the required pressure accurately as well as the fluid flow.

4. Sloshing is not present because the cylinder is always full and pressure is resisted by the stiff chamber walls and piston.

5. For a dual piston configuration, piston for fuel and piston for oxidizer can be mechanically interconnected and sized so that proper mixture ratio and control is always assured.

6. The incorporation of a floating piston eliminates the piston rod and the associated length increase.

Disadvantages

1. Thick walled cylinders are required for stiffness and fit thus invoking a weight penalty.

2. The incorporation of a piston rod adds length to the over-all expulsion device configuration.

3. Change of environmental conditions will affect seals, fits and sliding. Thus if a piston rod is employed, the aft piston and cylinder is open to spark environment.

4. Tolerances and machine surface finish may be critical, especially on large size configuration.

5. Piston configuration must have adequate length to diameter ratio to prevent cocking or jamming.

6. A flat head configuration is desirable but it induces a weight penalty to sustain the pressure loads.

PRESSURE-BALANCED PISTON DEVICE

A piston and cylinder with a double shell construction provides a pressure balanced inner shell. The outer shell acts as a protective cover to insure that damage inflicted through rough handling will not interfere with the free movement of the piston. The outer shell also acts as a gas container.

Characteristics of Pressure-Balanced Piston Device

Advantages

The advantages of the pressure-balanced piston device are the same as for the conventional piston configuration with the following additional characteristics:

1.   The pressure-balanced inner wall acts as a guide for the piston with little load on it to deform radially. As a result, sealing between piston and cylinder is not as critical as in the conventional piston design.

2.   The double wall also provides additional bending stiffness to over-all configuration.

Disadvantages

1.   Incorporation of flat heads on cylinder incurs a weight penalty and yet a flat head is desirable for such a combination.

2.   The double wall contributes an additional weight to the cylinder.

3.   Attachment of inner cylinder to heads may present a problem area because it is essential that transmission or head loads do not distort the thin inner shell.

FLOATING PISTON WITH BOURRELET

The piston resembles a ball that maintains a press fit in the circular tube. As shown in Figure 47 the so-called piston skirt is replaced with a bourrelet similar to those employed on artillery shells. The bourrelet will provide an interference fit as the piston travels along the tube, expanding the tube along its travel path and providing a seal between the tube wall and piston.

Characteristics of a Floating Piston With Bourrelet

Advantages

1.   Fluid container can be any smooth shaped cylinder such as a torus or part of a torus, ellipse, etc.
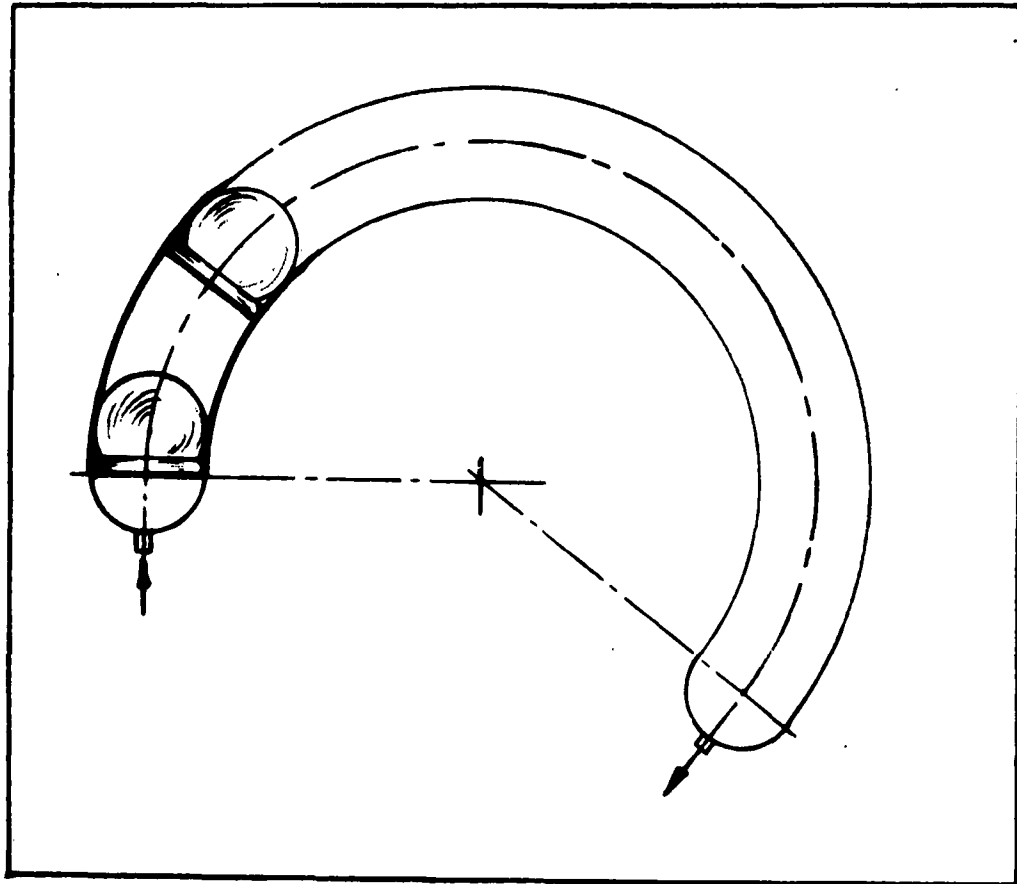
Figure 47.   Floating Piston with Bourrelet

2. Concentricity or circularity of tube is not as critical as in conventional piston device because of the initial press fit involved for the ball with bourrelet.

3. Unit is most efficient for continuous operation and rapid expulsion (fast time).

4. No seals are required other than the press fit.

Disadvantages

1. The device is a "one-shot" configuration.

2. Restraints or support points for the installation of the device could induce restrictions on tube expansion during operation.

3. Unit is restricted to low pressures because of the balance that must be maintained between the expansion of the tube by the ball and bourrelet and the expelled fluid pressure.

4. The pressure differential on the floating piston is relatively high because of the energy required to expand the tube in which it rides.

SQUEEZE-TYPE CONFIGURATIONS

The rotary squeeze-type configurations shown in Figures 48 through 50 are rather simple devices in principle. Fluid transfer is accomplished by a rotor mounted on an eccentric shaft which rotates within the squeeze tube geometry. This creates a progressive squeegee action on the fluid trapped between the liner of tube and the inside of the rigid body.

Rotating Squeegee Type Devices

Several designs of a rotating squeegee type expulsion device are indicated in Figures 48 through 50. It should be noted that Figure 48 is a slight revision of a commercially available pump that employs this flexible tube concept and uses double rotor for pumping.

Characteristics of Rotating Squeegee Type Devices

Advantages

1. Transfer of slurries is possible

2. No contact of parts with the material being pumped.

FILL & DISCHARGE

BLEED
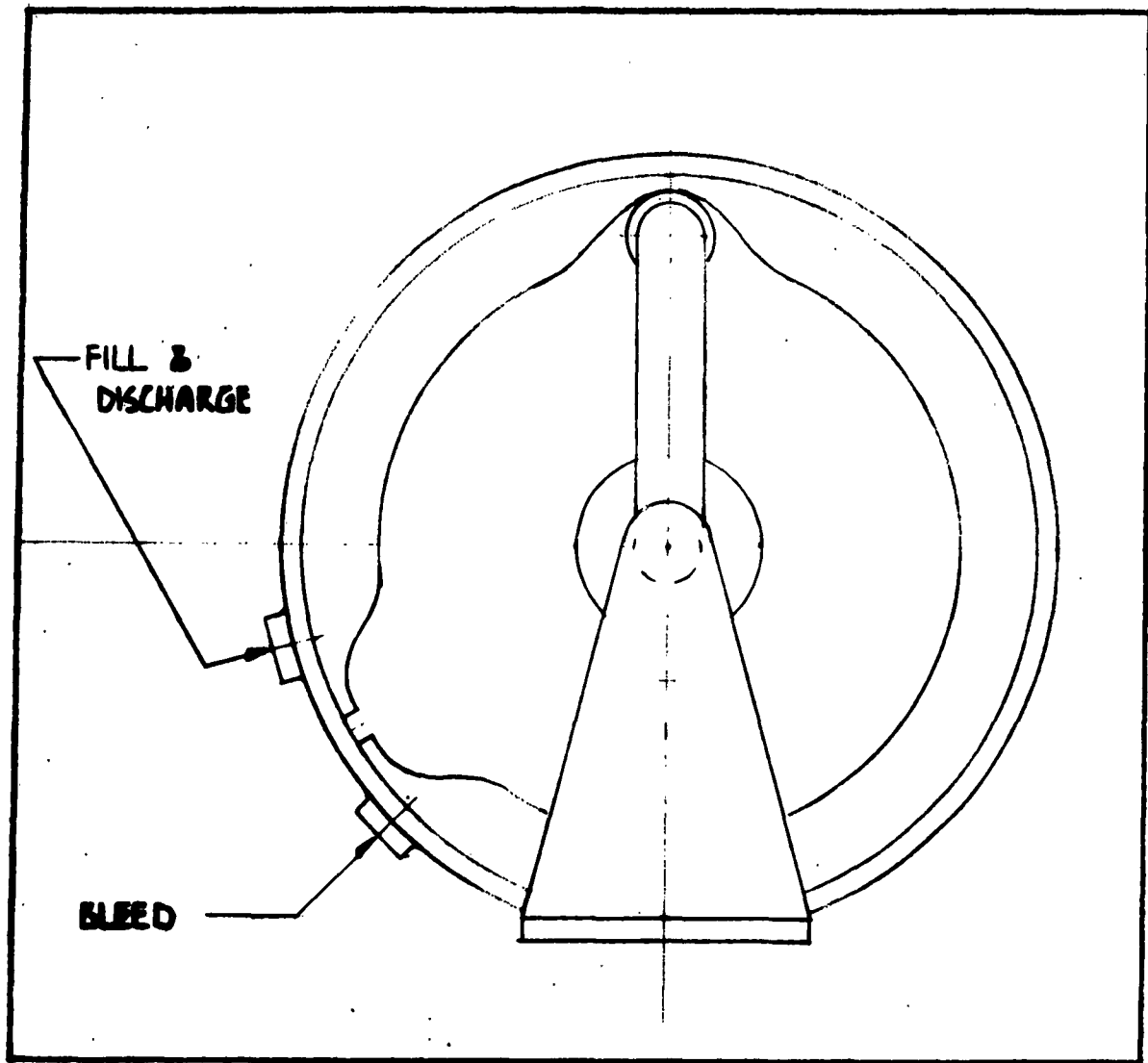
Figure 48.   Rotating Squeegee Type Device - Single Tube
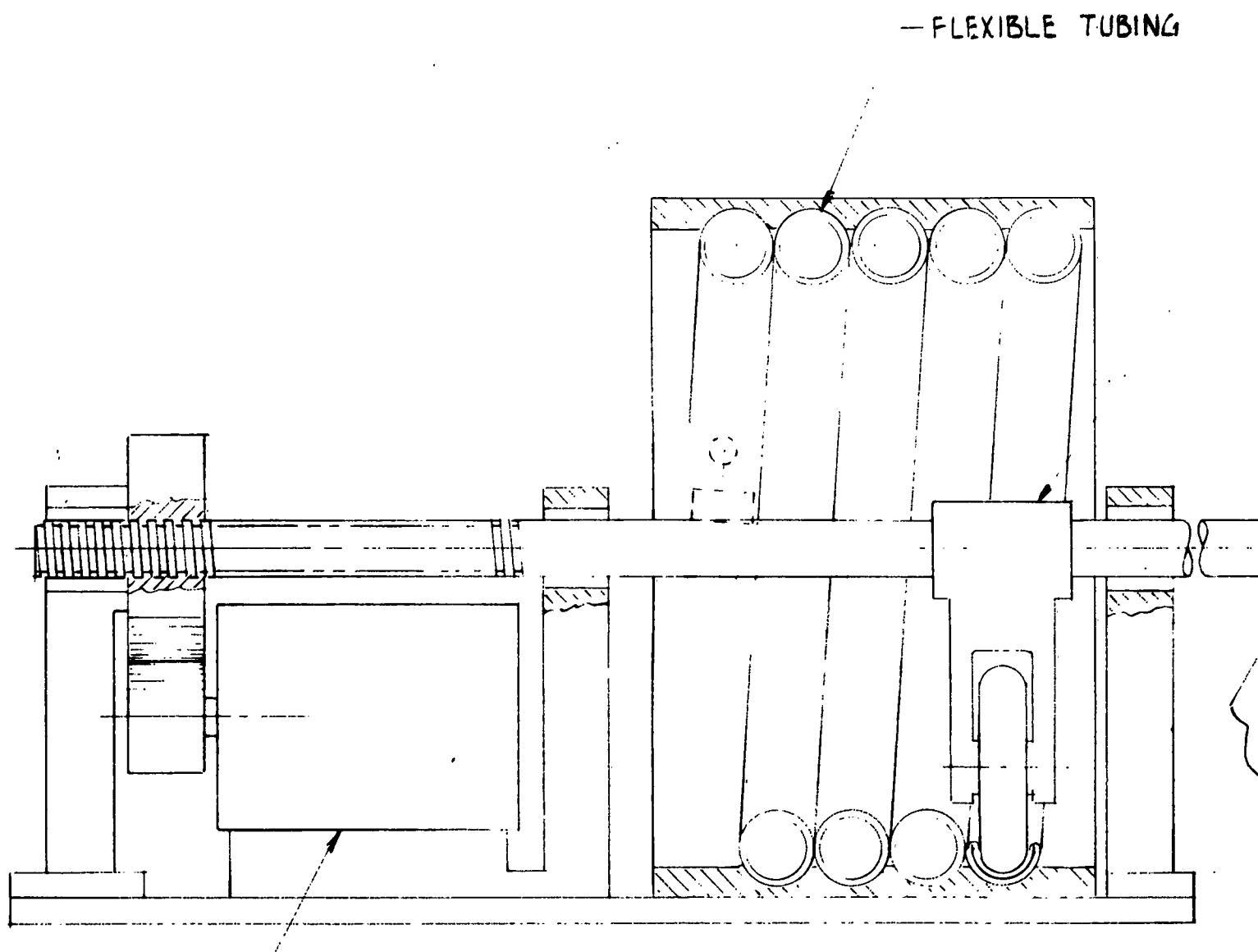
—FLEXIBLE TUBING

—GEAR MOTOR

1

FLEXIBLE TUBING

ROLLER MOUNT
FASTENED TO SHAFT
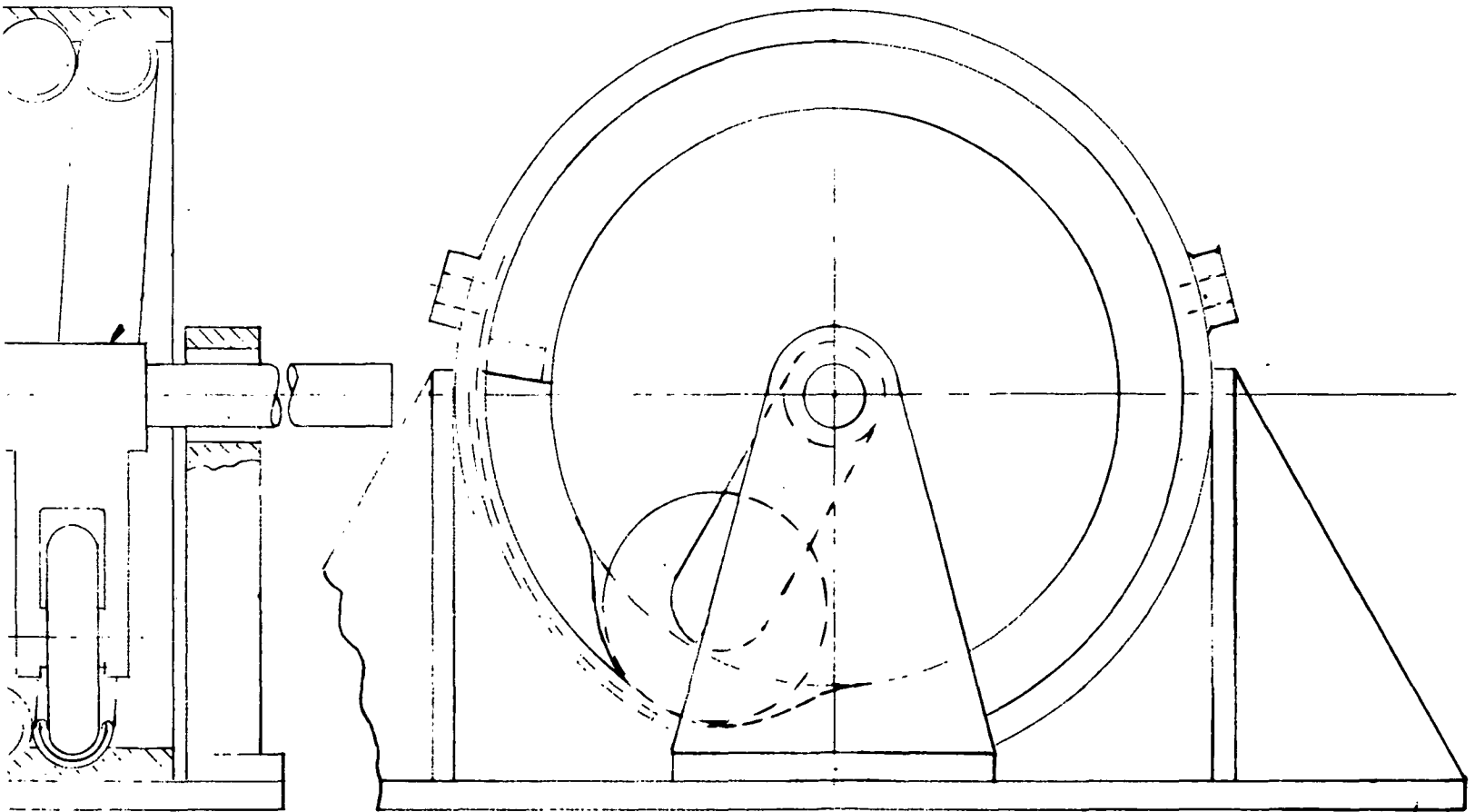
Figure 49.   Rotating Squeegee Type Device - Multiple Tube

BLEED

FUEL OUTLET
& FILL

SECTION B-B

B

B

A

MET

1

METAL DIAPHRAGM

SECTION A-A

2
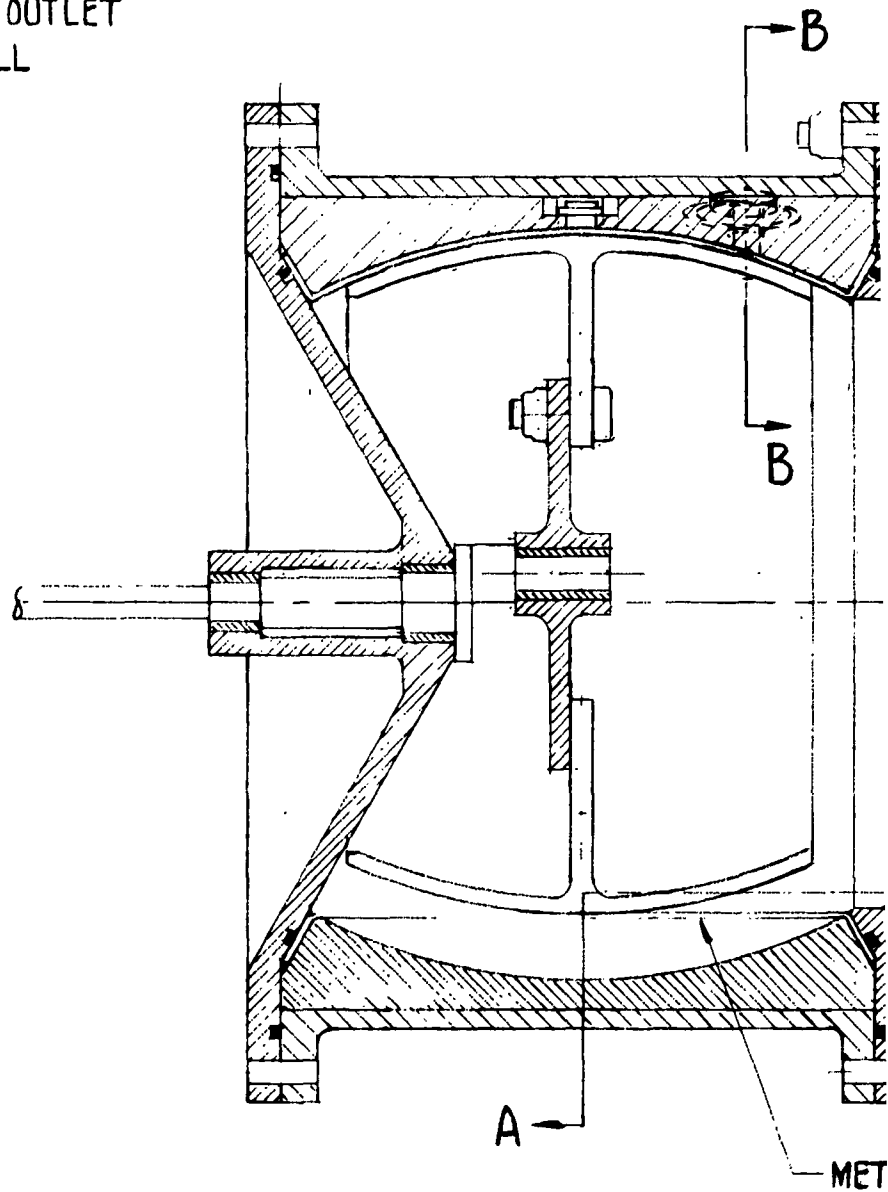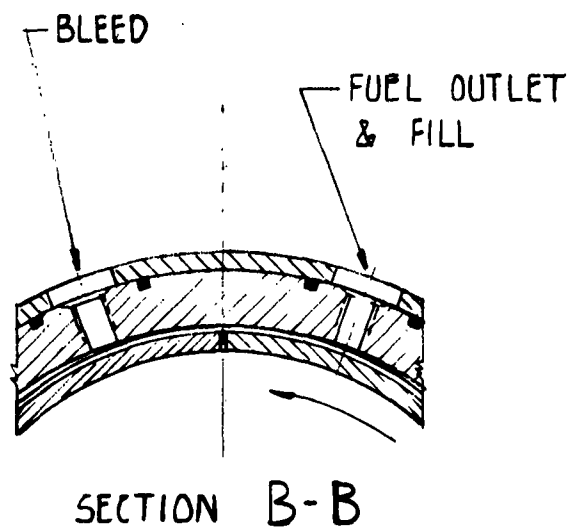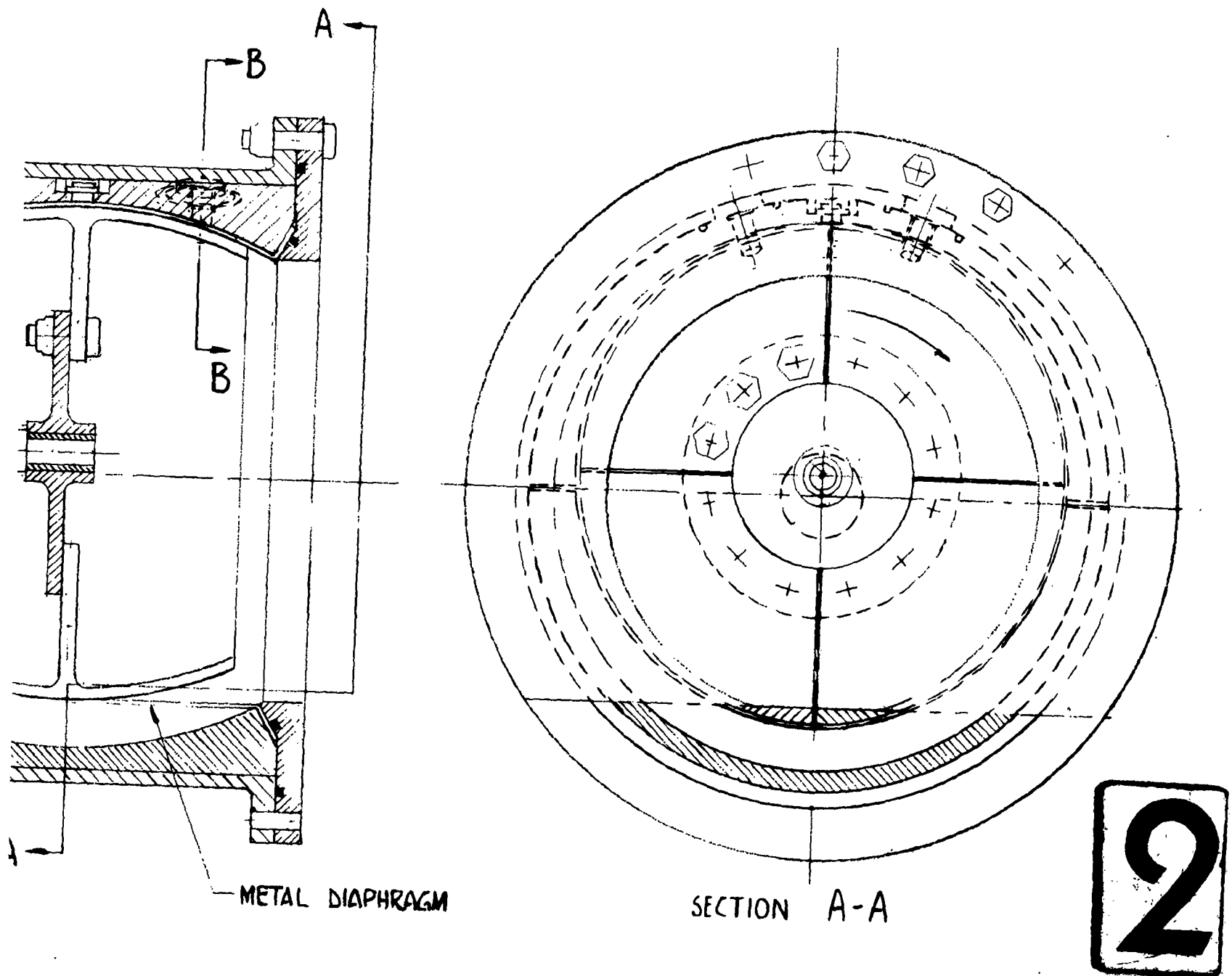
Figure 50.   Rotating Squeegee Type Device - Diaphragm

Disadvantages

1. Volume capacity is limited in comparison with the volume of over-all device.

2. The system possesses leakage when held in a given position for a length of time. Tube collapse by squeegee action is not complete and the small r/t in flattened tube is a source of leakage and pressure drop in the hold position.

3. Tube wall must resist the total fluid pressure.

TWISTING BLADDER

A presentation of a twisting bladder concept is indicated in Figures 51 and 52. The former diagram induces twist in a so-called uncontrolled manner whereby the ends are restrained from axial deformation. In the latter configuration, the shortening effect of the twisting bladder is not hampered by any axial restraint, except those due to friction forces. The pitch of this axial lead screw shown in Figure 52 is selected in such a manner that the axial contraction of the tube or bladder due to applied torque force is equal to the axial displacement produced by the head of the lead screw.

ROTATING TANKS

An illustration of a possible rotating tank construction is shown in Figure 53. Its major characteristics are given below.

Characteristics of Rotating Tanks

Advantages

1. Multiple restarts are available.

2. Gas-liquid separation is an inherent characteristic of the system.

Disadvantages

1. For very large tanks, a relatively large amount of energy will be required to obtain the desired acceleration forces.

2. Stopping a large rotating mass would produce undesirable end effects.

3. Safety hazards may be created by a rotating tank in the proximity of an orbital complex.

PRESSURE
EQUALIZER

BLADDER FILLED

BLADDER

APPLY
TORQUE

1

BLADDER EMPTY

PROTECTIVE COVER

ED

FUEL OUT
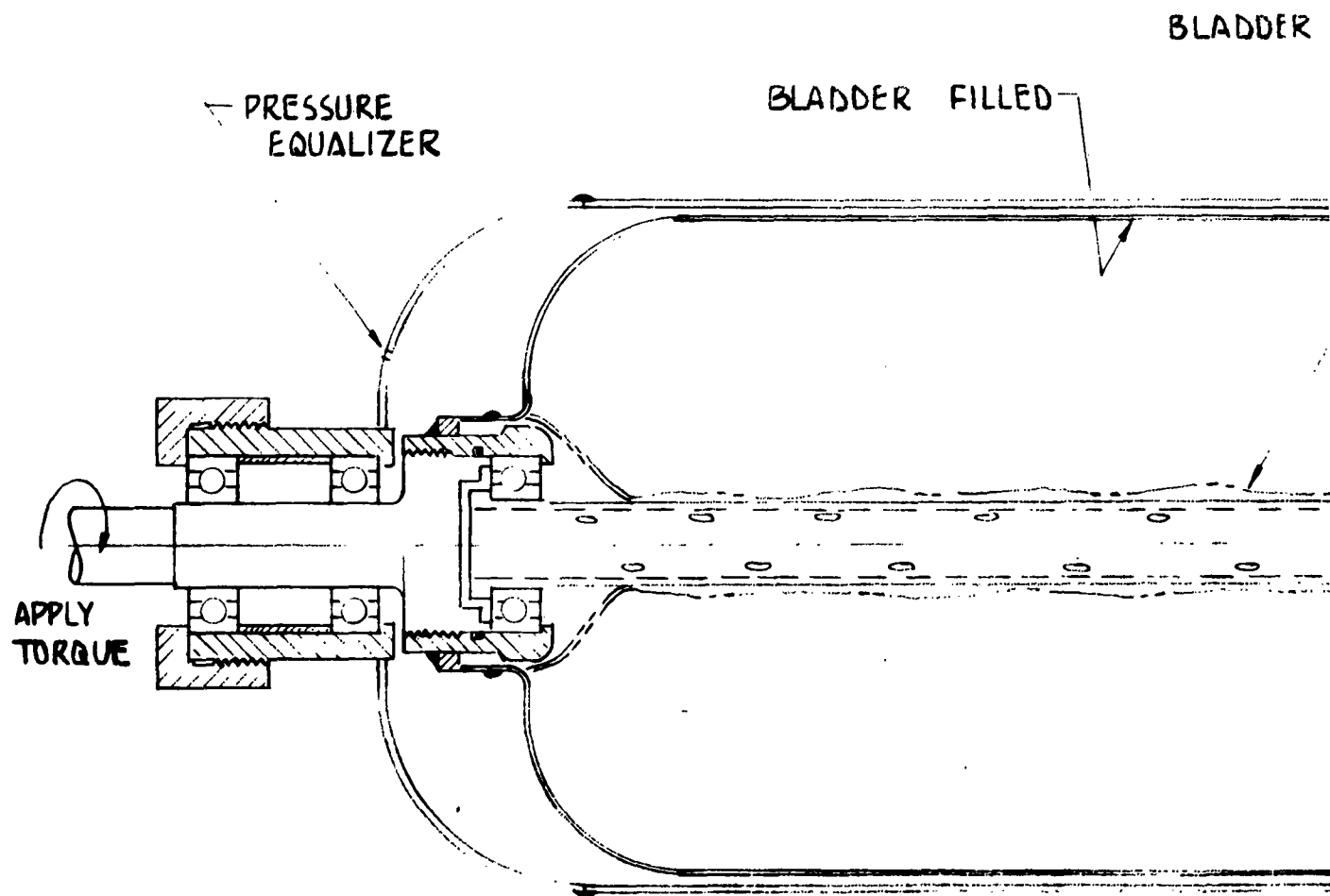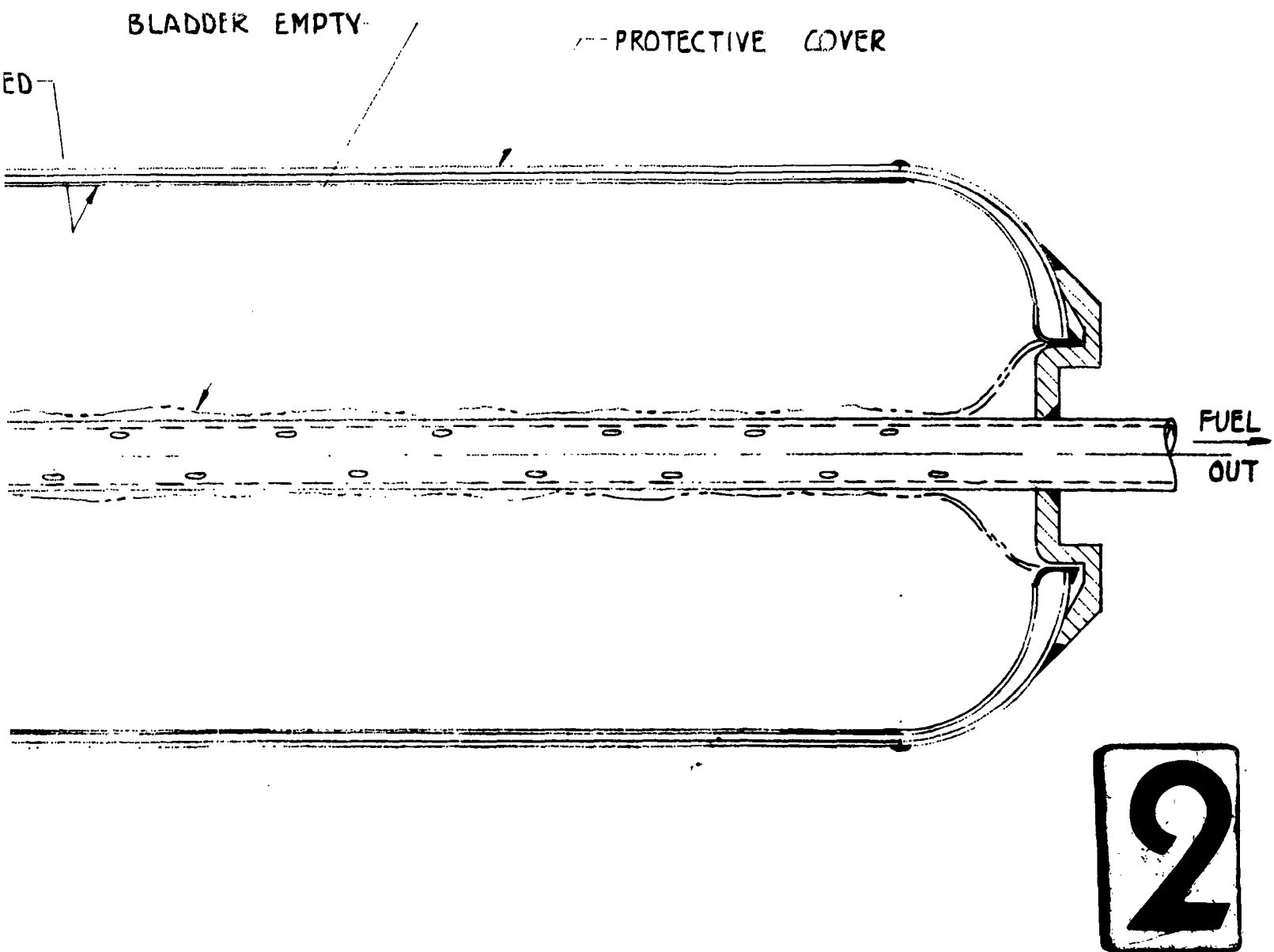
Figure 51.   Twisting Bladder - Uncontrolled
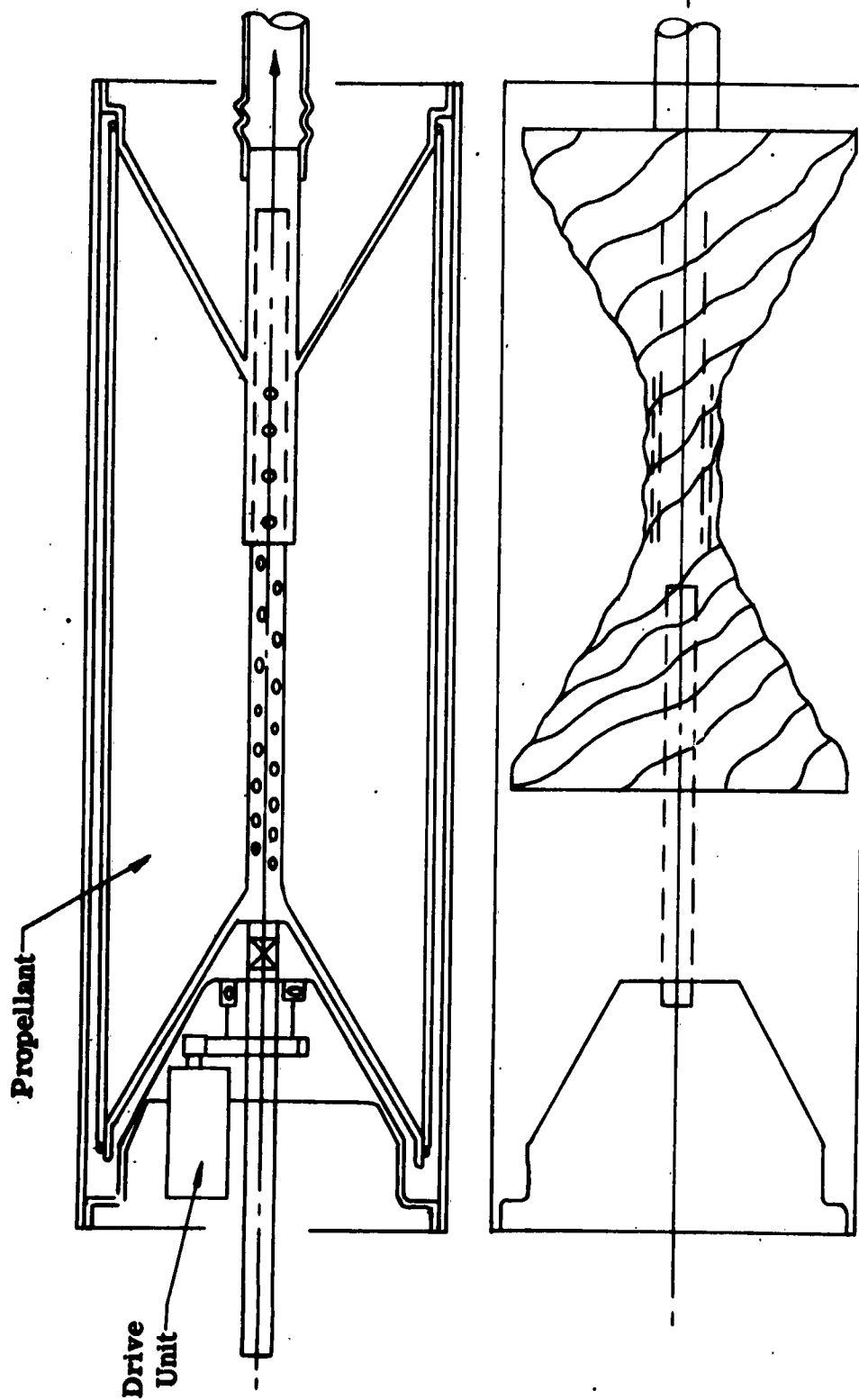
Figure 52. Twisting Bladder (Controlled)
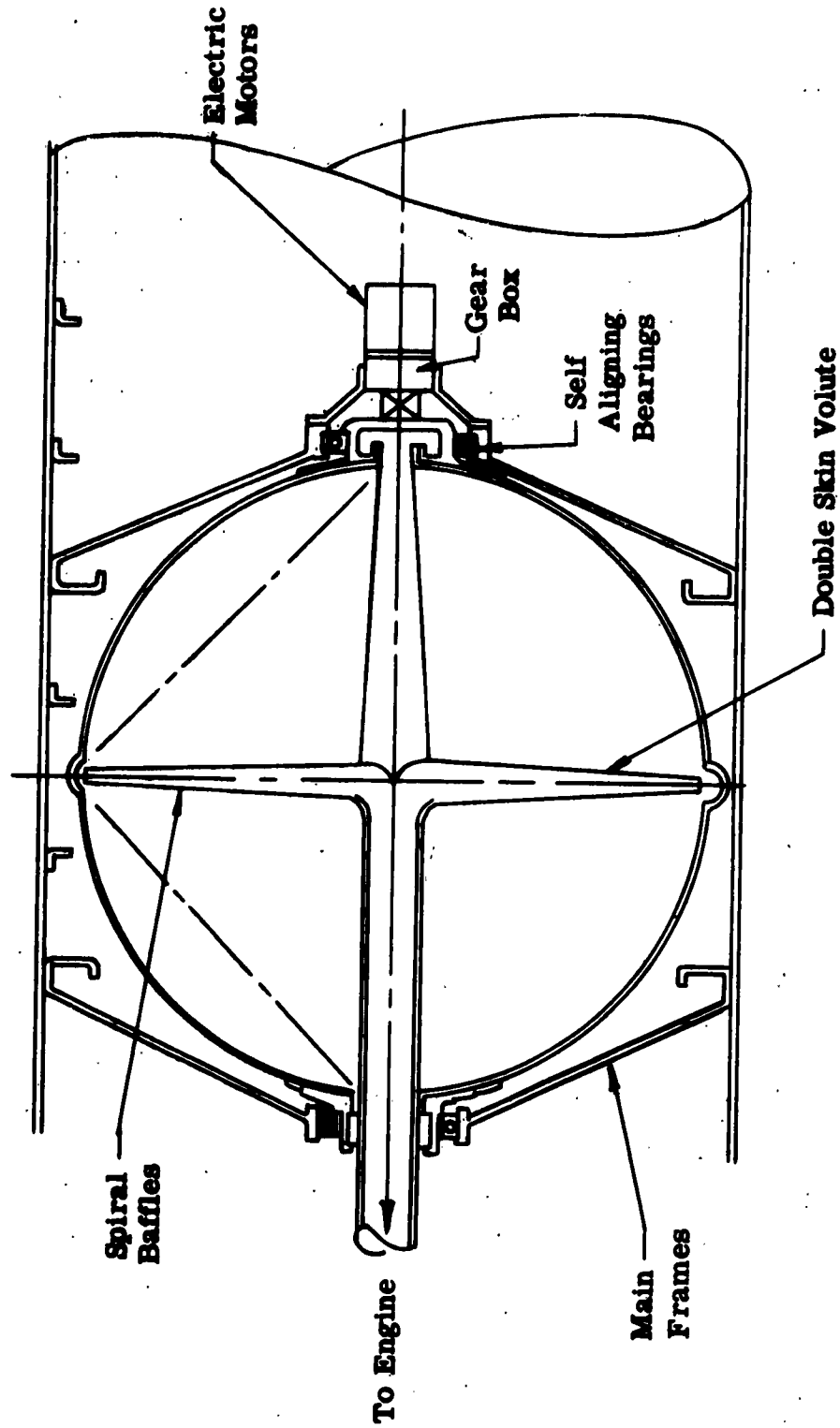
Figure 53. Rotating Tank

SURFACE FORCES

An expulsion device utilizing surface forces consists of two principal components; one component serves for the containment of the liquid to be expelled and the other is a displacing system. The nature of the containing system excludes the use of bladders or pistons for displacement. A containment system based on surface forces can be defined as a system which utilizes the adhesive force between liquid and solid and the tendency of the free liquid surfaces to assume a shape of minimum surface-energy for the confinement of the liquid into a given space.

Use of surface forces for containment is based on analytical and empirical evidence. If a liquid which wets the walls of its container is brought into a zero-gravity field, then the liquid will adhere to the wall and a void within the liquid will contain vapors and gases. On the other hand, if the wall-liquid constitutes a non-wetting combination, then the vapors and gases will contact the wall, while the liquid will aggregate inside of the bubble, away from the wall.

The distance to which the liquid moves in a capillary tube and wick is a function of the surface tension of the liquid, the contact angle between the liquid and the solid surface, the radius of the passage, the liquid density and the acceleration.

In the expression for capillary rise, the gravitational acceleration appears in the denominator. Theoretically, in the zero-gravity environment, one would expect an infinite capillary rise in an infinite capillary tube. In a finite tube, however, the liquid may rise only to the end of the tube and perhaps beyond.

    1.   Capillary Tubes

In the capillary action concept, capillary tubes of wetted material are places as a parallel bundle into that end of the container which adjoins the intake to the engine. The height of the bundle is determined by the volume of liquid necessary for initiation of a safe restart. The diameter of the capillary tubes is determined by the height of the liquid column to be contained, by the highest adverse axial acceleration imposed by the reaction control system during coasting, by the adhesion between capillary and liquid, and by the surface tension of the liquid.

    2.   Wicks

A wick can be considered as composed of randomly oriented capillary tubes of varying lengths and small diameters. The liquid rise in wick materials is similar to that in a capillary tube but is a far more complicated case.

The wick material itself must satisfy several criteria for application as an expulsion or containment device.

a. The storage capacity of the material for the fluid should be high.

b. The rate of rise of a liquid should be high.

c. The material should have a low density.

d. The material should be compatible with the fluid.

e. The material should be easily wetted.

f. Within the given operating range, the temperature dependence of the material properties shall not interfere with the operation.

3. Containing Grids (Screens)

The containing grids are in effect very short bundles of capillaries. They are places in the container at a point where adequate propellant will be trapped and maintained for engine restarting. The containing force consists of the adhesion between the liquid and the wires of the grid and by the surface force on the curved free surface of the liquid as bounded by the mesh. The greater the force on the free surface, the smaller the mesh required. The mesh width is determined by the same factors as a capillary tubes diameter. These are by the height of the liquid volume to be contained, by the highest adverse axial acceleration, by the adhesion between the mesh and liquid and by the surface tension of the liquid.

Information obtained at ASRMPE supported the contention that a wetting liquid will rise up to the grid and not cross it if exposed to a zero gravity. The grid tested has been placed slightly above the level of the water used in the tests. The gas, originally between water and grid, receded into a void in the bulk of the water.

CAPILLARY TUBES

The capillary tube concept of fluid movement is not new and capillary studies are undergoing laboratory tests by several organizations. The Jet Propulsion Laboratory at the California Institute of Technology is performing such theoratical laboratory tests.

Characteristics of Capillary Tubes

Advantages

1.   It is effective in the separation of the entrained gas from the liquid.

2.   No outside energy forces are required for operation.

3.   The possibility of utilizing sandwich cores as bundles of capillary tubes would produce simplified construction.

Disadvantages

1.   Flow resistance of capillary bundles is high.

2.   The system is sensitive to acceleration forces and the result could induce oscillatory motion to the fluid within the capillary tube.

3.   The pumping capacity is small.

WICKS

Characteristics of Wicks

Advantages

1.   No entrained vapors or gas bubbles are present.

2.   A natural phenomena is utilized that requires no outside energy sources for operation.

Disadvantages

1.   The time to reach equilibrium height in a wick material is greater than that for the same liquid in a straight tube. (The liquid has to travel through a large number of small passages oriented in all directions.)

2.   Flow resistance is high.

3.   Transport quantity of fluid is small.

ORIENTATION SYSTEMS

Orientation or containment of the fluid is either an inherent characteristic of an expulsion device or it must be provided within a specified location or area so that fluid movement only can be assured.

A liquid is said to be contained or oriented if it is at a given time in a predetermined part of its container. It could be assumed that the acceleration during the (n-1)-st restart oriented or transported the liquid to be contained into the space where it is expected to be at the time of the n-th start. The containing device should prevent the propellants escape during coasting of the vehicle and should not impede with the expulsion of the propellant during any period of the powered trajectory. Bladders, diaphragms and piston devices possess this inherent characteristic of containment.

Two typical orientation systems are

        1. Ullage Rockets
        2. Trap or Surge Tank

ULLAGE ROCKETS

The firing of an ullage rocket induces thrust and an associated acceleration. The resulting acceleration or inertia field provides the necessary forces for settling of the fluid at a prescribed location within the tank.

    Characteristics of Ullage Rockets

      Advantages

1. If one restart is required, small solid rockets will position the fuel in the tank.

      Disadvantages

1. For multiple-restart capability, the simple addition of more solid rockets can be employed but the system would introduce complexities.

2. If liquid propellants are employed for the ullage rockets, positive expulsion devices must be employed.

ANALYSIS DATA

Radiation Cooling of an Uncooled Rocket Nozzle

In the application of ullage rockets for main propellant orientation, the space environment and the design of heat-sink rockets induces several problems. In such a situation the heat-sink rocket is associated with the problem of heat conduction through the walls during firing and the dissipation of heat by means of radiation during the cooling period. Intermittent operation of an uncooled rocket engine also affects the selection of materials because of the associated and additative time-temperature environment.

The simulated evacuated ground testing of multiple firings of ullage rockets creates a time-consuming test facility operation. The cooling period between firings can involve an appreciable elapsed time in a given test facility when and if the restart firings are made at specified sink temperatures.

The carpet plot on Figure 54 represents the generalized solution of the radiation cooling equation presented in Reference 116. These curves provide the necessary data to establish the time required to attain a certain cooled body temperature when this sink temperature is known. The test time for multiple restarts is thus readily established.

The time carpet plot (in hours) is based on the equation,

$$ t = \frac{\rho c_p V}{\epsilon \sigma S T_s^3} \left[-\frac{1}{4} \ln \left| \frac{T_b + T_s}{T_b - T_s} \right| + \frac{1}{2} TAN^{-1} \left(\frac{T_b}{T_s} \right) - \frac{\pi}{4} \right] \qquad (72) $$

This equation is based on the assumption that the initial body temperature is large compared with the sink temperature, a condition that is readily met in practice both in simulated ground test and actual flight.

In addition, it was also assumed that none of the emitted energy from the body returns to the body.

The equation was further simplified to read

$$ t = K_c \left[\frac{\rho c_p V}{\epsilon S} \right] \qquad (73) $$
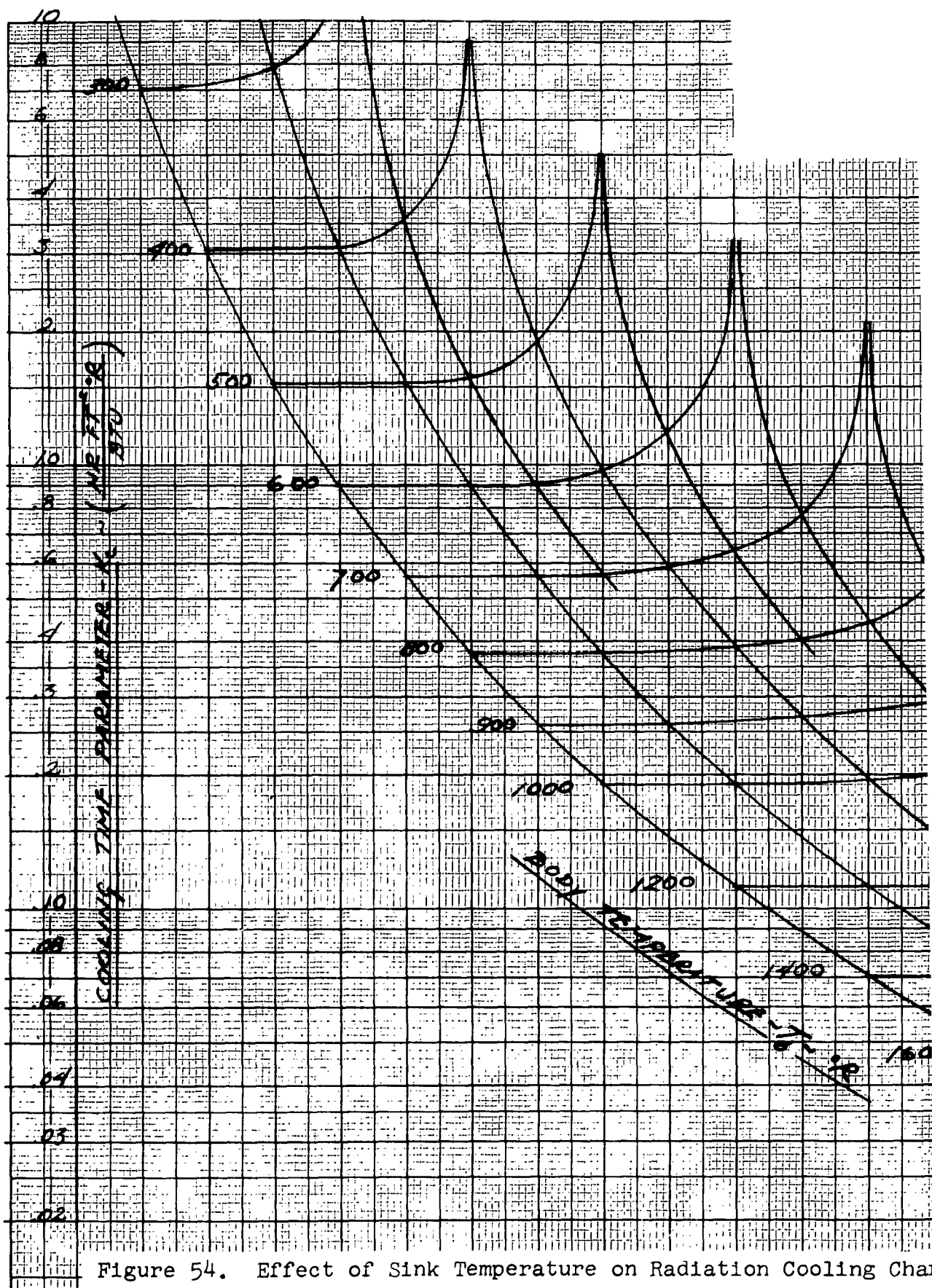
Figure 54. Effect of Sink Temperature on Radiation Cooling Chart

$$t_r = K_r \sqrt{\frac{\rho c_p V}{\varepsilon S}}$$

$$\frac{\rho c_p V}{\varepsilon S} = \frac{B T u}{F T^{\circ} R}$$

1400

1600

1800

2000

0
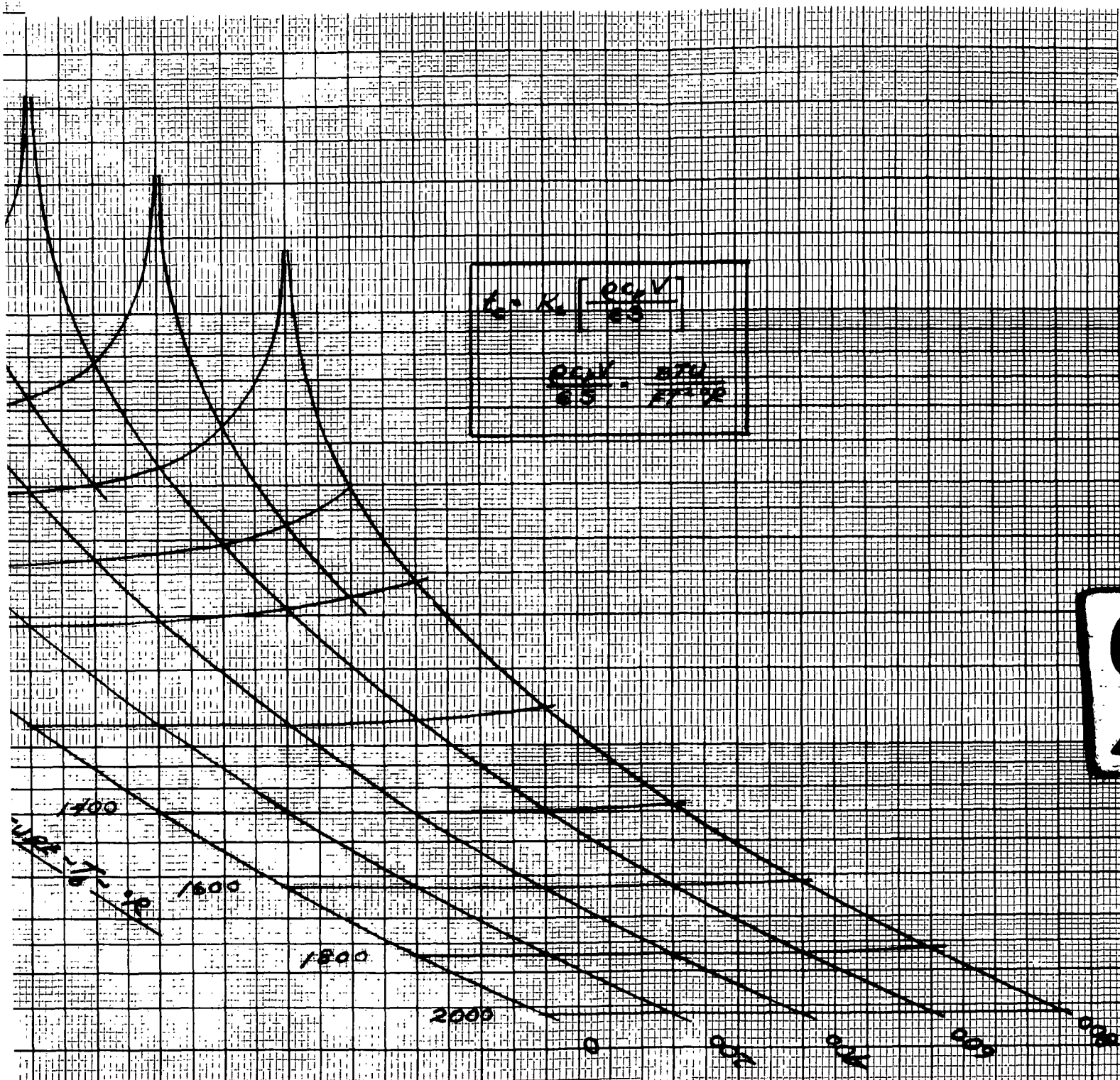
tion Cooling Characteristics of a Body in Space

SINK TEMPERATURE = °R X 10²

where

$$K_c = \left(\frac{1}{\sigma}\right)\left(\frac{1}{T_s}\right)^3 \left[\frac{1}{4}\ln\left|\frac{T_b + T_s}{T_b - T_s}\right| + \frac{1}{2}TAN^{-1}\left(\frac{T_b}{T_s}\right) - \frac{\pi}{4}\right]$$ (74)

and the units are:

$$K_c = \frac{HR\ FT^2\ {}^\circ R}{BTU}$$ (75)

$$\frac{\rho c_p V}{6S} = \frac{BTU}{FT^2\cdot R}$$ (76)

As obtained from the solution of the cooling time equations and carpet plot:

1. The cooling time of a body from one temperature to another in space is directly proportional to the volume-area ratio of the body, the density of the body and the specific heat of the body. The cooling time is also a function of the temperature of the surroundings and the emissivity.

2. The cooling time is insensitive to the initial temperature above temperatures of 2000°F.

3. For a fixed sink temperature, cooling time will increase as the final temperature approaches the sink temperature.

The carpet plot is more generalized than the curves presented in Reference 116. The sink temperatures are arbitrarily selected although under actual conditions it depends upon the specific mission of the vehicle. In simulated ground firing tests, however, the sink temperature is established or known.

In the selection of a material to withstand the time-temperature effects of an uncooled rocket nozzle, refractories are contemplated or employed. It is interesting to note that for the following four refractory materials, the values of ρc_p are almost constant.

TABLE IV.   PHYSICAL PROPERTIES OF REFRACTORIES

Material	$\rho(\#/Ft^3)$	c_p	ρc_p
Tungsten	1203	.032	38.5
Tantalum	1036	.036	37.3
Molybdenum	635	.061	37.7
Columbium	535	.065	34.8

Thus, for a given configuration of nozzle, emissivity is the predominant characteristic affecting cooling time (for a constant sink temperature) for these materials.

Figures 55 and 56 present the variation of specific heat with temperature for several materials, including the refractories. These values were taken from References 124 through 126.

In order to illustrate the procedure of computation and the use of the carpet plot in Figure 54, the following example is selected.

The material is a tantalum nozzle for a small ullage or control rocket with the following characteristics:

$$\epsilon = .90$$

$$\rho = 1036 \text{ lbs/ft}^3$$

$$c_p = .036 \text{ BTU/lb/}^\circ F$$

$$v/s = .009983$$

so that

$$\frac{\rho c_p}{\epsilon}\left(\frac{v}{s}\right) = \frac{1036\ (.036)(.009983)}{.90} = .4137$$

and

$$t_c = K_c\left[\frac{\rho c_p V}{\epsilon S}\right] = .4137\, K_c$$

From Figure 54 for selected values of body temperature, T_b, the cooling time coeff. K_c and cooling time t_c are summarized in Table V. The results are plotted in Figure 57.

TRAP OR SURGE TANK

The trap tank device is simply a small tank located at the lower region of a large tank and directly connected to the engine. The principle of this device is to keep the small tank completely full of propellant while the system is operating. At engine shut-down, the propellant is automatically trapped in the small tank by appropriate valving. Engine restart is assured since no ullage exists in this small tank. Initial acceleration immediately settles the remaining bulk of propellant thereby sustaining engine operation. Gas that is trapped initially while flowing
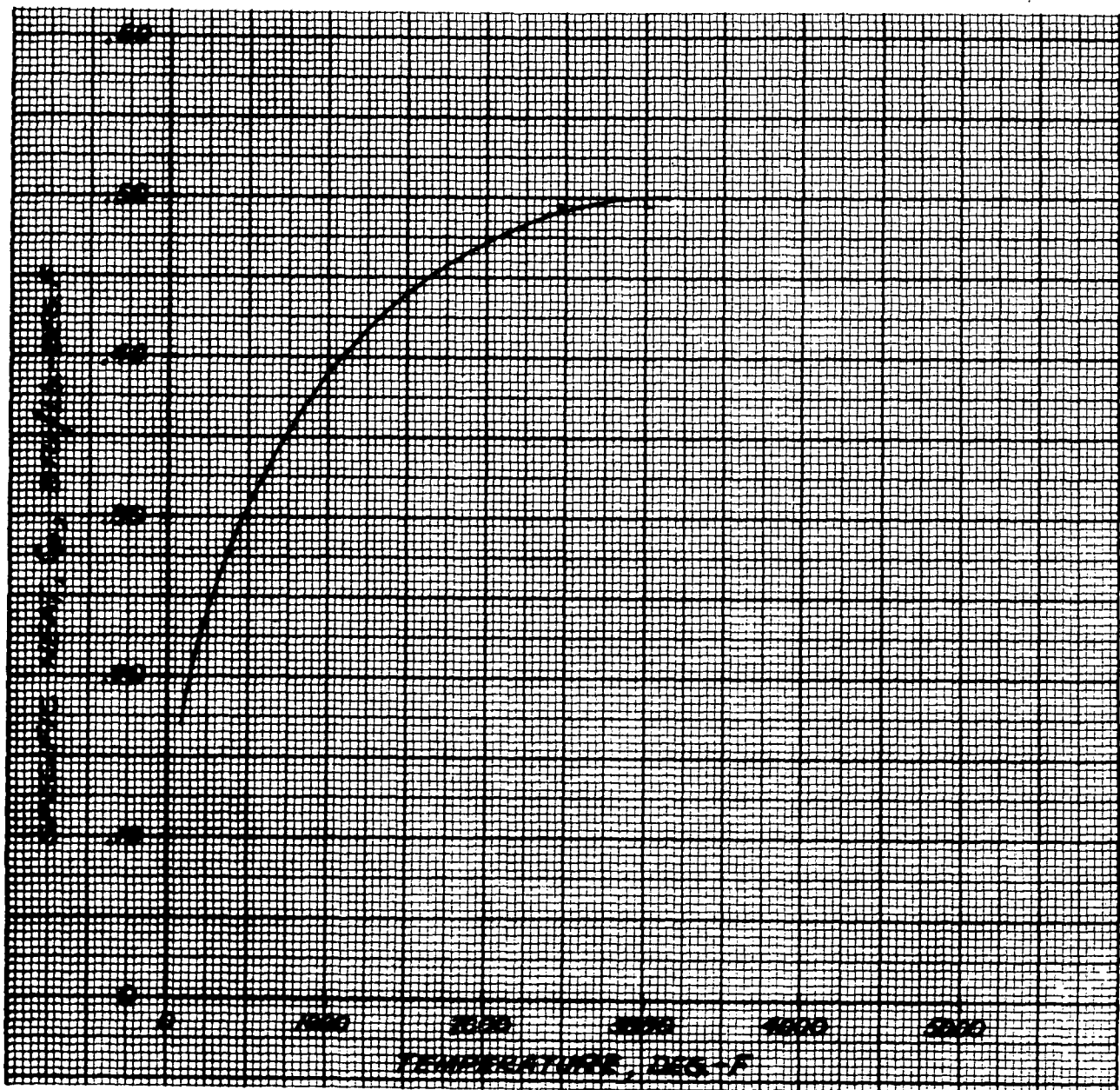
Figure 55.   Specific Heat of ATJ Graphite at
             Elevated Temperature
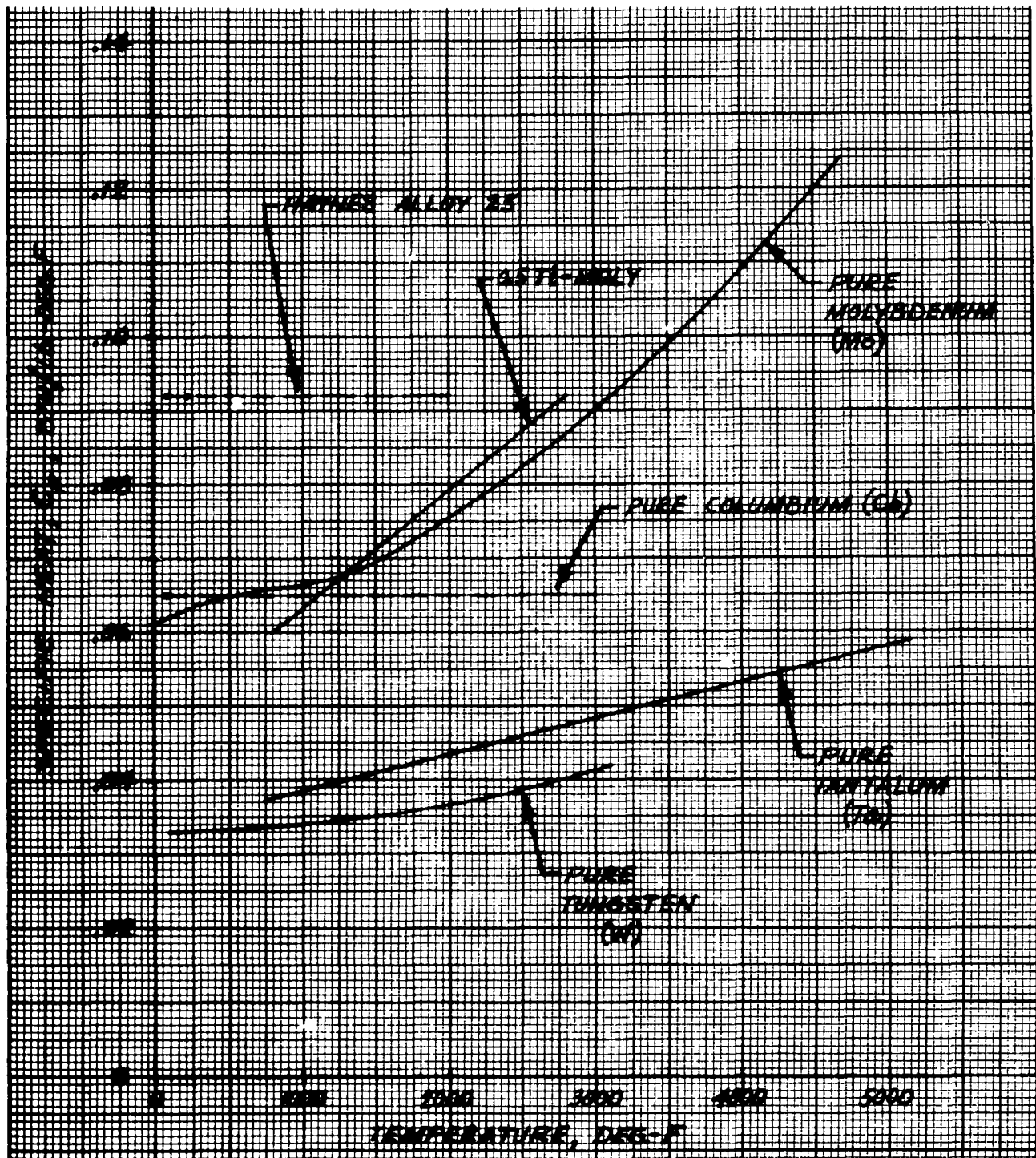
Figure 56.   Specific Heat of High-Temperature
Materials at Elevated Temperature

TABLE V

SAMPLE EVALUATION OF RADIATION COOLING TIME

(1)	(2)	(3)	(4)	(5)
T_b °F	K_c Fig.54	t_c(Hrs.) .41369x(2)	t_c(Min.) 60x(3)	T_b °F=°R-460
2000	.024	.009928	.5957	1540
1800	.033	.013652	.8191	1340
1600	.047	.019443	1.1666	1140
1400	.0705	.029165	1.7499	940
1200	.112	.046333	2.7799	740
1000	.20	.082738	4.9643	540
900	.282	.116660	6.9996	440
800	.41	.169613	10.1768	340
700	.67	.277172	16.6303	240
600	1.42	.587439	35.2463	140
560	1.95	.806695	48.4017	100
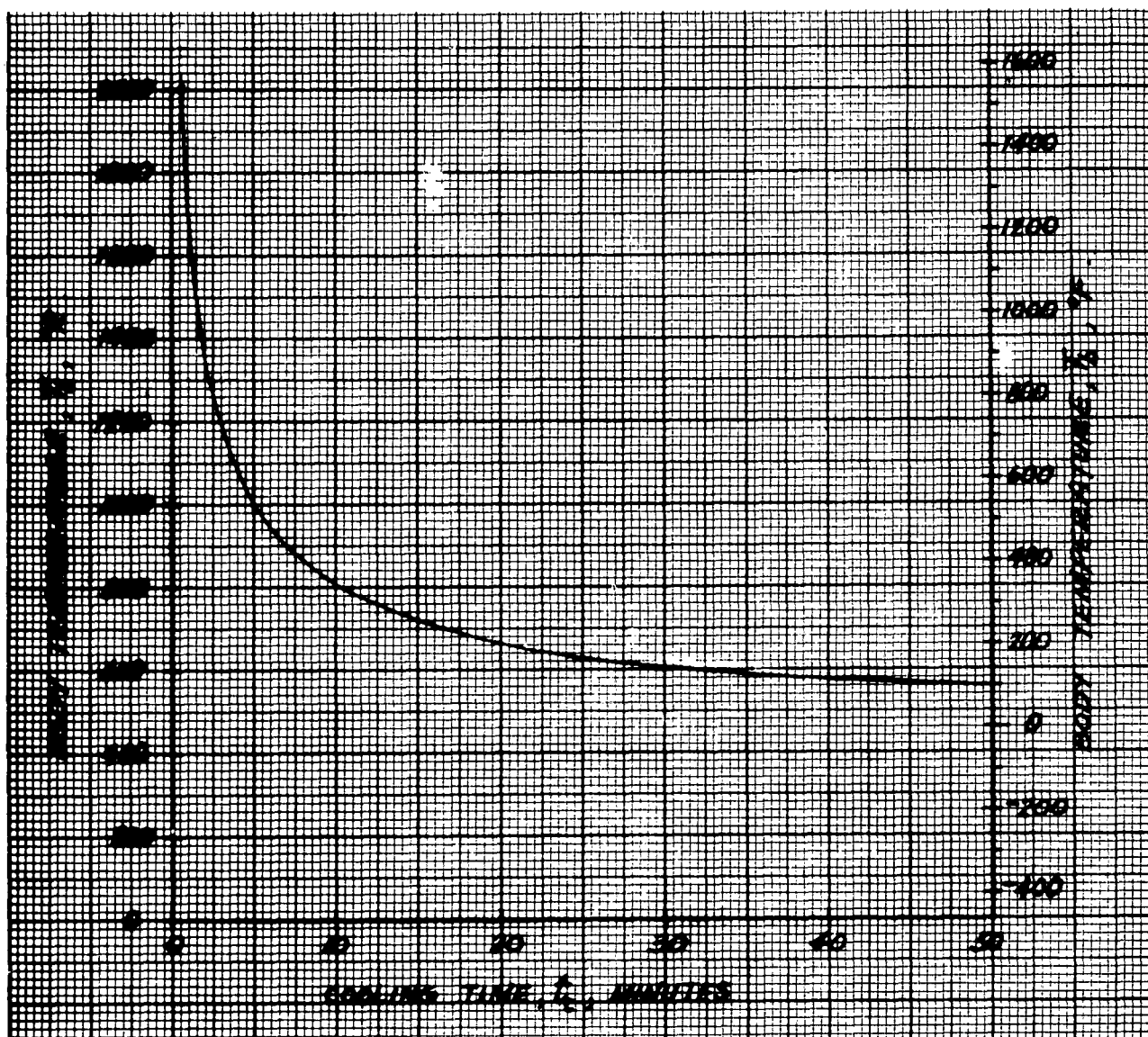
Figure 57.   Sample Calculation of Time-History
of Radiation Cooling

from the trap tank is bled off and returned to the top of the main
tank. The total propellant mass flow continues from the main tank
through the trap tank and to the engine for continuous operation.

Characteristics of Trap Tanks

Advantages

1. The tank is refillable during operation of each cycle
of acceleration.

Disadvantages

1. An elaborate plumbing and venting system is required.

CONTROLLED DEFORMATION OR FOLDING CONFIGURATION

Expulsion devices that depend upon large deformations and the collapsed state of a shell to provide the fluid flow introduces difficulties in trying to synthesize the deflection and the associated pressure loadings. In metallic versions, local yielding is greatly exceeded. Unpredictable wrinkles and their locations, creases, cambers and folds provide resistance to further deformation and induce additional complexities to analytical design solutions which, at present, are non-existent. In addition, sharp creases and folds can induce pin-hole leaks, tears and actual rupture of the component.

There are means, however, that can diminish these undesirable characteristics. Flexibility or controlled deformation can be insured by the incorporation of pre-formed shapes, local reinforcement, hinged or flexible joints and the fabrication technique of material indentation or scoring.

1. Bellows

The incorporation of bellows offers the best control of membrane movement. A bellows is basically a convoluted form of metal tubing, (thin wall circumferential corrugated metal elements). The amount of flexibility is dependent upon such factors as type of material used in fabrication, wall thickness, number of convolutions, etc. The action of a bellows under a load or force applied axially, is like that of an ordinary helical spring. The allowable motion of a given size bellows under a constant load is proportional to the number of active convolutions. With the wall thickness and load remaining constant, the stroke will increase proportionally as the number of active convolutions are increased.

2. Spoke and Membrane Construction

The spoked or reinforced membrane configuration is constructed in such a manner that the membrane tends to rotate about the spoke or reinforcement to which it is attached (flexible hinge). The expanding or collapsing action is similar to that of an ordinary umbrella. This system of spoke and membrane construction can be broadly described as an unfurlable container which is unfolded during operation.

3. Accordian Pleat Concept

The membrane shell is line scored (in the longitudinal direction) so that a flexible joint or fold can be initiated at this point. The shell is pre-formed into accordian-type pleats and inserted into the rigid container.

BELLOWS

~   For application to expulsion systems, bellows, be they metallic or nonmetallic, offer flexibility to absorb a high degree of axial freedom of motion. Bellows are corrugated cylinders which have a wall thickness that is relatively thin compared to the wall thick-ness of the shell in which it is used. Because the radial sides of these corrugations are extremely flexible, bellows possess a high degree of axial freedom of motion.

The ability to deflect axially is predicated by the flexibility of the bellows. Flexibility is dependent upon the modulus of elasticity of the material and the diameter of the bellows, the size, shape, thickness, and number of convolutions. Flexibility is directly proportional to the number of convulutions per given length if the size of convolutions and wall thickness are constant. Within the elastic limit, the action of a convoluted bellows is closely related to that of a helical spring and a frequent cause of bellows failure is fatigue. A bellows can be considered analogous to a spring mass. Critical frequencies are a function of the mass and the bellows spring rate. A higher spring rate or a lower mass results in higher resonant frequencies. These resonant frequencies of vibration in bellows are induced either by mechanical means, high noise levels (130 db and above), or by high-velocity compressible fluids impinging on the internal surfaces. Also, overstressing of bellows prior to installation can impair the life of the bellows. Hence, even though the stress experienced may be quite low, it should be taken into account.

The speed at which a bellows is operated has little effect on life expectancy, except at very high frequencies.

Some basic facts concerning bellows fatigue are:

1. Everything else being equal, an increased live length in the bellows gives longer life.

2. A metal bellows which is stress relieved after forming has a significantly shorter life than if the work hardened proper-ties during forming are retained.

3. Fatigue data indicate that life of bellows is directly proportional to total stress regardless of the configuration, i.e. shape of corrugations.

Metal bellows are usually either hydraulically or roll formed. Hydraulic forming is usually preferable because it produces more uniform corrugations with a minimum thinning of the bellows material. In addition, stresses developed during hydraulic forming are lower than those induced by rolling or drawing processes. Convolutions

are formed simultaneously during hydraulic forming, and wall
thinning of 10 percent or less can be obtained. The entire pro-
cess is a room temperature operation. With roll forming, con-
volutions are formed one at a time and wall thinning of 10 percent
or less is difficult to obtain.

Analysis Data

A considerable amount of literature is available for the
design of bellows and their configurations. Bellows have been
used extensively in various industries for various applications
and with various materials. The selection of a material for a
bellows-configuration-type expulsion device is dependent upon
numerous conditions some of which have been discussed under
MATERIAL CONSIDERATIONS. Once the material has been selected,
the actual design must be accomplished.

Within the elastic limit, the action of a bellows is closely
related to that of a helical spring and deflection is proportional
to the applied load. The evaluation of the spring rate which
defines the energy or pressure differential to expel the fluid,
can be evaluated with the aid of Figures 58 and 59 for the parallel-
sided bellows and triangular-shaped bellows. This data has been
obtained from Reference 104. Similar curves could be obtained
for other configurations.

There are numerous variations in contours of convolutions
for bellows, each of which has special characteristics. It is
not difficult to visualize the great many numbers and variations
of contours that are possible, from flat plates to shallow ripples,
deep ripples, S curves, toroids, and so on.

The nesting ripple bellows, which is a welded configuration
analogous to a stacked Bellville disc column welded at the inner
and outer edges, can be built so the free length is the nested
length and all the stroke is in extension. This nesting ripple
is an extremely efficient configuration and can be built in
relatively large diameters. However, quality control is an
important consideration because the required length of welding
also increases the possibility of leakage. The fabrication by
welding also introduces problems in material selection, thickness
and welding process.

Figures 60 through 63 represent the developed width of
corrugations which are directly applicable to bellows. This
information is extracted from Reference 105. The developed
width is a direct function of weight and can be employed to
establish weight values. Although the developed length also
bears some relationship to the maximum extended length of the
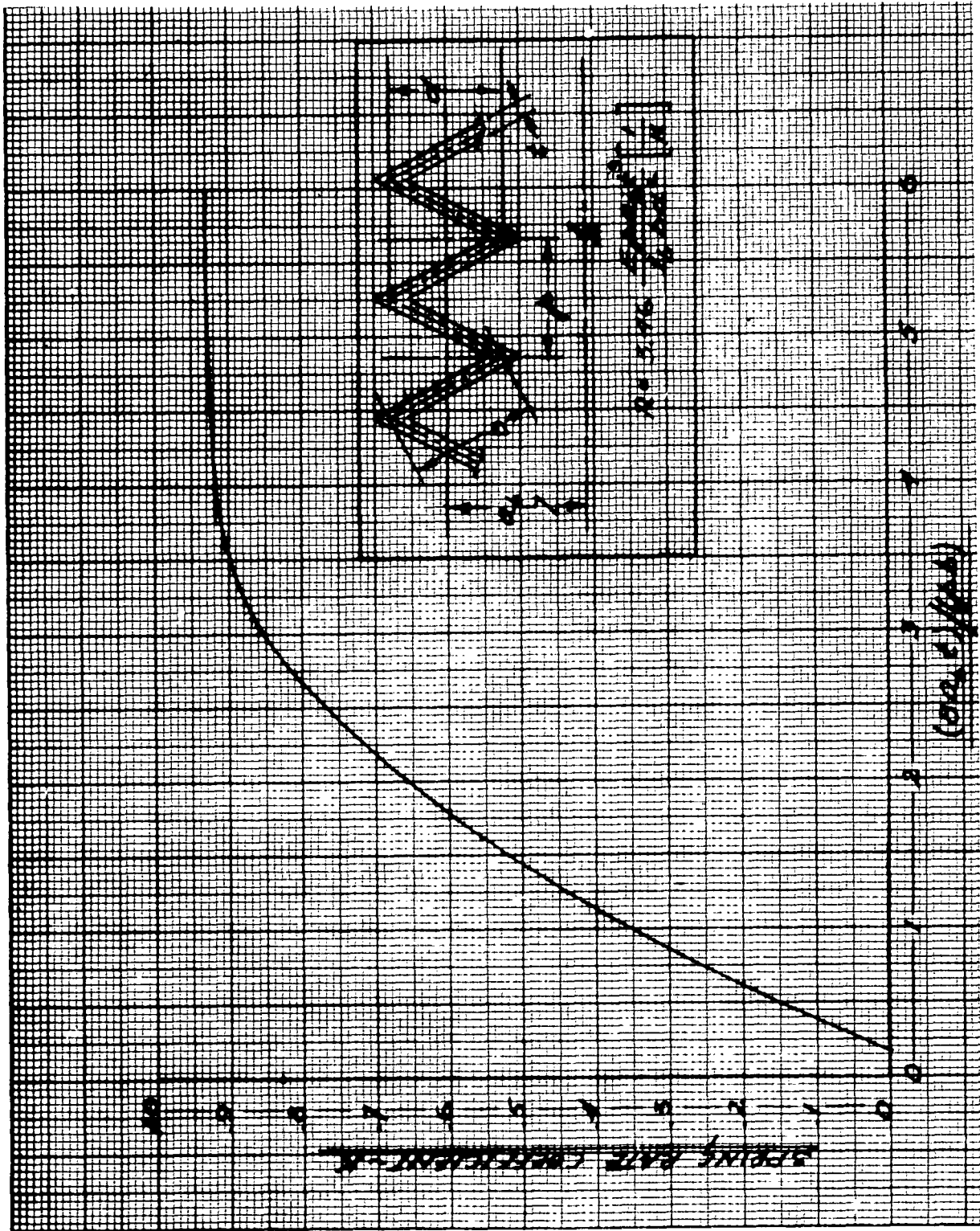
Figure 58. Spring Rates for Triangular-Shaped Bellows
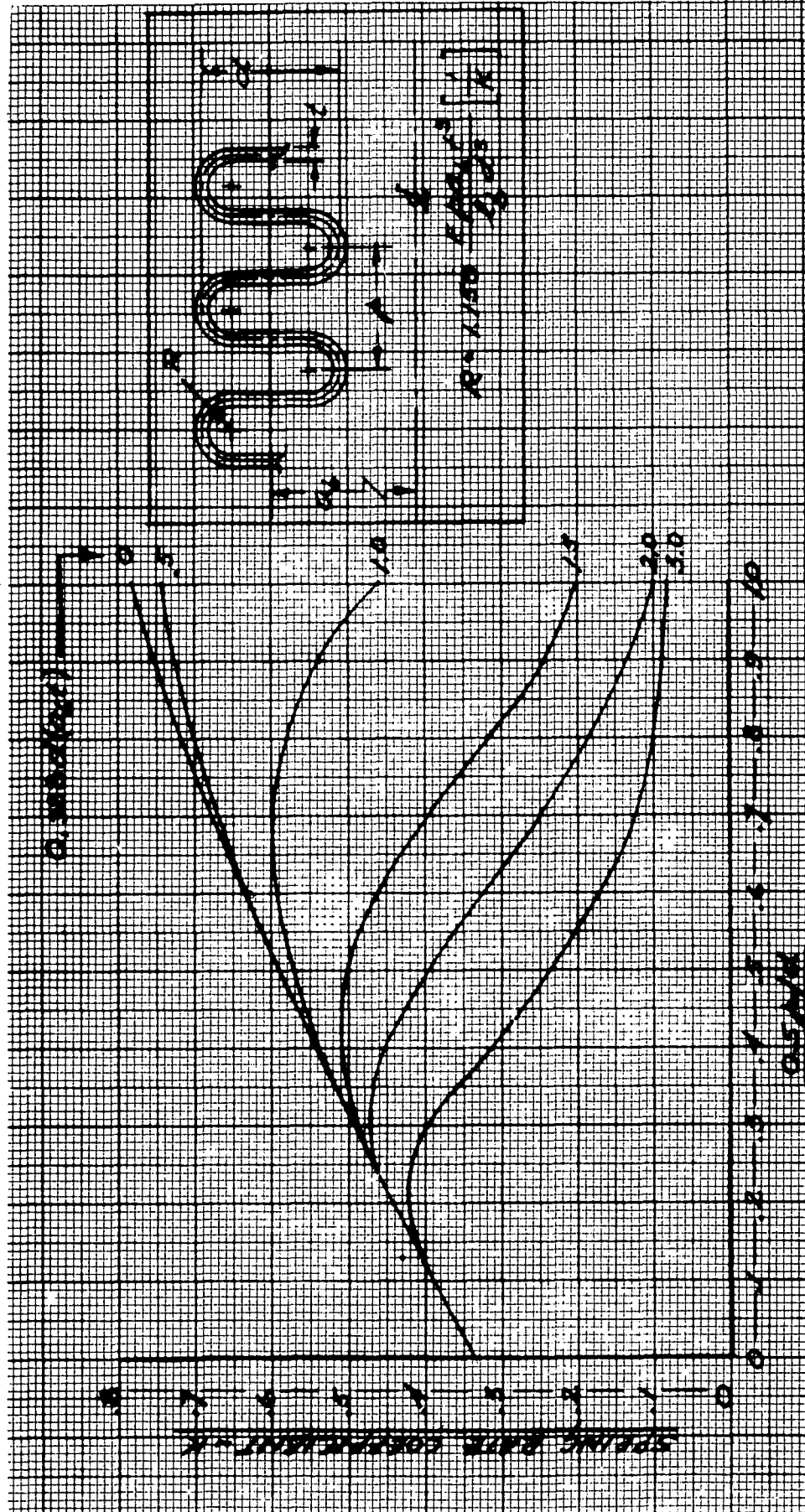
Figure 59. Spring Rates for Parallel-Sided Bellows
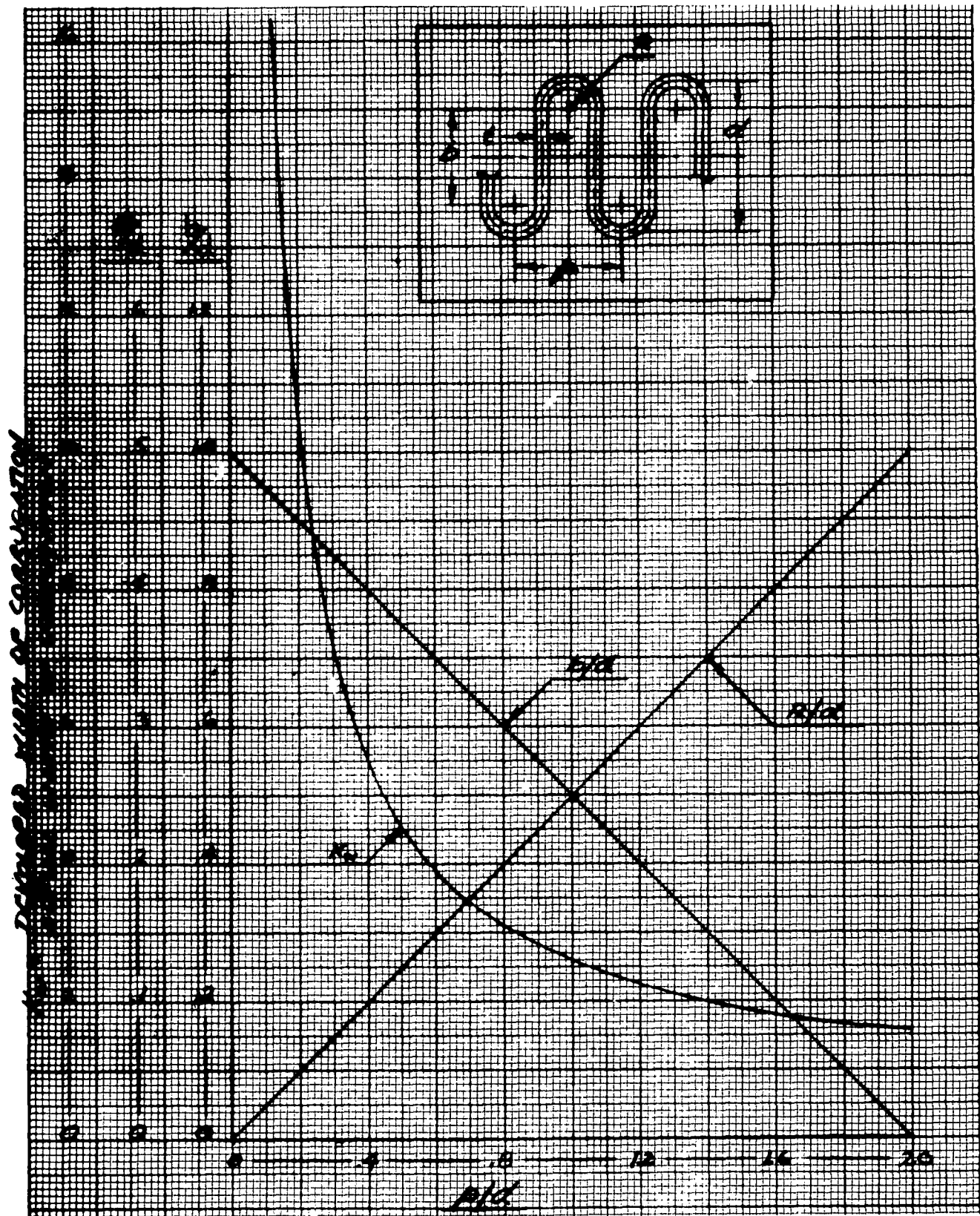
Figure 60.   Geometric Properties of
Parappel-Sided Corrugations
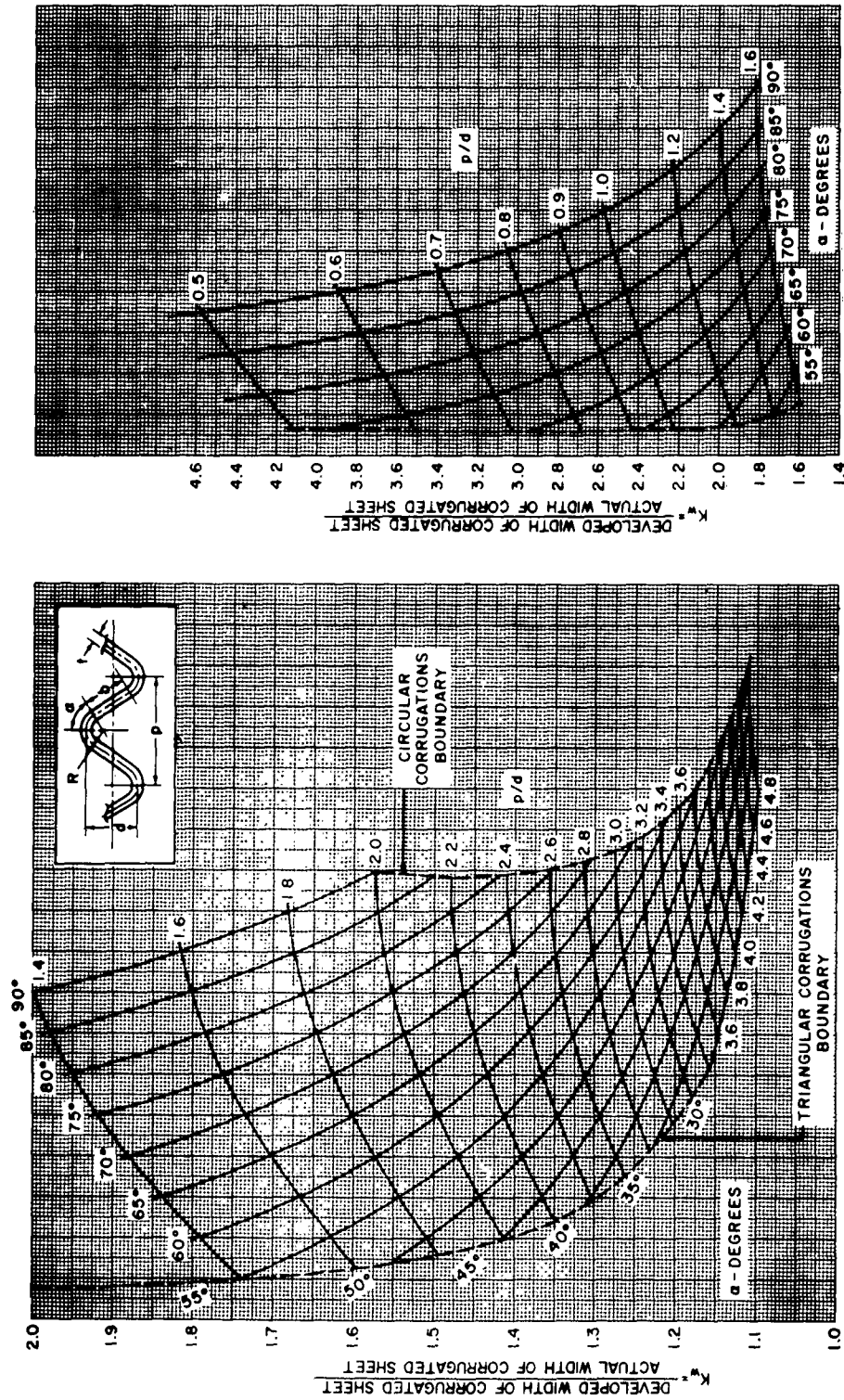
Figure 61.   Geometric Properties of Corrugations – Developed Width
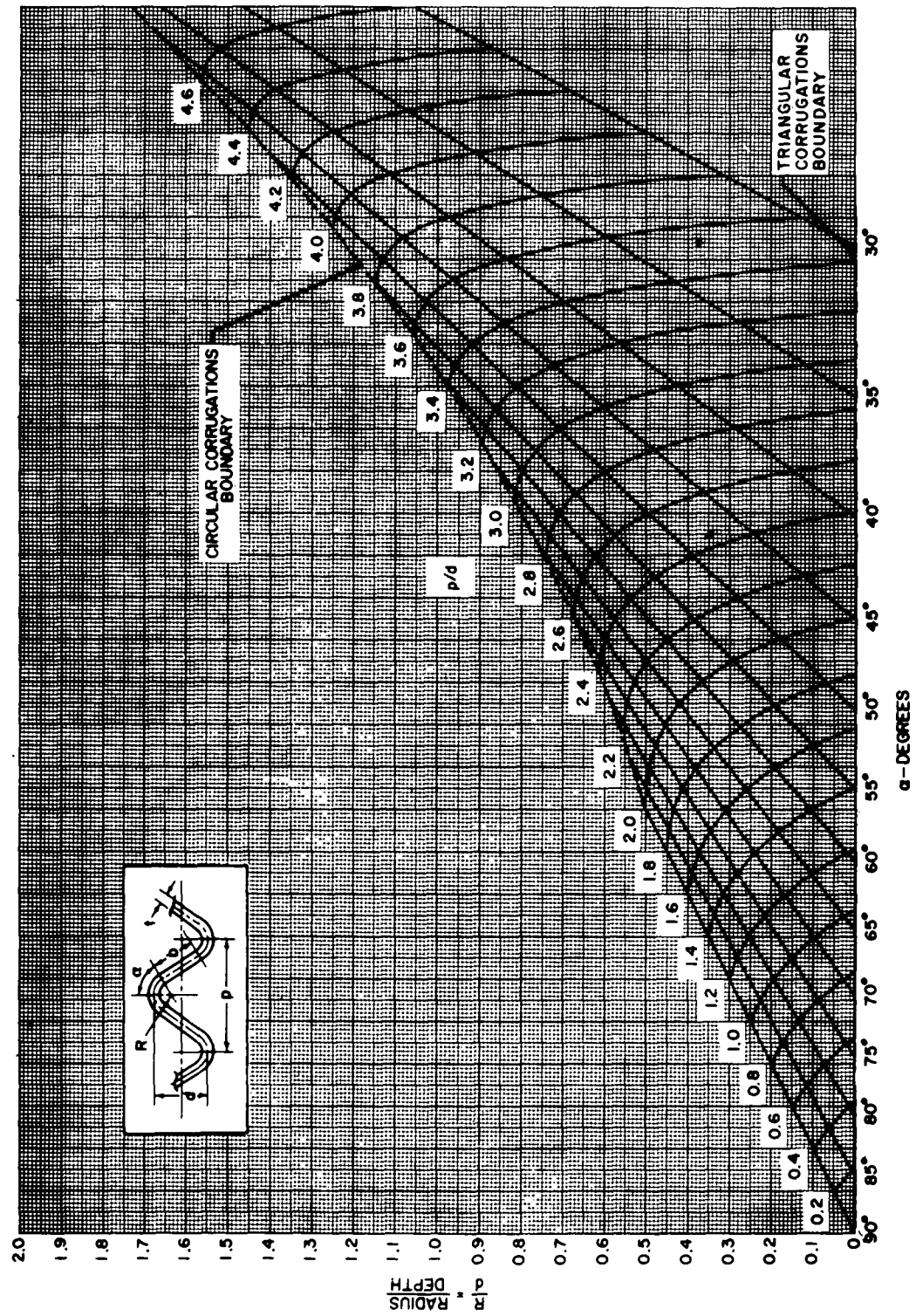
Figure 62.   Geometric Properties of Corrugations – Corrugation Radius
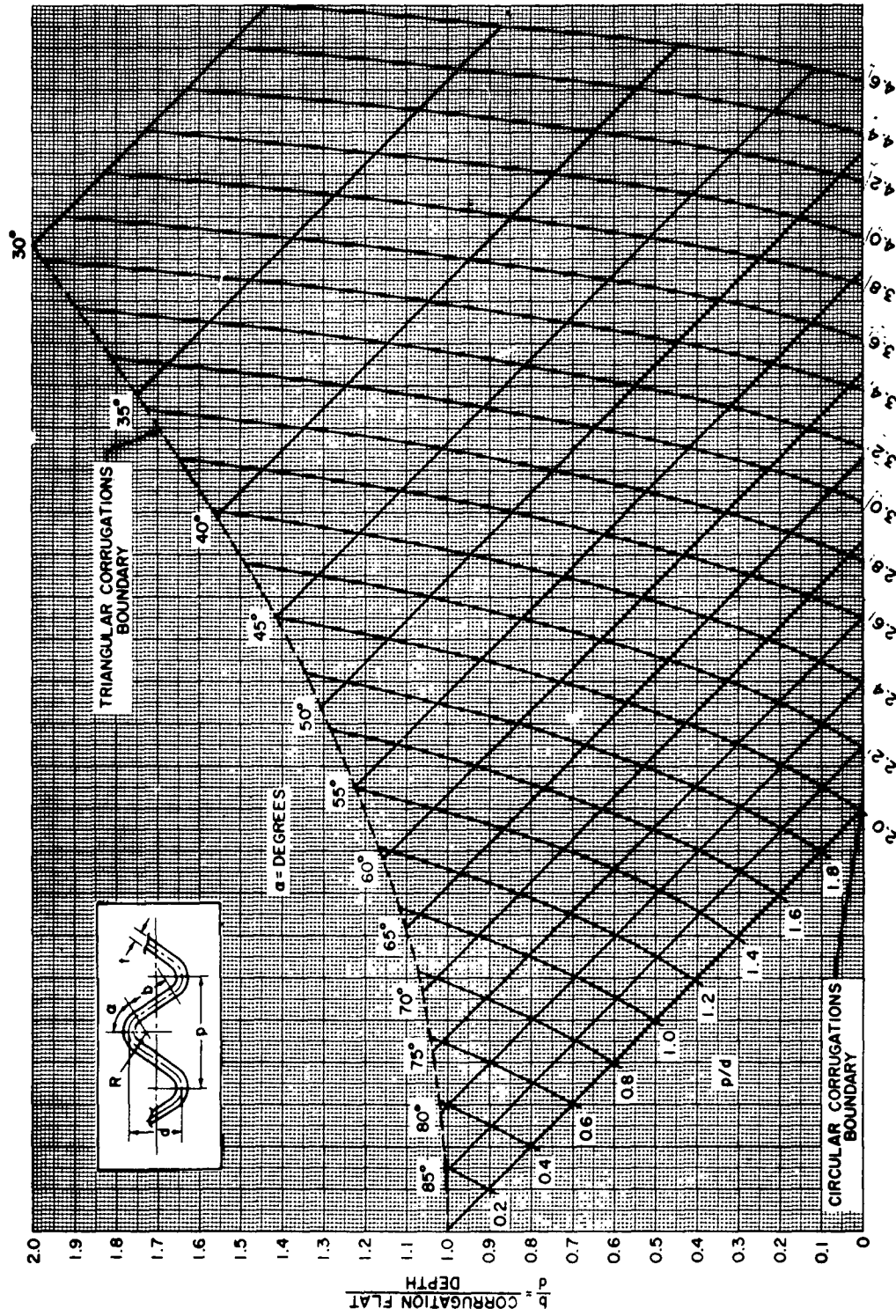
Figure 63.   Geometric Properties of Corrugations – Corrugation Flats

bellows, caution must be exercised in this application because the local buckling of the convolution could cause a primary failure or bending rupture.

MECHANICAL BELLOWS

A positive expulsion device employing bellows is shown in Figure 64. The illustrated unit incorporates an auxiliary bellows that aids in reducing the "dead volume" in the head. The various characteristics of the bellows system are enumerated below.

Characteristics of Mechanical Bellows

Advantages

1. The partial expulsion cycle test can be readily performed with the bellows system thus insuring reliability and performance.

2. In general, the bladder can be considered a two-piece component: bellows and head, so that assembly is relatively simple.

3. Bellows can be rolled or welded readily and many commercial outfits can perform the fabrication with relatively little lead time.

4. Squirm and buckling of bellows, which results when pressure is applied inside a bellows that is longer than its outside diameter, is minimized if not prevented due to the fact that the outside structural tank walls provide adequate guiding.

5. The three-corner or handkerchief-fold is eliminated in either the expansion or contraction of the bellows.

6. Bellows have excellent spring characteristics and pressure deflection curves.

7. Contours of "corrugations" can be varied to achieve desired characteristics.

8. The bellows can be designed for full and repeated expulsion cycles.

Disadvantages

1. The bellows system requires a larger tank to maintain required propellant volume because of the volume it displaces.

FUEL FILL AND OUTLET

BELLOWS

REVERSING DIAPHRAGM

GAS PRESSURE INLET
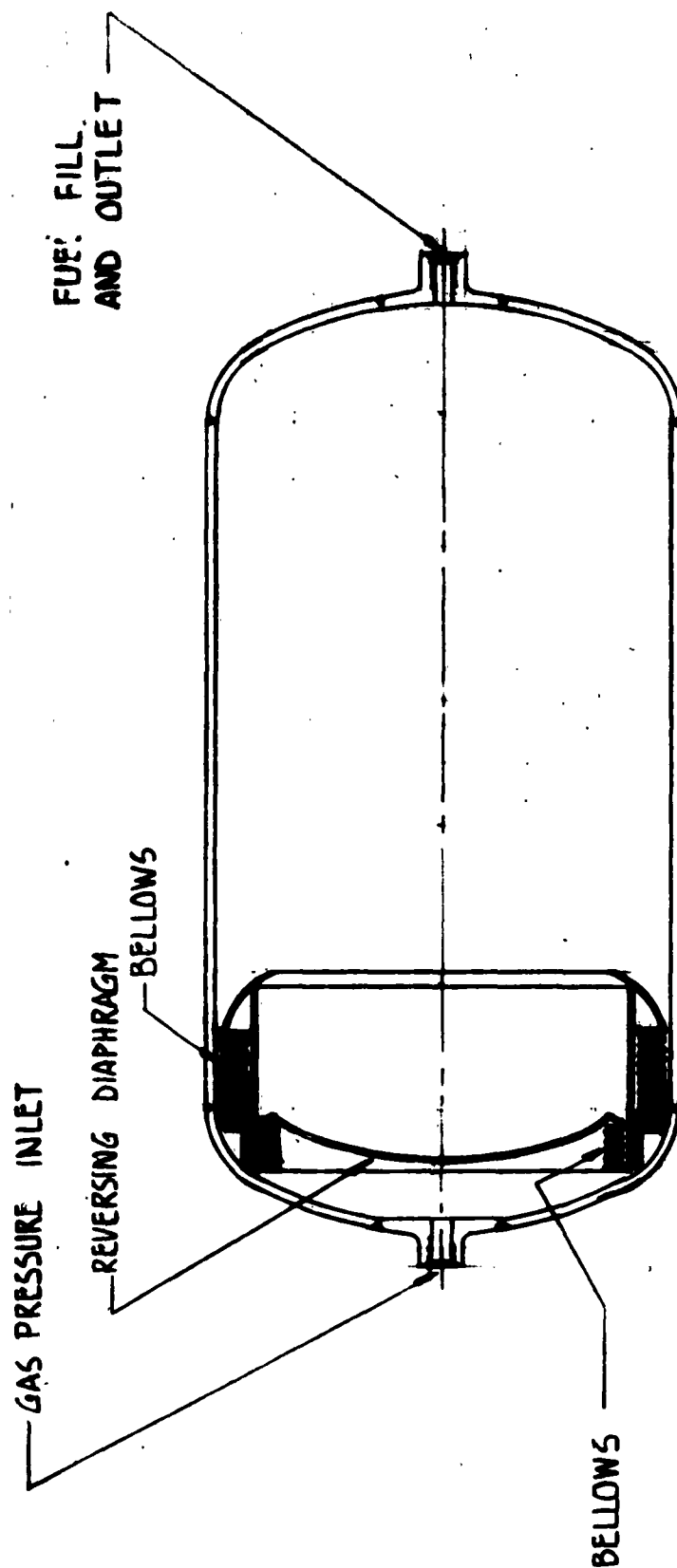
BELLOWS

Figure 64. Mechanical Bellows

2. There may be a limitation on the depth of the bellows that can be rolled or welded to insure that the extended length is at least equal to or greater than the tank length. A greater bellows depth can be realized by the use of a series of welded washers (similar to Bellville Springs). However, welding length is excessive and the problem of leakage is increased. In addition, the flexing of the bellows during expulsion induces localized stresses at the weld periphery of the welded bellow section.

3. Too long a bellows length introduces a long head within bellows to reduce the ullage volume so that buckling and collapse problems may arise. (Head and cylindrical portion folding on itself during expulsion).

4. It is possible, if the fluid is on the outside of the bellows that some fluid will be entrapped within the annulus produced by the inside tank wall and the expanded elements of the bellows. If the expulsion is in the opposite direction, the fluid may be entrapped within the annulus remaining within the bellows when fully compressed.

5. The use of bellows implies the use of cylindrical tank with flat heads as an ideal configuration. This involves a weight penalty.

6. Friction due to the rubbing velocity associated with the contraction or elongation of the bellows along the tank walls will increase Δp .

ACCORDIAN PLEAT CONTAINERS

The configuration shown on Figures 65 and 66 employs the so-called accordian-pleat concept to promote controlled deformation and expansion. In this type of expulsion device the container (which is a bladder in this case) is installed in the pre-folded condition with the propellant between the bladder and the structural container.

Characteristics of Accordian Pleat Containers

Advantages

1. The single and double folds that are incorporated in the bladder are controlled during the fabrication process thus minimizing their random formation and associated pin-hole leaks or fractures.

2. Partial expulsion cycles are possible with this pre-folded accordian-pleat configuration.

PROBABLE LIMIT OF
COLLAPSED BLADDER
(LONG DASHES)

SECTION A-A
BLADDER PARTLY EXPAND
HEAVY PHANTOM LINES

FUEL OUTLET
& FILL
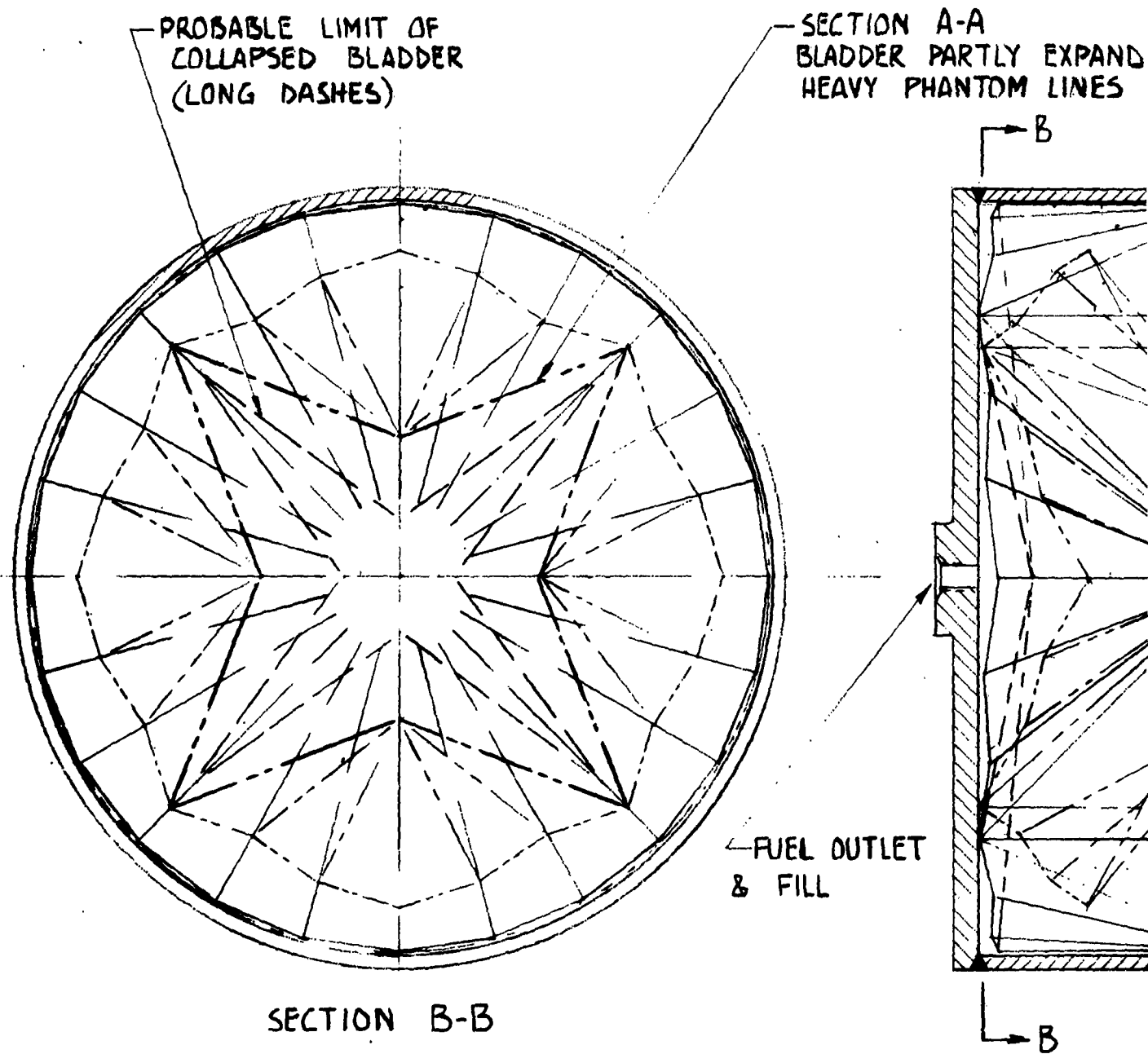
SECTION B-B

SECTION A-A
BLADDER PARTLY EXPANDED
HEAVY PHANTOM LINES

— BLADDER PARTLY EXPANDED
(PHANTOM LINES)

HOSE

GAS INLET

OUTLET

FUEL BLEED

SOLID LINES REPRESENT BLADDER
ALMOST COMPLETELY EXPANDED
(FUEL EXPELLED)
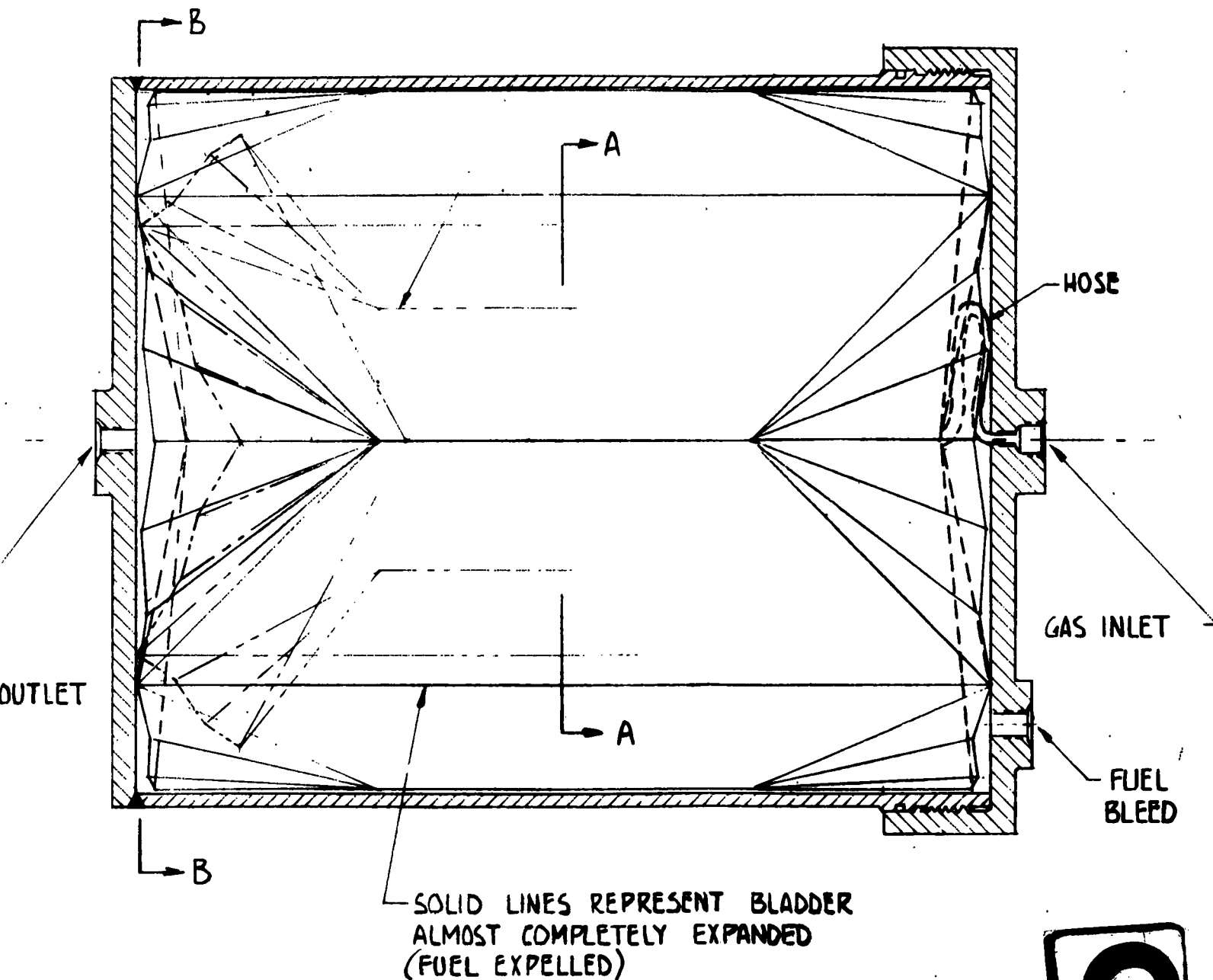
Figure 65. Pleated Folding-Type Bladder

GAS PRESSURE IN

END PLATE A
WHEN FUEL IS EXPELLED

ROTATING
TUBE
WELDED TO
PLATE A

END PLATE A
ONE HALF OF FUEL
EXPELLED

1

IN

FUEL OUT

STATIONARY TUBE
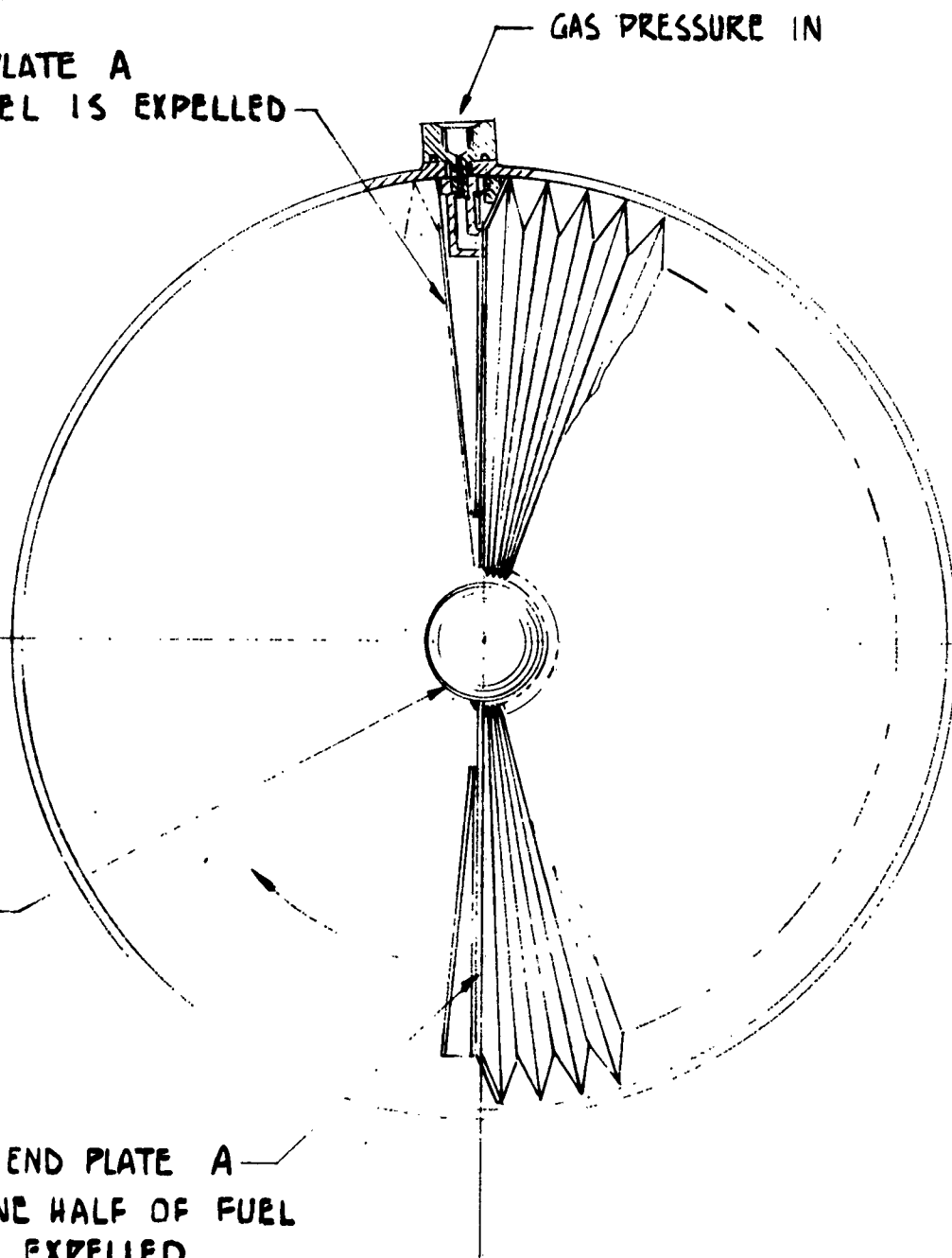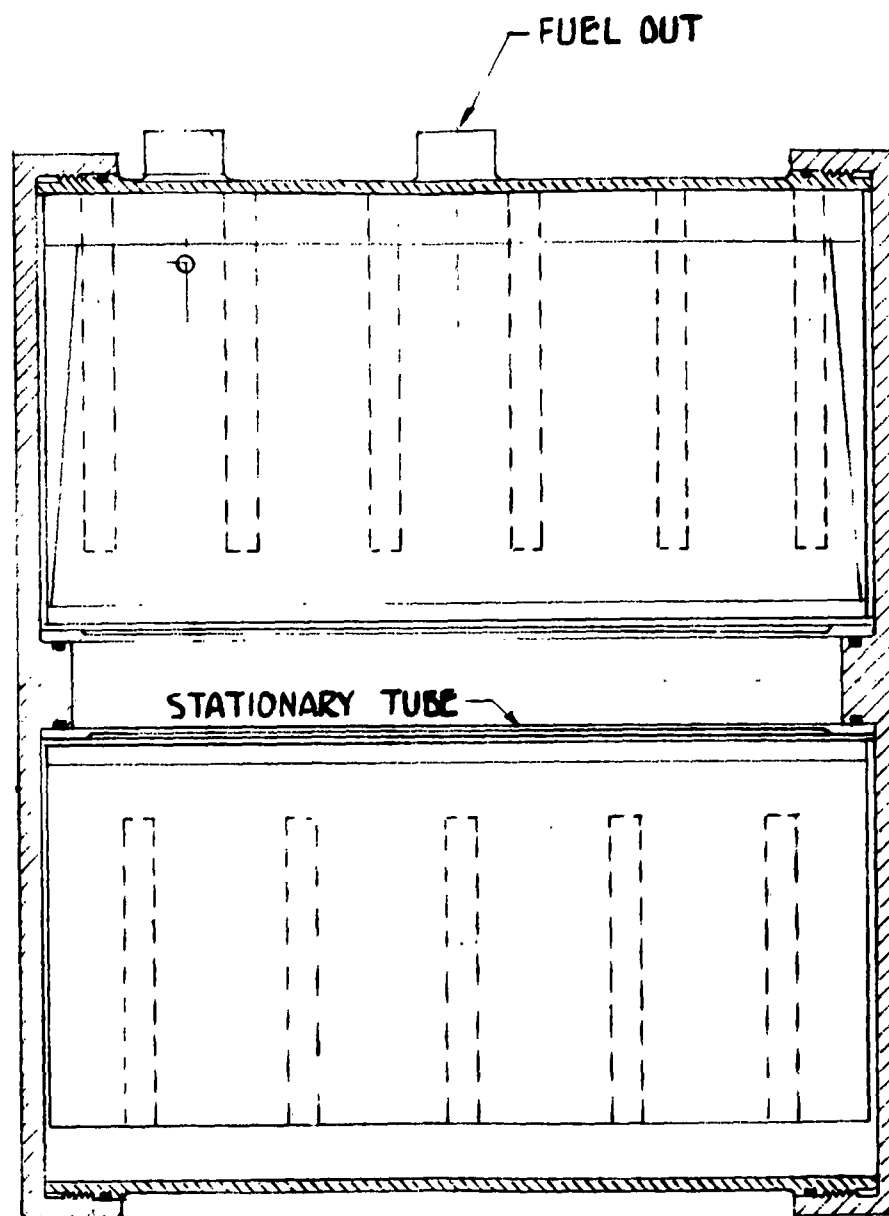
Figure 66. Roll Sweep Pleated Bladder

2

Disadvantages

1. Tank heads must conform to developed expansion of the bladder head shape.

2. Fabrication techniques must be developed to construct the metal pre-folded bladder and the associated welding to insure folding and unfolding of the bladder.

3. Complete folding of a metallic bladder may not be possible thus introducing a larger than required ullage volume.

HYBRID OR MISCELLANEOUS SYSTEMS

Hybrid, combination or miscellaneous systems appear to be likely candidates for consideration. In the case of combinations combining the different methods of expulsion, the advantages of each may be realized.

ROLL AND PEEL DIAPHRAGM

The expulsion device illustrated in Figure 67 is another example of a metallic rolling diaphragm with the notable exception that the diaphragm is adhesively bonded to the structural wall of the vessel and that its operation does not require the use of a piston. A major advantage is that the necessary ullage can be kept to a minimum.

The operation of the rolling diaphragm is dependent on the ability of the bond to keep the gas pressure from coming into contact with the external surface of the unrolled portion of the diaphragm. Conversely, sufficient gas pressure must be supplied to obtain the desired peeling action. During the resulting rolling process the free surface of the diaphragm increases progressively to a deep convolution.

Analysis Data

From an analytical viewpoint a rational analysis of the peeling action has yet to be made although considerable tests have been made and these are recorded in References 108 and 109. However, these tests are not completely representative for the present application. For example, the tests described in known literature are restricted to plain sheet action whereby the peeling strength of joints is determined. The A.R.L. (Reference 109) test involves bonding two metal strips together over a middle portion of their lengths and then rolled to a radius of 3 inches. The inner strip is then fixed on a freely rotating drum of 6 inches diameter, while the outer is pulled radially by one of its ends. Near the bonded end the strip is stressed by bending beyond its yield point and curves to a radius much smaller than the radius of the drum. The peeling force is then plotted against the unrolling of the flat strip and is found to vary considerably from point to point. Also, in those tests it is found that peeling may start before the strip bends upright and this is an indication that the stiffness of the strip is too high compared with the strength of the adhesive. For this condition it is found that a small force produces a strong bending moment at the point where the peeling starts. A slight increase of adhesive strength or a decrease of strip stiffness (e.g. thickness) may make the strip yield and bend more

pronouncely so that the moment is greatly reduced and a consider-
ably higher force is required to peel the strip. Even when the
bending of the strip is in the yield region a small change of
adhesive strength or strip thickness is found to result in a very
much larger variation of the peeling force. These observations
indicate that the peeling test is a very sensitive method for
the determination of small changes of strength.

It is generally conceded that the well known and very sensi-
tive ARL drum peel test used at SAAB and similar tests (Reference
111) is a very valuable aid for production quality control, how-
ever, it is not well suited for design purposes, i.e. for direct
judgment of peeling strength of actual structural elements. The
U.S. standard drum peel test (Reference 111, page 618) and modifi-
cations of it with varying joint geometry will give peel strength
data which are more directly applicable to actual designs.

From the above it would appear that even greater difficulties
can be anticipated with respect to the unrolling of the cylindrical
metallic diaphragm. It should be easy to appreciate that for this
application the stress distribution in such a joint is complex and
the force required to initiate and maintain stripping is consider-
ably influenced by the dimensions of the specimen and the mechanical
properties of the adherents as well as of the adhesive. In addi-
tion one must also deal with gas pressure effects and in particular
the adhesive must be capable of stopping the gas at the peeling
surface front. Additional problems to be resolved are those asso-
ciated with adhesive compatibility with various liquids or by-
products of gas generating systems, temperature changes and effects,
long time storage, method of applying and installing the bonded
diaphragm, inspection procedures, etc.

A number of adhesives that are applicable for roll-and-peel
expulsion devices have been tested in the Bell Aerosystems Company
Laboratories. The data presented in Table VI was extracted from
Reference 110.

TABLE VI

PEEL STRENGTH VALUES OF ADHESIVES

Adhesive	Peel Strength (Lbs/Linear Inch)
Araldite Type I	5.67
Bostick 7025	32.13
Cycle-Weld C-3	49.84
Cycle-Weld C-H	6.99
Metlbond M_3C N_2 tare	42.28
Plastilock GO1	61.81
Redux	27.07
3M-585	57.76

The peel test specimens that produced these values were cut from a bonded panel which consisted of an .025" 24ST clad aluminum sheet peeling from an .064" sheet. The angle of separation was about 180° and the stripping rate about six inches per minute. The force necessary to strip the thin member from the thick member was sensed by a calibrated strain-gaged load ring and recorded on an automatic strip recorder. Preliminary tests have indicated that a change in thickness of the thin member results in an appreciable change in peel strength values recorded.

This data is merely a screening operation and indicates the relative strength of the adhesives with respect to each other. In addition this test set-up follows rather closely the associated peeling action for the configuration under investigation, the roll and peel diaphragm.

Characteristics of Roll and Peel Diaphragm

The advantages and disadvantages of a roll and peel diaphragm as illustrated in Figure 67 are enumerated below.

Advantages

1. The peeling reaction provides a restraining force that induces a uniform rolling of the diaphragm thus eliminating random buckling.

2. Maximum utilization of volume, (fuel capacity) is possible.

3. A high expulsion efficiency is possible.

4. No mechanical devices are required for operation.

5. Device is adaptable to practically all containers formed by surfaces of revolution.

Disadvantages

1. The device is a one-shot configuration because of the destruction of the bond during the peeling process.

2. Additional gas pressure or greater energy is required to peel the diaphragm from the cylinder wall in combination with the rolling action of the metallic diaphragm.

3. Tolerances have to be observed between the outside diameter of the diaphragm shell and the inside diameter of the structural container to insure a uniform fit for the bond.
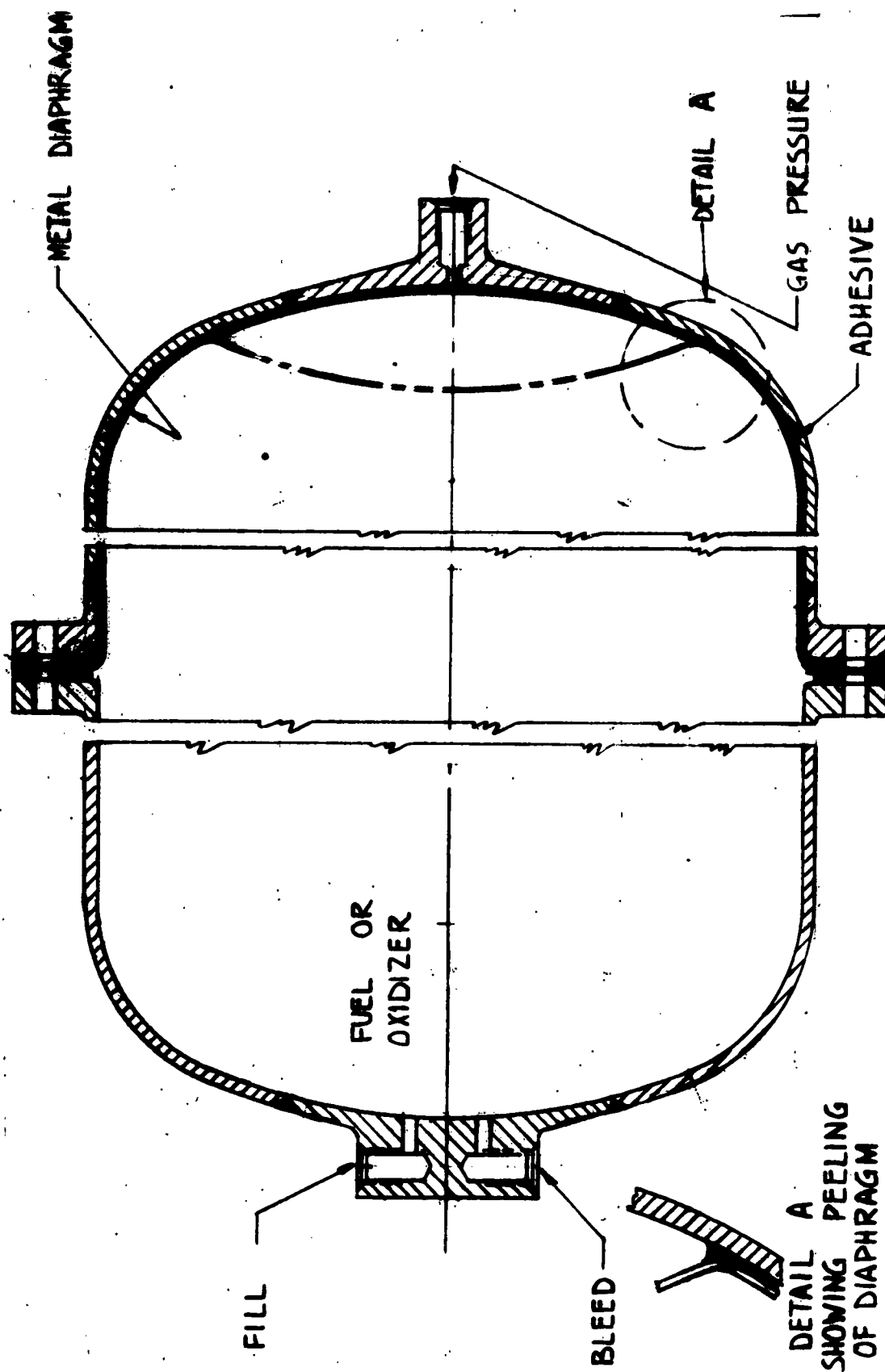
Figure 67. Roll and Peel Diaphragm

ELECTRIC AND MAGNETIC EXPULSION DEVICES

Several techniques employing electric and/or magnetic
fields, either directly or linked with a mechanical system can
be employed for positive expulsion. The devices described in
the following section can be listed in one of the following
categories:

1. Electric

An electric device can be defined as any device which
uses an electric field either alone or coupled with a mechanical
system in order to either pump or contain a substance.

2. Magnetic

A magnetic device utilizes a magnetic field to assist
in pumping or containment.

3. Electromagnetic

An electromagnetic device uses coupled electric and
magnetic fields for fuel expulsion. This resulting pumping
force is proportional to the product of the magnetic field and
the current density resulting from the presence of the electric
field.

In the application or evaluation of electric and magnetic
expulsion devices several items must be taken into considera-
tion. Some of these items constitute problem areas that may
arise when such devices are integrated into a vehicle system
as a whole.

Since the conductivities and magnetic susceptibilities of
presently considered fuels vary over a significant range, it
may be necessary to classify fuels in terms of applicable
electric or magnetic expulsion or confinement techniques. Other
considerations are the possibility of ignition due to either
high field concentrations and/or the possible ionization schemes,
and the weight and power requirements.

Power input considerations may lead to a dielectric confine-
ment system. However, a detailed study might reveal that power
input is an insignificant consideration as compared to pumping
and/or confinement rate. In general, a detailed study will be
necessary to fully evaluate technique versus fuel and/or mission.

The generated fields required for expulsion could introduce
interference effects on instrumentation, inertial guidance,
equipment and communications on the space vehicle. As a result,
shielding may be required in certain areas of the vehicle.

Finally, it is not implied that the categorical breakdown
given is in any way complete. One promising area not exploited
is the use of electric and/or magnetic waves to drive the fluid.

ELECTRICALLY DRIVEN MECHANICAL SYSTEMS

Many of the mechanical systems previously described can be
driven by an electromagnetic device. A familiar circuit breaker
device is illustrated in Figure 68.

Current is made to flow through circuit legs. I, II, III and
IV. The flow of current creates a magnetic field $\vec{H}$ which
couples with the current density $\vec{J}$ to produce a force propor-
tional to $\vec{J} \times \vec{H}$. This force pushes all current elements out-
ward. Element III which is linked to a piston is free to slide.

ELECTROSTATIC AND DIELECTRIC PUMPS

Several possible configurations for strictly electrostatic
devices are shown in Figure 69. In each of the devices sketched
fuel is contaminated with negatively charged particles. The
electric field moves the particles toward the positive elec-
trode. Neutral fuel is dragged along and ejected with the
charged particles in the manner shown in Figure 69. For details
see References 4 through 7. If necessary, a form of spark plug
may be incorporated to induce continual ionization.

The diagram shown in Figure 69c is also adaptable for
strictly dielectric liquids. Although positive expulsion is
not expected with a dielectric fuel, the fuel will be drawn up
between the "condenser plates" and contained therein. The
principle involved is not fully agreed upon, References 8 through
17; however, the phenomenon is observable. Other geometries
might be employed, utilizing either or both of the above
principles.

O. M. Stuetzer, Reference 4, has reported on the results of
experiments using so-called ion drag pumps to pump insulating
liquids. One of the liquids tested was kerosene which has
properties similar to JP-4 fuel. For the most part, the pumps
consisted of a circular cross section channel with an emitter
at one end and an accelerating electrode or collector grid
downstream. According to Stuetzer, the emitter serves to
supply ions to the liquid and these ions move under the action
of an electric field which is produced by applying a voltage
source across the emitter-collector electrodes. The ions
attain an average velocity which is dependent upon their mobility
and the field intensity, and they exchange momentum with the
fluid through friction, thereby building up a pressure in the
fluid.
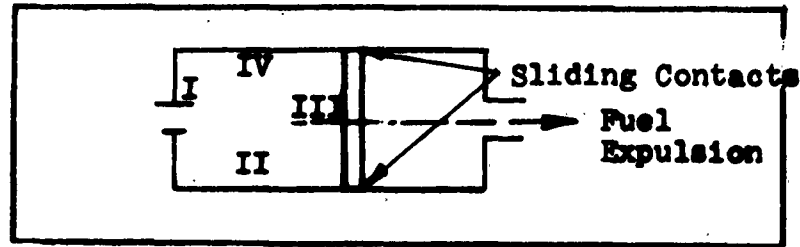
Figure 68.   Schematic of Electro-Mechanical System
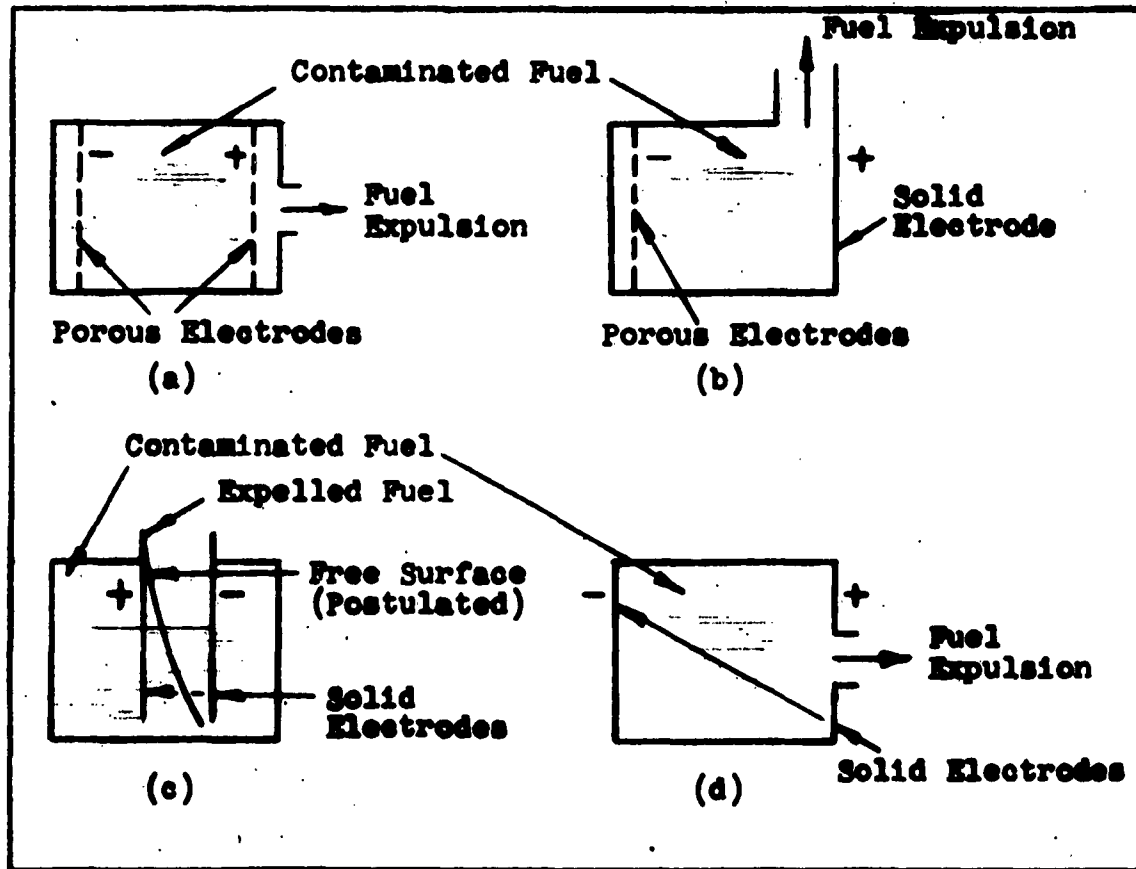
Figure 69.   Schematic of Electrostatic Devices

Data obtained with single stage pumps for both D.C. and
A.C. operation, are presented. The range of pump dimensions
employed were: diameter of channel 0.5 to 5 mm; spacing
between electrodes 0.6 to 10 mm. Some approximate performance
data as taken from graphs included in Stuetzer's paper are given
below.

	D.C. Operation	A.C. Operation
Applied Voltage (K.V.)	18	18 (peak)
Static Pressure (mm of H_2O)	550	700
Current-Static (μ amps)	0.23	
Current-Dynamic (μ amps)	0.48	
Volume Flow (cm^3/sec)	0.6	0.9

Photographic prints of two multi-stage pumps are presented.
One consists of seven single units arranged in parallel units,
arranged in series. The latter pump is described as pumping
8 cc. of kerosene per second, 1 meter high with an efficiency of
10%.

In adapting such devices as Stuetzer has described, for
application in space vehicle propulsion systems, there are a
number of factors which must be carefully examined. Many of
these have been pointed out by Stuetzer in his article. Oscil-
lations due to instability in the system are very likely to
develop unless damping techniques are included in the pump
system design. Because of the nature of the process, static
charge accumulations can develop and they can radically alter
the system performance. Alternating current operation tends
to reduce this problem. Since the performance is a function
of the mobility of the charge carriers, anything influencing
the mobility affects the performance. Impurities and gas
bubbles change the mobility value of the fluid being pumped.
If the dielectric fluid breaks down because of the high field,
the chemical properties of the fluid may change. This could
not only affect the pumping action but also the combustion
action of the fuel. For liquids, other than dielectrics, which
would undergo electrochemical decomposition, the system being
described here, is not applicable.

In the example of D.C. dynamic operation noted above, the
power input was approximately 8.7 milliwatts, with the applied
voltage some 18 KV. On this basis, it appears that the dielec-
tric pump type system can be mated with a high voltage-low
current power supply, e.g. nuclear battery.

ELECTROMAGNETIC PUMPS - CONVENTIONAL

It may be possible to employ the principles of operation of electromagnetic pumps to contain and/or pump certain propellant liquids. Such pumps have been chiefly used up to the present time, to pump liquid metals and they are frequently discussed in the literature relating to nuclear reactors, References 13 through 23. The principle of operation may be considered to be the so-called "motor" principle, i.e., if a current flows in a conductor which is placed in a magnetic field perpendicular to the current, the conductor will be acted on by a force, normal to both the current and the magnetic field. The conductor in this case is the fluid being pumped and thus the pumps work best with high conductivity liquids.

There are both direct current and alternating current type pumps. The direct current pumps are a direct application of the "motor" principle. There are two general categories of alternating current pumps viz., conduction and induction pumps. The conduction type pumps operate in a manner very similar to the direct current type and the magnetic field must reverse in synchronization with the current. In the induction pumps, currents are induced in the conducting liquid and these currents interact with the magnetic field of the pump so that motion of the fluid is produced.

The linear A.C. pump is a device which is rather similar to a linear induction motor (Reference 24). The polyphase field windings are arranged along a duct through which the conducting fluid moves. The duct is analogous to the squirrel cage rotor of the standard induction motor.

In all of the references cited above, specifications and characteristics of several electromagnetic pumps are given. Reference 22 presents a tabular listing of the characteristics of some commercial pumps manufactured by three different suppliers. Listed below are some typical characteristics of several different types of electromagnetic pumps. This information has been taken from Reference 19.

1. D.C. Conduction Electromagnetic Pump (Faraday Pump): 135 gallons per minute against a head of 21 feet; pump weight, 950 pounds; power requirements, 6000 amps at 1.25 volts.

2. Helical Flow A.C. Induction Pump: 400 gallons per minute against a 60-foot head; requires 1000 cubic feet per minute of cooling air; pump weight 1500 pounds, power supply, 25 cycle.

3. Linear Induction Pump: 1200 gallons per minute against a 110-foot head; pump weight, 6430 pounds; requires 2000 cubic feet per minute of cooling air; power requirements, 288 amps at 300 volts, 60 cycles.

According to Barnes in Reference 21, D.C. pump efficiencies range from 15 to 20 percent for small capacity pumps and up to 40 percent for larger systems. For A.C. conduction pumps, efficiencies range from 5 to 20 percent and for A.C. induction pumps, efficiencies may reach 40 percent.

Any or all of the types of electromagnetic pumps just described may have application for propellant containment or pumping. In general, the direct current devices are characterized by their simplicity of design and lack of insulation problems, since only low voltages are employed. They require, however, considerably larger currents than comparable A.C. systems and are heavier. In some applications, the use of direct current is also a detracting feature, especially where the primary power source is A.C. The most serious drawback to A.C. pumps is probably the insulation problem attendant with the use of higher voltages. The selection of one type of pump in preference to another, can only be made on the basis of a specific application.

MAGNETOFLUIDMECHANICAL PUMPS

A great deal of work is presently being published with respect to M.F.M. propulsion devices. Many of these devices can similarly be employed as fuel expulsion devices. Only two such devices are described since they are indicative of the field in general. An exhaustive literature search will undoubtedly yield several alternative geometries.

Multiple Exploding Wires

In the multiple exploding wires concept of expulsion, shown schematically in Figure 70, the wires I, II, III and IV are designed such that wire I explodes first ionizing fluid in its vicinity, then wire II explodes, etc. A magnetic field $\tilde{H}$ is created by the circuital current flow. This magnetic field, coupled with the current density $\tilde{J}$ forces the charged particles out of the tank. The expulsion force $\vec{F}$ is proportional to $\tilde{J} \times \tilde{H}$. As before, uncharged fuel is dragged along.

The properties of an exploding wire are expounded more completely in Reference 25. Another possible geometry is described in the last article of the above reference.

Channel Accelerator

.The channel accelerator utilizes segmented electrodes with
an applied magnetic field into and perpendicular to, the plane
of the diagram shown in Figure 71. If the fuel is partly con-
ducting then the current density j is perpendicular to both H
and the axis of the tank. A more detailed discussion of the above
device is given in Reference 26.

Many pinch engines have been discussed in the literature.
The pinch effect can be used to compress and thereby expel a con-
ducting liquid. To completely exhaust the various geometries
inducing the pinch effect would entail considerable effort.
Reference 27 shows one such geometry.

ANALYSIS OF SLIDING CONTACT TYPE DEVICES

Both the sliding contact device described under the elec-
trically driven mechanical system and the multiple exploding
wire device shown in Figure 70 share the same principle of
operation though the details of operation differ.

Consider the circuit shown in Figure 68. The magnitude of
the force F (in newtons) on any individual wire due to the mag-
netic induction B generated by the current in element I is given
by the following equation (Reference 28, page 21):

$$F = J\ell B \tag{73}$$

where ℓ is the length of element III and J is the current in
the circuit. Furthermore, (Reference 28, page   )

$$B = \frac{\mu_o m J}{4\pi}\left(\frac{\ell}{r^2}\right) \tag{74}$$

where r is the separation of elements I and III

     m is the number of current loops (circuits)   (75)

     $\mu_o = 4\pi \times 10^{-7}$ Henry/Meter

From Equations (73) and (74), it is seen that the force can be
increased by:

a.   increasing the number of current loops,
b.   using very high current sources,
c.   using a wide bore (large ℓ) short stroke (small r)
     piston.
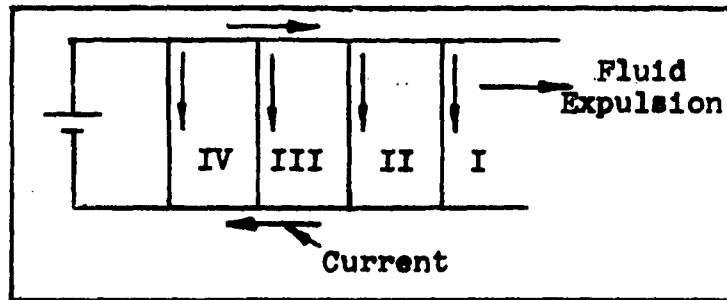
Figure 70.   Schematic of Multiple Exploding Wires
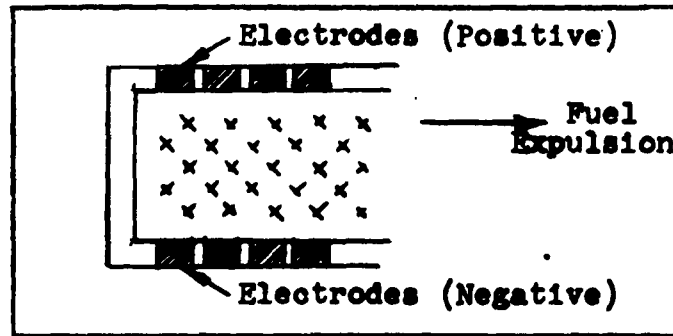
Figure 71.   Schematic of Channel Acceleration
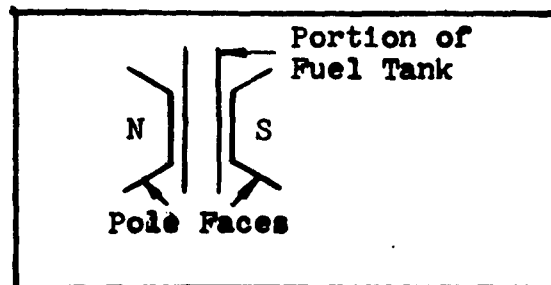
Figure 72.   Schematic of Magnetic Containment of Fluid
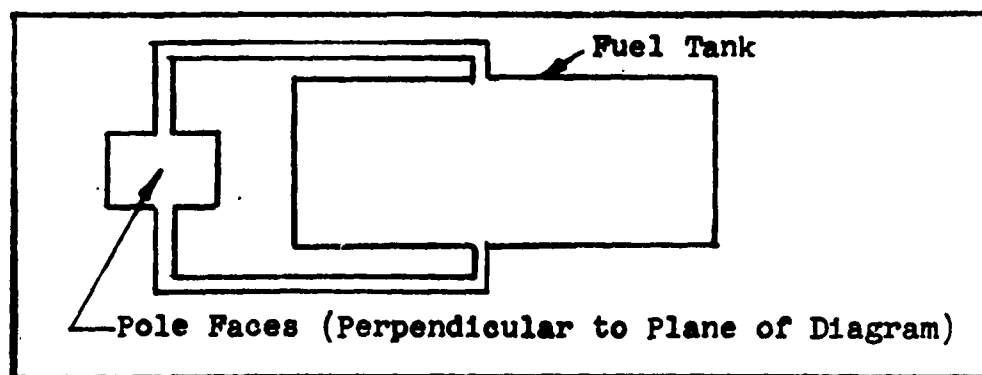
Figure 73.   Complete Magnetic Containment System

Since the weight of the system increases by less than the number
of loops (since a common piston is shared) and the available
force is proportional to the square of the number of loops and
the number of sliding elements also increase with m, the first
suggestion listed above appears particularly promising.

The available pumping rate (or piston velocity $\tilde{V}$) is
readily obtained as a function of either position or time by
integrating the equation of motion:

$$F = \frac{\mu_o J}{4\pi}\left(\frac{\ell^2}{r^2}\right) = m\frac{dV}{dt}$$

$$F = m\frac{dV}{dr}\left(\frac{dr}{dt}\right) = mV\frac{dV}{dr} \tag{76}$$

where m is the mass of the piston (or moving element).

Assume that $r = r_i$, and $V = 0$ when $t = 0$. Integration of
Equation (76) yields the value of V and r at a later time
as follows:

$$V = K\sqrt{\frac{1}{r_i} - \frac{1}{r}} \tag{77}$$

$$t = \frac{1}{K}\left[\sqrt{r_i(r^2 - r r_i)} + r_i^{3/2}\tanh^{-1}\sqrt{1 - \frac{r_i}{r}}\right] \tag{78}$$

where

$$K = \sqrt{\frac{\mu_o}{2\pi m}}\ (J\ell) \tag{79}$$

The above analysis reveals several significant points. Among
them are the following:

1.   The velocity asymptotically approaches the value $K/\sqrt{r_i}$

2.   If a given maximum time lag is specified to reach a
required pumping speed V then certain bounds will be placed
on the system variables J, ℓ, etc.

3.   Since the velocity V varies with distance r, the current
must be controlled to maintain a constant pumping rate.

4.   It follows from Equations (77) and (78) that the V ,
t -history varies with r . This places certain restrictions on
restartable operations.

5. Due to the purely electrical nature of the system, it is felt that greater reliability can be obtained than in a bladder type design.

6. In the case of the exploding wire, the resulting contamination of the fuel may prove undesirable.

A rather thorough discussion of the sliding contact device (and two alternative devices) can be found in Reference 29.

MAGNETOSTATIC SYSTEMS

It may be possible to employ static magnetic fields to contain liquid propellants. The use of such fields to pump propellants appears less feasible. With the notable exception of liquid oxygen, most propellant liquids are diamagnetic. Liquid oxygen is a paramagnetic material, whose mass susceptibility at $-310°F$ is 260×10^{-6} cgs-emu/gram.

Containment of paramagnetic propellants would be based upon the tendency of paramagnetic substances to move from a weak towards a more intense magnetic field. The force on a volume element of such a liquid is proportional to the gradient of the magnetic field. Thus the presence of an inhomogeneous magnetic field would be necessary to collect the liquid and then contain it at the desired location.

Diamagnetic materials, in the presence of an inhomogeneous magnetic field tend to move to a region of weaker magnetic field and thus they may also be collected and contained. The fact that paramagnetic and diamagnetic materials will be displaced by inhomogeneous magnetic fields, has been used in the design of several instruments for measuring magnetic susceptibility, References 17, 30 and 31. In the case of either class of material, the design objective is to produce a combination of magnetic field and container geometry, such that the propellant liquid will be collected and then contained as a continuous body of liquid. A possible containment scheme is shown in Figures 72 and 73.

The force $\tilde{F}$ due to a magnetic field $\tilde{H}$ is given by the following expression

$$\tilde{F} = K \, grad \, H^2 \tag{80}$$

where K is a positive constant for para- and ferromagnetic material and a negative constant for diamagnetic material. Furthermore, for the geometry shown:

$$H^2 = H_0^2 f(r) \tag{81}$$

where H_0 is the magnetic field at, and r is the magnitude of the distance $\vec{r}$ from, the center of the pole faces.

It can further be seen that:

$$\frac{df(r)}{dr} < 0 \tag{82}$$

since the field $\tilde{H}$ decreases with r (see Equation (81)).

Substitution of Equation (81) into equation (80) yields the following expression:

$$\tilde{F} = \left[K H_0^2 \frac{df(r)}{dr} \right] \frac{\tilde{r}}{r} \tag{83}$$

From Equations (82) and (83) and the remarks about the constant K in Equation (80), it is seen that a para- or ferromagnetic material is drawn into and a diamagnetic material is expelled from the region of the pole face (or the high field region) as was indicated (without proof) above.

In the foregoing discussion, emphasis has been placed upon the use of static magnetic fields to contain a liquid propellant. The same principles of containment may also have some application in pumping propellants. In either case, the forces produced are not expected to be very large. Forces which may be of sufficient magnitude to contain a propellant in a so-called "zero-gravity" condition may not be adequate to pump the same propellants. Unfortunately, the equipment required to produce a strong magnetic field is usually rather heavy and for space vehicle applications this may be a serious drawback. In the case of some propellants, it may be possible to increase the volume force by adding a compatible ferromagnetic material to the propellant and thereby increase its susceptibility.

As an example of the magnitude of force that might be expected with a given equipment weight, consider the problem of containing liquid oxygen by means of a permanent magnet with a magnetic field of 5,000 gauss and a pole separation of 1 cm. Such a magnet might be expected to have a mass of the order of 5 kg. For liquid oxygen the value of 2K (the magnetic susceptibility) is -310×10^{-6} cgs-emu/gm or -372×10^{-6} cgs-emu/cm^3. Equation (80) gives the force (per unit volume) drawing the column of liquid into the pole faces. The total force ΣF on either half of the liquid column is, therefore, given by the following expression:

$$\Sigma F = \int_0^z \tilde{F} \cdot \tilde{n} \, A \, dz \tag{84}$$

where A is the local cross-sectional area, $\tilde{n}$ is the local surface normal, Z is the coordinate along the length of the tube and $2Z_1$ is the length of the tube. It then follows from Equations (80) and (83) that:

$$\Sigma F = KA \int_0^{Z_1} GRAD\, H^2 \cdot \tilde{n}\, dz \tag{85}$$

$$\Sigma F = KA \int_0^{Z_1} \frac{dH^2}{dz} dz = -KA\left[H^2(0) - H^2(Z_1)\right] \tag{86}$$

$$\Sigma F = -KA\, H^2(0) \tag{87}$$

A more complete analysis will require a study not only of the integrated force on the liquid column but of the force distribution along the column. The following question must be answered: Can the resultant cohesive, viscous and magnetic force move a given element at a sufficient rate to maintain pumping?

A thorough analytical and experimental study of various fuel-magnet combinations (permanent and electromagnetic) will be necessary before a full evaluation of the above method can be made. The usefulness of the technique for a given mission can then be predicted.

CHEMICAL

In the incorporation of a system employing the effects of propellant chemistry, the propellant characteristics play a most important role. In this study on expulsion devices, only two concepts are considered under chemical expulsion. These are:

    1. Foam Displacement
    2. Supercritical System

FOAM DISPLACEMENT

Consideration of the possibility of using a light weight solid material that can be expanded to expel liquid fuels from a tank reveals that foams from such plastics as vinyls, phenolics, epoxys, polyesters and polyethers offer a unique method.

These foams are of relatively low density ranging from 1.5 to 15.0 lbs/ft^3, the density of the unexpanded plastic ingredients range from approximately 65 to 85 lbs/ft^3.

The general method of producing foams involves the reaction of the plastic resin and blowing agents and/or catalysts, with or without the addition of heat to form a cellular solid. This structure of the cells of these foams can be open or closed depending upon the foaming system involved. The density of the foam can be varied by controlling the proportions of the reactants and the temperature at which the reaction takes place. In some foaming systems there is a built-in heat of reaction and in others heat has to be added to cause expansion.

Foams will have volume expansions ranging from 10 to 200 times the original resin volume.

Characteristics of Foam Displacement Devices

Advantages

    1. There are no moving parts within the expulsion device.

    2. The system is relatively simple.

Disadvantages

    1. Foam must be immune to absorption and porosity must be low otherwise expulsion efficiency suffers.

    2. Compatibility of the foam with the various propellants may not be possible.

3. Temperature rise, if any, during the foaming process may produce adverse effects on the expulsion fluid.

4. Control of foam is not precise.

5. Clogging of entry tube and pile-up of foam may reduce outflow and limit restart capability.

6. Expulsion pressure may not be commensurate with required engine start pressure.

7. A lag in the system exists because foaming action will continue after foaming agent shut-off until equilibrium is established. A time lag exists for start of system.

8. Adhesion of foam to tank walls, unless it can be readily removed, will affect the test program cost and specimen numbers.

9. The required mixture of foaming agent and catalyst require valving, pressures and measuring devices.

10. Restart capability may be hampered by radiation environment on foam already present.

Analysis Data

Foamed Vinyls

Polyvinyl chloride or vinyl copolymers, resins or plastisols are premixed with a nitroso type blowing agent and introduced into a cavity heated to approximately 375°F, at which time the blowing agent decomposes releasing nitrogen gas which slowly expands the vinyl resin. The volume expansions achieved range from 10-50 times original volume and densities range from 4-10 lbs/ft^3.

This foaming system would probably be unsuitable for expulsion of fuels because heat would have to be added.

Foamed Polystyrene

Expandable polystyrene is produced as free flowing beads, approximately .020 inches in diameter, which contain an integrally mixed, expanding agent. These beads are expanded by blowing steam or injecting heat at around 250°F into the mass of beads. The polystyrene beads have a maximum expansion of 40-50 times their original volume and densities ranging from 1.5-4 lbs/ft^3.

These cells of the polystyrene foams are closed and the foam is relatively inert to acids and alkali.

This material will probably not be suitable because heat will have to be added.

Foam Phenolic and Epoxies

These plastic materials are generally expanded by the reaction between the resin and fixed proportion of acid or alkali catalysts. In general these foams will be prepared by mixing two components (i.e. the resin and catalyst) for five seconds and allowing the mixture to expand into a cavity; no addition of heat is required.

The maximum expansion volume of these systems ranges from 100-150 times the original volume resulting in approximate densities ranging from 1.5-15 lb/ft^3.

Foam Polyurethanes

Polyurethane foams are prepared by reacting polyester or polyether plastic resins with a catalyst and varying proportions of an isocyanate. The polyrethane foams usually consist of two components which must be mixed for five to ten seconds and then immediately introduced into the cavity to be filled. Because the reaction is an exothermic one, it us unnecessary to add heat to the system.

The volume expansion of these polyurethane foams ranges from 100 -200 times the original volume. The density of these foams will range from 1.5-15.0 lb/ft^3.

Discussion

Based upon practical application of these foaming systems to the problem of expelling propellants from a tank, the polyurethane foams appear to be the most suitable because they react rapidly without the addition of heat. They require very little mixing; they have high expansion volumes and low density. They have closed cells so they would not tend to absorb the fuel by capillary attraction, and once formed would be relatively inert to chemical action with many liquid fuels.

The problems involved with the use of polyurethane foams would be the mixing of approximately equal volumes of resin and the isocyanate prepolymer for five seconds and injecting the mixture into the tank cavity.

The foam would tend to adhere to the tank wall so it would be necessary to have the tank wall coated with a parting

agent such as polyethylene or similar inert plastic materials.
Another problem that might be encountered would be in controlling
the exact proportion of the two foaming components which would
react and expand to fill a specific volume, if the liquid fuel
were to be expelled in various volume increments.

At the foam liquid fuel interface, there might be some
local chemical reaction and/or absorption after -long time con-
tact of the foam and fuel. This problem might be overcome by
the use of a thin metal or plastic diaphragm which would separate
the foam and the liquid fuel.

SUPERCRITICAL SYSTEM

Characteristics of a Supercritical System

Advantages

1. A single phase fluid is always present so that mass
flow can be metered and monitored.

Disadvantages

1. Tank pressure must be greater than the critical
pressure of the fluid.

2. Tanks must be designed to withstand these high pres-
sures thus imposing heavier structures.

V. SPACE ENVIRONMENT

INTRODUCTION

The storing and expelling of propellants, including cryo-genics, during various flight and space missions, requires numerous considerations which are a function of the type of mission and its associated environment.

The various planned space missions cover the gamut of earth satellites with typical missions as low as 90 minutes to inter-planetary flight vehicles which have mission times of 3 to 6 months. For these configurations, propulsion must be provided to carry out midcourse and terminal trajectory corrections, steering, attitude control, orbital rendezvous, vernier orbit establishment, and planetary landing or take-off.

The outer space environment makes new demands on systems and materials. Some aspects of this new or space environment that are of concern to space vehicle operation are the extremely low pressure and the various radiation effects. These are also associated with a wide spectrum of possible design temperatures.

This section on space environment attempts to list the many facets of conditions surrounding a space mission that could be introduced during the life or operational period of a space vehicle and its associated equipment.

A brief summary of the space environment that is considered includes:

1. Temperature
2. High Vacuum
3. Radiation
   a. "Galactic" Cosmic Radiation
   b. "Solar" Cosmic Radiation
   c. Albedo Cosmic Rays
   d. Van Allen Radiation
   e. Auroral Radiation
   f. X-Ray and Ultraviolet Radiation
4. Extraterrestrial Environments
   a. Micrometeroids
5. Accelerations
6. Sonic Fatigue

TEMPERATURES

For thermal control, heat transfer to and from space vehicles is accomplished solely by radiation. Heat transmission by con-vection is precluded by the vacuum, and heat transmission by con-duction can take place within the vehicle only.

The primary source of thermal radiation for a space system located within the solar system, is the sun. The earth may also contribute to the thermal environment of the system and will be of greater importance for the lower altitude orbits. If these bodies were absent, for example, the system facing outer space, the equilibrium temperature which the system would achieve is approximately 5°R. A calculation of the equilibrium temperature for a black body at the mean earth-sun distance, based only upon the solar constant, yields a value of approximately 500°R. On the other hand, surfaces or systems facing the sun can reach temperatures as high as 1000°F where high ratios of absorptivity-to-emissivity are utilized. The temperatures may also vary continuously as on the surface of a spinning vehicle or they may be fixed by design as in cryogenic tank installations.

Depending upon the expulsion device location within the configuration, the unit is susceptible to a range of the above-mentioned temperatures. As a result, the characteristics of materials, in judging their suitability for service at these temperatures, must be considered. The tendency to brittle fractures of the materials must be expected to become more serious at the lower temperatures. Expulsion devices that incorporate folding membranes, creases and other large elastic and inelastic deformations in the cryogenic temperature range warrant additional studies or cryogenic laboratory tests because the material must be capable of flexing and folding at these cryogenic temperatures.

HIGH VACUUM

The pressure levels to be encountered by future space systems will be expected to vary from sea level values on earth to less than 10^{-12} mm Hg in the depths of space. Several deleterious effects can be expected from this high vacuum environment which must be carefully defined. A problem which will assume importance, especially for long duration missions, is vaporization of the materials from which a space capsule are constructed. Whenever the vacuum condition is such that the mean free paths of particles released from the surface of a solid material is greater than the size of the evaporating structure, the recondensation of vapors to the surface is insignificant. The rate of evaporation will then be a function of the vapor pressure of the material and its surface temperature. The vapor pressure for metals is an exponential function of temperature so that if sufficiently low structure temperature can be maintained the problem will be minimized. On the other hand, this effect, coupled with the erosion due to meteoroid collisions, may cause failure of pressurized compartments, propellant tanks, etc.

Another consequence of these extremely low pressures is that sliding friction between metals becomes very high, because of the absence of sufficient oxygen to renew an oxide film and thus prevent "cold welding" between the metallic surfaces. This phenomena may restrict the application of the sliding piston expulsion device. Although dry, non-volatile, lubricants such as molybdenum disulphide and graphite suggest themselves for service under their vacuum conditions, the propellant compatibility problem is introduced.

RADIATION

In space, the propulsion system will be exposed to many types of penetrating radiations which are both particulate and electromagnetic in nature. Commensurate with the intended use and location in the over-all system, subsystems and individual components must be designed to withstand these radiations for specified exposure periods. A brief description of the more important of these radiations and their possible effects is given in the following paragraphs.

a. "Galactic" Cosmic Radiation

This term is used by J. R. Winkler (Reference 71) and others to differentiate this radiation from the more recently discovered solar cosmic rays. The origin of the primary particles of this radiation is presumed to be galactic rather than solar, hence the name. The primary particles are composed of about 85% protons, better than 14% alpha particles and less than 1% heavy nuclei components (Reference 72). Their kinetic energies range from below 10^8 to slightly over 10^{19} electron volts, with an average of about 3.6×10^9 electron volts per nucleon. The flux density is very low, however, being about 3100 particules per square meter per second per steradian for particles with kinetic energy greater than 5×10^8 electron volts per nucleon. The ionization rate at these flux levels is about 24 milliroentgens per day.

Although these particles produce atomic dislocations in the material they penetrate, the damage produced is not expected to alter the bulk properties of structural metals used in space stations. Their effects on propellants, lubricants, fluids, and nonmetallic materials have not yet been adequately investigated.

Elastomers and fluids using materials whose structure includes the covalent bond will be the most sensitive. However, any effects are expected to be negligible in this case because of the low flux density. In this regard, it is interesting to note that for satellites in low altitude (i.e. 300-mile) orbits, addi-

tional filtering of the less energetic particles will be provided
in the lower latitudes by the earth's magnetic field.

b.   "Solar" Cosmic Radiation

This is sometimes referred to as "solar flare" radiation.
The name derives from the fact that a considerable fraction of large
flares on the sun give rise to almost pure streams of protons
(References 73 and 74). These protons eventually arrive at the
earth from 25 minutes to 10 hours after the flare reaches its
visible peak. They then continue to arrive for as long as 11 days
afterward. The flux density of these particles rises much more
steeply at the low energies than does that of the "galactic"
radiation, with a spectrum extending from 20-30 million electron
volts (possibly much lower) up to at least 500 million electron
volts. The flux of protons with energies greater than 75 million
electron volts is known to vary from 20 to 350 times that of the
galactic type. During the period from 1957-1960, the number of
flares ejecting such radiation numbered about 30.

Again, this radiation is not expected to significantly
alter the properties of structural metals used in space hardware.
The same materials and components enumerated in the preceding
section will also be the most sensitive here. Because of the much
higher flux densities, the effects are no longer apt to be negli-
gible. Furthermore, the high energies of these particles will make
difficult. The resultant situation is one which will require care-
ful analysis.

Brute force shielding may not be the only way of solving
such difficulties. It is known that this type of radiation occurs
more frequently during periods of high sunspot activity. More exact
prediction criteria are presently being established by K. A. Ander-
son (Reference 75) at the University of California. If sufficient
prediction accuracy becomes possible, the probability of encount-
ering this radiation might be reduced by moving vehicle to a
"safer" orbit prior to the event.

c.   Albedo Cosmic Rays

This is secondary radiation caused by the primary cosmic
particles striking the earth's atmosphere and disintegrating the
nuclei into lower energy particles which behave in a manner similar
to the parent particles. The portion of this secondary radiation
which is radiated into space is referred to as Albedo Cosmic Rays.
These secondary particles can cause molecular sputtering (knocking
off of molecules) of the skin and damage to components mounted at
the surface. While this effect might be negligible for deep space
or the higher orbits, extended exposure times at a 300 mile orbit

might produce significant effects. Again, further analysis of the situation as it pertains to the specified missions is indicated.

    d. Van Allen Radiation

        The inner Van Allen Belt extends from about 1000 to 3000 nautical miles altitude, lies in the plane of the geomagnetic equator, and extends from about 45°N to 45°S magnetic latitude. The outer Van Allen Belt extends from about 8000 nautical miles to 12,500 nautical miles altitude (Reference 76)

        It is not intended to imply that the space outside these regions is completely free of radiation. Actually, there is evidence that particle radiation is generally distributed throughout the near-earth space; the Van Allen regions being zones of high concentration because of the peculiar mechanisms by which the particles are trapped, the strength of the geomagnetic field and the energy and nature of the primary particle flux.

        The inner zone has exhibited a high degree of constancy both in intensity and spatial extent. On the other hand, the outer zone has shown immense temporal fluctuations. It is thought that this behavior of the outer zone is due to changes in the geomagnetic field as a result of strong corpuscular emission from the sun. The inner boundary of the outer zone remains essentially fixed following solar activity, whereas, its outer boundary has been noted to extend outward well beyond the 12,500 miles mentioned above. Further, the inner zone, lying as it does in the region of strong geomagnetic field, is relatively well isolated from direct solar influence.

        It is now fairly definite that the more penetrating component of the inner zone consists of protons having energies of the order of 100 MEV (References 77 and 78). In the heart of this zone, at an altitude of 1900 nautical miles on the geomagnetic equator, the ominidirectional intensity of protons having energies greater than 40 MEV is $2 \times 10^4/cm^2$-sec. At 660 nautical miles, Freden and White (Reference 79) have found protons having a moderately steep spectrum in the range of energies from 75 to 700 MEV.

        On the other hand, the particles of the outer zone are now believed to consist mostly of high energy electrons. Their energy spectrum resembles that of the auroral radiation. The ominidirectional flux of these electrons is of the order of 10^{11} particles/cm^2-sec for energies greater than 20 KEV (Reference 78). The position of the center of this zone fluctuates with time, being particularly sensitive to outbursts of solar activity. Data obtained from Explorer VI indicated that this outer zone shrinks

considerably in intensity and extent during periods of low solar
activity. During such times, there is evidence that two maxima
appear at altitudes of 5700 and 8900 nautical miles at the equator.

Within the range of geographic latitudes from about 40°N
to 40°S and for all longitudes, the Van Allen radiation appears
to be of little intensity below altitudes of about 400 nautical
miles. Consequently, for a 300 mile orbital mission, the effect
of this parameter on the space system should be less important.

For satellites which pass through the outer Van Allen
Belt, past satellite experiments have shown that a system in this
type of orbit may expect to be engulfed from time to time in very
intense radiation. The energetic component of this radiation, as
mentioned previously, consists mainly of electrons having
energies between 20 and 100 KEV.

Many reports have been published on the nature and
intensity of the particle radiation present in space. References
80 and 81 are two of these which have reached the stature of
initial specifications to which space vehicles and components
should be designed as recommended by LMSD and USAF, respectively.
Reference 82 contains calculations of anticipated yearly dosages
due to particulate space radiation as measured on the vehicle
surface (surface dose) and under a nominal satellite wall thick-
ness (internal dose). Reference 83 and other sources, generally
agree on 5×10^5 rads as a probable yearly internal dose for the
center of the inner Van Allen zone. A surface dose of as high as
10^{12} rads has been assumed by USAF, ASD.

With equipment shielded in about the manner that ordinary
minimum structural considerations for space vehicles would
dictate, i.e., about 0.1 inch of light weight material, dose rates
of some 10 roentgens per hour have been measured in the center of
the inner zone; and ones several times this level in the heart of
the outer zone. The dose rate in the inner zone is only slightly
reduced by the addition of 0.130 inch of lead due to the
penetrability of the high energy protons present there. The same
thickness of lead reduces the level in the outer zone by a factor
of at least fifty.

The exposure levels on the surface of the satellite or
space vehicle are much higher, especially in the outer zone, of
the order of 10^5 roentgens per hours.

Any charged particle emits electromagnetic radiation when
it is slowed down. The electromagnetic radiation is known as
"Bremsstrahlung", which in German means "braking radiation".

This rate of emission of radiant energy is nearly proportional to the energy of the particle and decreased rapidly with increase in the mass of the particle. Hence, it is usually important only in the case of electrons; the rate being so much less for protons. Bremsstrahlung production is much larger in matter composed of heavy atoms, such as lead, than in matter composed of light atoms, such as aluminum or beryllium. Such considerations have led to studies of optimum shield weights based on a laminated shield with a light weight material on the outside and backed by a heavy material like lead, which is effective in absorbing the resultant Bremsstrahlung radiation.

e.   Auroral Radiation

Auroral displays have been detected (References 84 and 85) at altitudes from 27 to over 550 nautical miles. The primary radiation associated with these complex auroral processes consists of electrons having fluxes as high as 10^8 electrons cm^{-2} sec^{-1}. Maximum electron energies of 200 KEV are attained. Proton fluxes of about 10^6 protons cm^{-2} sec with a maximum energy of 500 KEV have also been detected. Most of the activity observed occurs in northern and southern auroral zones, hence the name. The effects of auroral radiation will be similar to that produced by the outer Van Allen Belt but reduced in magnitude.

f.   X-Ray and Ultraviolet Radiation

Most of the "quiet" sun's X-radiation originates in its corona and in certain active regions of the chromosphere. These regions emit X-radiation at wave lengths greater than about 10 Angstroms and at energies around 10^4 electron volts. During solar flares, however, the sun emits bursts of high energy X-ray radiation. It has been reported that an 18-second burst of radiation peaked in the 200-500 KEV region occurring simultaneously with the flash phase of the solar flare. In a similar instance, X-rays with energies extending up to 70 KEV have been measured. The total energy contained in the emission tail above quantum energies of 20 KEV was of the order of 2×10^{-5} ergs/cm^2/sec.

In the auroral regions, collision of the primary electrons with the nuclei of gases in the earth's atmosphere is believed to generate "Brensstrahlung" X-rays. These X-rays have energies in the range of 10 to 100 KEV and fluxes of 10^3 ti k9^4 protons cm^{-2} sec^{-1}.

About 7.5% of the total radiation from the quiescent sun lies in the near ultraviolet (2000 - 3800 Angstroms); about 0.2% lies in the far ultraviolet (1-2000 Angstroms). While the total energy in these regions is small, the energy per proton is

relatively high, ranging from 4 to 125 electron volts as the wave
length shortens from 3000 to 100 Angstroms. The Lyman alpha line
of hydrogen is one of the more important in the ultraviolet
spectrum. The intensity of this line radiation increases by a
factor of 100 or more during the times when solar flare disturb-
ances are present. Above altitudes of about 200 miles, the
absorption of ultraviolet by the earth's atmosphere will be
negligible.

In metals, the ultraviolet radiation can produce photo-
electric emission. However, the flux is too low in this instance
to produce serious effects either in the surface layers or in the
bulk. The damage to plastics and elastomers caused by ultra-
violet irradiation results from ionization and excitation of
electrons. The changes are irreversible and include free radical
formation, polymerization and gas formation. Investigations of
the effects on various materials are now underway but data are as
yet rather sparse.

Practical considerations of the useful-life limit of long
orbiting satellite systems show that only nonmetallic materials
need be considered as likely to cause a malfunction. Metals and
metal-alloys do not begin to show gross changes in physical pro-
perties until a dose of between 10^{10} and 10^{11} rads; 1 rad is
defined as 100 ergs absorbed per gram of material. Therefore,
metals and alloys may be considered as being inert to the antici-
pated dosages during normal satellite life. Attention is again
directed to the surface dose being considerably higher.

Plastics and elastomers on the other hand, have threshold
doses considerably less, of the order of 10^4 to 10^6 rads; and
therefore must be considered as liable to failure during the
missions anticipated. These materials, such as Teflon, Kel-F,
mylar, etc. are widely used in attitude control systems because of
their excellent chemical and physical properties in propellant
service.

EXTRATERRESTRIAL ENVIRONMENTS

The environments evidenced at sites located on planetary
bodies other than Earth's are rather limited. The moon is
undoubtedly the side of man's first extraterrestrial colony. The
lunar environment will be similar in many respects to the space
environments discussed in the preceding paragraphs. This is so
since for all practical purposes, the moon is devoid of an atmos-
phere. An upper limit of 10^{-10} millimeters of Mercury has been
estimated for the moon's atmosphere based on astronomical measure-
ments. The lunar gravitational field has already been mentioned.

Dust layers on the surface of the moon have been postulated but are still speculative.

Although the environmental information for the moon is far from complete, out knowledge of the environments on Venus and Mars, Earth's nearest neighbors, is still more rudimentary. Recent measurements, for example, of surface temperature on Venus of a value of approximately 300°C and an atmosphere composed mainly of CO_2 have been made. Any detailed description on the conditions under which systems must work would of course require considerably more data from interplanetary probes before any detailed descriptions could be made.

a.   Micrometeroids

The effects of micrometeroids appear to be of importance more and more as the results of evaluation of the most recent satellite experiments become available. These data indicate a much greater population, particularly of particles of the very small size and, consequently, require a careful study of this environment and its penetration potential.

Examination of meteorites (meteroids which have survived passage through the Earth's atmosphere) reveals two distinct classes. The metallic or "iron" type has an average density of about 8 gm/cm^3. The "stoney" type, which outnumbers the "iron" type by a ratio of 9 to 1, has a density range from about 3 to 0.05 gm/cm^3. Velocities of both types at point of entry into the Earth's atmosphere range from about 40,000 to 230,000ft/sec. The heavier particles, from 10^{-5} to 10^3 gms, are usually completely destroyed after entering the Earth's atmosphere while the small-sized, low density (0.05 - 2.0 grams/cm^3), spongy ones pass through comparatively unharmed. Only the heaviest (above about 10^4 grams) survive the penetration of the Earth's atmosphere and reach the ground. In addition to the daily sporadic impacts of meteoroids with the earth, there are periodic "showers" which occur at about the same time each year. During a year's time there are about 17 known showers of this type. The number density of meteoroids during these times is several orders of magnitude greater than normal.

Existence of a "dust" belt around the earth is indicated by data obtained from U. S. and Russian satellite and rocket experiments. The heaviest concentration of particles is believed to occur at an altitude of about 100 miles, in the plane of the equator, and gradually fading away at distances 300,000 to 1,000,000 miles from the earth. The prediction of this belt appears to be confirmed by recent experiments conducted by the AFCRL with a special nose cone.

Two effects are of primary concern here, they are: penetration of the structure by the more massive particles, and erosion of the surface skin by the "sandblasting" action of the more numerous but much less massive particles. The meteoroid population, as directly measured in rocket and satellite experiments, has indicated contradictory results when compared with the extrapolations based on visual, photographic, radio or radar detection of meteoroids. Basically, the measured population of the low mass meteoroids is (by several orders magnitude) higher than the extrapolated values. In addition, the measured values (for the same meteoroid magnitude) varied over a large range up to five orders of magnitude.

For operations at altitudes below 400,000 feet (65 nautical miles) the effects of meteoritic bombardment are negligible, even for very long periods. During orbital or lunar missions, however, the vehicle may be exposed to increased micrometeoroid bombardment by the dust "halo" particles. The distribution of particle masses in this "halo" has not yet been adequately determined. However, there cannot be many particles having masses exceeding 10^{-5} grams, or they would have been detected previously by radar measurements.

Using the information on the penetrating effects of high velocity particles together with data on the incidence of meteoroids in space, References 86 and 87, conservative estimates of exposure time versus number of penetrations through aluminum skins of varying thicknesses can be made. For an aluminum skin thickness of .010 inches, about 3.6 to 360 penetrations per square meter per hour can be expected. The approximate radius of the hole of penetration is 0.01 inches or 3.14×10^{-4} square inches of area. Increasing the skin thickness to 0.10 inches, the flux density or encounter rate is 5.4×10^{-5} to 3.6 penetrations per square meter per hour. The radius of the hole, by Kornhauser's method, (Reference 86) is 0.1 inches for this condition. The probability of "holing" space vehicles or capsules is thus seen to be extremely sensitive to increases in skin thickness. The penetration itself is a very complex phenomenon because of the variable amount of energy dissipated in each of the different forms (heating, melting, radiation, evaporation, and deformation of material).

The second, so-called "sandblasting" effect, can be expressed numerically by the removal rate of the exposed surface material due to erosion. A calculation, made by Kornhauser, (Reference 86), results in a thickness loss of 0.0036 inch per year for an aluminum surface (outside the dust halo). Similar results can be expected for other material.

ACCELERATIONS

The acceleration during take-off in an Earth-launching may be in the order of 10 g. Vibratory acceleration from 10 to 40 g with frequencies of 5 to 2000 cycles per second have been mentioned. The latter accelerations are of very brief duration and have not been of profound concern.

Trajectory corrections, orbit rendezvous, etc. will induce accelerations of perhaps smaller magnitude than that experienced during an earth-launch. However, the direction of this acceleration and the orientation of the positive expulsion device may affect the performance of the device. For example, a piston type expulsion device can be oriented in such a manner (along the piston axis of symmetry) that the energy required to expel the fluid must take into account the force to overcome the acceleration acting on the piston head. Thus, some of the expulsion devices are g or acceleration sensitive.

SONIC FATIGUE

As engines become more powerful to provide the necessary thrust for future planned payloads and space missions, there will also arise an attendant increase in sound level. Some aircraft and missiles have already undergone extensive modifications to improve their ability to withstand these noise loadings. The prediction of fatigue behavior under noise loading requires an understanding of structural response under extremely complex loading conditions. Sirens and other discrete-frequency force generators are being considered and used, but the interpretation of the probable life from the test results obtained under such laboratory conditions is subject to question.

The acoustic noise environment will generally be in evidence at, and immediately following, launching, and possibly during boost separation and firing of the second or third stages. Application of thrust for steering, attitude control, orbit establishment, etc. in the near space vacuum should not induce any sonic or noise problems because of the lack of the medium to transmit the distrubance. On the other hand, planetary landing or take-off and the associated planetary atmosphere may be conducive to sonic excitation.

Table VII represents a brief summary of some of the effects of space environments presented on the previous pages and some of the design factors that require consideration in the study and analysis of a reliable space vehicle and its components.

Table VII. Summary of Space Environment Design Factors

Environment	Effects	Design Factors
Temperature	Thermal energy within vehicle produced by solar radiation, earthshine, earth radiation, & internal heating. No convection heating outside earth atmosphere.	Design for temp control by means of absorptive & reflective surfaced (α/ϵ ratio) w/heat control servo circuits. Isolate internal equip. thermally for temps. between 0° & 60°C depending on requirements. For heat transfer use radiation & conduction heat sinks. Spin space vehicle to eliminate temp. gradients around surface.
Vibration	Unimportant in space (except for launch environment). No acoustic, frictional, or combustion vibration problems except for special applications.	Any vibration, acceleration, or shock levels in space which may occur would be very small compared w/those during the boost phase. The equipment must be designed to withstand the levels during boost and therefore the lower levels encountered in space should pose no problems.
Acceleration	Unimportant in space except for special applications.	
Shock	Unimportant in space except for meteorite & micro-meteorite impacts.	
High Vacuum	Sublimation & evaporation of materials occur in high vacuum	Use materials w/low sublimation rates. Allow sufficient thickness for sublimation & evaporation over expected operating life.
	Chemical atmosphere produced by outgassing & sublimation may have corrosive, plating, or chemical effects.	Select material w/care to avoid hazardous conditions.
	Electrical arc-over or corona discharge.	Provide adequate insulation material & insulation paths.
Magnetic fields	No effects except for fine instrumentation.	Avoid use of instruments not shielded against variations outside earth's magnetic fields.
Gravitational fields	No effect on materials or parts.	None for materials or parts. For manned vehicles, physiological considerations

Factor	Effect	Protection / Consideration
	Electrical arc-over or corona discharge.	Provide adequate insulation material & insulation paths.
Magnetic fields	No effects except for fine instrumentation.	Avoid use of instruments not shielded against variations outside earth's magnetic fields.
Gravitational fields	No effect on materials or parts.	None for materials or parts. For manned vehicles, physiological considerations are involved.
Meteorites & micrometeorites	Collisions w/particles of varying sizes occur.	Statistically calculated risk is involved. Use preroughened surfaces or oxide finishes to minimize changes in α/ϵ ratio. Use sufficient outer skin thickness or a secondary outer shell to provide protection against small particles.
Ultraviolet light	Increase sublimation rates in high vacuum.	Minimize sublimation by selection of materials & by providing sufficient material thickness allowances.
X-rays & gamma rays	Ionization of material occurs, possibly causing atomic displacements which produces changes in material characteristics or composition.	Intensity of primary radiation is negligible but shielding with heavy material may be considered for secondary ionizing radiation effects.
Neutrons	Intensity too low to require consideration of atomic displacement effects.	No special precautions necessary because of low intensity.
Trapped Electrons	Ionizing radiation occurs primarily in Van Allen belts, possibly causing atomic displacements which produce changes in material characteristics or composition.	Protection required for externally mounted equipment such as solar cells. Space vehicle shell normally provides protection for internal equipment.
Trapped Protons	Ionizing radiation occurs primarily in Van Allen belts, possibly causing atomic displacements which produce changes in material characteristics or composition.	For low energy protons in outer Van Allen belts, protection requirements are similar to those for trapped electrons. For high energy protons in inner Van Allen belts there is no known adequate protection.

2

The description of the space environment indicates the existance of certain conditions and their physical order of magnitude that must be integrated with a material or component to witnstand these effects.

Materials are tested, within the physical capabilities of space simulation on earth, to ascertain their physical conditions when exposed to such environments. It is only on a simulated test basis that a material is selected to insure its performance characteristics. The effects of this space environment on several materials is presented in some detail in the section MATERIAL CONSIDERATIONS.

VI. MATERIAL CONSIDERATIONS

The selection of materials for positive expulsion devices depends upon many inter-related design parameters. In general, there are four very important characteristics required in materials for application in expulsion devices in a zero-gravity environment. These are:

> Material-Propellant Compatibility
> Permeability
> Radiation
> Elongation & Ductibility

These characteristics are discussed, in some detail, in this report in order to indicate their importance.

Other considerations are also stated but are treated more lightly. These considerations include:

> Temperature
> Yield Strength
> Ultimate Strength
> Modulus or Elasticity
> Work Hardening
> Metal-to-Metal Compatibility
> Vacuum Effects

Candidate materials should be considered with respect to their particular applications for which they are interested. For example, a minimum use temperature of -130°F for Teflon TFE does not mean that a Teflon bladder could be successfully flexed at this temperature. Similarly, it has been reported that Polyethylene and Polyvinyl Fluoride exhibit a lower than normal melting point when heated in the presence of unsymmetrical Dimethylhydrazine.

A list of possible candidate materials and their properties are given in Tables VIII, IX and X. Data for Table VIII has been abstracted from References 32 and 33. Table IX, on elastomers is necessarily brief. The active propellant compatibility of a basic elastomer such as silicone or butyl depends to a great extent on additives and compounding techniques utilized to prepare a rare gum stock and aslo upon curing techniques necessary to vulcanize the gum stock.

TABLE VIII

PROPERTIES OF PLASTIC FILM

Material / Property	(1) Teflon TFE	(1) Teflon FEP	(1) Polymonochloro-trifluoroethylene	(1) Polyamide (Nylon)	(1) Poly-Propylene	Polyet Low Density	M D
Specific Gravity	2.1-2.2	2.15	2.1-2.2	1.08-1.14	0.885-0.9	0.910-0.925	0.92
Tensile Strength, psi	1500-4000	2500-3000	6300-6600	9000	4500-10,000	1350-2500	2000
Elongation, %	100-350	300	90-300	Orients	Over 200	200-800	15(
Bursting Strength, 1 mil thickness, Mullen Points			42 (2 mil film)				
Tearing Strength, gm	10-100	125	200-350		32-1750	60-200	5(
Tearing Strength, lb/in.				1300		65-575	
Folding Endurance					Very high	Very high	Ver
Water Absorption, 24 hr, %	0.00	0.00	0.00	1.0-1.5	0.005 or less	0-0.8	N
Water Vapor Permeability, gms/24 hr/m^2/ mm thick/cm Hg at 25 °C	0.00	0.002	0.00	0.3-1.8	0.06	0.04-0.08	0.03-
Resistance to Heat, °F	500	400-450	300	180-380	190-220	200	2:
Resistance to Cold, °F	-130	-130	-80	-60	-60	-50	-(
Permeability Gases, 10^{-6} g/24 hr/m^2/ mm thick/ cm Hg at 21°C, 0% RH		CO_2-2		CO_2-160		CO_2-12,000	CO_2-
	N_2-2 O_2-6 H_2-14		Very low	O_2-25 (50% RH)		O_2-1900 N_2-400	O_2-

NOTES: (1) Data from Reference 17
(2) Data from Reference 18

TABLE VIII

ERTIES OF PLASTIC FILMS

(1) Poly-ropylene	Polyethylene (1)			Polyethylene Terephythalate (Mylar)(1)	(1) Polyvinyl Fluoride	(2) Polyvinylidene Fluoride
	Low Density	Medium Density	High Density			
85-0.9	0.910-0.925	0.926-0.940	0.941-0.965	1.38-1.39	1.37	1.76
)0-10,000	1350-2500	2000-3500	2400-6100	17,000-23,700	8000-15,000	6000-6500
/er 200	200-800	150-650	150-650	35-110	100-190	150-500
				45-60	40	15-20
2-1750	60-200	50-300	15-300	10-27	15-25	40-60
	65-575			650-1740		
y high	Very high	Very high	Very high	20,000	Excellent	75,000 cycles for 3 mil film, MIT Flex Life Endurance
)5 or ss	0-0.8	Nil	Nil	< 0.5	< 0.5	
06	0.04-0.08	0.03-0.06	0.02-0.04	0.05-0.15	190 g/100 meters sg/hr/mil	0.6 g/mil - 24 hrs-1000 in.^{2}
-220	200	220	250	300	220-250	300
)	-50	-60	-70	-80	-60	> -40
	CO_2-12,000	CO_2-9000	CO_2-6200-3300	CO_2 < 0.5	CO_2 <0.5	10^{-12} cc/sec/cm^2/mm thick/cm Hg
	O_2-1900	O_2-1500	O_2-800-450	O_2 < 0.5	O_2 < 0.5	CO_2-9
	N_2-400		N_2-100-50	N_2 < 0.5	N_2 < 0.5	O_2-24 N_2-5.5

TABLE IX

PROPERTIES OF ELASTOMERS

Material Property	Silastic S-9711(1) Dow Corning Corp. Silicone	Silastic LS-53(2) Dow Corning Corp. Fluoroalkyl Silicone	Viton A(2) E.I. du Pont de Nemours & Co. Fluoroelastomer	Compound 3496-7 Parker Seal Co. Butyl (3)
Specific Gravity	1.13	1.4		1.12
Hardness, Shore A	50	55	66	64
Tensile Strength, psi	950	1000	2375	2530
Elongation, %	520	170	350	1170
Tear Strength, lb/in.	100			
Compression Set, %	100 after 22 hr. at 300°F	20 after 22 hr. at 300°F		
Brittle Point, °F	-100	-90	-47	
Stiffening Point, °F	-67			
Specimen Cure	Press molded 5 min. at 260°F, cured 2 hr. at 480°F	Press molded 5 min. at 260°F, cured 24 hr. at 300°F		

Notes: (1) Data from Reference 34
        (2) Data from Reference 35
        (3) Data from Reference 36

TABLE X

PROPERTIES OF METALS

Material	Specif. Gravity	Density lb/in3	Melting Point °F	Tensile Strength x10³ psi	Modulus Elast. x10⁶psi	Expansion x10⁻⁶in/in/ °F	Conductivity BTU/ft.hr. °F/in.	Ref.
Lead	11.4	0.41	621	2	2	16.4	240	37
Alum. 1100-0	2.71	0.098	1190-1215	13	10.0	13.7	1540	38
Copper, Hard Temper	8.92	0.322	1980	52	16.0	9.3	2700	38
K-Monel, Hot Rolled	8.47	0.306	2400-2460	150	26.0	7.8	130	38
Gold (Pure) Hard Temp.	19.32	0.698	1945	32	13.0	7.8	2000	38
Nickel(Wrought) Hard Temp.	8.89	0.321	2615-2635	105	30.0	7.2	420	38
Platinum, Hard Temp.	21.40	0.772	3225	36	24.0	4.9	480	38
Silver (Pure) Hard Temp.	10.50	0.379	1760	43	10.5	10.6	2900	38
SS, Type 304- Annealed	8.02	0.29	2550-2650	85	28.0	9.6	113	38
Titanium, Annealed		0.164	3300-3480	78.7	16.8	4.7	1180	39, 40

MATERIAL-PROPELLANT COMPATIBILITY

The selection of any material for the fabrication of a positive expulsion device is governed primarily by compatibility with the proposed propellant. The compatibility is determined by changes in physical, mechanical, permeability, and chemical resistant properties of the material before and after immersion for a specific test period in the proposed propellant. It should be noted that materials listed as compatible with a given propellant should be tested for compatibility under anticipated service conditions. The effects of temperature and exposure time are important factors in measuring compatibility.

CYROGENIC FLUIDS

The major consideration in the selection of a material for the construction of a positive expulsion bladder for use with cryogenic fluids is the ability of the material to withstand flexing and folding at cryogenic temperature. If a material will fail when flexed and folded at the extremely low temperature in question, it cannot be used for this application. Of equal importance are the compatibility of the material with various fuels and oxidizers, impact sensitivity of the material with other strong oxidizers, and the effect of various types of radiation on the material. In addition, the material must be readily adaptable to fabricating techniques which are within the capability of current technology.

A series of materials were evaluated for use in positive expulsion systems for cryogenic fluids (Reference 41). Bladders were fabricated and tested for use with liquid hydrogen and liquid nitrogen. The following recommendations are based on data from Reference 41.

1. Materials for Use With Liquid Hydrogen and Liquid Nitrogen.

    a. Mylar

        Mylar was found to be the best material for use with these cryogenic fluids. Mylar film of 1/4 and 1/2 mil gauge was found to have excellent flexibility at the cryogenic temperatures involved.

        Bladder fabrication techniques proved to have a profound effect on bladder service life. Triple-membrane bladders of 1/2 mil gauge Mylar which were not bonded together exceeded 79 expulsion cycles and were retired from service while still in excellent condition. Bladders constructed of bonded membranes, (Mylar, Mylar/Dacron combinations) repeatedly failed in less than 10 cycles. The results indicate that unbonded

multiple-membrane construction is inherently superior to single-membrane or bonded multiple-membrane construction.

The bladders in this program were 11.37 inches in diameter and were contained in a 12 liter glass flask which allowed observation of the bladder during the expulsion cycles.

b. Teflon (FEP) and Trithene

Teflon and Trithene showed some potential value but were stiff at the temperature in question.

c. Metal Foil

Aluminum foil exhibited remarkable ductility at liquid nitrogen temperature. However, this material failed repeatedly when flexed and folded. Failures were due to excessive pin holing at points of maximum and multiple folds.

Table XI lists the physical properties of recommended materials for use with cryogenic fluids.

PROPELLANTS

1. Materials for Oxidizers

a. Nitrogen Tetroxide (N_2O_4) (References 42, 43, 44, 45, 46)

Nitrogen Tetroxide, which is hygroscopic in nature, exhibits a marked change in characteristics when contaminated with water; a 1.6% water content results in a solution which is equivalent to a 60 to 70% solution of nitric acid. Materials which may be completely compatible with anhydrous N_2O_4 are severly attacked by the watered propellant. A good example is tin.

The only known organic materials which are suitable for fabrication into bladders for use with nitrogen tetroxide are the perfluorinated hydrocarbons. All other polymers are rapidly degraded by extended contact with this oxidizer.

The perfluorinated hydrocarbons which are recommended for use with N_2O_4 are Teflon TFE and Teflon FEP. Polymers of the Kel-F series (chlorotrifluoroethylenes) are not recommended since these materials exhibit a tendency to stress crack in contact with this oxidizer.

b. Mixed Oxides of Nitrogen (MON) (Reference 47)

Materials recommended for bladders for use with MON are limited to the perfluorinated hydrocarbons. Of these Teflon TFE and Teflon FEP are recommended.

TABLE XI

PHYSICAL PROPERTIES OF BLADDER MATERIALS
FOR CRYOGENIC FLUIDS[1]

Composition	Mylar Polyethylene Glycol Terephthalate	Teflon (FEP) Perfluorinated Copolymer of Ethylene, Propylene	Trithene Chlorotrifluoro-ethylene
Grade	Type A		Type A
Gauge (mils)	1/4, 1/2, 1	1/2, 1, 2	2
Density, lb/cu.in.	0.050	0.078	0.076
Tensile Strength			
Yield	1300	≤1600	6456
Ultimate	17,000-25,000	300	6456
Ultimate at -321°F	31,000	13,500	16,500
Tensile Modulus (psi)	450,000-600,000	43,000	226,000
Impact Strength (kg/cm/mil)	60	4	-
Tear Strength (G/mil)	15	125	353 in machine direction, 201 in Trans. direction
Flex Life (cycles/mil)	20,000	4000	
Oxygen Permeability (G/100 M²/hr/mil)	0.90	30	0.14
Water Vapor Permeability (G/100 M²/hr/mil)	110/39.5°C	30/25°C	2.6

NOTE: (1) Data from Reference 41.

c.   Inhibited Red Fuming Nitric Acid (IRFNA)
     (References 43, 48, 49)

        Materials that show the greatest resistance to
inhibited red fuming nitric acid (IRFNA) are Teflon, Kel-F,
Genetron GC and polymers of polyisobutylene. It is reported
that Teflon FEP and Genetron GC are superior to Teflon TFE and
Kel-F at elevated temperatures (+160°F.).

d.   Perchloryl Fluoride (ClO_3F) (References 48, 49)

        There is little quantitative data available on
the compatibility of polymeric materials. However, the materials
which follow are resistant to anhydrous perchloryl fluoride up
to the temperature indicated and can be considered as potential
candidates for bladder construction

Teflon (TFE)	to 390°F
Kel-F	to 390°F
Fluorosilicones	to 390°F
Styrene Butadiene (SBR) Rubber	to 390°F
Silicone Rubber	to 390°F

e.   Chlorine Trifluoride (Cl F_3) (References 43, 48, 49)

        Chlorine trifluoride is an extremely active chemical
which can react violently with water and many organic materials.
The only known organic materials which show sufficient resistance
to chlorine trifluoride to be considered for bladder construction
are Teflon, Kel-F and Genetron GC.

        In all probability, metal diaphragms or bladders
would be required for long term storage. The most resistant
metals are nickel, Monel and stainless steel.

f.   Bromine Trifluoride (BrF_3) (References 48, 49)

        A literature search did not reveal any data on
the compatibility of organic polymers with bromine trifluoride.
Metals which form a protective fluoride coating such as nickle
and copper are resistant to corrosion. Metals which do not form
protective fluoride coatings are vigorously attacked. Examples
of such metals are molybdenum, tungsten, and titanium. Boron,
silicon and columbium all ignite in contact with liquid bromine
trifluoride.

g.   Iodine Pentafluoride (IF$_5$) (References 48, 49)

        Iodine pentafluoride is the least reactive of
the halogen fluorides. Little quantitative compatibility data
is available for this oxidizer. It is reported that most metals
are only slightly attacked at ordinary temperatures.

Organic materials rich in hydrogen, react to give HF and tend to ignite. Reaction with chlorine containing compounds results in the liberation of free elemental iodine.

Recommended materials for use with IF_5 are Teflon TFE and Teflon FEP.

h. Oxygen Difluoride (OF_2) (References 50, 51)

Although oxygen difluoride has a boiling point of -229°F it is classified among the fluorine compounds for ease of reference.

This oxidizer, because of its excellent performance characteristics and reported hypergolicity with many fuels, shows promise of wide spread future use. Very little data is available on the compatibility of organic polymers with OF_2. Teflon (TFE) has been reported compatible with OF_2 but it cannot be used for bladder construction at the extremely low environmental temperatures required for OF_2.

i. Hydrogen Peroxide (H_2O_2)

Extensive testing by Bell Aerosystems Company and the Becco Chemical Division of Food Machinery and Chemical has shown that silicone rubber can be used for bladders designed to contain 90% hydrogen peroxide. Dow Corning's Silastic S-9711 silicone rubber has shown good compatibility with concentrated hydrogen peroxide. Teflon has also demonstrated excellent compatibility with hydrogen peroxide.

Silastic S-9711 is a dimethyl silicone rubber made for mdical use, consequently it is of a high degree of purity with a minimum of metallic and non-metallic additives. It is quite possible that other silicone rubbers made to the same degree of purity would result in equal compatibility with hydrogen peroxide and provide higher initial physical properties.

2. Materials for Fuels

a. Hydrazine (N_2H_4) (References 42, 43, 44, 48, 52)

Materials which can be recommended for the construction of bladders for use with hydrazine are Teflon (TFE), Teflon (FEP), polyethylene, butyl rubbers, and cis-4-polybutadiene rubber.

Teflon - Samples of Teflon immersed in hydrazine at ambient temperature for 370 to 385 days showed no signs of deterioration.

Polyethylene - Samples of polyethylene in
contact with hydrazine at both ambient temperature and 194°F.
for periods up to one year showed no change in appearance or
weight, however, stress cracking may be a problem.

Butyl Rubber - Samples of butyl rubber in
extended contact with hydrazine are not completely unaffected.
The degree of change in the physical properties induced by the
hydrazine is highly dependent upon the composition of the rubber
and the compounding it has received.

Cis-4-Polybutadiene - Samples of cis-4-polybuta-
diene have shown excellent resistance to hydrazine, comparable
to, or better than the butyl rubber.

Hydropols - Hydropols, or hydrogenated
polybutadienes show good resistance to hydrazine.

b. Unsymmetrical Dimethyl Hydrazine (CH_3) $N-NH_2$
(References 42, 43, 53)

Polymeric materials suitable for fabrication
into expulsion bladders for use with UDMH are limited to
Teflon (TFE and FEP), butyl rubbers, cis-4-polybutadiene rubbers,
and some of the hydropol elastomers.

(1) Teflon - Teflon is unaffected by short term
(28 days) immersion in UDMH at ambient temperature. There is
no reason to believe that extended contact with UDMH would be
detrimental

(2) Butyl Rubber - All butyl rubbers are affected
to some degree by extended contact with UDMH. Selection
or proper composition and compounding techniques will reduce
these effects to a minimum. The following are some butyl rubbers
which show minimum changes in physical properties when in extended
contact with UDMH.

Precision Rubber Compound 925-70
Stillman Rubber SR613-75
Parker Appliance 37-014
Firestone Rubber D-432
Chicago Rawhide 20316-70
Parco Compound 805-70

c. Anydrous Ammonia (Reference 53)

On the basis of minimum changes in tensile strength
and volume, the following materials have been recommended for use
with anhydrous ammonia up to 160°F.

Butyl Rubber
Neoprene Rubber
Silicone Rubber
Teflon
Kel-F
Polyethylene

d.   JP-X Fuel Mixture (Reference 43)

Teflon has shown the greatest compatibility
with JP-X fuel mixture (UDMH and JP-4: 40/60) and is recommended
for uses requiring extended contact with this fuel.

PERMEABILITY

One of the major problems associated with a positive expulsion
system employing a non-metallic bladder or diaphragm separating
the propellant and the expelling medium is that of permeability.
In the preparation of this section on permeability, information
and data from References 54 thru 61 have been used.

In general, all materials are permeable to liquids and/or
gases to some degree; however, the permeability of metals is
generally so small that it need not be considered. Exceptions
to this statement might be thin metal foils in the presence of
certain low molecular weight gases. This should not be confused
with porosity which is a transfer of a gas or liquid from one
side of a membrane to the other through small pores (holes) by
capillary action. Porosity can occur with many materials, par-
ticularly cast materials, due to, in some cases, faulty manufacture.

Permeability, according to the classical theory, occurs in
three steps: (1) solution of the gas or liquid (the permeant)
into the surface of the membrane, (2) diffusion of the molecules
through the membrane, and (3) evaporation of the permeant from
the opposite surface of the membrane. This is, it might be
noted, a simplified description of an otherwise complex process.
These three steps will be discussed below.

The process of solution is related to a number of factors
including the heat of solution, heat of condensation, activation
energies, molecular attractions, and temperature. The process of
evaporation is related to the boiling point of the permeant.
These two processes are governed to a degree by Henry's Law.
The rate at which these occur is a function of the environmental
conditions - temperature and pressure.

The process of diffusion, governed by Fick's Law, is a
function of several factors including the molecular size of
the permeant (i.e., the molecular weight), the temperature,
and the driving force or concentration gradient across the
interior of the membrane.

The over-all permeability, i.e., the amount of material that has transferred from one side of the membrane to the other, is the product of the solubility and diffusivity. Since the latter is a function, among other things as stated above, of molecular size, it is obvious that the permeation rate of various materials through a given membrane differs widely.

The first permeability test apparatus constructed to determine these differences with a modified Dow cell is described in ASTM D-1434-58. This is essentially a test cup partitioned by the test membrane; one side contains the propellant vapor or liquid and the other side is evacuated. The propellant passing into the evacuated side causes a pressure rise. (Figure 74 is a schematic of the apparatus). Knowing the volume of the apparatus, a gas transmission rate is calculated over the linear or steady-state portion of the "Pressure-Time" curve. Figure 75 is a typical pressure-time curve.

The term gas transmission rate is defined as the steady-state volume of test gas, converted to standard temperature and pressure, which passes through a known area of specimen per unit time. It is expressed in units of cubic centimeters of gas per 100 square inches per 24 hours per one atmosphere of pressure differential of test gas.

Gas transmission rate is the product of the diffusion rate and solubility of the test gas in the specimen.

The term steady-state is defined as the state of the test condition at which the volume of test gas transmitted becomes linear with time.

Steady-state is achieved when:

1. A stationary concentration gradient of test gas in the specimen is obtained.

2. The loss of water or other volatiles from the specimen are negligible.

Table XII is a tabulation of typical results obtained from this apparatus.

The gas transmission rates shown in Table XII should not be considered as absolute values. A number of factors such as variation in thickness or individual specimens, temperature, pressure differential across membrane, actual area of specimen permeating due to contact with the support grid, effect of possible reaction between propellants and mercury in manometer,
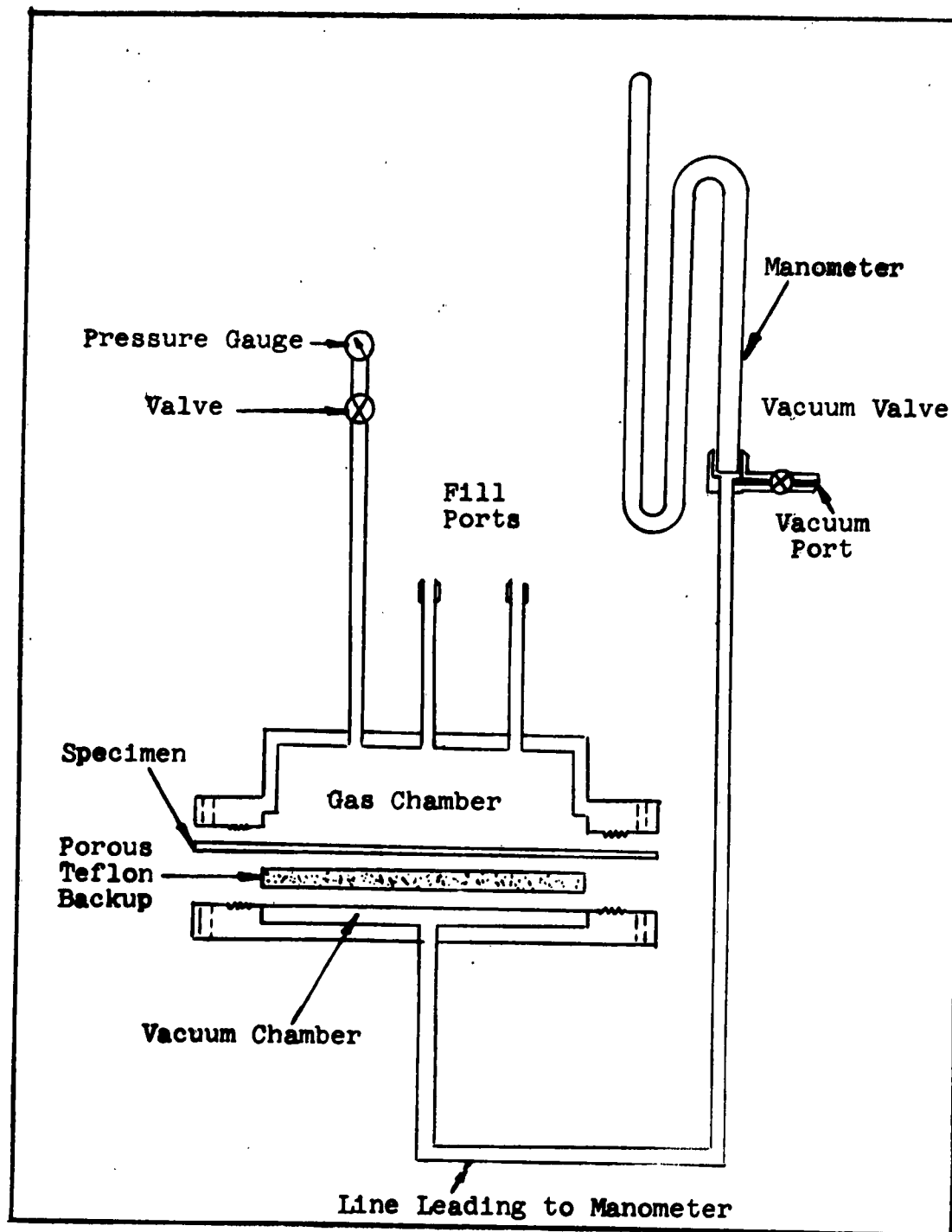
Figure 74. Dow Cell Apparatus Schematic Diagram
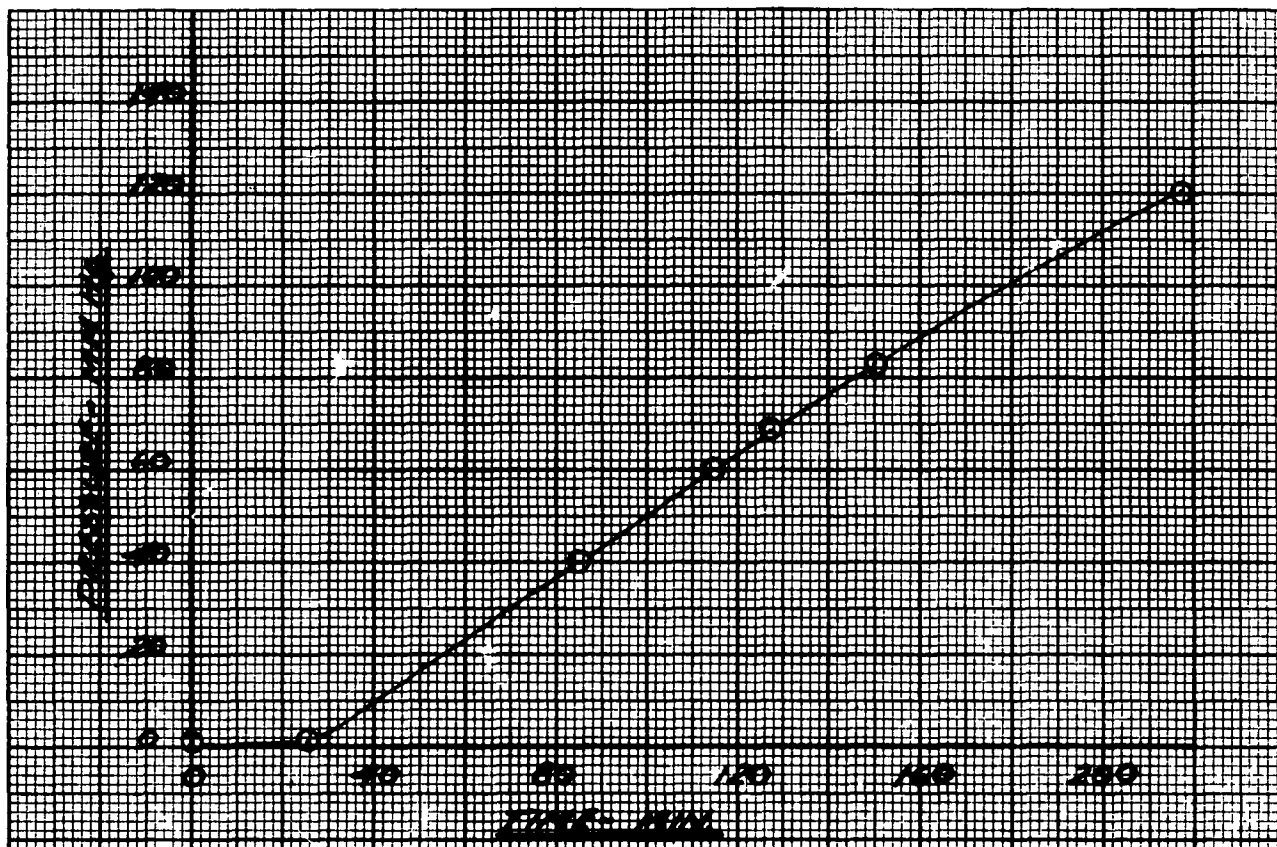
Figure 75.   MON vapor Transmission Thru Teflon
             (6.8-7.0 Mil Laminate)
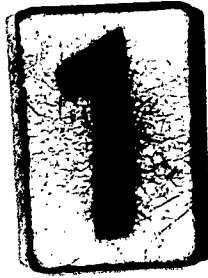
TABLE XII

GAS TRANSMISSION RATES OF VARIOUS MEMBRANES
(cc/100 in^2 · 24 hrs.)

TEFLON SPECIMENS	Test Gases		
	Air 14.7 psi	MON 16.7-17.7 psi	UDMH 14.7 psi
4 mil cast Teflon TFE	53	2274	--
10 mil sprayed Teflon TFE	45 (23)	585 (13)	28 (9)
10 mil sprayed co-dispersion of Teflon TFE and FEP	85 (3)	438 (2)	27 (1)
16 mil sprayed Teflon TFE (high density & crystallinity)	25 (4)	353 (2)	13 (2)
6 mil sprayed Teflon laminate (3 mil TFE/3 mil FEP)	45 (115)	310 (58)	28 (57)
20 mil (double ply) sprayed Teflon TFE	30	184	--
6 mil sprayed Teflon Laminate (3 mil TFE & FEP co-dispersion/3 mil FEP), CO$_2$ quenched	34 / 41	152 / 127	-- / --
10 mil extruded Teflon FEP			
14 mil sprayed Teflon laminate (10 mil TFE/4 mil FEP)	22 / 28 (5)	127 / 107 (3)	-- / 6 (2)
10 mil sprayed Teflon FEP			
20 mil (double ply) sprayed Teflon FEP	15	35	--
7 mil FEP-1/4 mil al foil-3 mil FEP (Al foil perforated in two specimens)	3 (3) / 5	5 (3) / 2	0.7 / --
Metal Specimens (Electroformed)			
1 mil Nickel, not annealed			
2 mil Nickel, not annealed	7	3	--
2 mil Nickel, annealed 1/2 hr. at 1600°F	7	7	--

Teflon FEP	15	(3)	35	(3)	
7 mil FEP-1/4 mil al foil-3 mil FEP (Al foil perforated in two specimens)	3				-- / 0.7
1 mil Nickel, not annealed	5		2		--
2 mil Nickel, not annealed	7		3		--
2 mil Nickel, annealed 1/2 hr. at 1600°F	7		7		
Metal Specimens (Electroformed)					
3 mil Nickel, not annealed	1		0.3		?23 air / ?39 UDMH
3 mil Nickel, annealed	8		1		
3 mil Tin	5		.1		?84 for 5 hrs. / ?34 for 24 hrs.

NOTES

1. The transmission rate for UDMH liquid is with 1 atmosphere of pressure differential. The transmission rate for air is also at 1 atmosphere of pressure differential. The transmission rate for MON gas is with 16.7 to 17.7 psi differential pressure. Transmission rates in the table are the arithmetic mean of the number of specimens circled, e.g. 45 (23) equals arithmetic mean of 45 for 23 specimens tested.

2. All sprayed Teflon specimens were prepared by spraying and fusing Teflon TFE or Teflon FEP dispersions individually, collectively (as dispersion) or in sequence (laminate).

3. Specimen thickness was recorded during each test, since the gas transmissions values calculated are for actual thickness of the film. The above thickness values are average values.

4. Pinholes in 1 mil annealed Nickel prevented test.

5. Difficulty in sealing 2 and 4 mil tin specimens prevented test.

6. All metal specimens prepared by EMCO Industries, Buffalo, New York.

and the use of extrapolation are not known or measured. These
rates should only be used for the purpose of comparing one
material in relation to another.

These variables, coupled with the fact that the test condi-
tions were quite different from the conditions that exist in an
actual expulsion system, resulted in a new apparatus being con-
structed that was aptly called the zero differential pressure
permeability apparatus.

These are the conditions that exist in a typical tank/
bladder expulsion system: A flexible Teflon bladder is filled
completely with MON. The bladder is externally pressurized with
N_2 and a small percentage, 2%-5%, of the MON is expelled provid-
ing an ullage space between the tank and bladder. The entire
inner surface of the bladder is exposed to MON, and the differ-
ential is essentially zero. Figure 76 is a schematic of a
bladder tank test assembly. Figure 77 is a schematic of the zero
differential pressure permeability test apparatus and Figure 78
is a photograph of this test device.

Briefly the operation of the apparatus is as follows: Mon is
charged into the propellant reservoir at 40°F; the Mon is allowed
to fill the liquid side of the test cup. The system is pres-
surized to 200 psia with N_2 and held at 70°F (in a controlled
temperature chamber) while maintaining zero differential pressure
across the bladder material; zero differential pressure is main-
tained by adding or removing N_2 from the liquid side; gas samples
were taken at the end of prescribed times, e.g., 1, 4, 10 days,
for analysis.

Figure 79 shows the results of several tests. The amount
of propellant that will permeate depends on the ullage volume
and not on the bladder material. The latter merely determines
how rapidly the ullage space will become saturated with propel-
lant. Figure 80 shows the variation of the amount of propellant
that will permeate versus the ullage volume at several temperatures.

The practical aspects of the permeability of a bladder or
diaphragm in a positive expulsion device range from that of a
slight weight penalty to that of complete system failure.

Following are some of the problem areas with a tank and
Teflon bladder filled with MON and pressurized with N_2.

a. Loss of propellant due to permeation to the gas side,
thereby reducing the design capability of the mission.

1. MON Pressure Pick-up
2. N_2 Pressure Pick-up
3. MON Temp. Probe
4. N_2 Temp. Probe
5. N_2 Pressurization Valve
6. N_2 Taber Isolation Valve
7. MON Fill & Dump Valve
8. MON Taber Isolation Valve
9. Dump Valve for Taber Line
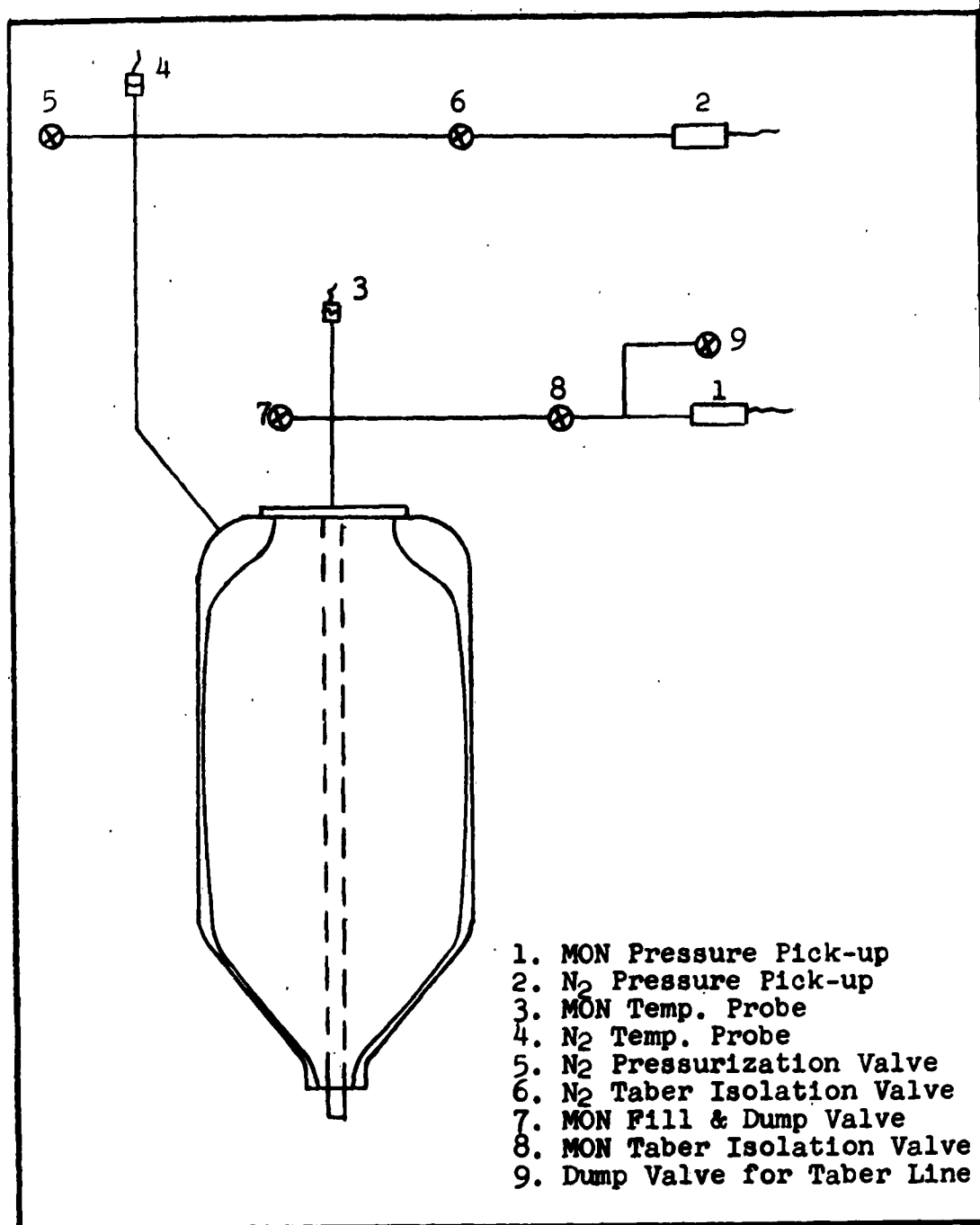
Figure 76.   Bladder Tank Test Assembly
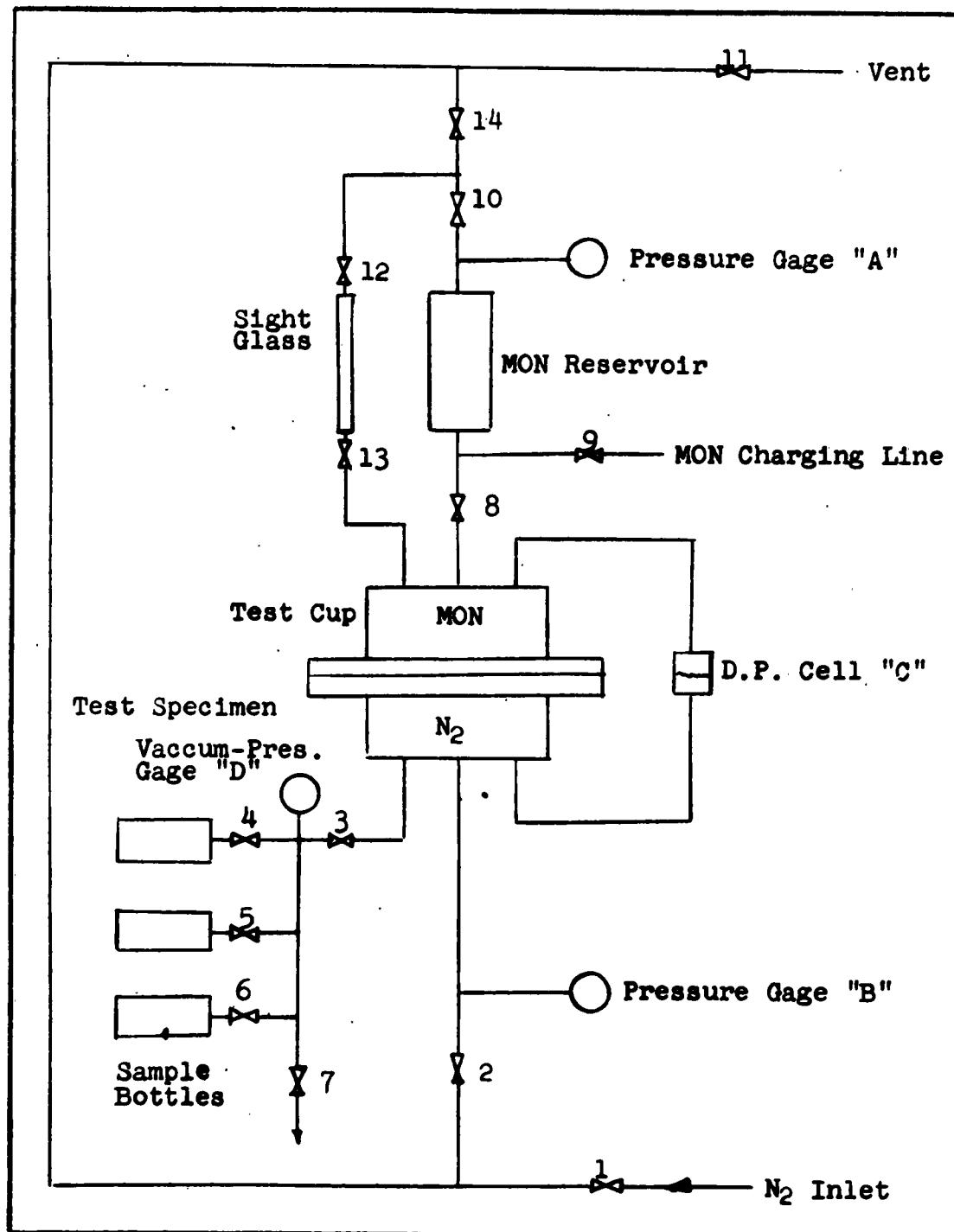
Figure 77. Zero DP Permeability Apparatus
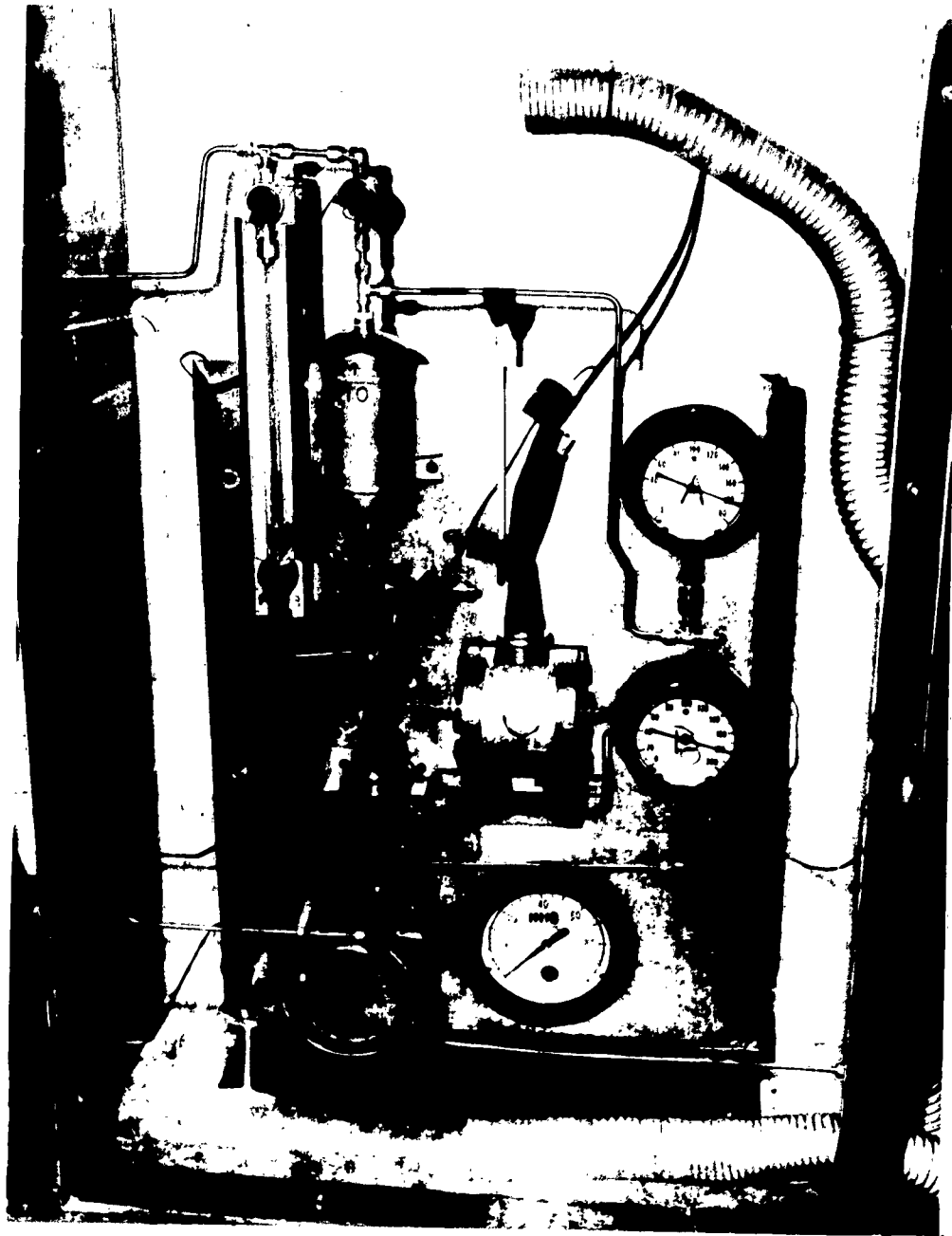
Figure 78.   Zero ΔP Permeability Apparatus
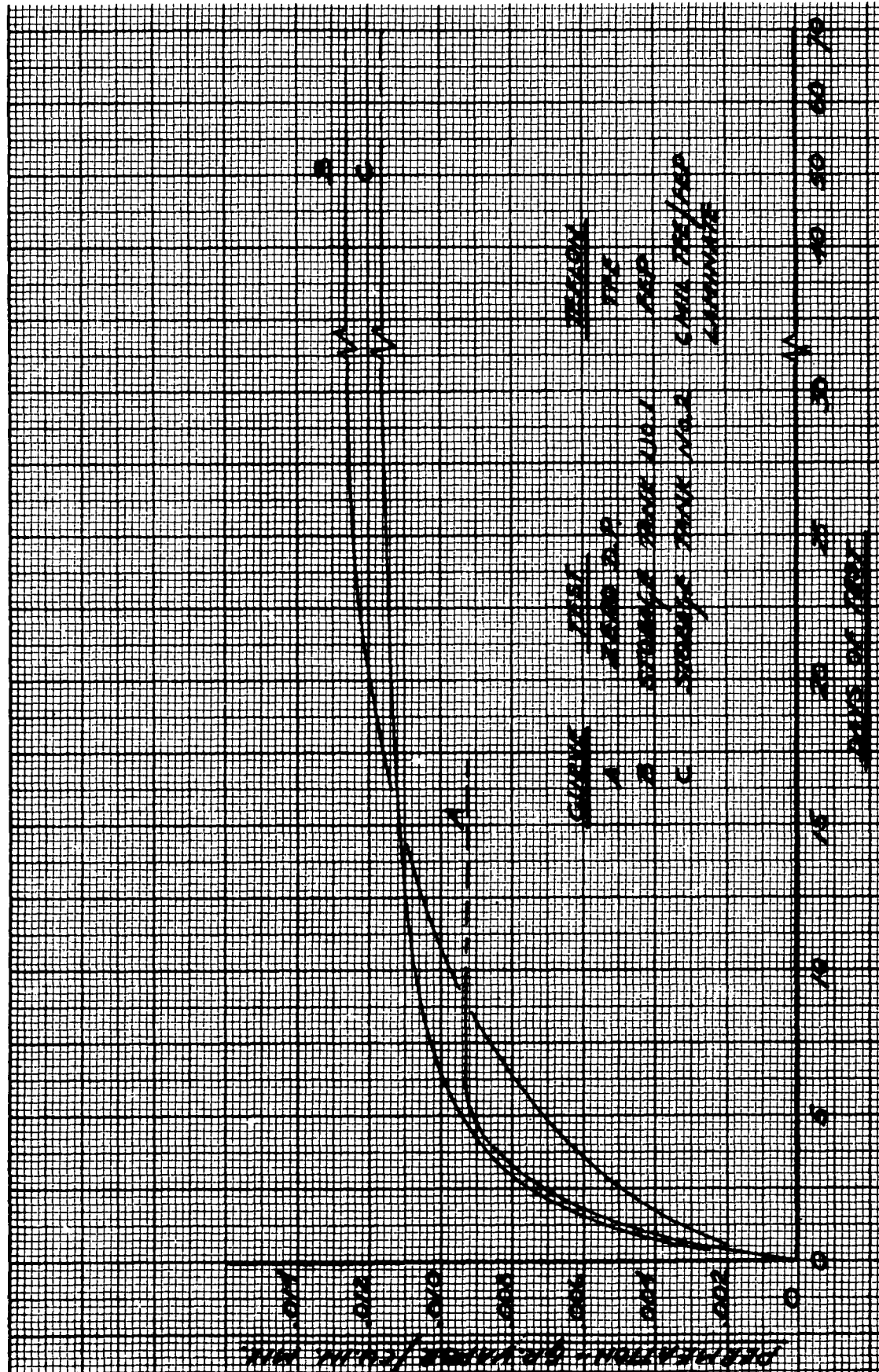
Figure 79. Permeation of MON Through Teflon at 70°F
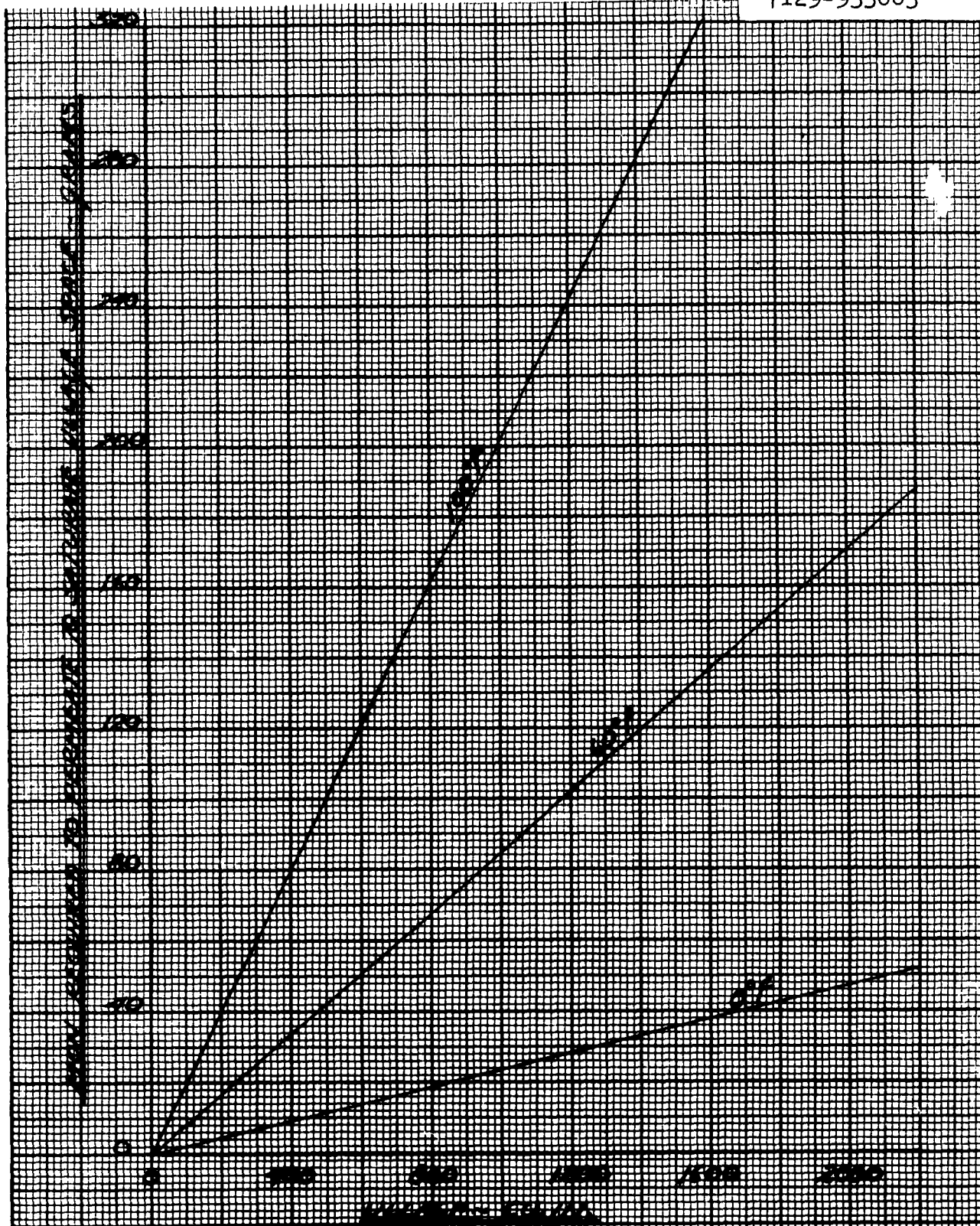
Figure 80.   MON Saturation Level Vs Ullage

Calculations, supported by test work at 70°F at Bell Aerosystems Company, indicate the loss of MON to be less than 1% by weight of the original charge of MON. If, however, due to temperature cycling and poor heat transfer rates the tank wall is always cooler than the bladder and propellant, then condensation could occur on the tank wall, the gas space would never become saturated, and permeation could continue at a high rate. Further calculations at Bell indicate this loss could be of the order of 25% by weight for a prolonged mission.

b. In addition to the propellants permeating into the ullage space, the pressurizing gas also permeates to the propellant side of the bladder. If this gas is soluble in the propellant as in the case of nitrogen, a pressure drop will occur, or make-up gas will be required. Figure 81 shows the solubility of nitrogen in MON at various pressures. The nitrogen loss could be reduced or eliminated by saturating the propellant during loading. Figure 82 graphically illustrates the pressure loss that results when pressurizing with N_2 over a 6 MIL Teflon bladder containing mixed oxides of nitrogen.

c. Pressurizing gas permeating into the propellant could also cause, under zero "g" conditions, a dispersion of gas bubbles or pockets in the propellant, thereby causing combustion instability or failure of the thrust chamber to perform satisfactorily.

d. If the fuel and oxidizer bladders are in the same tank or in tanks fed by a common pressurization line so that the permeant of both bladders could mix, then the result could be total loss of the mission.

RADIATION

Space systems must be capable of operating in a-nuclear radiation environment. These systems will be subjected to either space radiation or that from nuclear reactors present in the vehicle, or both. In the case of the natural or space radiation, the dose rate or intensity to which a vehicle or satellite is subjected is dependent upon the orbit parameters or mission trajectory. The existence of the Van Allen radiation zones surrounding the earth is well established. These are regions of high concentration of nuclear particles, protons and electrons. These particles are trapped in the geo-magnetic field. If a celestial body has no magnetic moment it is believed very unlikely that it will be surrounded by such radiation zones. A recent lunar probe, instrumented with radiation detectors, measured no increase in the radiation level in the vicinity of the moon. This is the first direct indication that the moon has a zero or very small magnetic moment. Data from satellite and probe missions indicate that
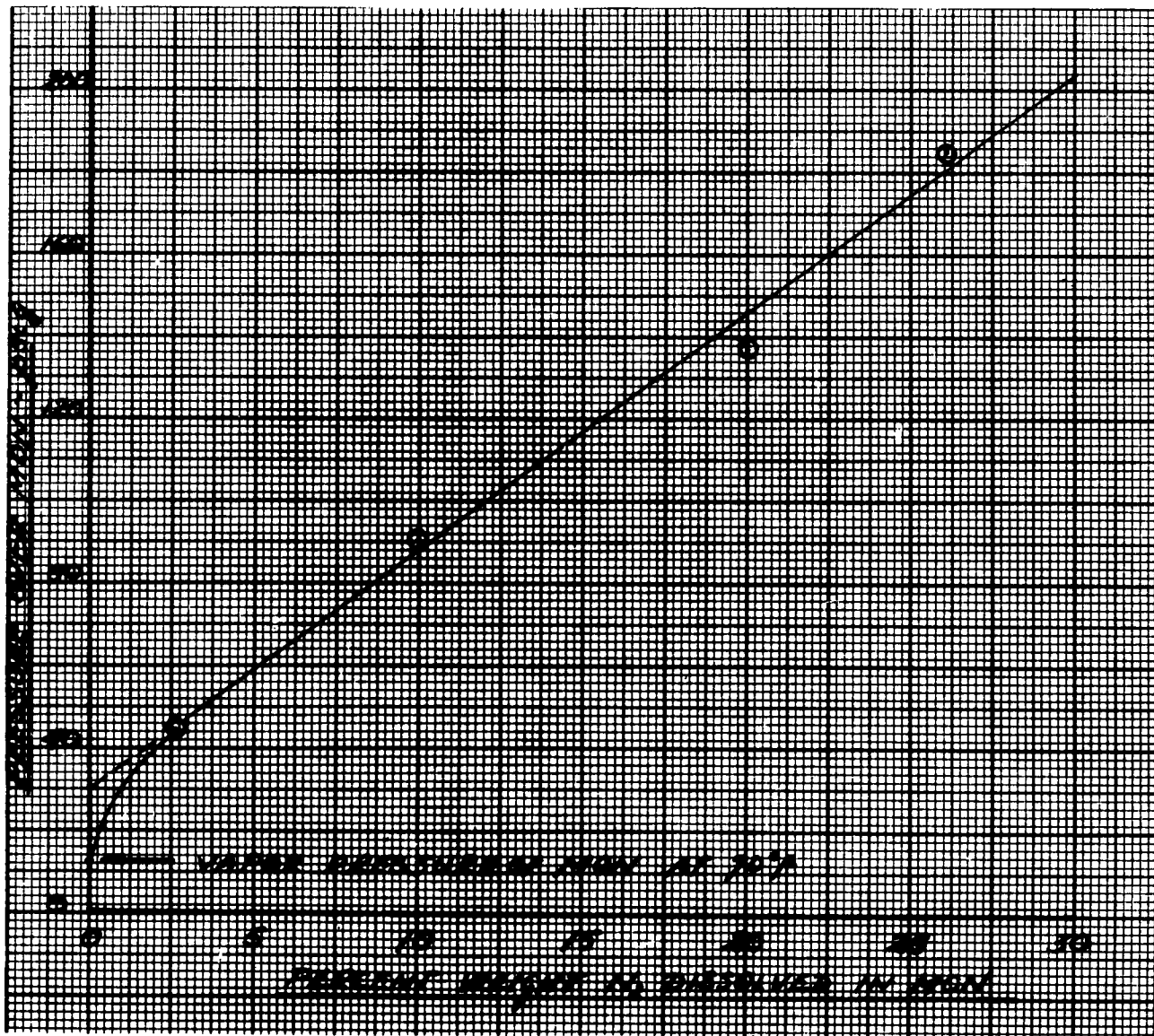
Figure 81. Solubility of N_2 in 10% MON Vs Total
Pressure Over MON at 70°F
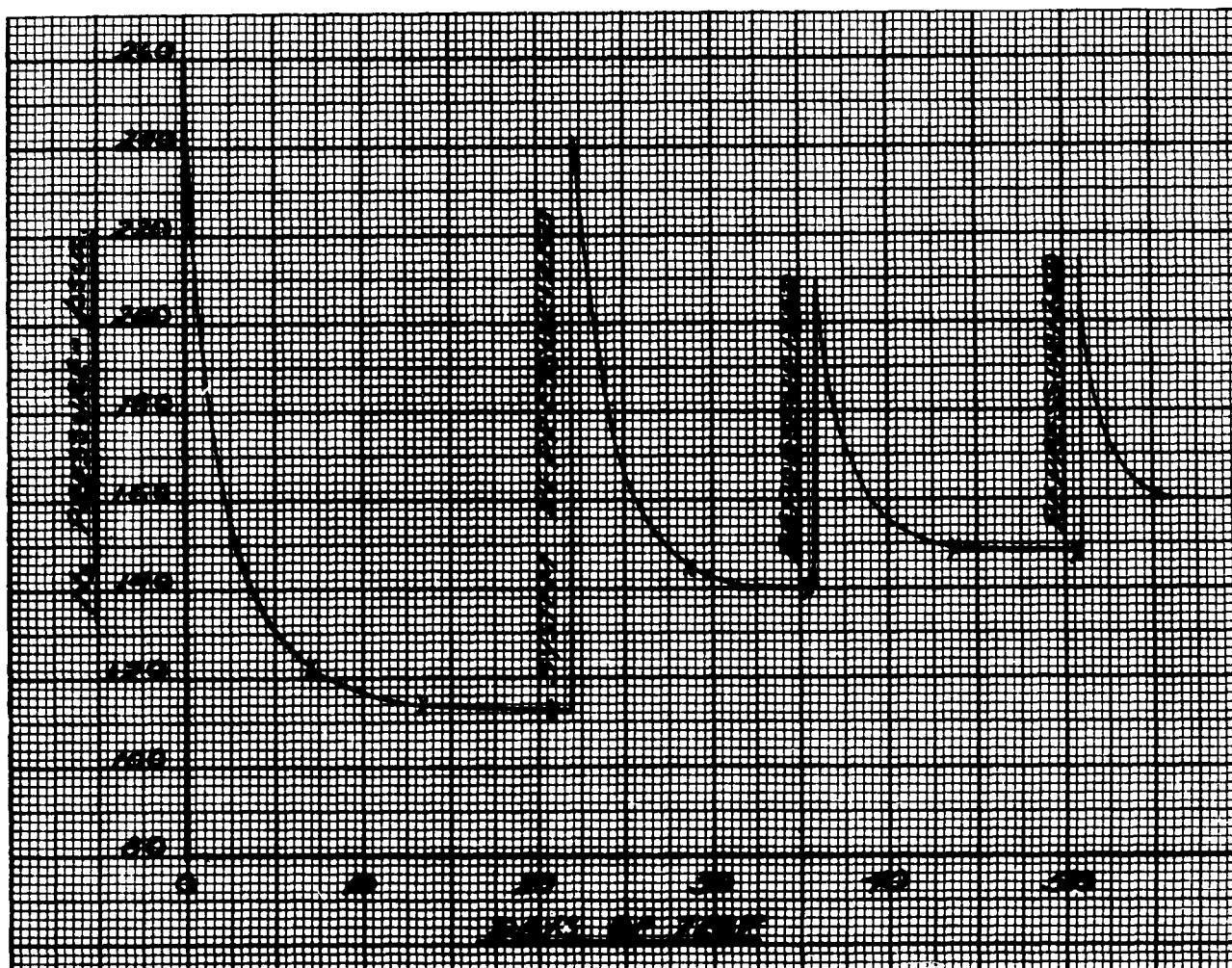
Figure 82.   Variation of Nitrogen Pressure in
MON When Tested at 70°F

the inner Van Allen region is quite stable with time in both intensity and spatial extent. The outer boundary of the outer zone, however, appears to expand considerably during solar eruptions, with a consequent change in intensity within the band. Another geo-effect associated with solar activity is the great increase in particle intensity at earth-satellite altitudes in the higher geo-latitudes.

Nuclear reactors will be employed on space vehicles for electrical power and propulsion. Associated systems will therefore be subjected to this source of radiation in addition to the space radiation. This means the components will receive gamma and neutron radiation in addition to the higher energy proton radiation (in the inner Van Allen belt) and the Bremsstrahlung radiation (X-ray) due to the electron in either the inner or outer Van Allen zones.

Except for surface exposed to the direct flux, components and materials of construction will actually not absorb electron radiation since the penetration depth is very small. However, in the process of being stopped by the wall, the electrons give rise to Bremsstrahlung, or braking radiation. For the electrons in the Van Allen belts, the energy of the electromagnetic radiation produced is about $1/4$ Mev. The protons in the inner belt are more penetrating and some of them will deposit their energy in internal components and system parts. The total amount of radiation which any material received is obviously a function of the intensity of the ambient, incident flux on the surface of the space vehicle. At present, the momenta spectra for the incident space radiation are incomplete, especially for the important higher energy electrons, i.e. energy $\geq$ 100 kev. These higher energy electrons are the most important since the efficiency of a wall material for production of Bremsstrahlung radiation varies as E^2, where E is the energy of the electron. Many reports are available on the nature and intensity of this radiation. References 62 and 63 give details on the number of energy spectra of the various space radiation elements. However, the important factor in determining the effect of radiation on design of components is the ability of the material to perform properly after receiving a certain dose of radiation. Therefore, the important parameter is the integrated absorbed dose; not the incident flux.

Organic materials are susceptible to all types of radiation because of the ease with which the molecular structure of polymers can be rearranged. The molecular structure can be reoriented in any of several different ways: (a) the formation of new bonds between chains, (b) the breaking of chains, (c) the formation and evolution of gases, and (d) reaction with environment such as the absorption of oxygen. These four methods of degradation may be

grouped into two broader classifications: 1. crosslinking and 2. chain scission.

1. Crosslinking - When radiation impinges on a polymeric material, the weakest bond present (the carbon-hydrogen bond in materials like polyethylene) may be broken. When this occurs on adjacent polymer chains, a new carbon-carbon bond may be formed, accompanied by the formation of hydrogen. This new bond now joins two previously independent chains resulting in a crosslink. Crosslinking results in restricted freedom of motion, increased hardness, and increased density.

The following polymers are examples of potential bladder materials which crosslink when exposed to radiation:

> Polyethylene
> Natural rubber
> Neoprene rubber
> Silicone rubber
> Polyvinyl chloride

2. Chain Scission - As the name suggests, this method of polymer degradation proceeds by a breaking chain mechanism which results in lowered molecular weight. This effect is prominent in perfluorinated polymers such as Teflon where the carbon-carbon bond in the polymer chain is weaker than the carbon-fluorine bond.

The following materials undergo chain scission when exposed to radiation:

> Teflons and Fluoro-elastomers
> Polyesters
> Nylon
> Melamines

When metals are exposed to radiation, ionization and excitation occur, but most of the energy absorbed appears as heat and produces a temperature rise in the metal. However, when the radiation causes atomic displacement within the material, the situation becomes serious. In general, there is little indication that the properties of metals such as thermal conductivity or density undergo any appreciable changes upon irradiation, even with fast neutrons. However, the properties of metals which are structure sensitive, such as yield strength, hardness, ductility, etc., usually experience a considerable change upon prolonged exposure to fast neutrons.

Radiation embrittlement is another degradation effect. This is the result of bombardment with high-energy particles. This radiation embrittlement by neutrons and ionized particles at ordinary temperatures is usually insignificant for integrated

fluxes below 10^{19} particles per square centimeter for metals.
For space missions which do not involve the use of a nuclear
reactor the only significant radiation will be in the form of
high-energy protons. This flux is expected to be less than 10^4
particles/Cm^2 and the integrated does for a one-year period
(3.15 x 10^7 seconds) should not cause significant radiation
damage. One important point in this connection is the observa-
tion that the resistance of metals to radiation damage is largely
a result of annealing-out of radiation damage at ordinary temper-
atures. At low temperatures this process is significantly reduced
and the cumulative radiation damage which would result from an
extended mission which involves the use of a nuclear reactor
might be significant.

Figure 83 presents some test data on the effect of nuclear
radiation on the relative radiation stability of elastomeric and
plastic materials. This information has been extracted from
Reference 64 and gives the effects of gamma radiation for tests
conducted on relatively thin specimens in an environment of air.
Metals do not show any appreciable change in properties for
radiation dosages below 10^{12} rads.

Bell Aerosystems Company has been conducting a radiation
test program in connection with a USAF liquid rocket propulsion
system contract for the past two years. This system, under
Air Force Contract AF 04(647)-563, employs positive expulsion,
bladder-tankage systems containing storable liquid propellants.
The design orbit is such that the system must be capable of oper-
ating one year in an orbit that extends to the center of the
Van Allen band. Assuming a nominal skin thickness of 0.030" to
0.050" of light weight material, a yearly integrated does of
2.0 x 10^5 rads has been established as a design requirement for
the Teflon bladders. The radiation test program will further
establish the maximum radiation dosage at which the various com-
ponents will still function properly. The test results are sum-
marized below.

Swatch tests were conducted whereby Teflon test coupons
were immersed in the liquid propellant in glass test tubes and
irradiated to various dosages. Tensile and elongation were
measured and compared to standards which were immersed for the
same time and under the same conditions but not irradiated.

More sophisticated tests were then conducted whereby Teflon
tubes were used to contain propellants and the outside of the tube
was pressurized using N_2 gas, thus, simulating on a reduced scale
the tank configuration and bladder application environment.
Figure 84 shows the test assembly in various phases of assembly
for this test.
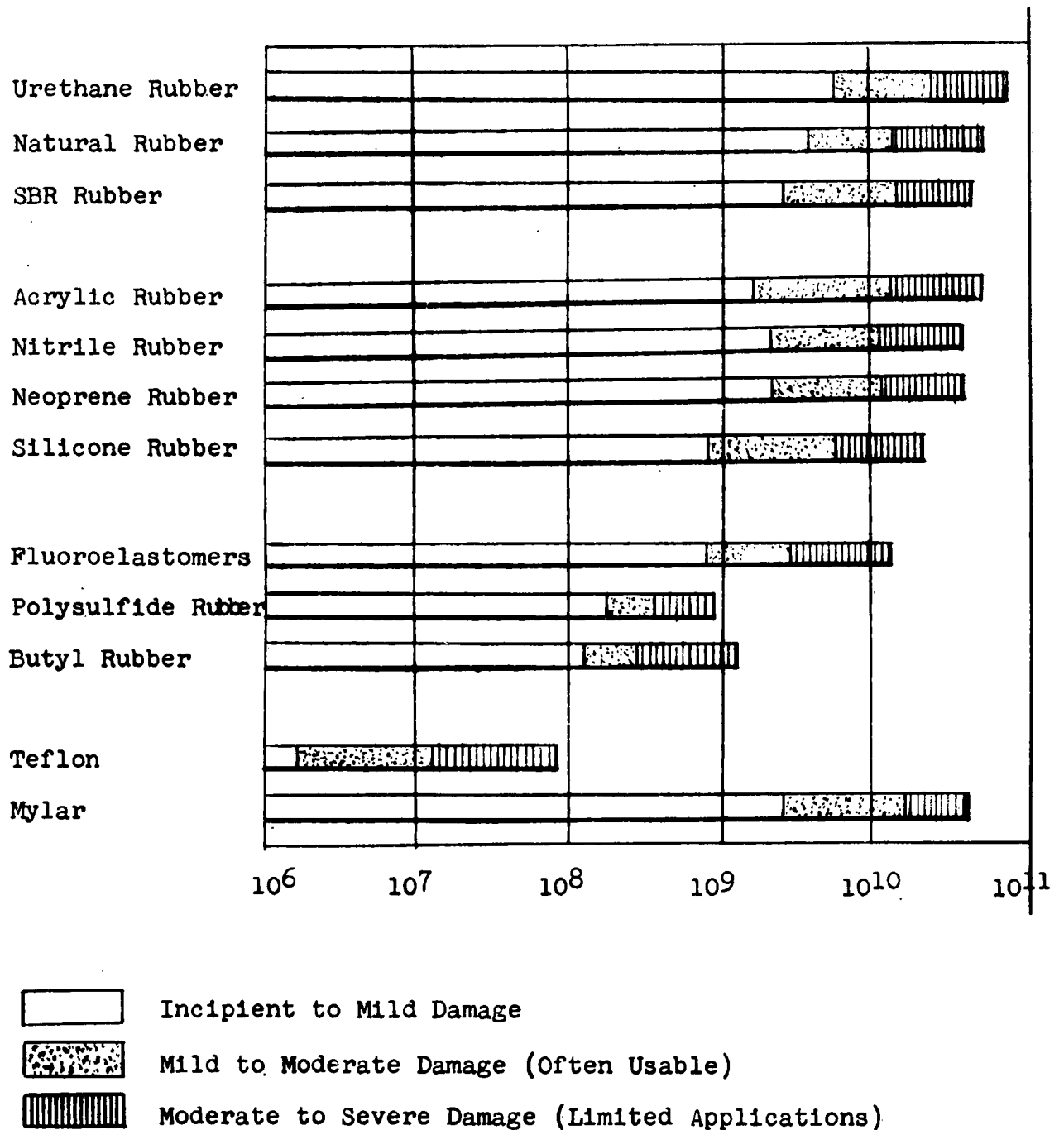
Figure 83. Relative Radiation Stability of Materials

(a) Simulated Teflon Bladder

(b) Disassembled Unit

(c) Assembled Unit

(d) Total Rack Unit

Figure 84. Radiation Test Specimen Set-up for a Simulated Bladder

All irradiations were performed at Argonne National Labora-
roty's High Level Gamma Facility using spent fuel rods as the
source of gamma radiation. Figure 84d shows the irradiation rack
constructed for the Teflon test tube tests. The nuclear fuel
rod is placed in the center of the rack facilitating dosimetry.

The physical property data versus radiation dosage is given
in Figures 85 through 88. The effects of a simulated test
(including Teflon, nitrogen and MON) is indicated on these figures
when Teflon was subjected to radiation in MON only. This data is
now being analyzed to establish the reasons for the variations
indicated.

Based on these data and a knowledge of the bladder physical
properties required in service, full size propellant tank tests
were performed. Each tank system was loaded approximately 25%
full of propellant and inserted in a specially designed irradia-
tion chamber. These chambers are heavy-walled stainless steel
pressure shells to guard against the event of an explosion or
leaking inner propellant tank.

Each tank, oxidizer and fuel, received 1/2 million rads dosage
at a dose rate of approximately 100,000 rads per hour. It was
concluded that this dosage did not cause a malfunction of either
tank assembly.

Samples of propellants subjected to the various dosage levels
received on this Air Force Contract were analyzed before and after
radiation test. MON showed no change in composition up to an
integrated dosage of 2.3×10^7 rads. UDMH did show some decom-
position.

Based on the radiation data gathered to date on the tank
assembly, the following generalizations and conclusions can be
drawn.

a. Teflon, a favored material of construction for positive
expulsion system bladders, is not per se as radiation sensitive
as originally thought. The ambient environment in which the
Teflon receives the radiation determines to a large extent the
radiation dosage at which a given change in physical properties
will occur.

b. For the conditions and dose rates employed during these
tests, Teflon does not exhibit any appreciable dose rate dependence.
The integrated dose is the principal parameter determining the
depreciation of physical properties.

c. The upper level to which this type of bladder should still
be operable is between 1 and 2 million rads. This is much higher
than that which would have been predicted based upon presently
published results.
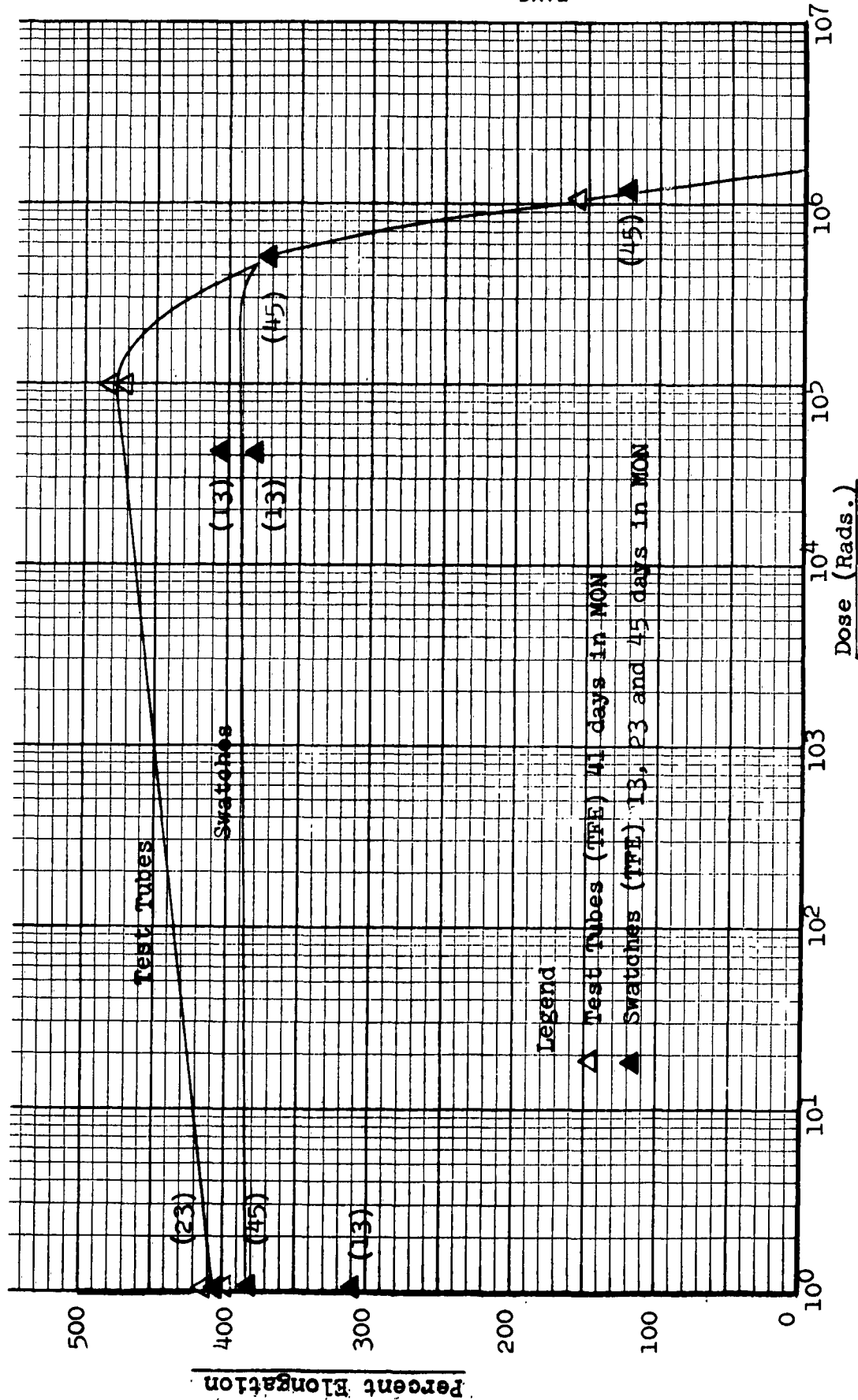
Figure 85. Percent Elongation of Gamma Irradiated Teflon (TFE) as a Function of Dose
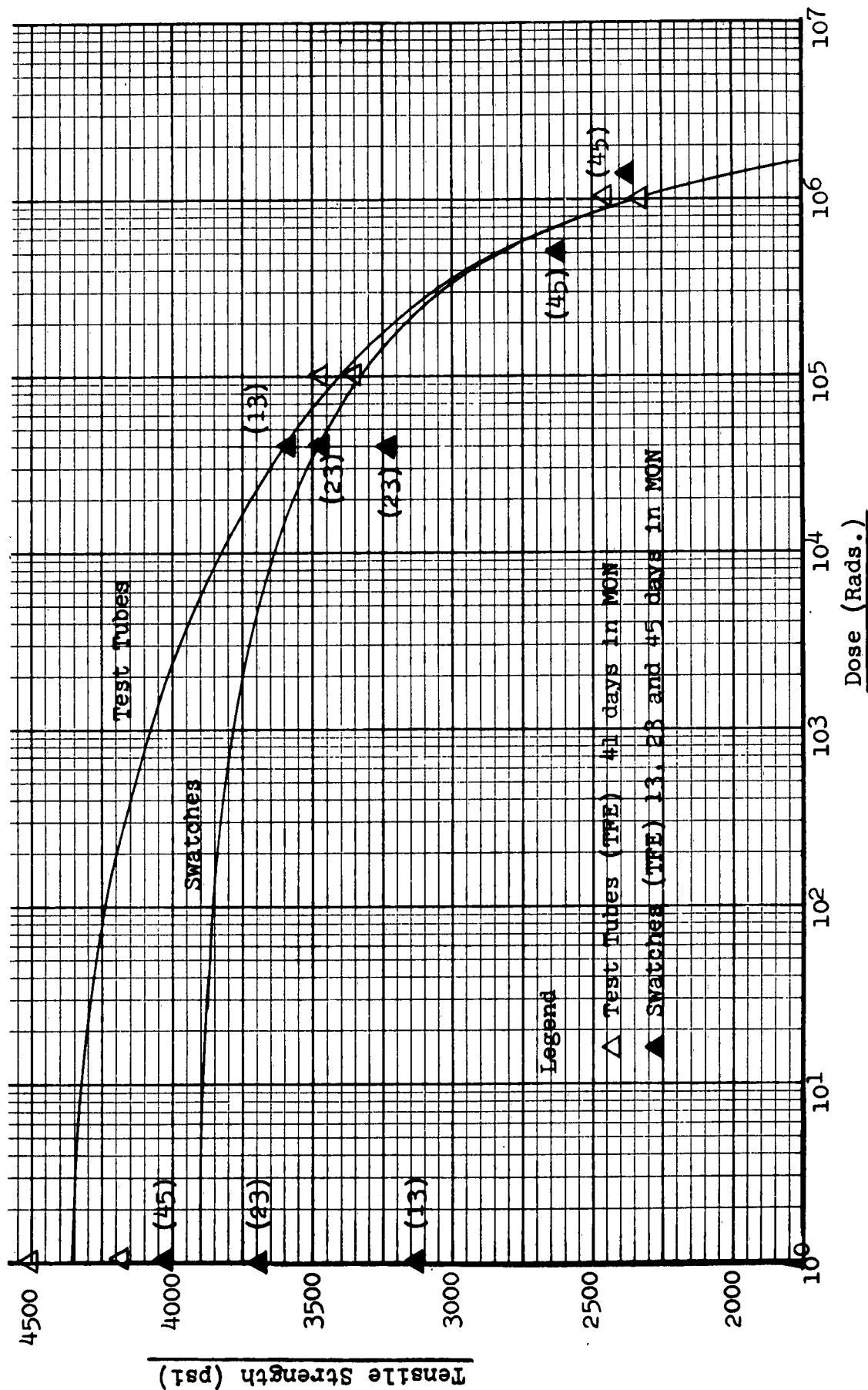
Figure 86. Tensile Strength of Gamma Irradiated Teflon (TFE)
as a Function of Dose
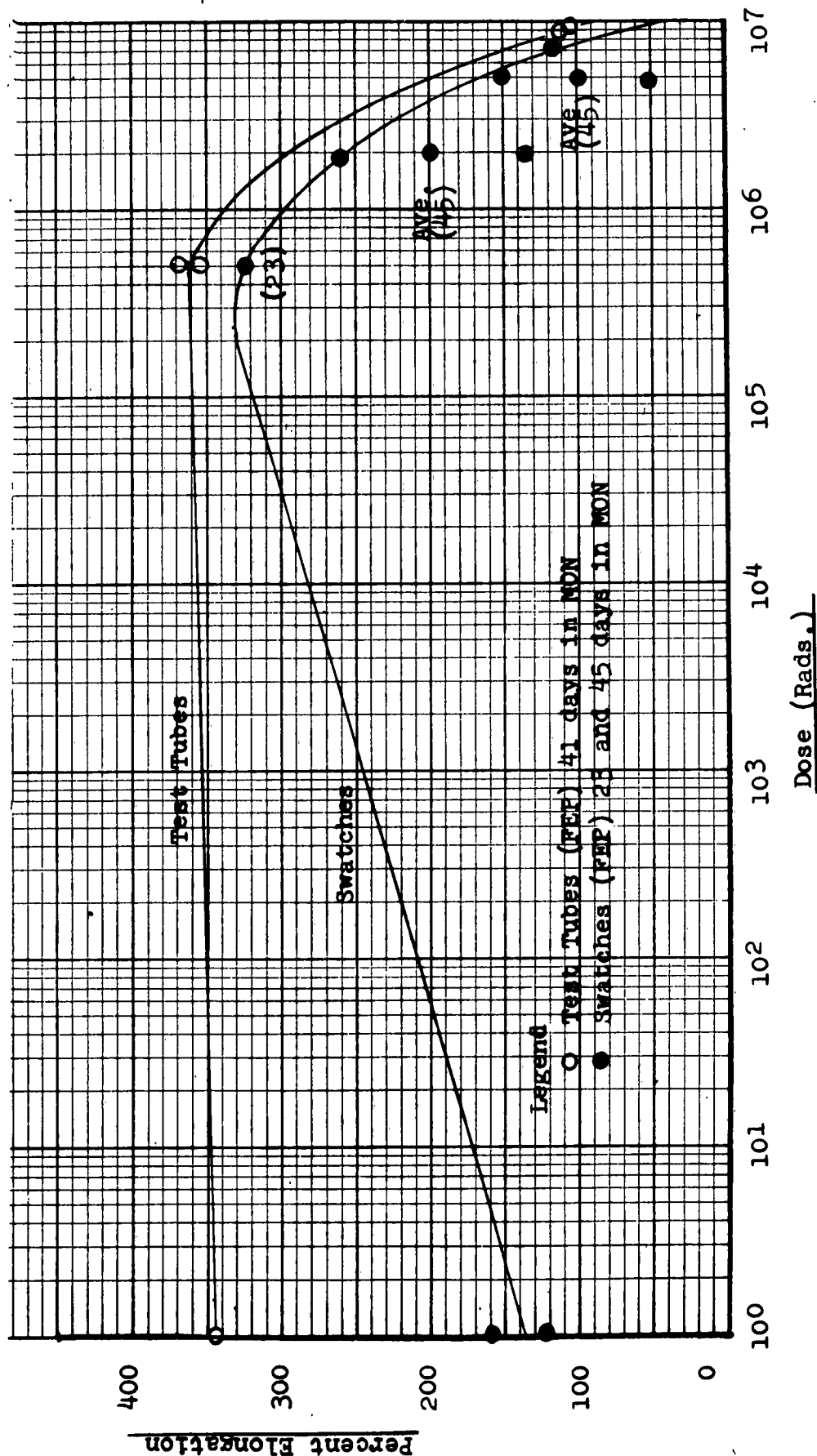
Figure 87. Percent Elongation of Gamma Irradiated Teflon (FEP)
as a Function of Dose
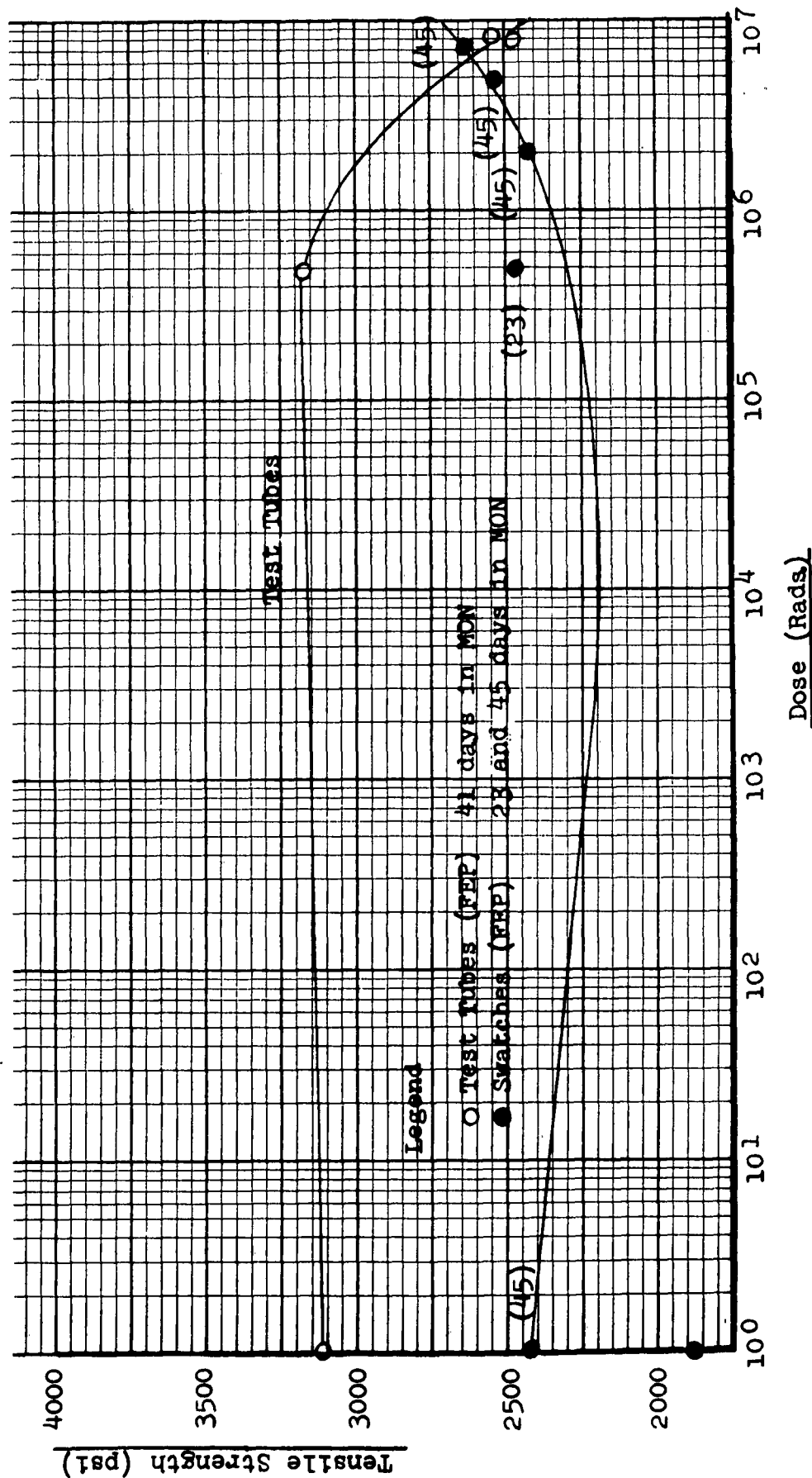
Figure 88. Tensile Strength of Gamma Irradiated Teflon (FEP)
as a Function of Dose

Table XIII has been inserted to indicate the effect of nuclear radiation on the properties of metals. Although some of the data is based on rather meager tests it has been gathered as an aid for design.

ELONGATION AND DUCTILITY

The structural design of an expulsion device employing a bladder or diaphragm does not present an opportunity for a detail stress analysis and the associated material selection. The primary requisite for the material for such a configuration is a capability to withstand folding, buckling, and wrinkling without tearing or rupturing. Thus, elongation and ductility is an important structural characteristic, leaving very little basis for the selection of a material gage on the basis of structural requirements be it a metal, plastic or composite.

The property of uniform elongation in a material is closely allied with the work hardening properties of the particular metal, however, it can also be affected by local variations in heat treatment and non-uniformity in alloying. Desirable materials from this standpoint are pure and non-heat treatable metals.

The elongation properties of several aluminum alloys and plastics suitable for expulsion devices are shown in Figures 89 and 90. The effect of temperature, from +100°F to -400°F, is indicated on these charts.

TEMPERATURE

The material of the expulsion device must be capable of withstanding the temperatures of the surrounding environment, the operational temperature of the propellant and the resulting gas pressurization system temperatures if such a system is employed. The use of a cryogenic propellant or fluid imposes another restriction on plastic or pliable material choice for incorporation in a bladder, diaphragm or controlled deformation device because of the flexing and folding requirements desired at this low temperature.

The effect of temperature on the typical mechanical properties of candidate materials for expulsion devices is presented in Figures 91 through 94. This information has been gathered from References 65 through 68. The temperature range considered for its effect on material characteristics varies from the cryogenic value to room temperature.

TABLE XIII

EFFECTS OF NUCLEAR RADIATION ON PROPERTIES OF METALS

| Property	Effect
Yield Strength	Increases up to 450 percent for annealed metals and to a lesser extent for cold-worked metals at moderate temperatures
Tensile Strength	Increases up to 75 percent for annealed metals and to a lesser extent for cold-worked metals at moderate temperatures
Ductility	Generally decreases at moderate temperatures
Elastic Constants	Little or no change in engineering materials
Impact Properties	Ductile-brittle transition temperature raised as much as 100°C
Creep Rate	Usually unaffected for steel alloys
Fatigue Strength	No effect in ordinary materials (according to limited data)
Hardness	Increases generally less than 100 Bhn for commonly used materials
Damping Capacity and Internal Friction	No change (according to limited data) at ordinary temperatures
Density	Generally increased by as much as 0.2%.
Diffusion Coefficient	Possible very slight change
Electrical Resistivity	Increased, generally by less than 10% at room temperature
Phase Changes	Possible in certain systems
Microstructure	No significant change
Thermoelectric emf	Little change at ordinary temperatures
Thermal Conductivity	No change, according to limited data
Residual Radiation	Appears to be unimportant for space environments
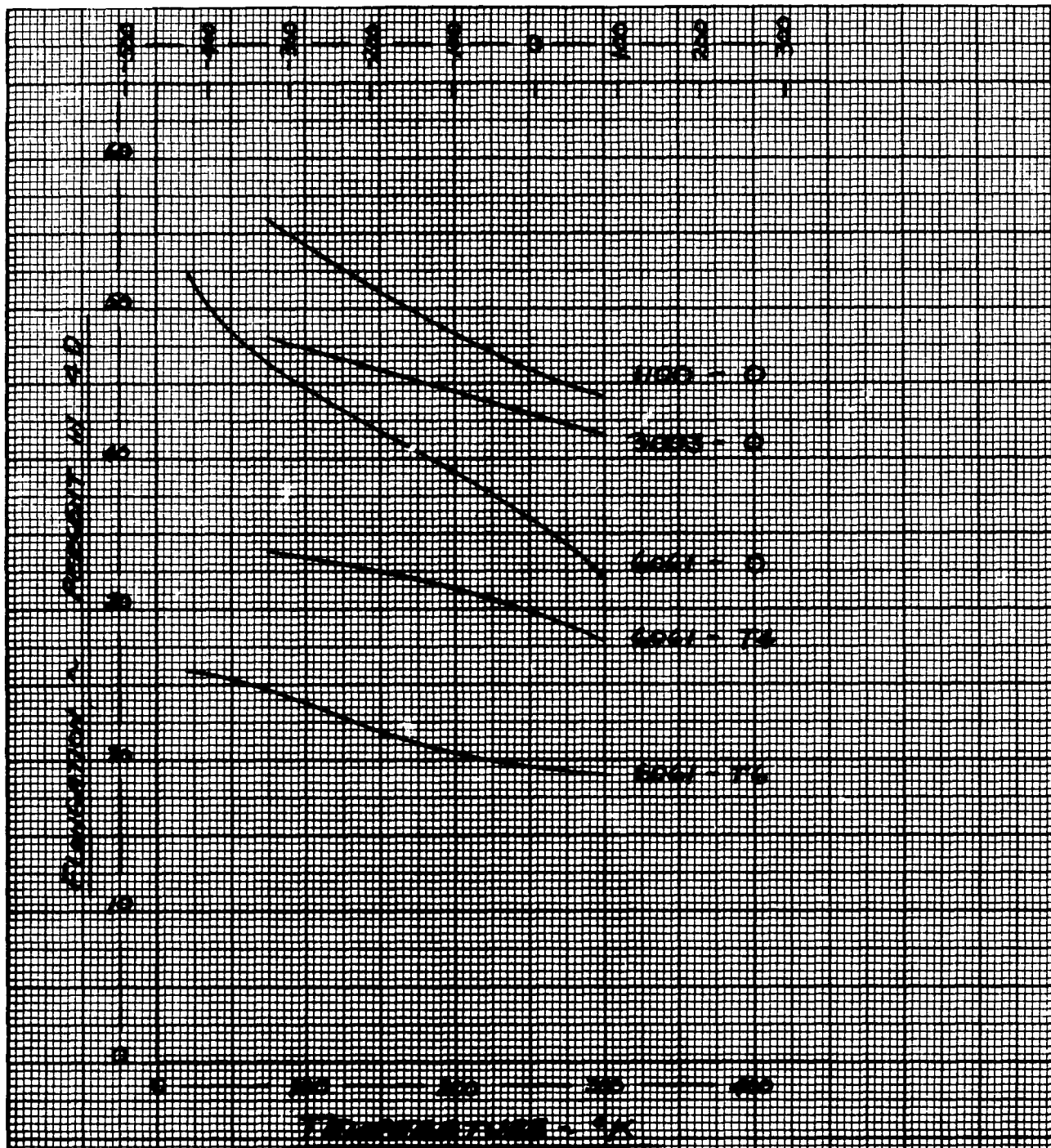
Figure 89.   Cryogenic Properties of Aluminum
             Alloys Elongation
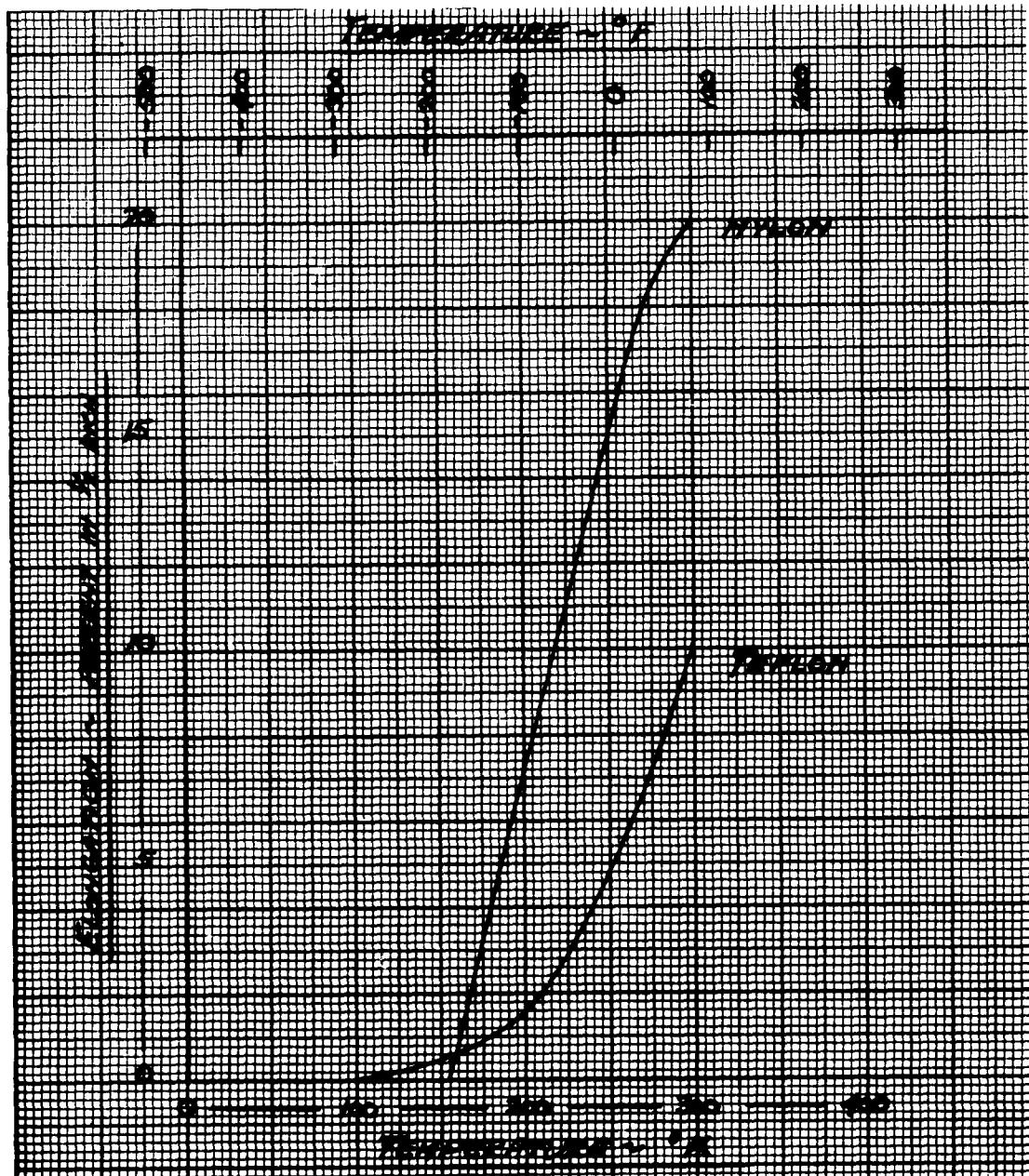
Figure 90.   Cryogenic Properties of
             Plastics Elongation

YIELD STRENGTH

The yield strength is important when one considers the collapsing pressure required to achieve the complete collapse of a bladder for maximum expulsion efficiency. A low yield stress is desirable because it will increase this efficiency and allow the buckling to continue into the plastic range. This is contrary to the conventional aircraft stress analysis and material selection. Some typical values of yield strength for several aluminum alloys and Teflon are shown in Figures 91 and 92, respectively.

ULTIMATE STRENGTH

For the bladder and diaphragm configurations, high ultimate strength is less important than yield strength. However, its value must be of sufficient magnitude to prevent premature failure of the material in critical areas. As a secondary consideration, the spread between yield and ultimate should be large. The burst pressure of the structural container incorporating an expulsion device is a function of the ultimate strength of the material.

Ultimate strength values for several candidate materials are shown in Figures 93 and 94.

MODULUS OF ELASTICITY

Another desirable property for the material in the application of bladders or diaphragms is a low modulus of elasticity. Buckling or collapsing of the shells for such configuration is a direction function of the modulus of elasticity.

Values of the modulus of elasticity of several plastic materials for a range of temperatures is illustrated in Figure 95.

WORK HARDENING

Resistance to work hardening becomes important when plastic deformation occurs during forming, installation or repeated expulsions. Although annealing can be accomplished on the material itself, this may be impractical when a bladder or diaphragm configuration is installed in a tank assembly. Work hardening also increases the strength properties of the material which is an undesirable characteristic, for example, for a collapsing bladder configuration.
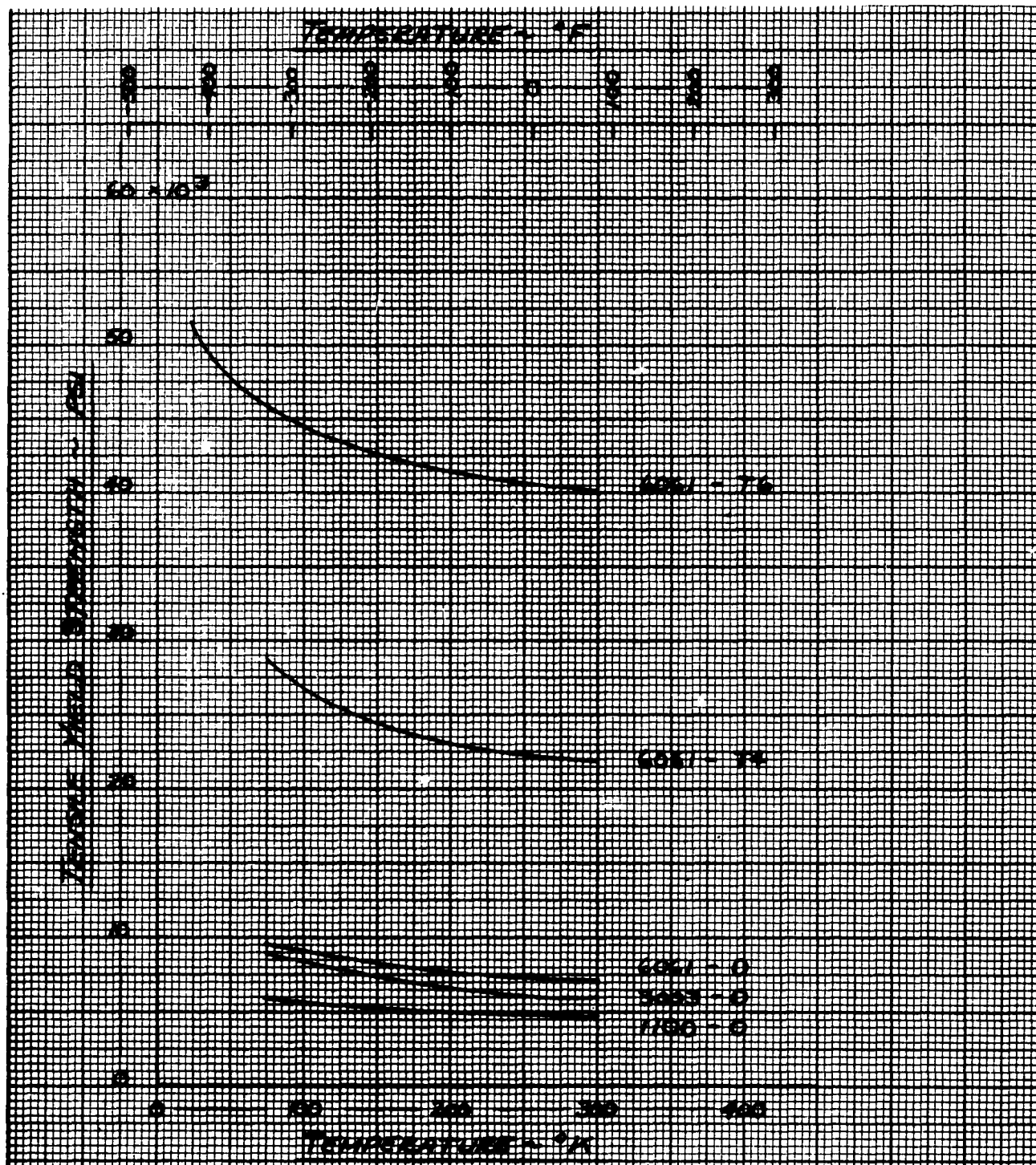
Figure 91.   Cryogenic Properties of Aluminum Alloys
Tensile Yield Strength
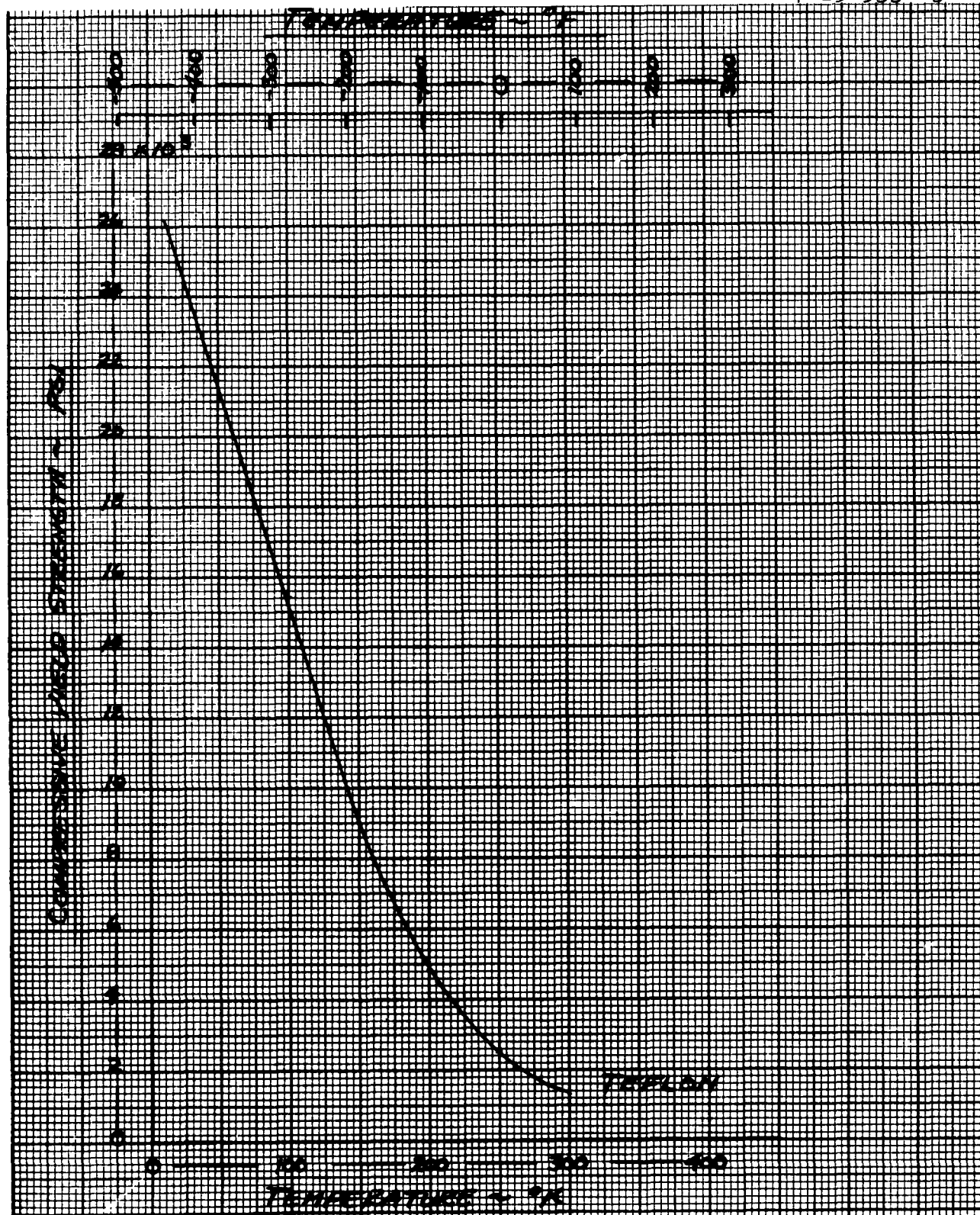
Figure 92.   Cryogenic Properties of Plastics
Compressive Yield Strength
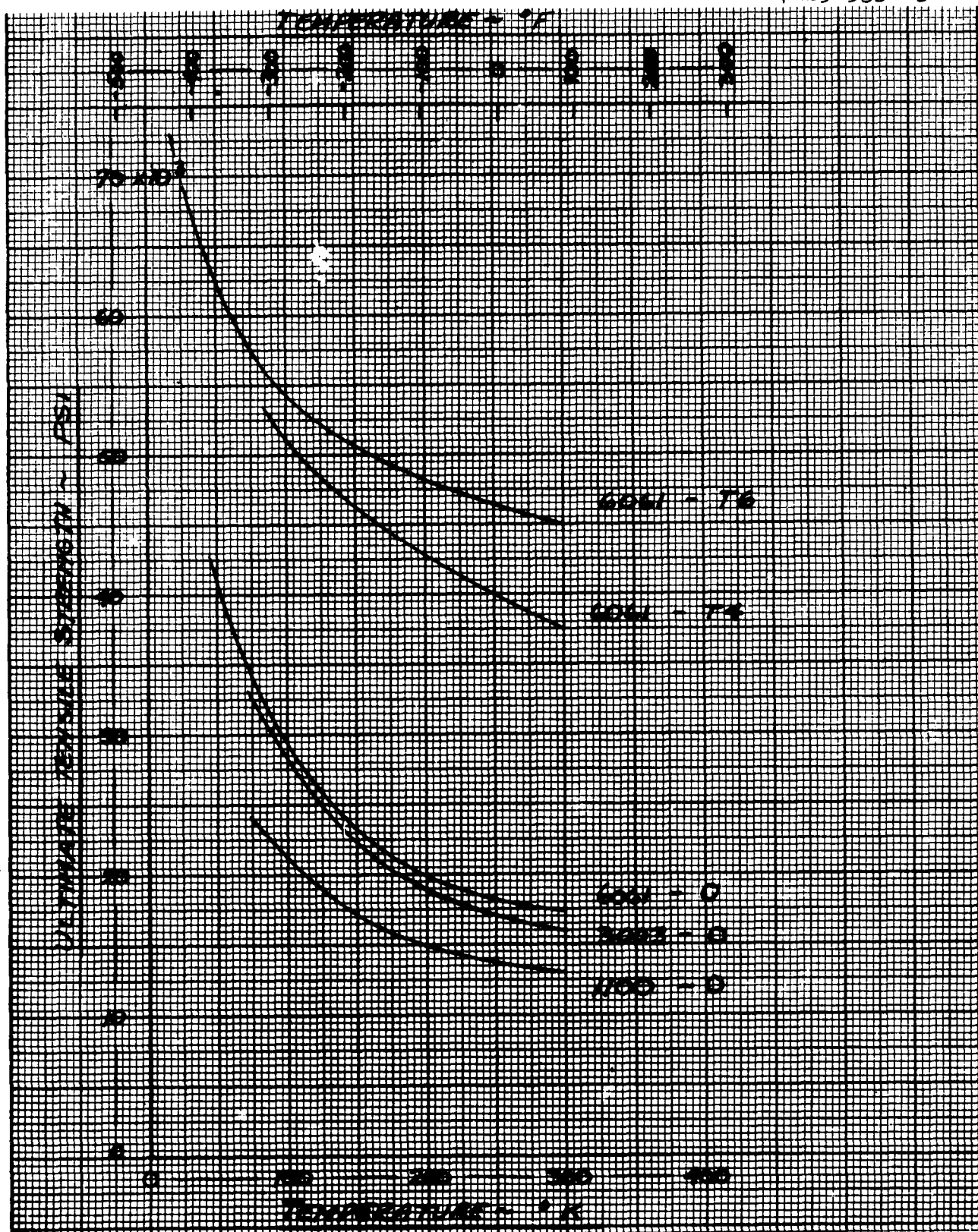
Figure 93.   Cryogenic Properties of Aluminum Alloys
Ultimate Tensile Strength
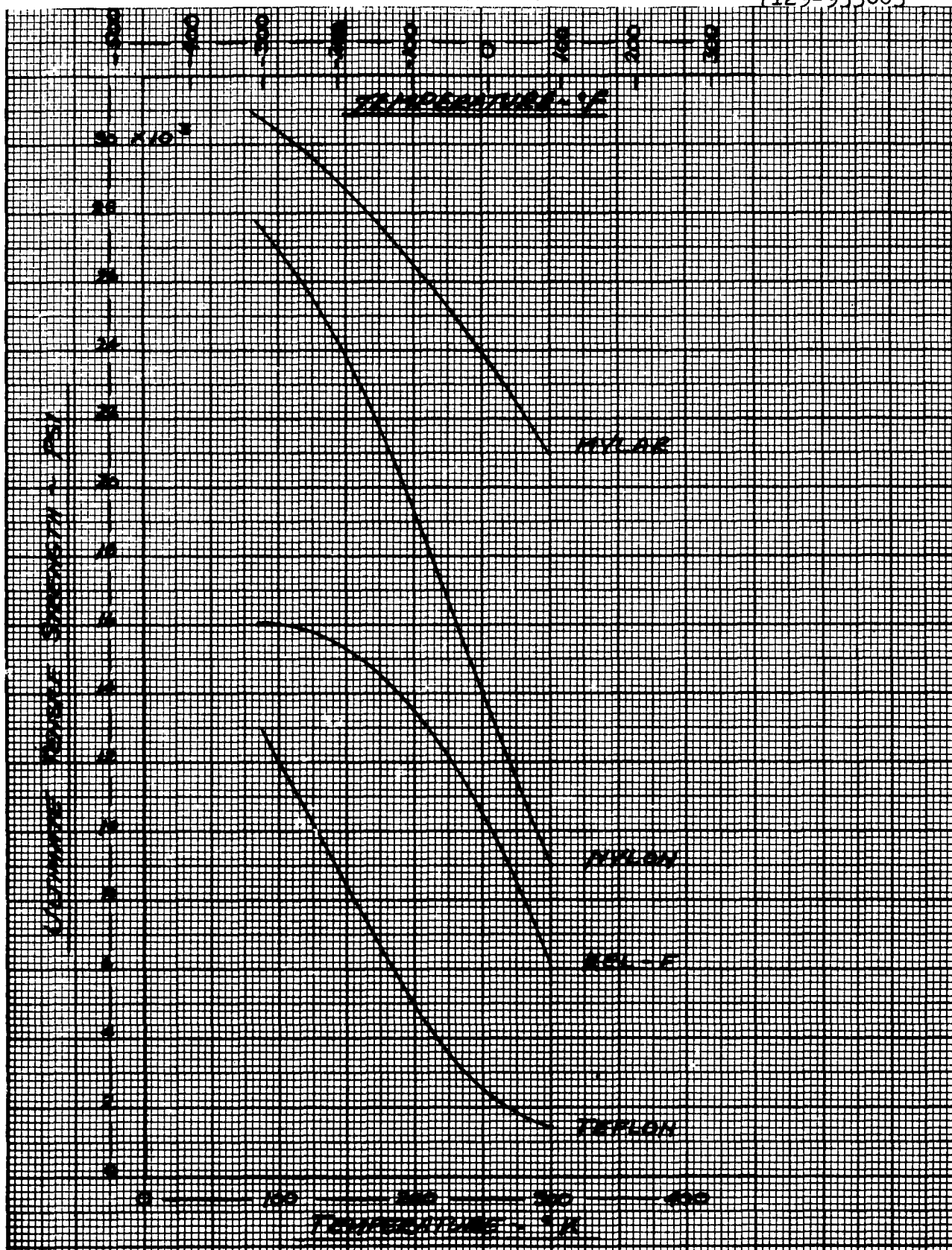
Figure 94. Cryogenic Properties of Plastics
Ultimate Tensile Strength
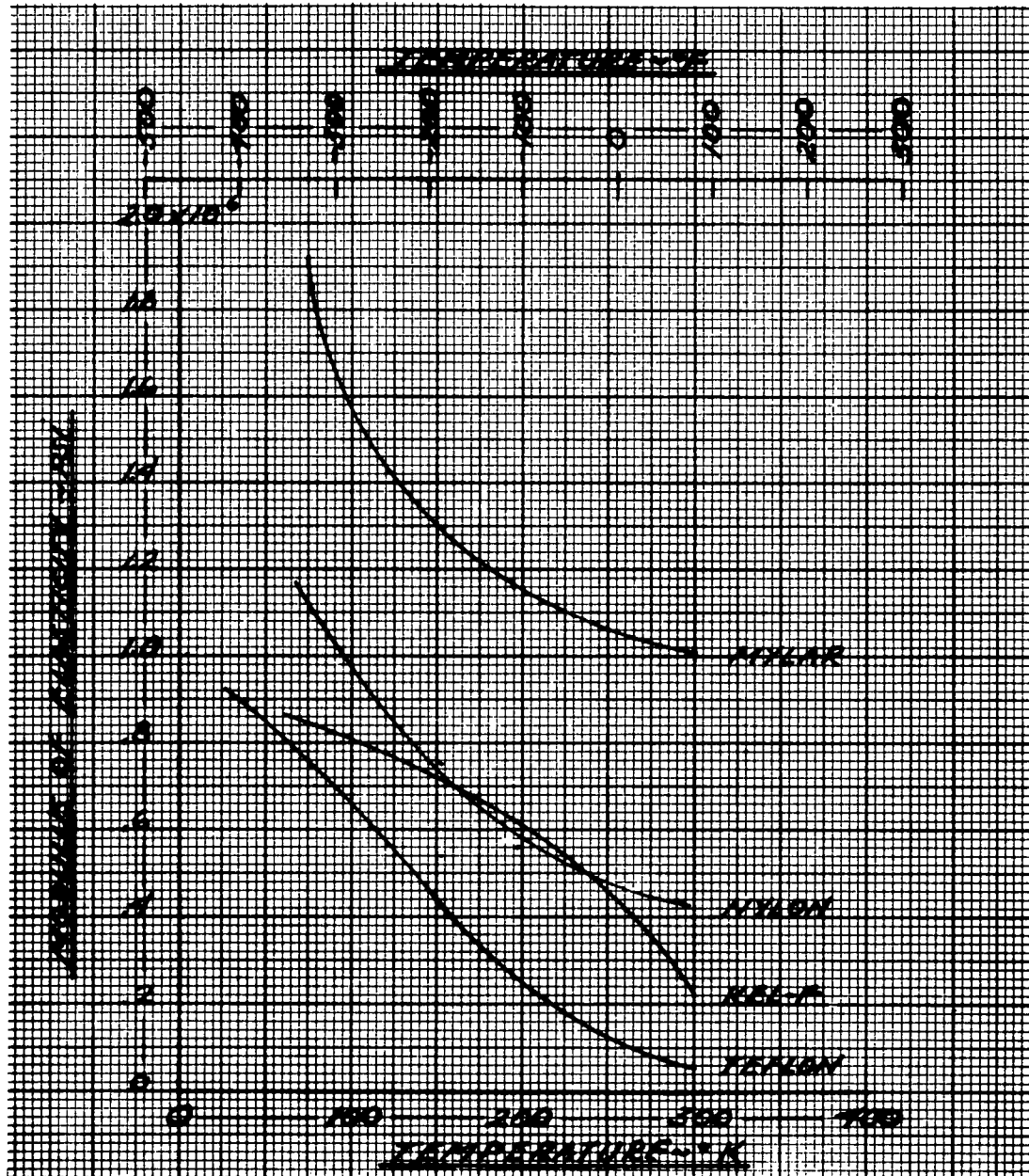
Figure 95.   Cryogenic Properties of Plastics
              Modulus of Elasticity

Examples of materials having desirable work-hardening prop-
erties for application to deforming-type expulsion devices are
gold and tin. Three-hundred-series stainless steel and nickel
exhibit a high degree of work hardenability. Aluminum alloys
exhibit work hardening properties which are related to their
alloying constituents. Therefore, pure aluminum and 1100
aluminum are the least affected by this phenomena.

METAL-TO-METAL COMPATIBILITY

When designing positive expulsion devices incorporating metal
diaphragms, bellows, etc., consideration should be given not
only to compatibility with propellants but also to the compati-
bility of metals in the system with themselves. Dissimilar metal
combinations are often sources of galvanic corrosion. In order
to minimize the effects of galvanic corrosion, metals and alloys
should be selected which are close to one another in the electro-
motive series. Relative surface areas of dissimilar materials
should be considered. Small components attached to a relatively
large surface area of a dissimilar metal should be fabricated of
a metal or alloy which is electropositive or cathodic to that
metal to avoid pitting corrosion.

Another factor to consider with respect to galvanic corrosion
is the homogeneity of the surface of individual metals. Small
pieces or inclusions of foreign material imbedded in the surface
during fabrication or removal of passive films in selected areas
can produce potential differences which cause corrosion. There-
fore, parts should be given suitable chemical treatments prior
to assembly to provide a surface which is as clean and homogeneous
as possible within the limits of the alloy or metal specification.

In addition to non-homogeneous metal surfaces, variation in
concentration of the contacting medium may produce concentration
cell corrosion. Fabricating techniques should therefore be
employed which minimize seams and junctures which will act as
capillaries and trap solution. Due to lack of circulation, this
trapped solution will vary in concentration from the main body
of solution and produce a potential difference in the adjoining
metal which can lead to corrosion.

Also in the compatibility area, on galvanic corrosion, the
use of aluminum, one of the least noble metals with other metals
of higher nobility could well make the aluminum the sacrificial
element. On the other hand, the use of gold and platinum would
create the greatest galvanic potential when used in the presence
of a conducting medium and aluminum since they are the most noble
metals.

VACUUM EFFECTS

In considering the effect of low pressure on the vaporization process of metals, the number of gas particles at various altitudes and the mean free path of gases at these altitudes are, therefore, of interest. Values taken from ARDC Model Atmosphere 1959 (Reference 69) are given in Table XIV.

When the environmental pressures are very low, the mean free paths of the vaporized metal particles are long, relative to the size of the evaporating vehicle structure, the recondensing of metal vaporized becomes negligible and the rate of metal volatization depends only on the temperature and corresponding vapor pressure of the metal. Experimental data on the vapor pressure-temperature and evaporation rates of metals in vacuum have been compiled by Dushman (Reference 70) and are shown graphically in Figure 90.

Since the amount of evaporation from metal surfaces for such refractory metals as Cb, W, Ta and Mo per year in high vacuum is extremely low, it can be postulated that these metals employed in structures operating in natural space environment will not suffer significant deterioration in structural strength for exposure periods of one year or less.

In considering the use of any plastic material exposed to a high vacuum and temperature, the vapor pressure of a specific plastic composition at a specific temperature and pressure must be known if any reasonable estimates of the amount of deterioration due to volatilization are to be made. Jensen (Reference 88) has determined vapor pressure of thermoplastic materials at temperatures ranging from approximately 0° to 235°F at pressures of 10^{-6} MM Hg. These data are shown in Figure 97. No data on the vapor pressure of reinforced plastic laminates at various temperatures and pressures have been found.

TABLE XIV

VARIATION OF PRESSURE, NUMBER OF PARTICLES
AND MEAN FREE PATH WITH ALTITUDE

| Altitude, Ft.	Pressure, MM Hg	Particles/Cu.Ft.	Mean Free Path, Ft.
0	760	7.2139×10^{23}	2.1758×10^{-7}
50,000	85	1.1043×10^{23}	1.4211×10^{-6}
100,000	8.3	9.746×10^{21}	1.6104×10^{-5}
200,000	1.9×10^{-1}	1.8568×10^{20}	8.4532×10^{-4}
300,000	7.5×10^{-4}	1.241×10^{18}	1.254×10^{-1}
400,000	8.8×10^{-6}	7.200×10^{15}	2.180×10^{1}
500,000	3.1×10^{-6}	9.478×10^{14}	1.656×10^{2}
600,000	1.7×10^{-6}	3.502×10^{14}	4.482×10^{2}
700,000	9.4×10^{-7}	1.779×10^{14}	8.715×10^{2}
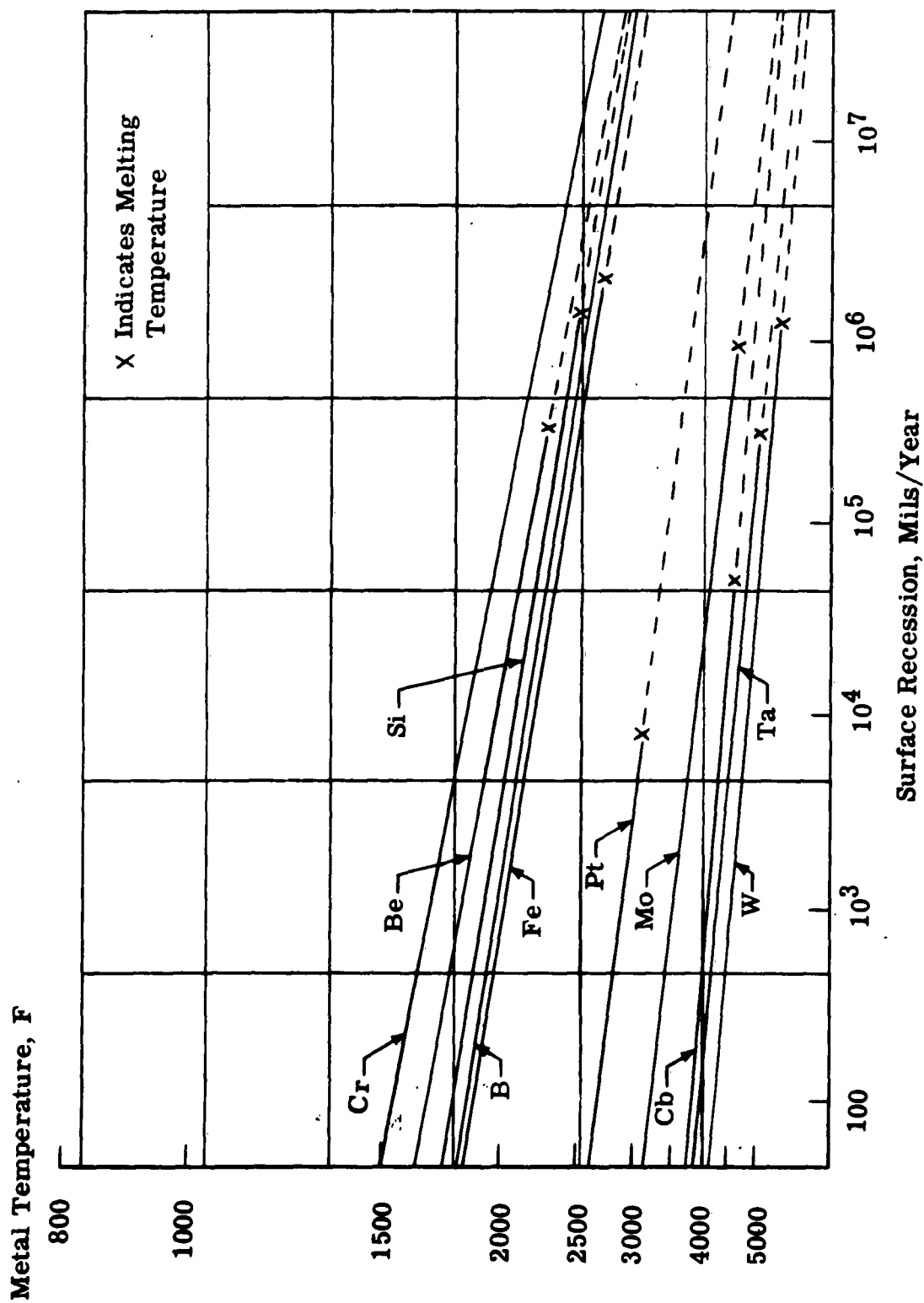
Figure 96. Volatilization of Metals in Space
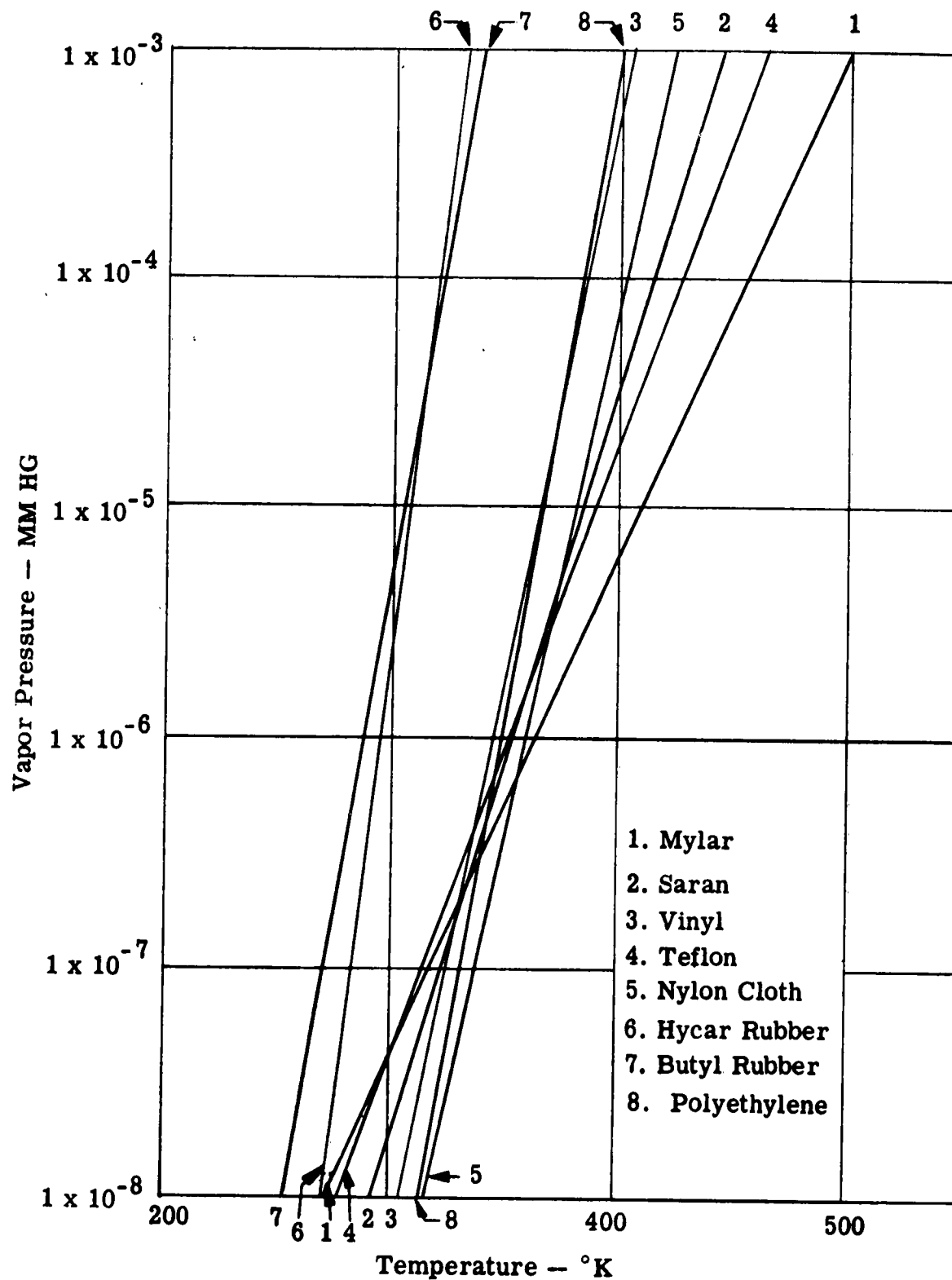
Figure 97. Vapor Pressure of Plastic Materials

VII. SLOSH AND VIBRATION CONSIDERATIONS

INTRODUCTION

In establishing the suitability and reliability of positive
expulsion devices it will be important to ultimately establish
that oscillatory motions of the fuel, fuel pressures due to
missile accelerations, and the process of fuel expulsion do not
singly or in combination overstress or fatigue bladders, diaphragms
or other devices in the system. Evaluation of expulsion devices
in this area in the present study must be done largely on a
qualitative basis since:

1. Much depends on detail design and the environment supplied
by the service application.

2. Analytical methods of predicting fluid motions, and par-
ticularly amplitudes are generally crude, or nonexistent.

3. Physical properties and resistance to fatigue of bladder
and diaphragm configurations are heavily dependent upon the
details of the manufacturing techniques as well as material prop-
erties which are as yet poorly defined particularly at cryogenic
temperatures.

Oscillations in tanks containing fuel may be divided into
three categories distinguished principally by the form of the
potential energy storage and secondly by the location of the lower
natural frequencies in the over-all frequency spectrum. These
categories in the order of increasing natural frequencies are:
(a) slosh modes; (b) elastic tank modes; and (3) acoustic modes.

Like all oscillations these modes represent the transfer of
energy back and forth between the kinetic and potential form.
The kinetic energy in each case appears as fuel velocity, the
potential energy storage mechanism however is different in the
three cases. For slosh modes it is due to fuel displacement in
the direction of tank acceleration; for elastic modes it is due
to elastic deformation of the tank; and for acoustic modes,
energy is stored in the fuel because of its compressibility.
Slosh modes will typically fall in a frequency band from .1 to
10 cps depending on tank geometry, tank size, and acceleration
applied to the tank. Tank elastic deformations, fuel density,
pressurization and viscosity play no significant part in determin-
ing fuel slosh frequency in practical tanks. The bladders involved
will have negligible elasticity and will not significantly influ-
ence the slosh mode.

Fuel modes involving tank elasticity will tend to fall into a frequency band from 10 to 100 cps depending on tank size, material, skin gages and fluid density. For elastic modes to exist the tank must be full or the fluid must be held toward one side or end of the tank by acceleration or by the pressurization system to give a preloading effect to maintain a linear elastic system and a static pressure within the fluid which will prevent cavitation within the fluid and spray at the free surface for small amplitudes of oscillation. As the amplitude of oscillation is increased the oscillating pressure plus the vapor pressure of the fluid can be made to exceed the compressive or preloading pressures and fuel spraying from free surfaces and cavitation within the fluid must be expected. These nonlinear effects will change the response characteristics in accordance with the nature of the nonlinearity and will add greatly to the effective damping of the system.

The lowest acoustic mode will have a frequency $f = c/2\ell$ where C is the speed of sound in the fluid (2000 to 6000 fps) and ℓ is the distance between reflecting surfaces. Fuel peak displacements in acoustic modes will generally be less than 0.001 inch. Very small amplitudes at these frequencies will allow spray formation at the free surface and local cavitation against tank walls with an accompanying dissipation of energy. The small amplitudes, and energy dissipation characteristics will prevent these modes from becoming destructive in most tank configurations.

Each of these areas of fuel oscillation and their implications on positive expulsion systems are discussed further in the subsequent sections.

BLADDER CONSIDERATIONS

The following discussion applies to bladders where the bladder acts through membrane stresses (carries no bending moment), and supplies negligible elastic restraint in the dynamic system. Such bladders have been extremely important in the past due to their relatively low weight as compared to other positive expulsion systems.

A major problem of bladder configurations is their tendency to crease at double bends with a possible rupture of the bladder material resulting when these double bends are further flexed by fuel sloshing. Missile boost flight is a period of particular vulnerability to fuel sloshing because of the many sources of disturbances which tend to exicte the lower lateral elastic modes of boost configurations and the tendency of such modes to fall into the same frequency range as important lateral slosh modes, thus exciting these modes.

No problem will exist if bladder tanks are always full during
boost, however, such a condition cannot be considered for a
vehicle of any general utility as any fuel weight not needed to
achieve a particular orbit or mission can generally be used to
great advantage in the payload to increase the capability or
reliability of payload functions. Many flights might therefore
call for less than full fuel in positive expulsion systems.

The chief difficulty with bladders, of course, is in selecting
materials that will withstand the chemical and temperature environ-
ment imposed by the fluid and will at the same time withstand
service fuel sloshing conditions. Bladder material properties
are discussed under MATERIAL CONSIDERATIONS.

When the designer has selected the best available bladder
material compatible with the particular propellant involved, he
will next be concerned with achieving a detail design that will
minimize slosh vulnerability. Wherever possible, the slosh fre-
quencies of the bladder tank should be designed to avoid the
lateral natural frequencies of the boost configuration.

The determination of the natural frequencies of multistage
boost configurations is necessary for flight control system
design and for load studies as well as for slosh coupling studies.
Because of these important applications considerable effort is
justified in both analytical and experimental procedures to
establish these modes and frequencies. Reference 117 is an excel-
lent illustration of such an effort.

DETERMINATION OF SLOSH FREQUENCY

Only limited means are available to the designer in his
attempt to make his bladder tank slosh frequencies avoid airframe
natural frequencies since only tank geometry and tank accelera-
tion will influence slosh frequency. Slosh frequency may be
expressed as

$$\omega_n = K_n \sqrt{\frac{ng}{D}} \tag{88}$$

where D is a characteristic dimension usually the tank diameter
or width, n is the acceleration of the container in g units, and
K is the Froude number characteristic of the tank configuration
and fuel level.

Analytical derivations of K values or its equivalent are
available in the literature for flat bottomed cylindrical tanks
with a variety of cross-section shapes, and for a few containers
with nonflat bottoms, notably spherical and conical. For a

review of literature on techniques of fuel slosh analysis see
Reference 118.

Where slosh frequencies for complex tank shapes are required
but the Froude constant K cannot be obtained from analytical
solutions in the literature, it may be obtained experimentally
generally, at a small fraction of the cost of the corresponding
analytical exercise.

Equation (88) is used in the form

$$K_n = \omega_n \sqrt{\frac{D}{ng}} \tag{89}$$

where ω_n is the observed slosh mode natural frequency and $n=1$
in the laboratory. This value of K may then be used in Equation
(88) to obtain the frequency of this mode for any geometrically
similar tank and fuel condition, for any flight acceleration n g.

The speed and low cost of the experiment determination of
K is due to the following: (1) Tank elasticity will not be a
significant factor and a rigid model may be used; (2) Water may
be used to represent any fuel since neither fuel viscosity or
density are significant in determining slosh frequencies;
(3) A laboratory model tank with a length of 10 or 12 inches will
give accurate data for any size prototype. Bladders will generally
have a negligible elastic restraint on the prototype fluid and
will therefore show little effect on the lower natural frequencies
although the flexing of severe bladder creases may contribute con-
siderable damping.

The variations of the Froude constant K_n, (termed the fluid
frequency parameter in Reference 121), with depth are indicated
in Figures 98, 99 and 100 for the modes of spherical tanks and
transverse modes of horizontal circular cylinders, longitudinal
modes of horizontal circular cylinders, and modes of the upright
circular cylinders, respectively. Figures 98 and 99 utilize the

fluid frequency parameter $\lambda_n = \omega_n (R/g)^{1/2}$ and Figure 100 the

fluid frequency parameter $\delta_n = \omega_n \sqrt{\frac{R}{g \, \epsilon_n \, TANH \, (h/R)}}$

where ϵ_n is the nth zero of the first derivative of the Bessel
Function of the first order and the first kind. The above figures
from Reference 121 have been included as they represent the most
commonly used tank configurations
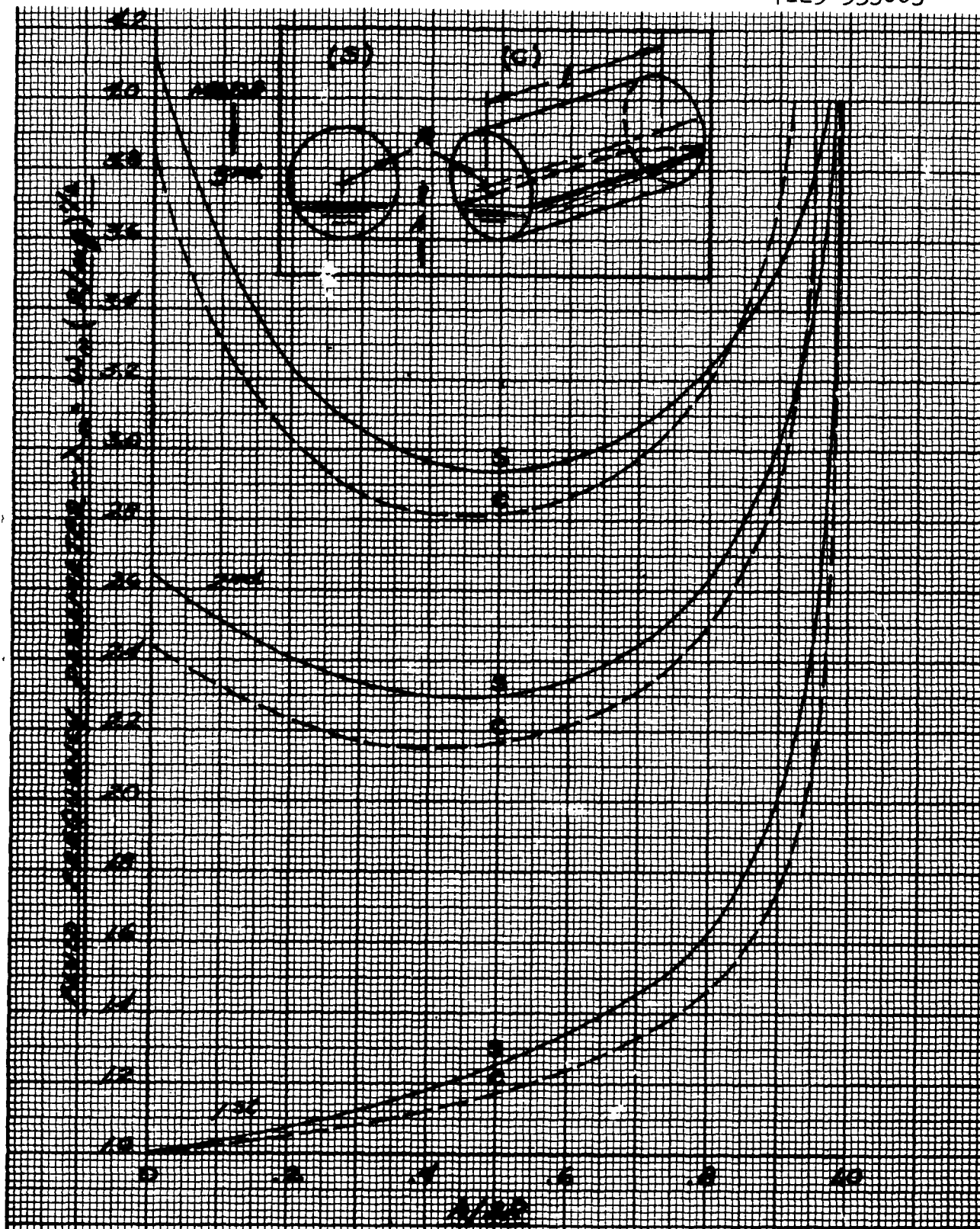
Figure 98.   Variation of Fluid Frequency Parameter with Depth
             for Spherical Tanks and Transverse Modes of
   Horizontal Circular Cylinders
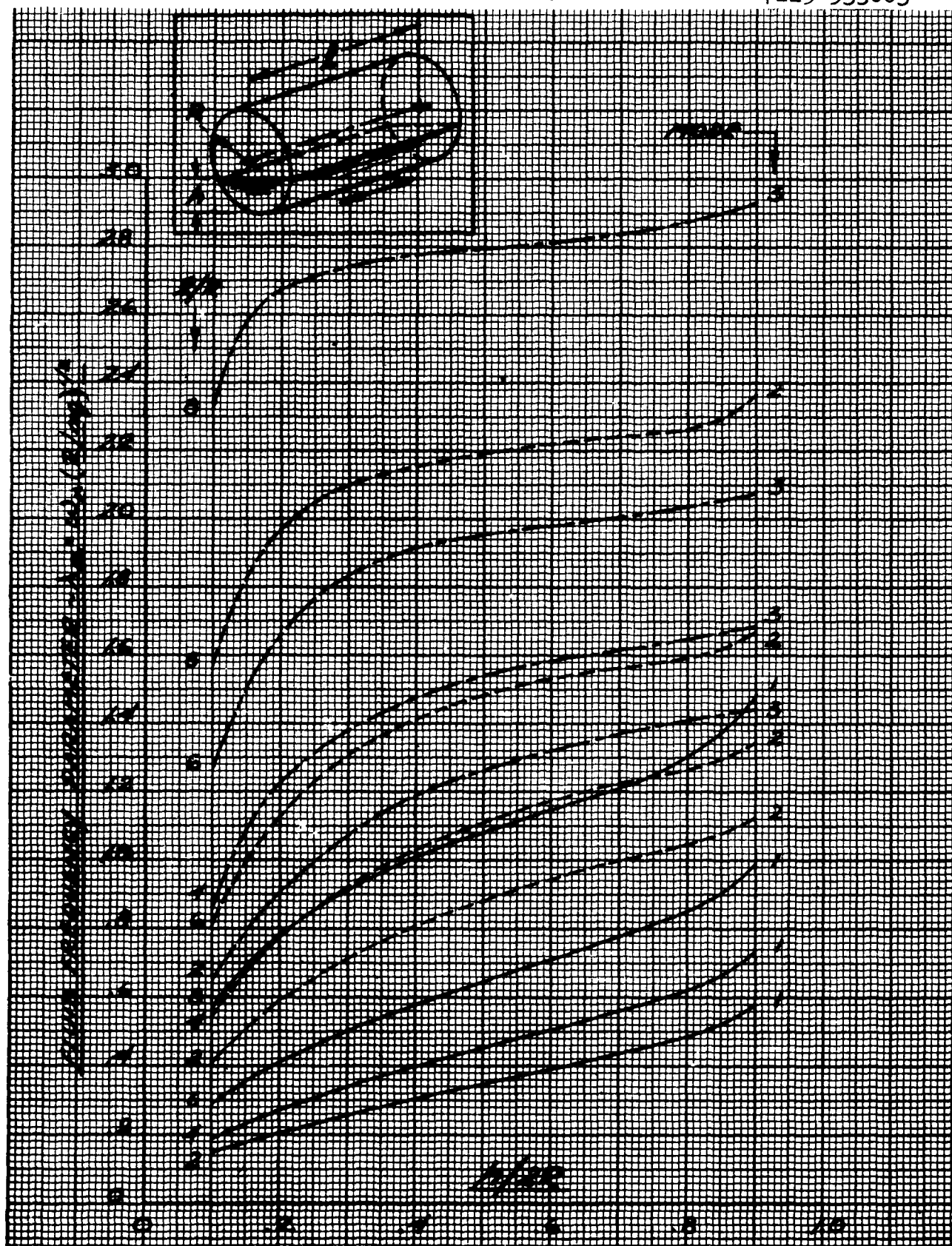
Figure 99.   Variation of Frequency Parameter with Depth for
              Longitudinal Modes of Horizontal Circular Cylinders
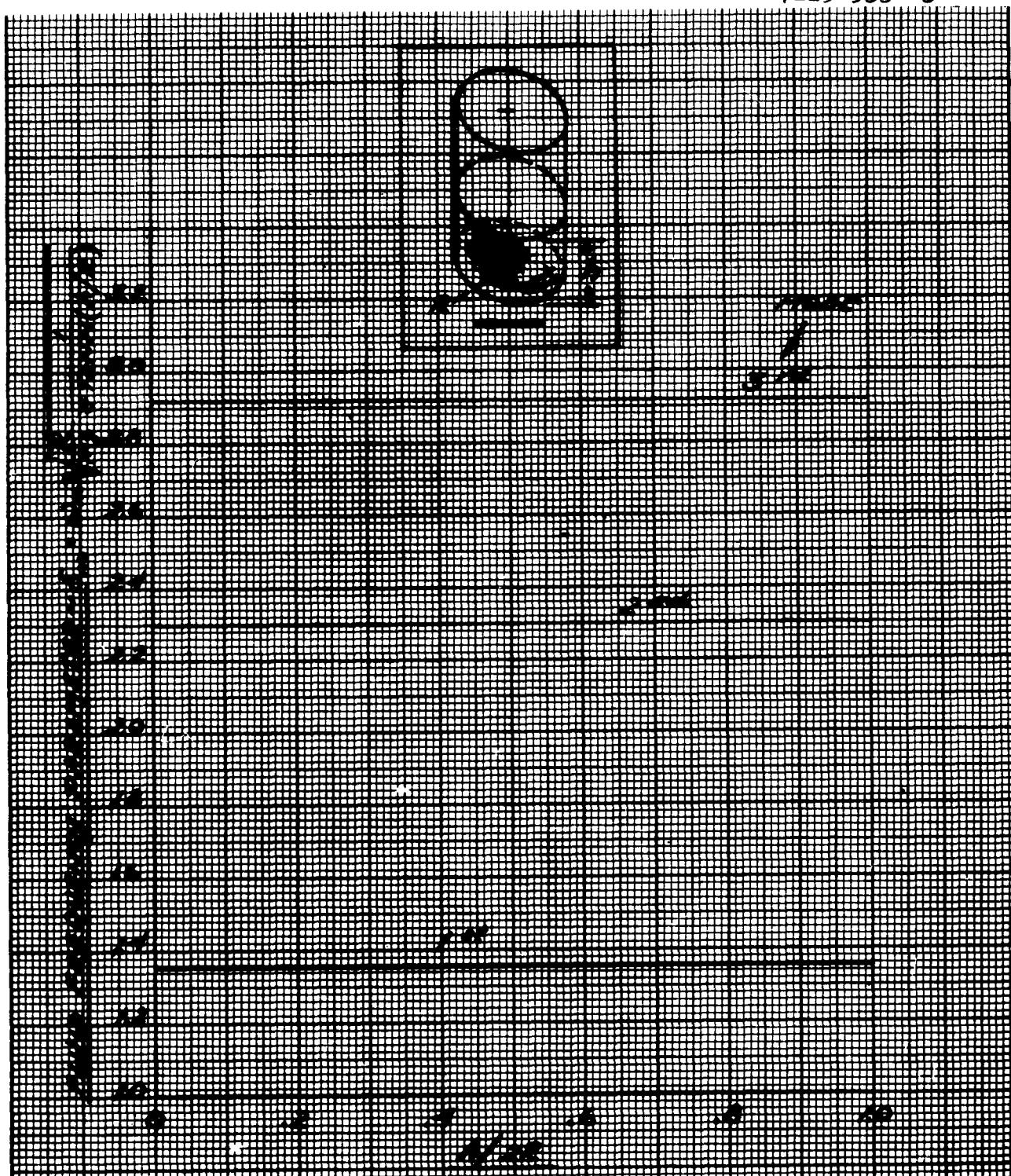
Figure 100.   Variation of Fluid Frequency Parameter with
Depth for Vertical Circular Cylinders

DETERMINATION OF BLADDER LIFE IN SERVICE SLOSH CONDITIONS

Analytical methods of determining bladder adequacy in a sloshing environment are hampered by the following: (1) The severity of bladder working as a function of the amplitude of slosh induced in the fluid by the forced excitation of the tank. This amplitude is critically dependent on the total effective damping in the fluid and bladder material. At the present time damping constants cannot be assigned with sufficient accuracy to allow reliable computation of slosh amplitude as a function of excitation amplitude; (2) There is no method of established accuracy for determining the sharpness of the double folds that must exist in a tank partly filled with fuel or for determining the severity with which such double folds will get flexed during sloshing; (3) Methods of testing bladder materials for flexing failure characteristics are not sufficiently correlated with bladder service conditions to allow computed bladder flexing conditions to be used in service life estimates.

On the basis of the foregoing it appears that bladder suitability and reliability will be established by direct experimental tests for some time to come. In setting up a laboratory slosh test for this purpose it is likely that a substitution will be made for the service fluid, and perhaps a model of less than full scale will be necessary. Both of these changes will affect the Reynolds number correspondence between model and prototype. Since Reynolds number matching should be correct to assure the correct slosh amplitude in the model, it is important that Reynolds number be accounted for in establishing the equivalence of model and prototype. For a review of basic slosh model similitude requirements see References 119 and 120.

DETERMINATION OF REYNOLDS NUMBER CORRELATION

Reynolds number matching will be exact when

$$\frac{D_{model}}{D_{prototype}} = \left[\frac{\left(\frac{\mu_{model}}{\mu_{prototype}} \right)}{\left(\frac{\rho_{model}}{\rho_{prototype}} \right)} \right] \left[\frac{(ng)_{model}}{(ng)_{prototype}} \right]^{-\frac{1}{3}} \tag{90}$$

where $\dfrac{D_{model}}{D_{prototype}}$ = length scale factor, μ = fluid viscosity, ρ = fluid mass density, and n×g is tank acceleration.

In applying Equation (90) to important liquid propellants and convenient laboratory fluids it will be found in many cases that little or no reduction in model size is possible, and in some cases a model larger than the prototpye is called for. It is obviously desirable to use full scale tanks and the actual propellants wherever possible both from the above standpoint and because of the cost and practical difficulty of scaling bladders to different sizes. Many fuels, of course, particularly the cryogenic fuels are quite awkward and should be avoided if possible in these tests.

Satisfying Equation (90) for practical model sizes in many cases calls for model fluids of significantly lower viscosity and higher density than are available. In such cases the inevitable Reynolds number deviation may be corrected for in bladder slosh tests by the following scheme for linear oscillation amplitudes.

Solving Equation (90) for μ model

$$\mu_{\substack{MODEL \\ REQ'D.}} = \mu_{PROTOTYPE} \left[\frac{\rho_{MODEL}}{\rho_{PROTOTYPE}} \right] \left[\frac{D_{MODEL}}{D_{PROTOTYPE}} \right]^{3/2} \left[\frac{(ng)_{MODEL}}{(ng)_{PROTOTYPE}} \right]^{1/2} \tag{91}$$

If model size and model fluid are selected on the basis of convenience for test purposes then Equation (91) will give the model fluid viscosity required for exact Reynolds number matching. This value will usually be considerably lower than the actual viscosity of the model fluid. Defining the ratio of required to actual viscosity as

$$R_{\mu} = \frac{\mu_{MODEL\ ACTUAL}}{\mu_{MODEL\ REQ'D.}} \tag{92}$$

it is required that test conditions be adjusted so that the factor R_{μ} will not invalidate test results in deviating from unity.

If a single degree of freedom system with viscous damping coefficient C is forced at its resonant frequency by displacement of the supporting structure with amplitude S_o, then the amplitude of response y_o will be given by

$$\frac{y_o}{S_o} = \frac{K}{C} \tag{93}$$

where K may be considered for present purposes merely the constant of proportionality, and C is well below critical damping. Response amplitude at resonance is then inversely proportional to fluid damping.

Applying this result to the case at hand indicates that if the fuel tank is excited with a force displacement S_o corresponding to prototype service displacements the effect of a viscosity error factor R_μ will be to change the response amplitude by the factor $1/R_\mu$. Since the fluid response amplitude is directly proportional to the support structure excitation amplitude the proper slosh amplitude may be restored by changing the tank excitation amplitude from S_o to $S_o R_\mu$. Thus if Equation (91) showed that the model fluid were twice as viscous as it should be, shaking the tank at the specified input level S_o would give only half the proper slosh amplitude. Doubling the excitation amplitude would then give the correct model slosh amplitude for proper representation of the prototype.

Where a "room temperature" model fluid is used to simulate a cryogenic prototype fuel, the bladder service life characteristics must be corrected for the difference in physical properties of the bladder at room temperature as compared to the properties at the prototype fuel temperature. At the present time insufficient data from the bladder materials tests are available to allow room temperature bladder test data to be extrapolated to cryogenic performance predictions.

BLADDER CONFIGURATION FUEL ENTRAPMENT

The problem of fuel isolation in a flexible bladder system is closely tied to the more serious companion problem of fluid exit port sealing by part of the flexible bladder. Since fuel pressurizing pressure will then be applied across the face of the bladder where it spans the exit port there may be a chance of bladder rupture as well as fuel flow stoppage.

Exit blockage is due to the high velocity of fluid flow in the vicinity of the exit port. If the velocity is high close to the bladder, a pressure difference will exist across the face of the bladder and it will be drawn into the high velocity stream. The bladder, in the vicinity of the exit port, is therefore actually attracted to the port and can seal it off.

The use of collector tubes running from the exit port up into the tank has been found to be an excellent method of solving both the fuel isolation and exit seal problems at the same time, and is routinely used on most flexible bladder expulsion systems.

FOAMING AND FOAM SUPPRESSION

Foaming tendency is a function of the ability of a fluid to exert a membrane tensile force characteristic on its free surface. Any gas or vapor bubble rising to the free surface will tend, rather than to break through this free surface, to have this membrane stretch around it forming a bubble floating on the free surface.

Liquids being handled or sloshed at pressure-temperature combinations close to boiling may foam with vapor bubbles. Where a bladder or diaphragm is used in a positive expulsion device under the above circumstances, a vapor pocket would be created between the fluid and the bladder or diaphragm. Since operation close to the liquid boiling point also raises the danger of cavitation at pump intake, design operating conditions of such a system should allow pressures to be maintained well above the boiling pressure for the expected fuel service temperature conditions. This should eliminate any vapor foam problems.

Where a bladder is used, gas filled foam bubbles should not be caused by sloshing since the pressurizing gas is isolated from the fluid. Gas filled bubbles can result from gas being mixed into the fluid during filling. Also, liquids which do not wet the surface of the container or bladder may, during filling, trap gas against the wall. Some of this gas may later collect into bubbles and rise to the surface. The volume of gas thus accumulated is probably small but perhaps should be vented off if there is danger of pump malfunction due to air lock, or if a short thrust drop-off in the engine were objectionable.

CAVITATION AND FUEL SPRAY

While descriptions of vibration tests of tanks containing fuel may be found in the literature with brief descriptions of fuel spray encountered, no accompanying analytical studies are presented which predict fuel spray or cavitation conditions.

The reason for this situation is believed to be the fact that while analytical methods have been developed to study the effects of tank elasticity for a few special tank slosh frequency conditions, the action of fuel at the higher frequencies of the elastic modes will vary between configurations and modes, may contain major nonlinearities and in many cases apparently is not well understood. Mathematical models suitable for analyses in this area are as a consequence virtually nonexistent.

Since fuel spray and cavitation are an important phenomenon associated with these modes of vibration, the lack of vibration analysis techniques automatically limits the analytical considerations of spraying and oscillatory cavitations accompanying

elastic mode oscillations. However, since fuel spray and cavitation are closely tied to the total absolute pressure at the free surface and within the fluid, a start can be made in this area by considering the pressure within the fluid of a rigid cylindrical tank in a forced oscillation in the axial direction, as shown in Figure 101.

Figure 101 may be considered as an upper stage of a multistage missile oscillating in its fundamental axial mode. When the tank of Figure 101 is oscillated at frequency ω and half amplitudes h in the axial direction the pressure P at a point a distance $\ell-y$ from the free surface will be given by

$$p = p_i - p_v + \rho(\ell-y)(a + \omega^2 h \sin \omega t) \tag{94}$$

where a = missile steady acceleration

p_i = total absolute pressure of all gases and vapors above the fluid

p_v = vapor pressure

If the pressure above the fluid, p_i is due only to fluid vapor pressure giving $p_i = p_v$, and if $a = \omega^2 h$ there will be one instant at the peak of each oscillation when there will be no net pressure at any point within the fluid and at the free surface. If the amplitude of container oscillation is then increased further, Equation (94) indicates a negative pressure. Since the fluid has no tensile strength and is not attached to the bottom of the container it cannot be expected to keep up with the displacement path of the container during the period of acceleration reversal, and cavitation should result at the bottom of the container. Cavitation is less likely to appear at other depths of fuel because of the inertia of the fluid and the lack of forces to move part of the fluid to allow a cavity to form, except where baffling or other flow restriction exists.

Since free surface wavelet peaks represent highly localized velocity fluctuations relative to and normal to the free surface, when the total pressure within the fluid drops to zero during tank oscillation peaks, a cresting wavelet at that instant has an upward velocity with nothing to resist it but surface tension. During these intervals then, surface spray should result. If a bladder were lying on the free surface the damping of the bladder would severely dampen any wavelet that tended to form, and the inertia of the bladder would be sufficient to restrain any individual spray pellets.
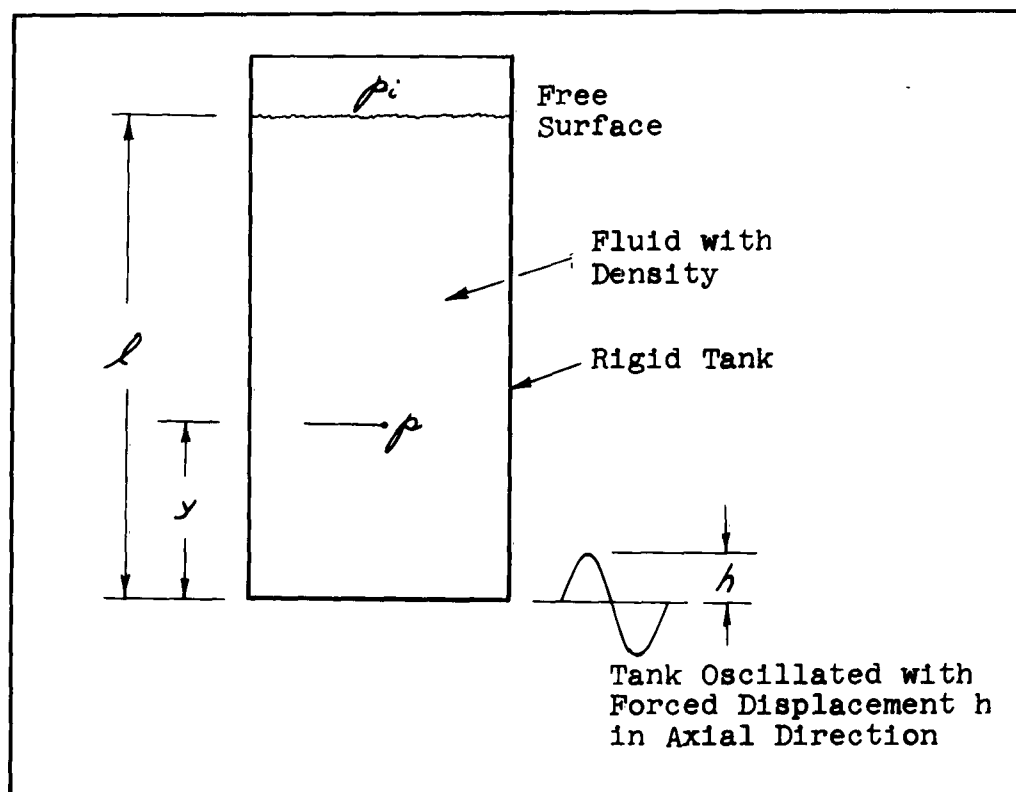
Figure 101. Rigid Tank With Fluid Subjected to
Displacement Excitation in Axial
Direction

Consider now the preceding case without bladder, and modified only by the addition of pressurizing gas. If the container is oscillated axially with an acceleration $\omega^2 h$ equal to the steady container acceleration a , the pressures due to acceleration will be cancelled at each cycle peak. However, when the amplitude of container oscillation h is increased to give a reversal in the sign of the net acceleration, the container tendency to pull away from the fluid and form a bottom cavity during this time period will cause the fluid pressure at the bottom of the tank to drop below $p_i - p_v$ the effective surface pressure, and the resulting pressure differential should force the fluid downward in a piston-like action against the tank bottom and prevent cavitation until the peak amplitude of oscillation h is increased to the point where

$$p_i - p_v + \rho(\ell - y)(\omega^2 h - a) \tag{96}$$

The pressure p_1 will not be effective in reducing spray at the free surface since the pressure will be felt uniformly throughout the wavelets and no pressure differential due to p_1 will develop which would affect wavelet dynamics. Spray should be expected with $\omega^2 h = a$. A bladder on the free surface will be very effective in eliminating spray since no cavity can be formed between the free surface and the bladder without developing a pressure on the fuel side of the bladder of $p_i - p_v$.

For the bladder to be raised from the fuel surface by a spray pressure p_s it will be necessary that

$$p_s > p_i - p_v$$
$$p_i < p_s + p_v \tag{97}$$

Since spray pressure must be the result of fluid particles with a velocity component normal to the bladder surface it seems most improbable that a significant pressure could be developed from this source with practical values of pressurization p_1.

ELASTIC TANK BREATHING MODE

It was initially stated that a class of liquid tank vibration modes exists apart from the conventional slosh modes and distinguished from sloshing by the potential energy storage mechanism. An investigation into practical cases of such modes is considered necessary if important oscillations and natural frequencies of positive expulsion devices are to be evaluated. In sloshing modes the potential energy storage is due to liquid movement in

the direction of tank steady acceleration, while in the case of
elastic tank vibration modes the potential energy storage is due
to the elastic deformation of the tank walls when subject to
fluid pressure oscillations.

As an illustration of the effects of this fundamental dif-
ference it may be stated that: (1) Pressurization does not affect
fuel sloshing but can affect the upper amplitude limit of liquid
elastic tank vibration modes; and (2) forms of pressurization
which hold the fuel to one end of the tank will allow an elastic
tank mode to exist under zero-g conditions, in constrast with
slosh modes where tank acceleration is essential to the existence
of the mode.

In order to allow some quantitative feel for frequency range,
cavitation, and spray susceptibility of an elastic mode, a method
of analysis has been established to determine natural frequency,
and amplitude-pressure relationships in the oscillating liquid
of an important cylindrical tank breathing mode. A summary of
the result is presented in the following paragraphs, and the
analytical procedure is covered in Appendix C.

CONFIGURATION DESCRIPTION AND ANALYSIS RESULTS

Figure 102 illustrates an elastic breathing mode involving
radial motion of the fuel in the lower part of the tank with
accompanying hoop strains or breathing in the cylinder walls at
these stations due to the accompanying pressure oscillations.
The fluctuations in tank volume occurring near the bottom of the
tank will cause corresponding vertical oscillations of the fuel
level at the free surface. This mode will exist during periods
of tank acceleration or where there is some means of pressurizing
which will hold the fluid toward one end of the container and
maintain a positive pressure within the fluid and against the
tank walls. This base supported cylinder is considered of par-
ticular interest since it represents a missile stage tank and
this mode should be observed when vibrating such a configuration
in the axial direction. This mode of oscillation is only very
slightly coupled to other masses or stages attached to either
end of the tank through the Poisson's ratio shortening of the
tank accompanying the hoop tension in breathing.

A method of computing the frequency of oscillation, pressure
distribution and wall mode shape is shown in Appendix C for an
idealization of Figure 102 which is illustrated in Figure 103.
This idealization considered the cylinder without ends and rest-
ing on a solid frictionless surface. Elimination of the tank
ends allowed the basic breathing mode to be investigated
analytically in its simplest form and eliminates the need to
qualify results by associating them to a specific set of end
conditions.
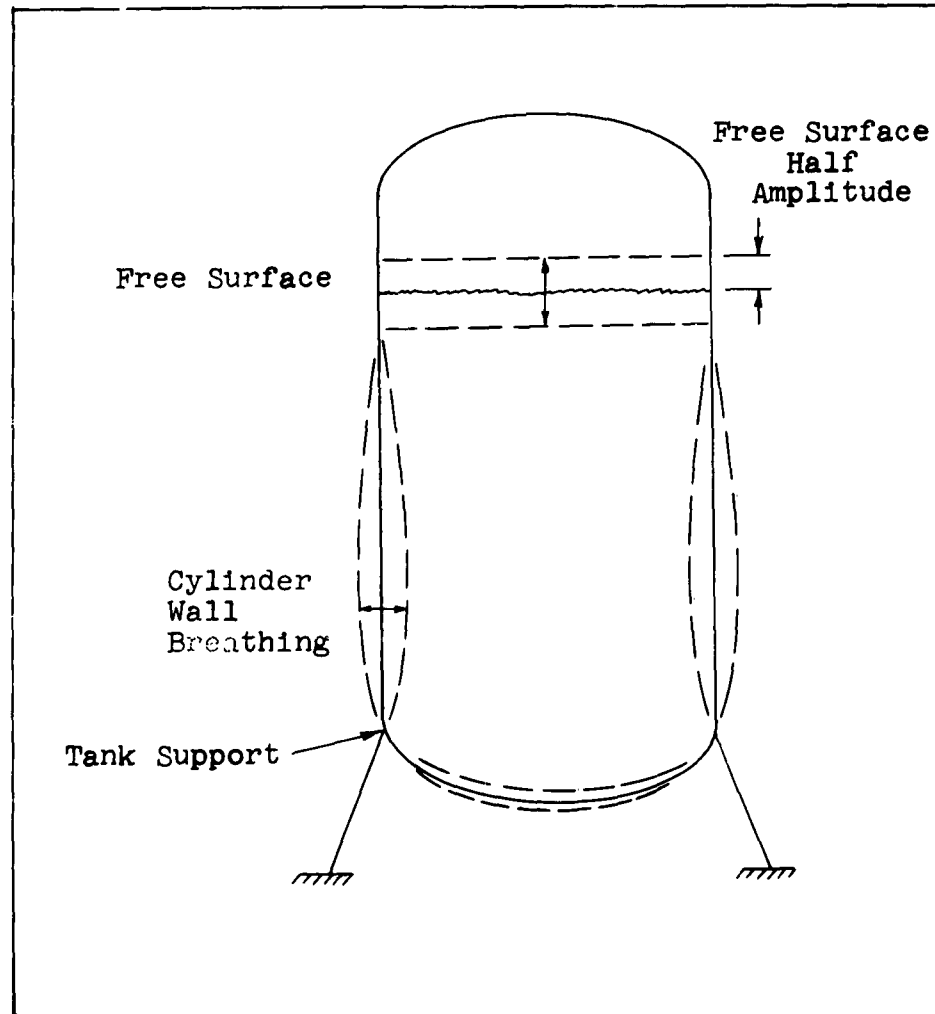
Figure 102. Illustration of Cylindrical Tank
Breathing Mode
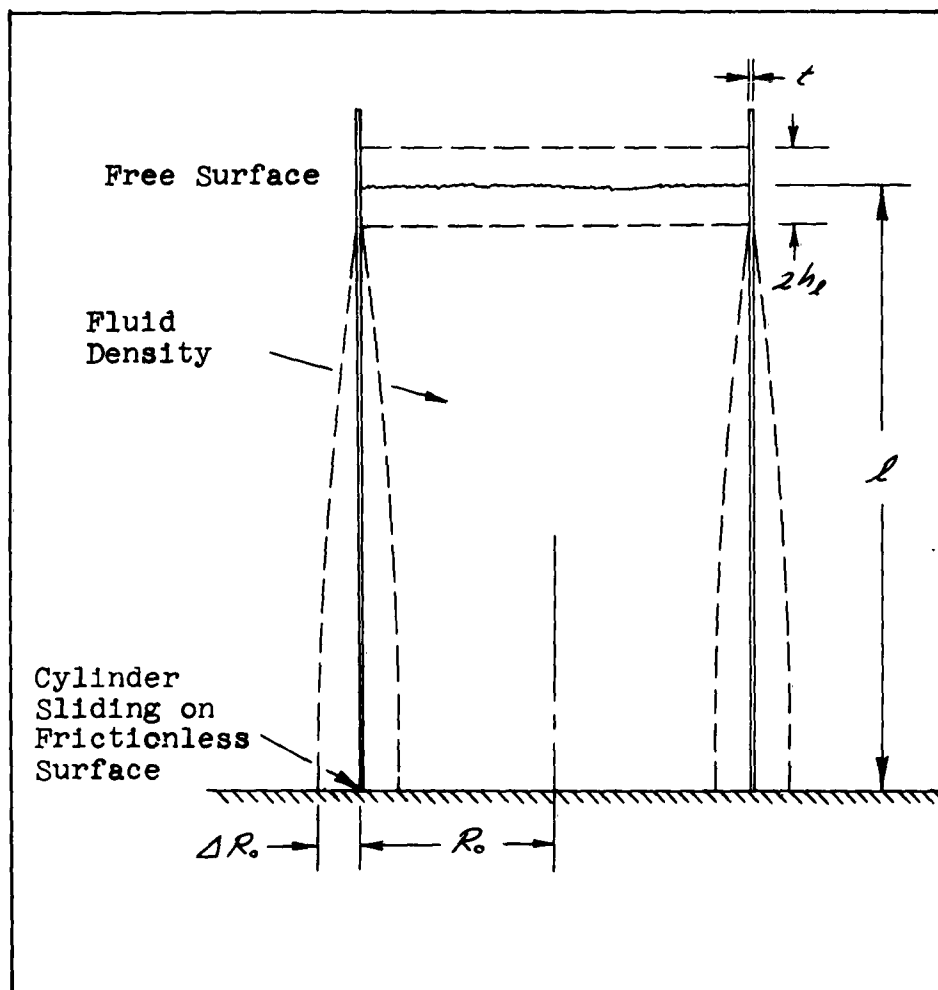
Figure 103.   Idealization of Cylindrical Tank
Breathing Mode for Analysis

Employing the following notation,

ℓ = the distance from the bottom of the cylinder to the free surface,

ΔR_0 = the half amplitude of the radial breathing at the cylinder bottom,

R_0 = the cylinder radius,

E = the cylinder material modulus of elasticity,

t = the cylinder wall thickness, and

ρ = the fluid density

it is shown in Appendix C that,

1.   The half amplitude displacement h_ℓ of the free surface will be given by

$$h_\ell = 1.27\ell \, \frac{\Delta R_0}{R_0} \tag{98}$$

2.   The natural frequency ω of the breathing mode will be given by

$$\omega = \frac{1.11}{\ell} \sqrt{\frac{Et}{\rho R_0}} \tag{99}$$

3.   The half amplitude of the oscillating pressure at the bottom of the cylinder will be given by $p_{o_{osc.}}$

$$p_{o_{osc.}} = 0.79 \, \frac{h_\ell}{\ell}\left(\frac{Et}{R_0}\right) = 0.639 \, h_\ell \omega^2 \ell \rho \tag{100}$$

The pressure at the bottom of the tank will be

$$p_o = p_i - p_v + \rho \ell a + \left(0.639 \, h_\ell \omega^2 \ell \rho\right) \sin \omega t \tag{101}$$

and when $\sin \omega t = -1$

$$p_o = p_i - p_v + \rho \ell a - \left(0.639 \, h_\ell \omega^2 \ell \rho\right) \tag{102}$$

In applying Equation (102) it will be found that p_o will become zero for extremely small values of h and bottom cavitation will appear before surface spray appears for this configuration and mode where no bladder is used. Surface spray would be expected when $a = \omega^2 h$, since this is the peak value of the oscillatory acceleration at the free surface.

The frequency Equation (99) has been used to predict the breathing frequency of a small cylinder tested in a laboratory. The experimental breathing mode frequency was within 5 percent of the computed frequency.

ACOUSTIC MODES

Acoustic excitation, while frequently a threat to critically located airframe skin panels and sensitive equipment, does not appear to be a significant threat to tanks containing fluids. Sound level studies such as are described in References 122 and 123 for missile during take-off, show values from 140 to 168 db. 168 db represents pressure fluctuations of 0.05 psi RMS. While such pressure fluctuation may be felt by the outside of a tank it should be remembered that these pulses will tend to be random in nature and the RMS pressure cannot be multiplied by a tank surface area to obtain an effective force acting on any significant area of the tank.

The RMS pressure level that can be transmitted into the fluid by the impingement of this acoustic excitation on a fluid free surface (assumed for simplicity) depends on the transmission coefficient

$$\alpha_t = \frac{4r}{(r+1)^2} \tag{103}$$

where $r = \dfrac{\rho_2 c_2}{\rho_1 c_1}$, ρ_1 and ρ_2 are the mass densities of air and fluid respectively, while c_1 and c_2 are the speed of sound in air and the fluid, respectively.

Considering water, liquid oxygen and liquid hydrogen as the fluids,

a. water $r = 3490$, $\alpha_t = 0.0011$

b. liquid oxygen $r = 2526$, $\alpha_t = 0.0016$

c. Liquid hydrogen $r = 148$, $\alpha_t = 0.0267$

The sound pressure level of 0.05 psi RMS of air would be attenuated by these factors giving transmitted pressure levels of

a. water   0.000055 psi RMS

b. liquid oxygen   0.000080 psi RMS

c. liquid hydrogen 0.001335 psi RMS

If resonance buildup inside the tank allowed an amplification
factor of 100, the RMS pressures existing within the tank would
be

   a.   water   0.0055 psi RMS

   b.   liquid oxygen   0.0080 psi RMS

   c.   liquid hydrogen   0.1335 psi RMS

Extremely minute local amplitudes of fluid motion will be asso-
ciated with these pressures and acoustic frequencies, and damage
from this source seems extremely improbable.

   Some idea of the upper limit of possible fluid motion may
be obtained by considering the fundamental one-dimensional axial
mode of oscillation in a long cylindrical tank. Here the maximum
amplitude y_o of motion will occur at the longitudinal center of
the tank and will be given by

$$y_o = \frac{p\ell}{2\rho\pi c^2} = \frac{p\ell}{2\pi K} \qquad (104)$$

where p = maximum value of the fluctuating pressure,

   ℓ = tank length,

   ρ = fluid mass density,

   C = speed of sound in the fluid, and

   K = bulk modulus of fluid.

   Missile propulsion liquids with the exception of liquid
hydrogen have bulk modulus values in a range between 10.0×10^6
and 50.0×10^6 lbs/in^2. The limiting value of oscillation
amplitude y_o will be that value which causes the peak value of
fluctuating pressure p in Equations (104) to be equal to p_c

where $p_c = p_i - p_v$

when p_i = total absolute pressure in the fluid

and p_v = fluid vapor pressure

   Amplitudes of oscillation greater than this will result in
fluid cavitation with a resulting damping and nonlinearity that
will limit oscillation amplitude. If a tank 15 feet long were

filled with a fluid with $K = 10.0 \times 10^6$ and was pressurized to 100 psi above the fluid vapor pressure then Equation (104) gives $y_o = .00028$ in. half amplitude. A fluid with a bulk modulus $K = 50 \times 10^6$ would give $y_o = .000056$ in. half amplitude. It seems most improbable that such amplitudes of fluid motion could induce stresses in and part of the tank system that would contribute to a tank failure.

Liquid hydrogen is in a class by itself with a bulk modulus $K = 110,000$ lbs/ft^2 per unit volume. Using this fluid with the foregoing tank conditions gives $y_o = 0.0261$ in. half amplitude. Amplitudes of this size are considered to give this liquid a greater damage potential than would be the case for other liquids.

The foregoing amplitude computations are idealized by assuming that the tank ends are completely rigid and flat reflecting surfaces allowing a plane wave to oscillate along the length of the tank. In practice a more complex situation will exist since the reflecting surfaces will generally be curved and will deflect underload, thus giving the dynamic system additional degrees of freedom and causing some dispersion of the traveling wave. The tank deflections in particular should be taken into account where accurate fluid motion predictions are required.

VIII. RECOMMENDATIONS

During the investigation it was disclosed that there are certain areas that require further work and carry-on effort. Such efforts are presented as recommendations directed toward providing better inputs to the designer, improvement of available analysis methods, studies to establish analysis methods not presently available, experimental verification of analysis methods, and improvement of testing methods and capabilities for simulating operational improvements. The need for work in these general areas is apparent.

1. Methods are required for the analysis of the cumulative degradation of bladders and diaphragms under flexing cycles with application to non-homogeneous or composite materials, including metals and plastics and various mesh screens, or orthotropic construction.

2. It is necessary to define the radiation exposure levels associated with various missions so that a reasonable material selection can be made on the basis of this environment.

3. Permeability test data and procedures on fluids and gases and combinations should be standardized to avoid duplication of effort by numerous organizations. At present data is somewhat of a screening operation that indicates one material is better than another under the same test conditions and procedures. Quantitative values are not susceptible to comparison among various organizations or agency data.

4. Consideration must be given to the performance rating of the device itself.

5. In-space storability of the propellants coupled with insulation requirements and the expulsion device warrants investigations of the complexities that can arise in such combinations.

6. Power or energy requirements for the operation of the devices require coordinated studies between the devices and the various possibilities of power generation and/or availability.

7. It is necessary to design, fabricate, test and demonstrate the working feasibility of a promising system.

8. In the incorporation of the field force principle and the associated magnetic contamination of the propellants, the effects of the contaminants on the propellant characteristics must be studied and tested to provide information on combustion characteristics, specific impulse, compatibility, storage and handling characteristics, etc.

IX. REFERENCES

1. Zwicky, F.: Tasks We Face. Journal of the American Rocket
    Society, No. 84, March 1951, pp 3-20.

2. Vogel, J. M.: A Quasi-Morphological Approach to the Geometry
    of Charges for Solid Propellant Rockets: The Family Tree
    of Charge Designs. Jet Propulsion, Vol. 26, No. 2,
    February 1956, pp 102-105.

3. Zwicky, F.: Morphology and Nomenclature of Jet Engines.
    Aeronautical Engineering Review, Vol. 6, June 1947, pp 20-23.

4. Stuetzer, O. M.: Ion Drag Pumps. J. Appl. Phys., Vol. 31,
    No. 1, January 1960, pp 136-146.

5. Stuetzer, O. M.: Ion Drag Pressure Generation. J. Appl.
    Phys., Vol. 30, No. 7, July 1959, pp 984-994.

6. Stuetzer, O. M.: Ion Transport High Voltage Generator.
    Rev. Sci. Instr., Vol. 32, No. 1, January 1961, pp 16-22.

7. Ernsberger, F. M.: Mechanism of Frictional Electrification
    of Dielectric Liquids. J. Appl. Phys., Vol. 27, No. 4,
    April 1956, pp 418-419.

8. Pohl, H. A.: Some Effects of Nonuniform Fields of Dielectrics.
    J. Appl. Phys., Vol. 29, No. 8, August 1958, pp 1182-1188.

9. Pohl, H. A.: The Motion and Precipitation of Suspensoids in
    Divergent Electric Fields. J. Appl. Phys. Vol. 22, No. 7,
    July 1951, pp 869-871.

10. Pohl, H. A. and Schwar, J. P.: Factors Affecting Separations
    of Suspensions in Nonuniform Electric Fields. J. Appl. Phys.,
    Vol. 30, No. 1, January 1959, pp 69-73.

11. Pierce, E. T.: Effects of High Electric Fields on Dielectric
    Liquids. J. Appl. Phys., Vol. 30, No. 3, March 1959,
    pp 445-446.

12. Middendorf, W. H. and Brown, G. H.: Liquid Dielectrics in
    an Electric Field. Trans. A.I.E.E., Vol.77, Part III,
    "Power Apparatus and Systems," October 1958, pp 795-799.

13. Birks, J. B.: Electrophoretic Deposition of Insulating
    Materials, Progress in Dielectrics, Vol. I, edited by
    Birks, J. G. and Schulman, J.H., Heywood and Company Ltd.,
    London (1959), pp 273-312.

14. Lewis, T. J.: The Electric Strength and High-Field Conductivity of Dielectric Liquids, Progress in Dielectrics, Vol. I, edited by Birks, J. B., and Schulman, J. H., Heywood and Company Ltd., London (1959) pp 90-140.

15. Abraham, M. and Becker, R.: The Classical Theory of Electricity and Magnetism. Second Edition, Hafner Publishing Co., Inc., N. Y., 1949, pp 100-103.

16. Panofsky, W. K. H. and Phillips, M.: Classical Electricity and Magnetism. Addison-Wesley Publishing Co., Inc., Reading, Mass., 1956, pp 100-103.

17. Harnwell, G. P.: Principles of Electricity and Electromagnetism. Second Edition, McGraw-Hill Book Co., Inc., N. Y., Toronto, London, 1949, pp 71-72.

18. Barnes, A. H.: Direct-Current Electromagnetic Pumps. Nucleonics, Vol. 11, No. 1, January 1953, pp 16-21.

19. Cage, J. F., Jr.: Electromagnetic Pumps. Machine Design, Vol. 25, No. 3, March 1953, pp 178.

20. Blake, L. R.: Conduction and Induction Pumps for Liquid Metals. Proceedings of the Institution of Electrical Engineers, Part A, Power Engineering, Vol. 104, 1957, pp 49-67.

21. Barnes, A. H.: Pumping of Liquid Metals. Proceedings of the International Conference on the Peaceful Uses of Atomic Energy, Vol. 9, Reactor Technology and Chemical Processing, United Nations, New York, 1956, pp 259-264.

22. Pumps for Reactor Coolants. Special Report, Nucleonics, Vol. 13, No. 7, July 1955, pp 78.

23. Etherington, H.: Nuclear Engineering Handbook. McGraw-Hill Book Co., N.Y. (1950), Sec. 13, pp 89.

24. Laithwaite, E R.: Prospects for Linear Induction Motors. New Scientist, Vol. 12, No. 255, October 5, 1961, pp 42-45.

25. Chase, W. G. and Moore, H. K.: Exploding Wires. (Based on Conference on the Exploding Wire Phenomenon, April 1959, conducted by Geophysics Research Directorate) Plenum Press, Inc., N. Y. (1959).

26. Carter, A. F., Wood, G. P., Sabol, A. P. and Weinstein, R. H.: Experiments in Steady-State High-Density Plasma Acceleration. Second Symposium on the Engineering Aspects of Magnetohydrodynamics (Sponsored by A.I.E.E., I.A.S. and I.R.E.), March 9 and 10, 1961.

27. Republic Plasma Pinch Engine to Fly in Early '62. Missile and Rockets, Vol. 9, No. 14, October 2, 1961, pp 40-41.

28. Roth, H. L.: Foundation of Electromagnetic Theory. Bell Aerosystems Research Report 9102-920001, December 4, 1961.

29. Radnik, J. L. and Lathan, B. F.: Electromagnetic Projector Study. ASD-TR-61-35, July 1961.

30. Michaelis, L.: Determination of Magnetic Susceptibility. Physical Methods of Organic Chemistry, Vol. I, Part II, edited by Weissberger, A., Interscience Publishers, New York (1949), pp 1885-1926.

31. Kaufmann, A. R.: Magnetic Methods of Analysis. Physical Methods in Chemical Analysis, Vol. II, edited by Berl, W. G., Academic Press Inc., New York (1951), pp 229-254.

32. Anon: Film Chart, Modern Plastics Encyclopedia Issue for 1962, Vol. 39, No. 1-A, September 1961.

33. Anon: Kynar, Vinylidene Fluoride Resin, Bulletin VF2R-61, Pennsalt Chemicals Corp., Philadelphia, Pennsylvania, 1961.

34. Anon: Silastic S-9711, Bulletin No. P-9-303, Dow Corning Corp., Midland, Michigan, January 1958.

35. Riley, M. W.: The Fluoro-Elastomers. Materials in Design Engineering, Vol. 46, No. 1, July 1957.

36. Anon: New Butyl Compound, B496-7, For Use in Nitrogen Tetroxide. Bulletin No. 9, Parker Seal Company, Culver City, California, July 22, 1960.

37. Gardner, A. R.: Heavy Metals Solve Weight Problems. Product Engineering, July 21, 1958.

38. Anon: Rocket Design Data Handbook, 4th Edition. Bell Aerosystems Company, Buffalo, New York, 1961.

39. Anon: Metals Handbook. The American Society for Metals, Metals Park, Novelty, Ohio, 1960.

40. Gardner, A. R.: Willing and Able Exotic Metals Seek Employment. Product Engineering, March 17, 1958.

41. Spieth, E. W. et al: Development of Positive-Expulsion Systems for Cryogenic Fluids - Phase I. AFFTC-TR-60-70, January 1961.

42. Green, J., Levine, N.: Polymer Compatibility in Rocket Fuels and Oxidizers. Reaction Motors Division of Thiokol Chemical Co., 6th Joint Army, Navy, Air Force Conference on Elastomers, October 1960.

43. Baldridge, J. H., Inskeep, M. D.: Research on Rubber Like Materials for Applications Involving Contact with Liquid Rocket Propellants. WADC TR 57-651, Part II, May 1960.

44. Liberto, R. R.: Titan II - Storable Propellant Handbook. AFFTC-TR61-32, 1961.

45. Ault, G. R.: Screening of Twenty Elastomers for Compatibility in Nitrogen Tetroxide. Report MN-146, Research and Development Dept., Aerojet General Corp., Sacramento, California, October 1958.

46. Tomlinson, E. M.: Development of Elastomers for Use with Nitrogen Tetroxide Rocket Systems. Report No. 8160-03M-8, Aerojet General Corp., Sacramento, California, March 1960.

47. Foertter, L. I.: Materials for Use in Contact With Mixed Oxides of Nitrogen (MON) of 10% NO (Nitric Oxide) Content in Model 8101. Inter-Office Memo 964:60:0906-1:LIF, Bell Aerosystems Company, Buffalo, New York, September 1960.

48. Anon: Compatibility of Rocket Propellants With Materials of Construction. DMIC Memorandum 65, Defense Metals Information Center, Battelle Memorial Institute, Columbus, Ohio, September 1960.

49. Anon: Performance and Properties of Liquid Propellants. Brochure (no number), Aerojet General Corp., Sacramento, California, March 1961.

50. Anon: Nitrogen Tetroxide. Product Bulletin, Nitrogen Division, Allied Chemical Co., New York, New York, 1961.

51. Judge, J. F.: OF$_2$-Promising As Space-Storable Fuel. Missiles and Rockets, Volume 9, No. 24, December 11, 1961.

52. Lee, D. H.: A Survey of the Compatibility of Various Materials With Hydrazine and Mixtures of Hydrazine, Hydrazine Nitrate, and Water. Memo 20-152, Jet Propulsion Laboratories, Los Angeles, California, December 1957.

53. Baldridge, J. H.: Resistance of Elastomers and Plastics to Rocket Propellants: A Survey. WADC-TR57-472, August 1957.

54. Anon: ASTM Procedure D1434-58, Gas Transmission Rate of Plastic Sheeting.

55. Cartwright, L. C.: Measurement of the Gas Permeability of
       Sheet Materials. Analytical Chemistry, June 1947, pp 393.

56. Van Amerongen, G. J.: Influence of Structure of Elastomers
       on Their Permeability to Gases. Journal of Polymer Science,
       Vol. V, No. 3, pp 307-332.

57. Norton, F. J.: Permeation Problems in High Vacuum. 1954
       Vacuum Symposium Transactions.

58. Pinsky, J. et al.: Investigation of the Shelf Life of
       Liquids in Polyethylene Bottles. WADC TR 53-133.

59. Rogers, C. E., Stannett, V., and Szwarc, M.: The Sorption,
       Diffusion, and Permeation of Organic Vapors in Polyethylene,
       Journal of Polymer Science, Vol. XLV, pp 61-82 (1960).

60. Binning, R. C. et al.: Separation of Liquid Mixtures by
       Permeation. Ind. and Engrg. Chem., Vol. 53, No. 1, pp 45-50
       (Jan. 1961).

61. Perry: Chemical Engineer's Handbook. 3rd Ed., McGraw Hill
       Publishing Co.

62. General Environmental Specification for Agena Satellite
       Program. Lockheed Aircraft Corp. Report No. LMSD6117B,
       July 1, 1960.

63. Space Environmental Criteria for Aerospace Vehicles. USAF
       Specification Bulletin No. 523, 28 Nov. 1960.

64. Mayer, Ramona, Broadway, N. J., and Palinchak, S.: The
       Effect of Nuclear Radiation on Silicone Elastomeric and
       Plastic Materials. REIC R9, Battelle Memorial Institute,
       October 15, 1959.

65. Javitz, A. E.: Cryogenics-Environment, Phenomena, Applica-
       tions. Part I. Electro-Technology, Vol. 68, No. 3,
       September 1961.

66. McClintock, R. M. and Gibbons, H. P.: Mechanical Properties
       of Structural Materials at Low Temperatures. A Compilation
       from the Literature, U. S. Department of Commerce, National
       Bureau of Standards, Monograph 13, June 1, 1960.

67. Durham, T. F., McClintock, R. M., and Reed, R. P.: Cryogenic
       Materials Data Handbook. U. S. Department of Commerce,
       National Bureau of Standards, PB 171 809.

68. Watson, J. F., Christian, J. L., and Hertz, J.: Cryogenics-
       Selection Data for Structural Materials. Electro-Technology,
       Vol. 68, No. 5, November 1961.

69. Geophysics Research Directorate 1959, Abbreviated English Tables of Model ARDC Atmosphere.

70. Dushman, S.: Vacuum Techniques. John Wiley and Sons, Inc., (1949).

71. Winkler, J. R.: Non-Relativistic Protons From Solar Flares, Symposium on Upper Atmosphere Solar Relations, Chicago, Illinois, December 23, 1959, American Association for the Advancement of Science.

72. Ney, E. P. and Winkler, J. R.: High Altitude Cosmic-Ray Measurements During the International Geophysical Year, Geophysical Monograph No. 2, American Geophysical Union, Washington, D. C., July 1958.

73. Meyer, P., Parker, E. N., and Simpson, J. A.: Solar Cosmic Rays of February 1956 and Their Propagation Through Interplanetary Space, Physical Review, Vol. 104, 1956.

74. Winkler, J. R.: Cosmic-Ray Increase at High Altitude on February 23, 1956, Physical Review, Vol. 104, 1956.

75. Anderson, K. A.: Solar Particles and Cosmic Rays. Scientific American, June 1960, pp 64-71.

76. Van Allen, J. A., and Frank, L. A.: Survey of Radiation Around the Earth to a Radial Distance of 107,400 Kilometers. Report SUI-59-2, State University of Iowa, Iowa City, January 1959.

77. IGY Satellite Report No. 11, June 1960, National Academy of Sciences, National Research Council, Washington 25, D. C.

78. Van Allen, J. A.: On the Radiation Hazards of Space Flight. Report SUI-59-7, State University of Iowa, Iowa City, May 1959.

79. Freden, S. C. and White, R. S.: Protons in the Earth's Magnetic Field. Physical Review, Vol. 3, 1959, pp 9-11.

80. General Environment Spec. for Agena Satellite Programs. LMSD Report No. 6117B, 17 August 1960.

81. Space Environmental Criteria for Aerospace Vehicles. USAF Spec Bulletin No. 523, 28 November 1960.

82. Robinson, J. V.: Particle Radiation at 2000 Nautical Miles Altitude. Bell Inter-Office Memo 966:60:0115-1, 15 January 1960.

83. Proposal to Assess the Long Term Effects of Proton and
     Electron Irradiation of Infrared Detectors Currently Used
     in Near Space Applications. Bell Report No. D9119-953001,
     January 1962.

84. Meredith, L. H. Gottlieb, H. B. and Van Allen, J. A.: Direct
     Detection of Soft Radiation Above 50 KM in the Auroral
     Zone. Physical Review, Vol. 97, pp 201-205, 1955.

85. Van Allen, J. A.: Direct Detection of Auroral Radiation
     with Rocket Equipment. Proceedings of the National Academy
     of Sciences, Vol. 43, pp 57-92, 1957.

86. Kornhauser, M.: Current Estimates of the Effects of
     Meteorites on the Skin of a Satellite Vehicle. Advanced
     Space Vehicle Engineering Memo, General Electric, MSVD.

87. Anon: Liquid Propellant Losses During Space Flight.
     Report No. 63270-00-003, Arthur D. Little, Inc., November
     1961.

88. Jensen, Niels: Vapor Pressure of Plastic Materials. Journal
     of Applied Physics, 27-12 p. 1460.

89. Hoffman, O. and Sacks, G.: Introduction to the Theory of
     Plasticity for Engineers. McGraw-Hill Book Company, Inc.,
     New York, 1953, pp 266-272.

90. Hill, R.: The Mathematical Theory of Plasticity. Oxford
     University Press, New York, 1950.

91. Lubahn, J. D. and Sacks, G.: Bending of an Ideal Plastic
     Metal. Trans. ASME, Vol. 72, pp 201-208, 1950.

92. Shaffer, B. W. and Ungar, E. E.: Mechanics of the Sheet-
     Bending Process. Journal of Applied Mechanics, Vol. 27,
     March 1960, pp 34-40.

93. Schroeder, W.: Mechanics of Sheet-Metal Bending. Trans.
     ASME Vol. 65, 1943, pp 817-827.

94. Gerard, G.: Effect of Bend Width Upon Minimum Bend Radii.
     Journal of Aero. Sci., Vol. 13, 1946, pp 161-170.

95. Swift, H. W.: Plastic Bending Under Tension. Engineering
     Vol. 166, October 1948, pp 333-335.

96. Sachs, G.: Fundamentals of the Working of Metals. Pergamon
     Press, Ltd., 1954.

97. Coffin, L. F. Jr.: A Study of the Effects of Cyclic Thermal
     Stresses on a Ductile Metal. Transactions, Am. Soc. of
     Mech. Engr., Vol. 76, 1959, pp 931.

98. Coffin, L. F. Jr.: The Problem of Thermal Stress Fatigue in Austenitic Steels at Elevated Temperatures. ASTM Special Tech. Pub. No. 165, June 1954.

99. Padlog, J. and Rattinger, I.: Low-Cycle Fatigue Strength of Pressurized Components. ASTM Special Tech. Pub. No. 274, June 1960, pp 65-77.

100. Padlog, J. and Schnitt, A.: A Study of Creep, Creep-Fatigue and Thermal-Stress-Fatigue in Airframe Subject to Aerodynamic Heating. WADC TR 58-294, July 1958.

101. Millar, G. L.: Tantalum and Niobium. Academic Press, Inc., 1959.

102. Metals Handbook, ASM, Vol. 1, 1961.

103. Voorhees, H. R., and Freeman, J. W.: Aluminum and Magnesium Alloys. ASTM, STP No. 191, 1960.

104. Sokolnikoff, I. S., and Sokolnikoff, E. S.: Higher Mathematics for Engineers and Physicists. McGraw-Hill Book Company, Inc., New York, 1941, pp 227.

105. Matheny, J. D.: Bellows Spring Rate for Seven Typical Convolution Shapes. Machine Design, Vol. 34, No. 1, January 4, 1962, pp 137-139.

106. Krivetsky, A.: Section Properties of Shapes Bounded in Part by Circular Arcs. Report No. 9010-18-002, Bell Aircraft Corp., October 2, 1957.

107. Nadai, A.: Plasticity. McGraw-Hill Book Co., Inc., New York, 1931.

108. DeBruyne, N. A. and R. Hauwink, R.: Adhesion and Adhesives. Elsevier Publishing Company, New York, 1951.

109. Anon: Bonded Aircraft Structures. CIB (A.R.L.) Limited, Duxford, Cambridge, 1957.

110. Lund, R. F. and Provenzano, J.: Bell Aerosystems Engineering Laboratory Report BLR 52-38, 10 June 1952.

111. Anon: Tentative Method for Climbing Drum Peel Test for Adhesives. ASTM D1781-60T, 1960.

112. Timoshenko, S.: Theory of Elastic Stability. McGraw-Book Company, First Edition, 1936.

113. Sturns, R. G.: A Study of the Collapsing Pressure of Thin-Walled Cylinders. University of Illinois, Eng. Exp. Station, Bulletin No. 329, 1941.

114. Bijlaard, P.P.: Buckling Under External Pressure of Cylindrical Shells Evenly Stiffened by Rings Only. Bell Aircraft Corporation Report No. 02-941-002, April 1954.

115. von Karman, T. and Tsien, H. S.: The Buckling of Spherical Shells by External Pressure. Journal of the Aeronautical Sciences, Vol. 7, No. 2, December 1939, pp 43-50.

116. Robbins, W. H.: Analysis of the Transient Radiation Heat Transfer of an Uncooled Rocket Engine Operating Outside Earth's Atmosphere. NASA TND-62, December 1959.

117. Runyan, H. L. and Rainez, A. G.: Launch Vehicle Dynamics. NASA TM X-607 (Classified Document, Title Unclassified).

118. Cooper, R. M.: Dynamics of Liquids in Moving Containers. ARS Journal, August 1960, pp 725-729.

119. Abramson, H. N. and Ransleben, G. E.: Simulation of Fuel Sloshing Characteristics in Missile Tanks by Use of Small Models. ARS Journal, July 1960.

120. Landorff, P. E.: Principles of Design of Dynamically Similar Models for Huge Propellant Tanks. NASA TN D-99.

121. McCarty, J. L. and Stephens, D. G.: Investigation of the Natural Frequencies of Fluids in Spherical and Cylindrical Tanks. NASA TN D-252.

122. Tedrick, R. N. and Dorland, W. D.: Anticipated RMS Sound Levels Around Static Tests of Large Vehicles. NASA Marshall Space Flight Center, MTP-Test-61-60.

123. Mayes, W. H. and Milton, D. A.: In-Flight Noise Measurements for Three Project Mercury Vehicles. NASA TN D-997.

124. Goldsmith, A., Watermann, T. E. and Hirschhorn, H. J.: Thermophysical Properties of Solid Materials, Vol. 1, Elements. Armour Research Foundation, WADC TR 58-476, Revised Edition, August 1960.

125. Anon: Haynes Alloy No. 25. Haynes Stellite Company, Div. of Union Carbide Corporation, Kokomo, Indiana. Publication, September 1960.

126. Fieldhouse, I. B., Lang, J. I. and Blau, H. H., Jr.: Investigation of Feasibility of Utilizing Available Heat-Resistant Materials for Hypersonic Leading Edge Applications, Vol. IV, Thermal Properties of Molybdenum Alloy & Graphite. Armour Research Division and Arthur D. Little, Inc., WADC TR 59-744, July 1960.

APPENDIX A

GLOSSARY

In the preparation of the report and due to the numerous subject areas involved, it was deemed advisable to present a short table of definitions of the various terms employed. Terms not clarified within the text are defined on the following pages of the subject Appendix A.

ALPHA PARTICLES

Helium nuclei containing two neutrons and two protons. They have great ionizing power but very little penetrating power and are dangerous to living tissues. They are emitted during radioactive disintegration, have a mass number 4 and atomic number 2. They are thus identical with nuclei of ordinary helium atoms.

BETA PARTICLES (beta rays)

High speed electrons, positive or negative, emitted during radioactive disintegration. They travel several feet in air and are dangerous to living tissues.

BEV

Billion electron volts. An amount of energy equal to 1.6×10^{-3} ergs.

CONTAMINATION (radioactive)

Deposition of radioactive material in any place where it is not desired, and particularly in any place where its presence can be harmful. The harm may be in vitiating the validity of an experiment or a procedure, or in actually being a source of danger to persons.

DIAMAGNETIC SUBSTANCE

A substance whose susceptibility is negative. It is repelled when placed near a magnetic field.

DIELECTRIC

A substance through which an electrical current cannot pass. (Electrical conductivity is zero: non-conductor or insulator).

DOSE

The quantity of radiation delivered to a specified mass or volume. Dose units are: the roentgen (r) for gamma rays, the rad for gamma and beta rays. In radiology the dose may be specified in air, on the skin, or at some depth beneath its surface; no statement of dose is complete without specification of location at which the dose is considered. Unless otherwise specified, usually dose refers to the dose in air, measured without backscatter.

DOSE RATE

Dose per unit time.

EFFICIENCY

Expulsion Efficiency is defined as:

$$\eta_\epsilon = \frac{\text{Loadable Propellant Weight - Residual Propellant Wt.}}{\text{Loadable Propellant Weight}}$$

Volumetric Efficiency is expressed as:

$$\eta_v = \frac{\text{Total Tank Volume - Usable Volume with Device}}{\text{Total Tank Volume}}$$

ELECTROSTATIC DEVICE

A device that utilizes Coulomb's forces or a device that employs an electric field to displace a charged body.

EV.

Electron volt. An amount of energy equal to 1.6×10^{-12} ergs.

GAMMA RAYS

Electromagnetic radiation of short wavelength and correspondingly high frequency, emitted by nuclei in the course of radioactive decay. They have tremendous penetrating power and are dangerous to living tissues.

MEV

Million electron volts. An amount of energy equal to 1.6×10^{-6} ergs.

NEUTRONS

Electrically neutral components of atomic nuclei. Neutron radiation is highly penetrating. Free-neutrons are often classified according to their speed or temperature, as thermal, slow, intermediate, and fast.

PARAMAGNETIC SUBSTANCE

A substance whose magnetic susceptibility is positive but small. -

PRESSURE DROP

Pressure drop is defined as the loss in pressure from the tank pressurization inlet to the propellant outlet. This pressure drop occurs as a result of the work required to expel the fluid.

PROTON

The nucleus of ordinary light hydrogen and a constituent of all nuclei.

RAD

The unit of absorbed dose, which is 100 ergs/g. The rad is a measure of the energy imparted to matter by ionizing particles per unit mass of irradiated material at the place of interest. It is a unit that was recommended and adopted by the International Commission on Radiological Units at the Seventh International Congress of Radiology, Copenhagen, July 1953.

RADIATION

Energy propogated through space. As commonly employed in radiology, the term refers to two kinds of ionizing radiation: (1) Electromagnetic waves (X-rays, gamma-rays), and (2) corpuscular emissions from radioactive substances or other sources (alpha and beta particles, etc.).

Primary Radiation. Radiation coming directly from the source, including useful beam (that part of the primary radiation that passes through the aperture or collimator of the radiation source enclosure) and Leakage (Direct) Radiation (all radiation coming from the source, except the useful beam).

Scattered Radiation. Radiation that, during passage through material, has been deviated in direction and usually has also had its energy diminished.

Secondary Radiation. Radiation emitted by any irradiated material.

Stray Radiation. Radiation not serving any useful purpose; includes leakage and scattered radiation.

RADIOACTIVITY

Disintegration of unstable atomic nuclei by the emission of radiation with a definite half-life.

RHM

Roentgens per hour at one meter.

ROENTGEN (r)

The quantity of X- or gamma radiation such that the associated corpuscular emission per 0.001293 g of air produces, in air, ions carrying 1 esu of quantity of electricity of either sign.

SPECIFIC WEIGHT RATIO

The specific weight ratio can be represented as

$$R_W = \frac{\text{Tank Weight with Device - Weight of Device}}{\text{Tank Weight with Device Installed}}$$

The numerator corresponds to the weight of the propellant tank with all elements of the expulsion device removed and tank structure added as required to preserve required propellant storage capability.

SPRING RATE

A theoretical number describing the ratio of applied load to the resultant deflection and is usually expressed in lb/in. A 10 pound load that moves a bellows 0.20 inches will establish the spring rate as 10/.2 = 50 lb/in.

ULLAGE

This represents the volume above the free surface of the fluid.

APPENDIX B

VOLUME AND WEIGHT CHARACTERISTICS OF PRESSURE VESSELS

INTRODUCTION

Pressure vessels or containers constitute an appreciable portion of the structure of a space vehicle configuration, and for most of the positive expulsion devices presented herein, the structural enclosure for the device is a pressure vessel. In the design of such pressure vessels, certain simplifying assumptions can be introduced in the analytical approach, especially in the weight characteristics, that do not materially affect the desired result and at the same time provides a powerful tool for preliminary design estimation purposes. Weight penalties involved in shapes other than a sphere, weight-volume ratios, etc., are such useful design information.

This Appendix B includes condensed versions of the development of the required volume and weight equations of pressure vessels and the graphical representation of these equations for direct application in design. The work has been categorized into two parts: (1) Volume of pressure vessels and (2) Weight characteristics of pressure vessels.

The shapes of configurations that have been considered include:

(a) An ellipsoidally-capped cylinder
(b) A biconvex spherical cap vessel
(c) A two-radii contour configuration.

For the two-radii contour configuration, the volume characteristics only have been presented. Due to the positive and negative Gaussian curvature that is a characteristic of this configuration, the latter curvature regime introduces a considerable amount of bending in the shell. It became quite obvious, from the weight standpoint, that the alleviation of these bending stresses by the use of increased shell thickness in the negative Guassian curvature region would restrict its application. The establishment of a weight equation, neglecting these bending stresses, would introduce too great an error for general application.

VOLUMES OF PRESSURE VESSELS

In the determination of the volumes of pressure vessels or containers that constitute a configuration of an expulsion device, the mathematical expressions for the various shapes have been

transformed into graphical representation for convenient use. A condensed version of the development of these volume equations is given on the following pages.

Ellipsoidally-Capped Cylinder

The volume of an ellipsoidally-capped cylinder, see Figure B-1, is given by

$$V_t = \frac{4}{3} \pi a^3 \left(\frac{1}{K}\right) + 2 \pi a^3 \left(\frac{L}{D} - \frac{1}{K}\right) \tag{B1}$$

where the first term represents the volume of the two ellipsoidal caps or ellipsoid of revolution and the second term represents the volume of the straight circular cylinder portion of the tank.

With the aid of some geometric relationships and algebraic manipulations, the above volume equation reduces to

$$V_t = K_v (\pi a^2 L) \tag{B2}$$

where

$$K_v = 1 - \frac{\left(\frac{1}{3} K\right)}{\left(L/D\right)} \tag{B3}$$

The volume coefficient, K_v, is plotted on Figure B-3. This coefficient also represents the volume ratio of an ellipsoidally-capped cylinder of a given length to that of a right-circular cylinder of the same length and radius. The lower limit of the K_v curve is the sphere.

Biconvex Spherical-Cap Configuration

The volume of a biconvex spherical-cap configuration, as illustrated in Figure B-2, is given by the expression,

$$V = K_{vb} (\pi a^2 L) \tag{B4}$$

where

$$K_{vb} = \frac{1}{2} \left[\frac{1}{3} \left(\frac{L}{D}\right)^2 + 1 \right] \tag{B5}$$

The volume expression can be obtained from any handbook reference and the expression has been rearranged into terms defined on Figure B-2.
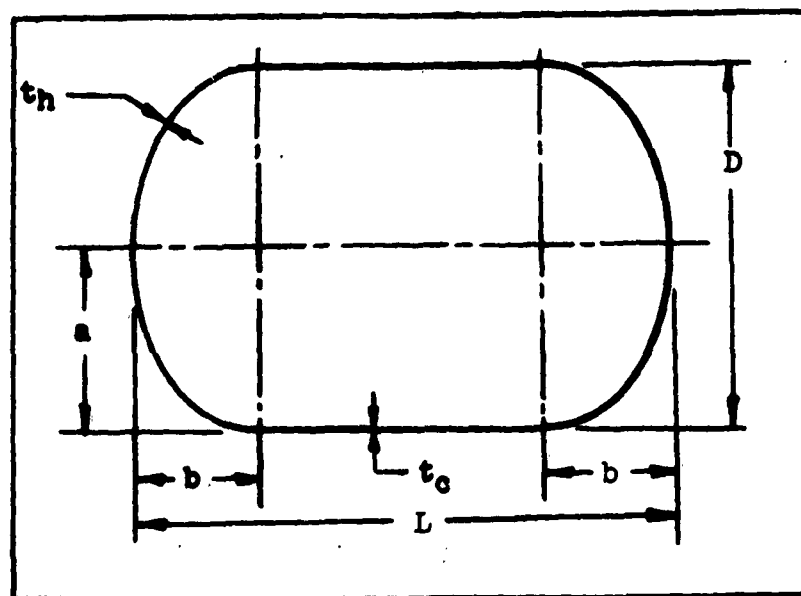
FIGURE B1   ELLIPSOIDALLY-CAPPED CYLINDER
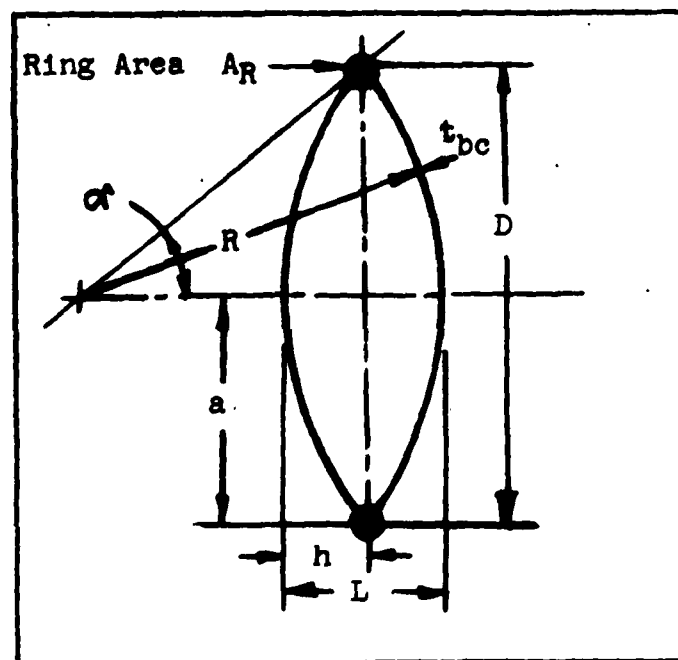
FIGURE B2   BICONVEX SPHERICAL CAP VESSEL

Figure 2. Design coefficients for rectangular cross sections

BELL AEROSYSTEMS COMPANY
DIVISION OF BELL AEROSPACE CORPORATION
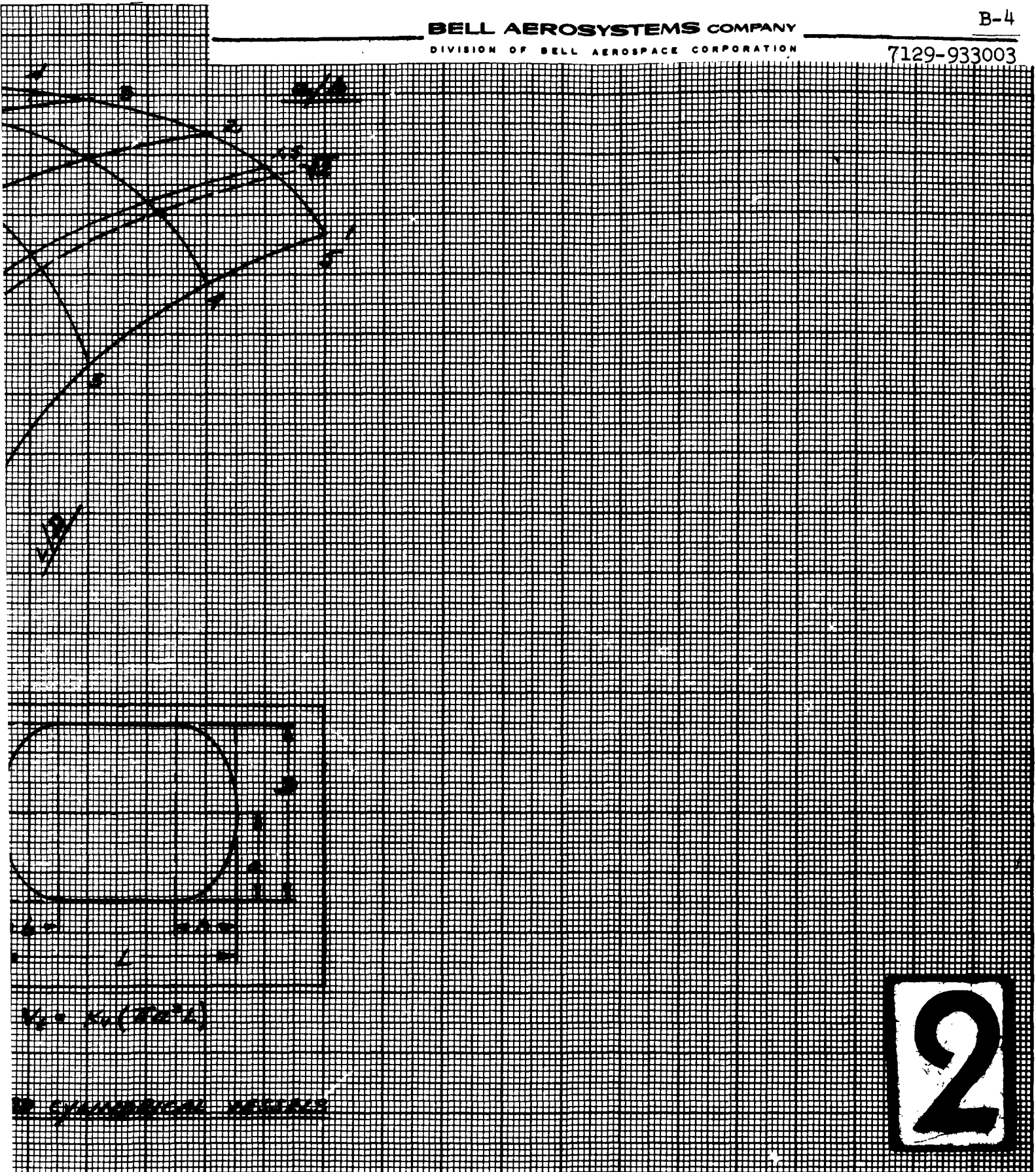
The volume coefficient K_{vb} is plotted on Figure B-4. The upper limit of the biconvex section is a sphere, when $L/D = 1$. For the biconvex configuration L/D is less than one.

Here again the volume coefficient K_{vb} can be interpreted as the ratio of the biconvex configuration volume to that of a right-circular cylinder of the same length L and radius, a.

Two-Radii Contour

The two-radii contour, which can be employed as a container for a diaphragm-type expulsion device, is depicted in Figure B-5. In the determination of the volume for such configurations, use is made of the Pappus Theorm and the notation and geometric relationships indicated in Figure B-6. In the application of the Pappus Rule, the indicated plane area is segmented into three sections: (a) The triangle OLQ, (b) The circular segment, LMN, and (c) The circular segment, NPQ. The subtraction of the latter plane area from the former two values produces the required area for the two-radii-contour figure.

The total volume for the surface of revolution can be shown to be:

$$V = 2 \left\{ \frac{2\pi a^2 y}{6} + 2\pi \left(\frac{2}{3}\right) R_1^3 \sin^4\left(\alpha/2\right) \right.$$

$$\left. - 2\pi \left[\frac{R_2^2 a}{2} \left(\alpha - \sin\alpha\right) - \frac{2}{3} R_2^3 \sin^4\left(\alpha/2\right) \right] \right\} \qquad \text{(B6)}$$

With the use of appropriate geometric relationships and algebraic manipulation, the volume for a two-radii-contour reduces to

$$V = K_{VTR} \left(\pi a^2 L\right) \qquad \text{(B7)}$$

where

$$K_{VTR} = 2 \left[\frac{1}{6} + \frac{1}{6} \left(\frac{1}{1+\cos\alpha}\right)\left(1 - 3z + 3z^2\right) - \frac{1}{2}(1-z)^2 \frac{\alpha - \sin\alpha}{\sin\alpha(1-\cos\alpha)} \right] \qquad \text{(B8)}$$

This volume coefficient is represented graphically on Figure B-7. A more detailed derivation of the volume equation for a two-radii contour vessel can be found in Reference B1.

The volume coefficient K_{VTR} has been presented in such a manner that it can be defined as the ratio of the volume of the two-radii-contour to that of right-circular cylinder of the same length L and radius a.
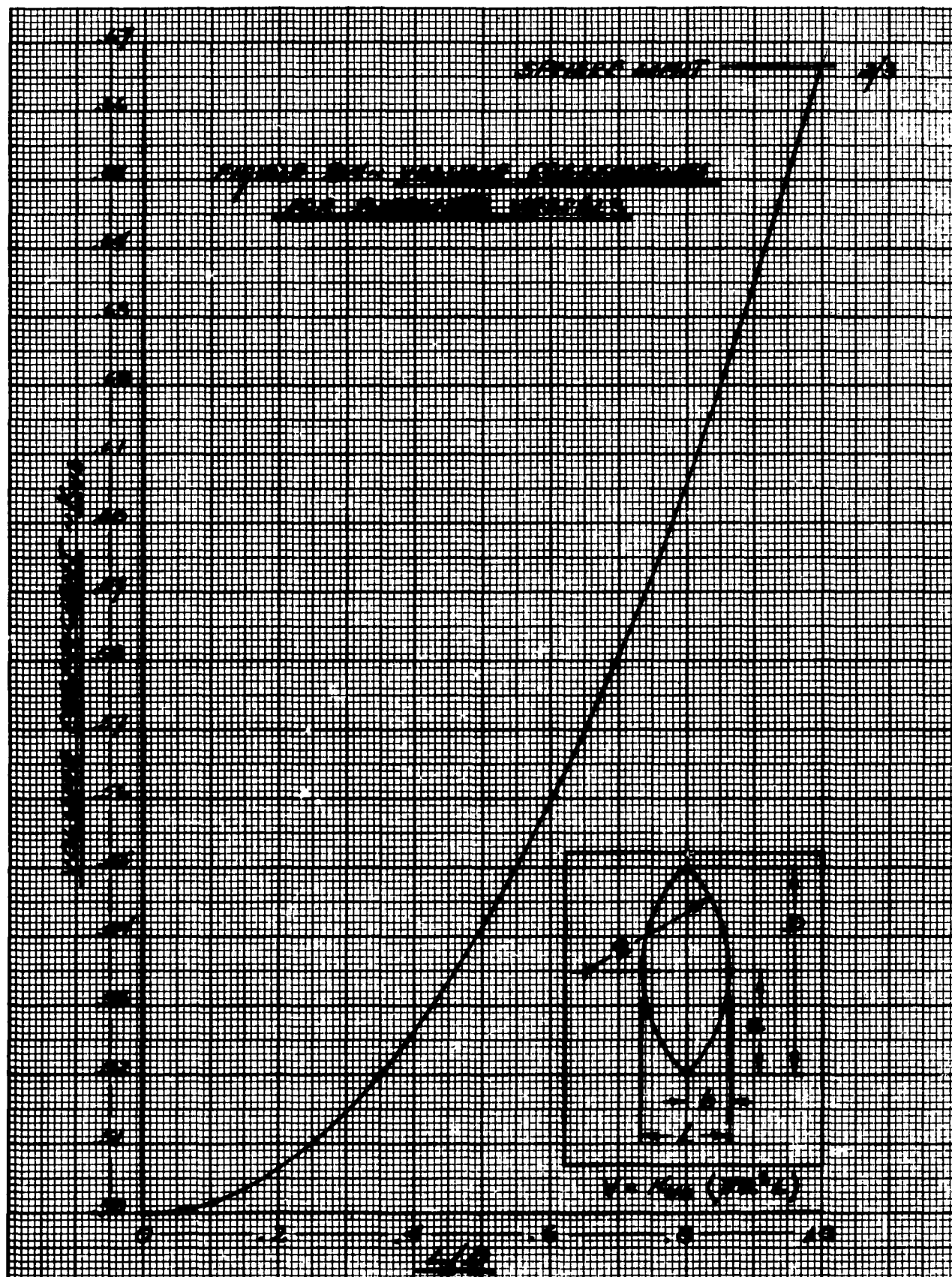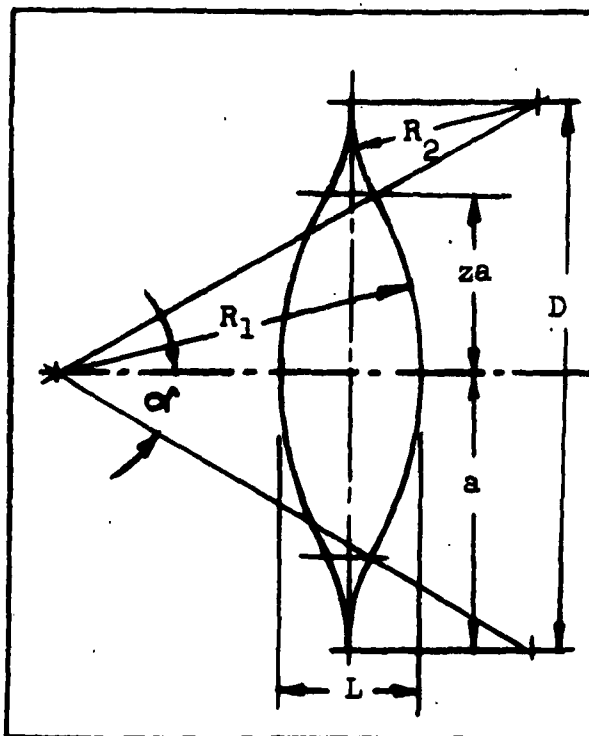
FIGURE B5 TWO-RADII CONTOUR VESSEL

$$z = R_1/(R_1 + R_2)$$
$$y/a = \sin\alpha/(1 + \cos\alpha)$$
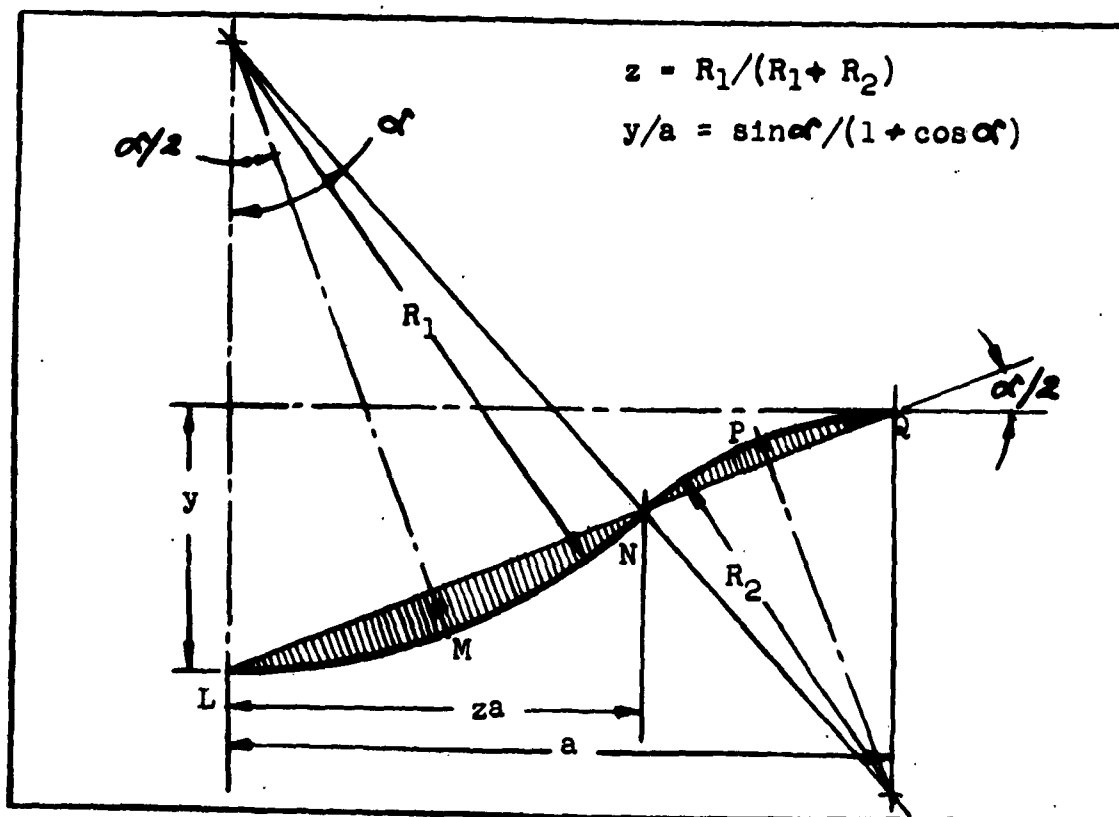
FIGURE B6 TWO-RADII CONTOUR VESSEL NOTATION
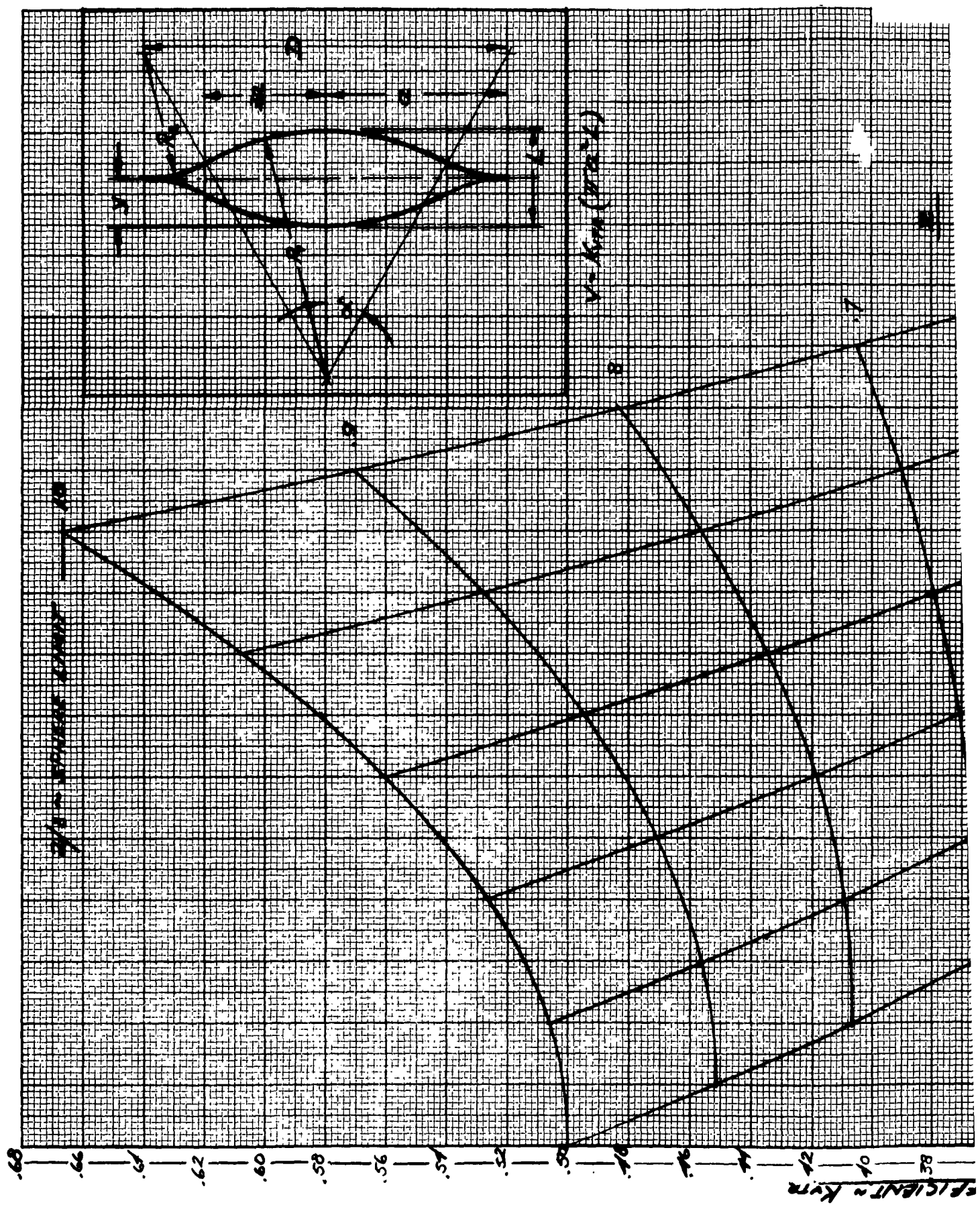
BELL AEROSYSTEMS COMPANY
DIVISION OF BELL AEROSPACE CORPORATION
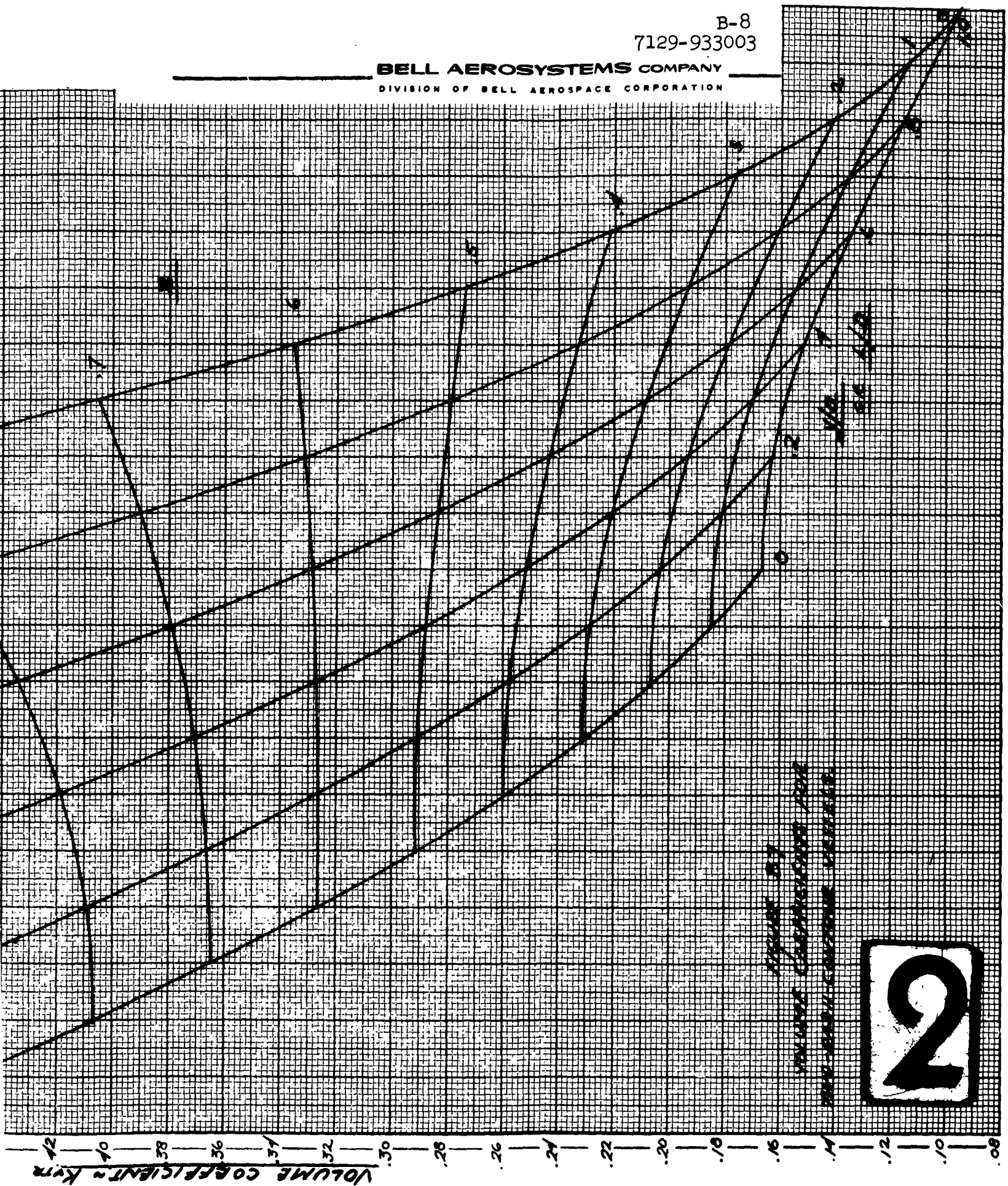
VOLUME COEFFICIENT ~ kv/k

It is interesting to note the shapes of the cross-section of the surface of revolution when certain limits or values are imposed on the R_1 and R_2 values and on z.

When $z = 1$ and $R_2 = 0$, the resulting cross-section of the surface of revolution is a biconvex configuration ($R_1 < y$).

When $z = 1$ and $R_1 = a = L/2 = y$, a sphere is obtained ($R_2 = 0$).

When $z = 0$ and $R_1 = 0$, the cross-section resembles an evolute of ellipse shape.

When $z = 0$ and $R_2 = a = L/2 = y$, a double symmetric cross-section resembling a hypocycloid of four cusps or astroid if produced ($R_1 = 0$).

WEIGHT CHARACTERISTICS OF PRESSURE VESSELS

Ellipsoidally-Capped Vessels

Many concepts of positive expulsion devices require a structural container or pressure vessel to sustain the pressure involved and to contain elements of the device. Cylindrical pressure vessels with ellipsoidal caps or heads are usually employed. Ellipsoidal caps are utilized more frequently because of the space advantage they have over those that incorporate hemispherical caps.

For certain ranges of geometry, the ellipsoidal cap has a drawback because compressive hoop or membrane stresses are generated in portions of the cap when under a uniform internal pressure. These compressive stresses occur over a small area of the ellipsoidal cap within the region of the head-to-cylinder joint. However, for ellipsoidal heads whose ratio of $a/b < \sqrt{2}$, the membrane stresses due to uniform pressure are always positive.

A collection of relationships is presented on the following pages that makes it a relatively simple matter to establish the preliminary structural size of a pressure vessel. The derivation of the equations and the resulting graphs are based on the following assumptions:

(1) The hoop stress in the cylindrical portion of the vessel is based on membrane theory and constant wall thickness.

(2) The ellipsoidal cap thickness is assumed constant and based upon the maximum stress at the center of the head.

(3) Local bending or discontinuity stresses are not considered.

The surface area of an ellipsoidal cap is given by, (See Reference B2),

$$A_c = 2\pi a^2 + \frac{\pi b^2}{e} \, \ell_n \left(\frac{1+e}{1-e} \right) \tag{B9}$$

For a constant thickness ellipsoidal cap, the above equation can be modified so that the weight of such a cap at both ends of a cylinder gives

$$W_{he} = \pi a^2 \rho t_h \left\{ 2 + \frac{1}{K(K^2-1)^{1/2}} \, \ell_n \left[\frac{K + (K^2-1)^{1/2}}{K - (K^2-1)^{1/2}} \right] \right\} \tag{B10}$$

where

ρ = density of the structural head material

t_h = thickness of head

If the ellipsoidal heads are incorporated in conjunction with a right-circular cylinder (see Figure B-1) it can be shown that the total weight of the container is

$$W_{te} = \pi a^2 \rho t_h \left\{ 2 + \frac{1}{K(K^2-1)^{1/2}} \, \ell_n \left[\frac{K + (K^2-1)^{1/2}}{K - (K^2-1)^{1/2}} \right] + 4 \left(\frac{t_c}{t_h} \right) \left(\frac{L}{D} - \frac{1}{K} \right) \right\} \tag{B11}$$

Although a cylindrical pressure vessel is always heavier than a spherical one of equal volume, subjected to the same internal pressure, it is interesting to note the influence of L/D and cap shape on the ratio of their weights. The ratio of weights of an ellipsoidally-capped cylinder to that of a sphere is:

$$\frac{W_{te}}{W_s} = \frac{1}{2} \left[\frac{1}{3\left(\frac{L}{D}\right) + \frac{1}{K}} \right] \left\{ 8 \left(\frac{L}{D} - \frac{1}{K} \right) + K \left[2 \cdot \frac{1}{K(K^2+1)^{1/2}} \, \ell_n \left(\frac{K + (K^2-1)^{1/2}}{K - (K^2+1)^{1/2}} \right) \right] \right\} \tag{B12}$$

The detailed derivation of Equation B12 is given in Reference B4 and the numerical values of this equation are plotted in carpet form in Figure B-8. This curve actually represents the weight penalty involved in the use of an ellipsoidally-capped container. It should be noted that regardless of the head shape considered, a limiting value of $4/3$ is approached when the L/D is increased and approaches infinity.

Another useful ratio for the design of pressure vessels or containers is the weight-volume ratio. The weight-volume ratio is a function of stress or material employed and on the basis of membrane stresses (Reference B3) given by
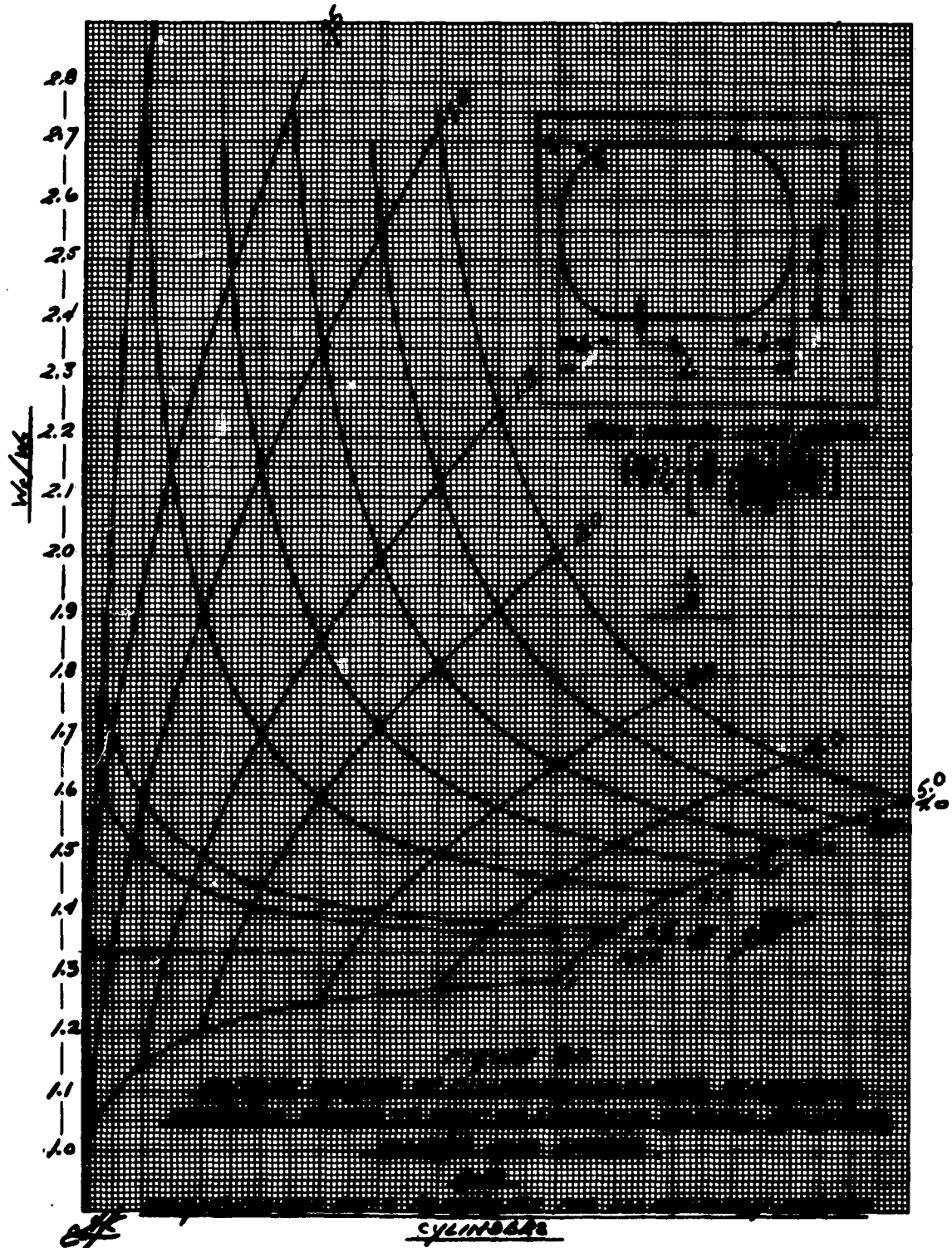
$$t_h = \rho a K / 2\sigma$$
$$t_c = \rho a / \sigma \tag{B13}$$

The desired expression is

$$\left(\frac{W}{V}\right)_{te} = \frac{1}{2}\frac{\rho}{\left(\frac{\sigma}{\rho}\right)}\left\{ \frac{B\left(\frac{b}{D}-\frac{1}{K}\right)+ K\left\{2+\frac{1}{K(K^2-1)^{1/2}}\ln\left[\frac{K+(K^2-1)^{1/2}}{K-(K^2-1)^{1/2}}\right]\right\}}{\frac{2}{3}\left[3\left(\frac{b}{D}\right)-\frac{1}{K}\right]} \right\} \tag{B14}$$

This $(W/V)_{te}$ expression is 1.5 $\rho/(\sigma/\rho)$ times the W_{te}/W_s expression whose plot is shown in Figure B8. As a result

$$\left(\frac{W}{V}\right)_{te} = 1.5\frac{\rho}{\left(\frac{\sigma}{\rho}\right)}\left(\frac{W_{te}}{W_s}\right) \tag{B15}$$

The minimum value of $(W/V)_{te}$ is obtained when the vessel is a sphere which results in the expression

$$\left(\frac{W}{V}\right)_{te} = 1.5\frac{\rho}{\left(\frac{\sigma}{\rho}\right)} \tag{B16}$$

For an infinite length cylinder, W_{te}/W_s approaches $4/3$ (See Figure B-8) and the familiar expression

$$\left(\frac{W}{V}\right)_{te} = 2.0\frac{\rho}{\left(\frac{\sigma}{\rho}\right)} \tag{B17}$$

is obtained.

With the aid of Equation B11 and employing the material thicknesses required by Equations B13, the weight of an ellipsoidally-capped pressure vessel can be obtained. Thus,

$$W_{te} = C_{we}\left(\pi a^3\right)\frac{\rho}{\left(\frac{\sigma}{\rho}\right)}$$

where

$$C_{we} = \frac{K}{2}\left\{2+\frac{1}{K(K^2-1)^{1/2}}\ln\left[\frac{K+(K^2-1)^{1/2}}{K-(K^2-1)^{1/2}}\right]+\frac{8}{K}\left(\frac{b}{D}-\frac{1}{K}\right)\right\} \tag{B18}$$

The values of the weight coefficient, C_{we}, are plotted on Figure B-9. The lowest points on the curve, indicated by the dashed line, represent the weights of the ellipsoidal caps only. This is also the minimum L/D values for such tank configurations, ellipsoids.

The total weight formula given by Equation B11 for an ellipsoidally-capped cylindrical vessel can be readily modified to yield the weight of constant thickness container. Such a container is actually a bladder. The weight equation for such a bladder configuration is presented graphically in Figure B-10.

These curves are represented by the equation:

$$C_{ecb} = \frac{1}{\left(\frac{L}{D}\right)} \left\{ 2 + \frac{1}{K(K^2-1)^{1/2}} \ln \left[\frac{K + (K^2-1)^{1/2}}{K - (K^2-1)^{1/2}} \right] \right\}$$ (B19)

which is the parameter for the weight equation

$$W_{teb} = C_{teb} \left[\pi a^2 t \rho \frac{1}{\cancel{}} \right]$$ (B20)

Equations B19 and B20 are merely modifications of Equation B11.

Biconvex Spherical-Cap Configuration

Another configuration utilized for the structural shell of positive expulsion devices is the biconvex spherical-cap pressure vessel (Figure B-2).

This configuration consists of two partial spherical caps and a stiffening ring located at the junction of both caps. When uniform internal pressure is applied to the vessel, compressive hoop stresses are generated in the ring, and also in small border zones of the caps adjacent to the ring.

Weight relationships are derived on the following pages which establish the preliminary structural size of the biconvex pressure vessel. The derivations of weight equations and resulting graphs are based on the following assumptions:

(1) Stresses in partial spherical caps are based on membrane theory and constant wall thickness.

(2) Ring area is considered to be concentrated at a finite point, at the intersection of both caps.
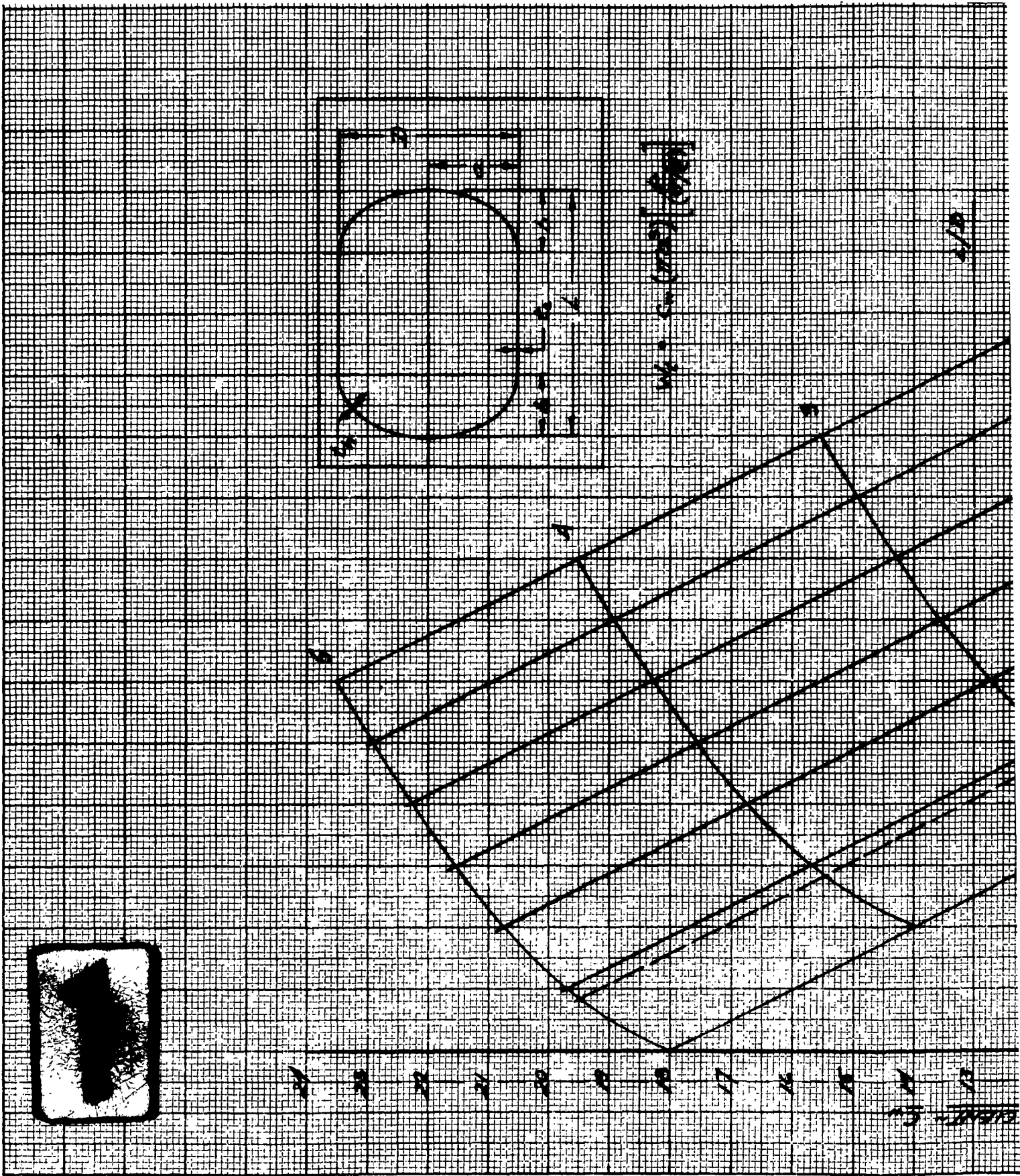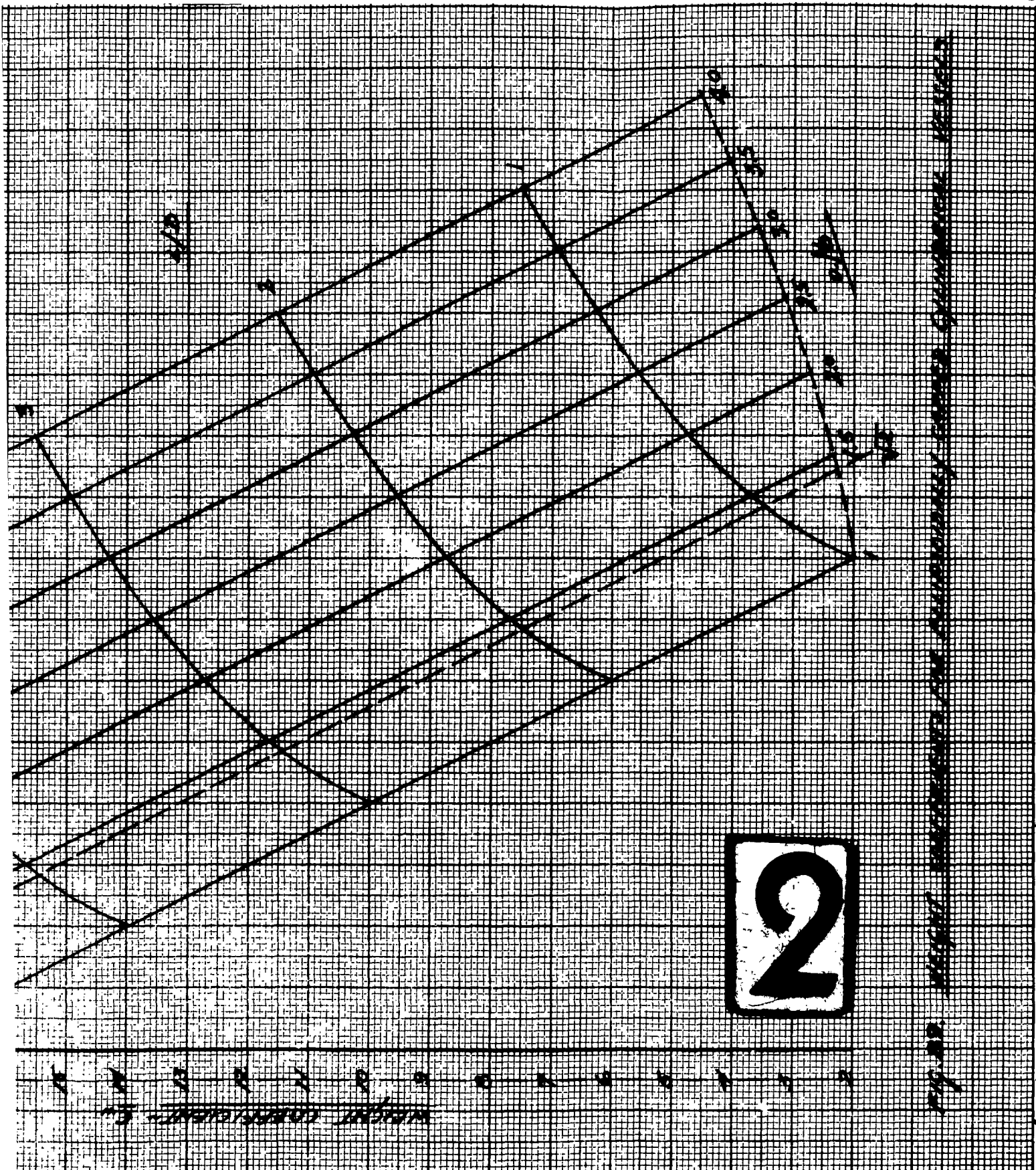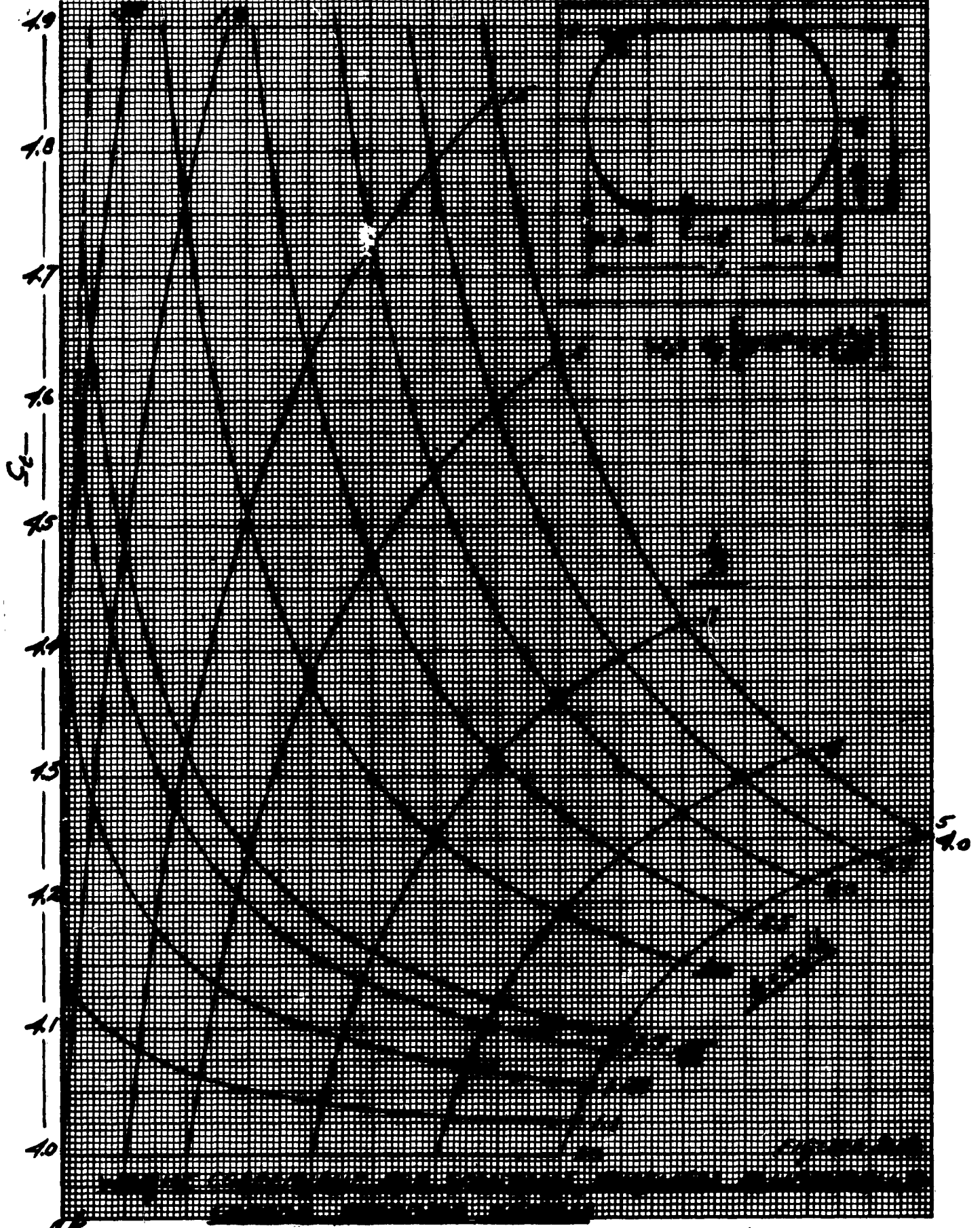
(3) Local bending or discontinuity stresses are not considered.

When uniform internal pressure exists in the vessel, the constant wall thickness required for each cap, corresponding to tensile strength of material used, is (Reference B2)

$$t_{bc} = \frac{\varphi a}{2\sigma_T \sin \alpha} \tag{B21}$$

The surface area of a single partial spherical cap is

$$A_c = 2\pi R h - 2\pi a^2 \left(\frac{1-\cos \alpha}{\sin^2 \alpha}\right) \tag{B22}$$

Hence, the weight of both caps is

$$W_{bc} = 2A_c t_{bc} \rho = 2\pi a^3 \rho \left(\frac{1}{\left(\frac{\sigma}{\rho}\right)}\right)\left(\frac{1-\cos \alpha}{\sin^2 \alpha}\right) \tag{B23}$$

The net force on the ring due to membrane stresses in the caps is

$$H_R = \rho a \cot \alpha \tag{B24}$$

From applied ring stress equal to allowable ring stress, for the area critical mode of failure of the ring, the cross-section area of the ring required is

$$A_R = \frac{H_R a}{|\sigma_R|} = \frac{\rho a^2}{|\sigma_R|} \cot \alpha \tag{B25}$$

Where σ_R is the absolute value of allowable compressive stress for the ring.

The weight of the ring is given by:

$$W_R = 2\pi a A_R \rho \tag{B26}$$

$$W_R = 2\pi a^3 \frac{\rho}{\left(\frac{|\sigma_R|}{\rho}\right)} \cot \alpha \tag{B27}$$

The weight of the biconvex spherical-cap vessel is then

$$W_{tbc} = W_{bc} + W_R \tag{B28}$$

$$W_{tbc} = 2\pi a^3 \frac{P}{\left(\frac{\sigma_t}{\rho}\right)}\left[\left(\frac{L}{D}\right)\frac{1}{SIN^2\alpha} + \left|\frac{\sigma_t}{\sigma_R}\right| \frac{1}{TAN\alpha}\right] \qquad (B29)$$

where:

$$\frac{L}{D} = \frac{h}{a} = \frac{1-COS\alpha}{SIN\alpha} \qquad (B30)$$

Although a biconvex spherical-cap pressure vessel is always heavier than a complete spherical vessel having equal volume and strength, subjected to the same internal pressure, it is interesting to note the influence of L/D and $|\sigma_t/\sigma_R|$ on the ratio of their weights. Hence, the ratio of weights of a biconvex spherical-cap vessel to that of a complete sphere is:

$$\frac{W_{tbc}}{W_S} = \frac{4}{3}\frac{\left(\frac{L}{D}\right)\frac{1}{SIN\alpha} + \left|\frac{\sigma_t}{\sigma_R}\right| \frac{1}{TAN\alpha}}{\left(\frac{L}{D}\right)\left[1 + \frac{1}{3}\left(\frac{L}{D}\right)^2\right]} \qquad (B31)$$

Numerical values of this equation are plotted in carpet form in Figure B-11, for the following ranges: $0.3 \leqq L/D \leqq 1, 1 \leqq |\sigma_t/\sigma_R| \leqq 3$

As expected, when $L/D = 1$, a complete sphere, the weight ratio is unity which indicates that the sphere is a minimum-weight configuration. This is true because the horizontal component of meridional membrane force is nonexistent at $\alpha = \pi/2$ therefore, no ring is required in this case.

Another useful ratio employed in the design of pressure vessels is the weight-volume ratio. This ratio is a function of strength or material used, and based on membrane stresses, it is expressed as

$$\left(\frac{W}{V}\right)_{tbc} = 2\frac{P}{\left(\frac{\sigma_t}{\rho}\right)}\left\{\frac{\left(\frac{L}{D}\right)\frac{1}{SIN^2\alpha} + \left|\frac{\sigma_t}{\sigma_R}\right| \frac{1}{TAN\alpha}}{\left(\frac{L}{D}\right)\left[1 + \frac{1}{3}\left(\frac{L}{D}\right)^2\right]}\right\} \qquad (B32)$$

This expression of $(W/V)_{tbc}$ is 1.5 $P/(\sigma_t/\rho)$ times the W_{tbc}/W_S expression shown on previous page; as a result

$$\left(\frac{W}{V}\right)_{tbc} = 1.5 \frac{P}{\left(\frac{\sigma_t}{\rho}\right)}\left(\frac{W_{tbc}}{W_S}\right) \qquad (B33)$$
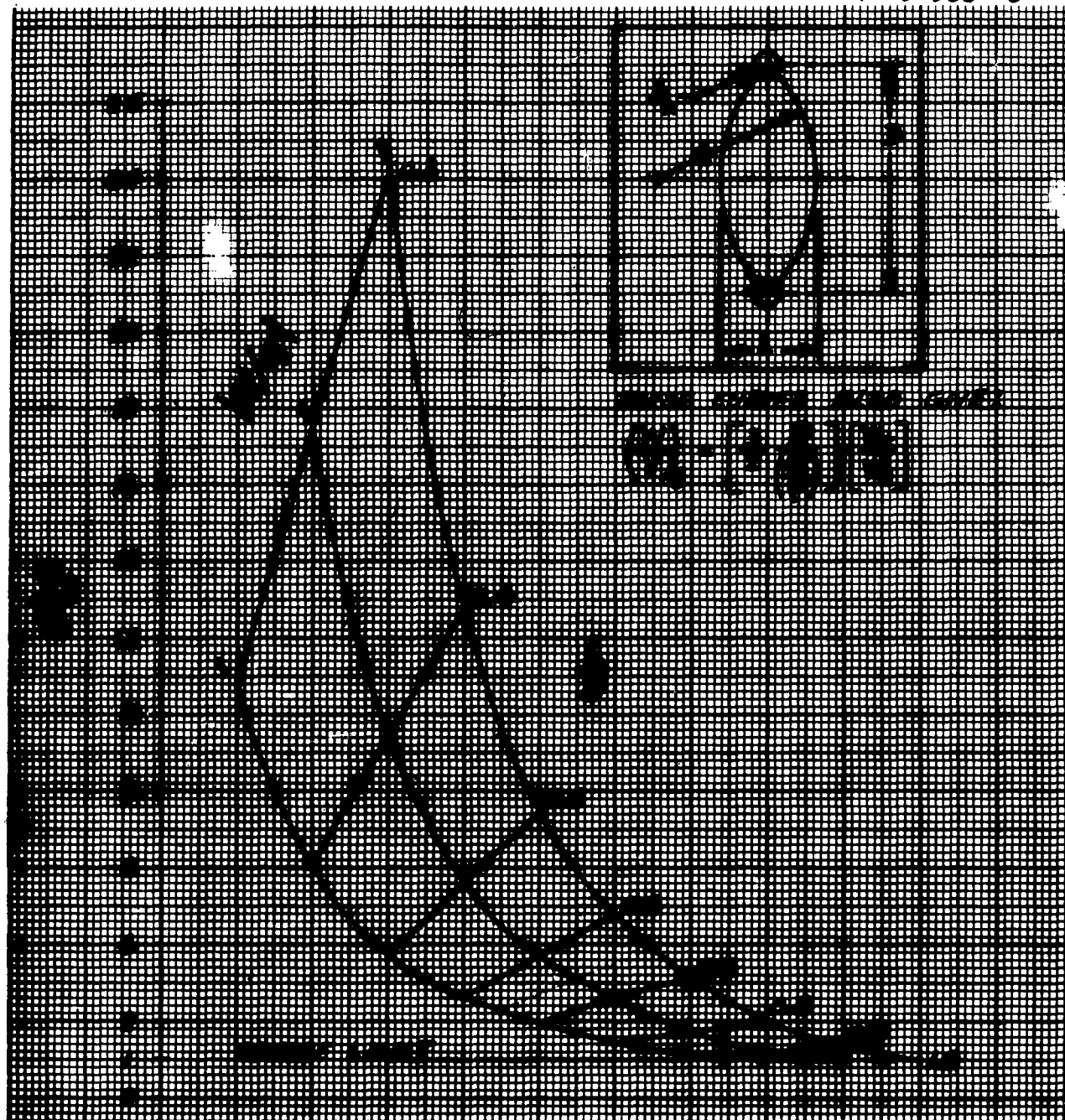
FIGURE B11

RATIO OF WEIGHTS OF BICONVEX SPHERICAL-CAP
PRESSURE VESSELS TO THAT OF SPHERICAL
VESSELS OF EQUAL VOLUME AND STRESS

AND

WEIGHT-VOLUME RATIO PARAMETER FOR BICONVEX
SPHERICAL-CAP VESSELS

The minimum value of $(W/V)_{tbc}$ is obtained when the vessel is a sphere which again results in the expression

$$\left(\frac{W}{V}\right)_{tcb} = 1.5 \frac{\rho}{\left(\frac{\sigma_t}{\rho}\right)} \tag{B34}$$

With the aid of Equation B29, an alternate expression for weight of a biconvex spherical pressure vessel is obtained, which is

$$W_{tbc} = C_{wbc}(\pi a^3)\left[\frac{\rho}{\left(\frac{\sigma_T}{\rho}\right)}\right] \tag{B35}$$

where

$$C_{wbc} = 2\left[\left(\frac{t}{b}\right)\frac{1}{\sin^2\alpha} + \left|\frac{\sigma_T}{\sigma_R}\right| \frac{1}{\tan\alpha}\right] \tag{B36}$$

The values of the weight coefficient, C_{wbc} are plotted in Figure B-12.

REFERENCES

B1. Krivetsky, A.: Volume of a Two-Radii Contour Pressure Vessel. Bell Aerosystems Company Report No. 7129-933005, March 1962.

B2. Wong, R. E.: Rapid Weight-Strength Analysis of Pressure Vessels. Product Engineering, Vol. 28, No. 14, October 14, 1957.

B3. Timoshenko, S.: Theory of Plates and Shells. McGraw-Hill Book Company, Inc., New York. First Edition, 1940.

B4. Krivetsky, A.: Weight and Volume Characteristics of Ellipsoidally-Capped Pressure Vessels. Bell Aerosystems Company Report No. 7129-933004, March 1962.
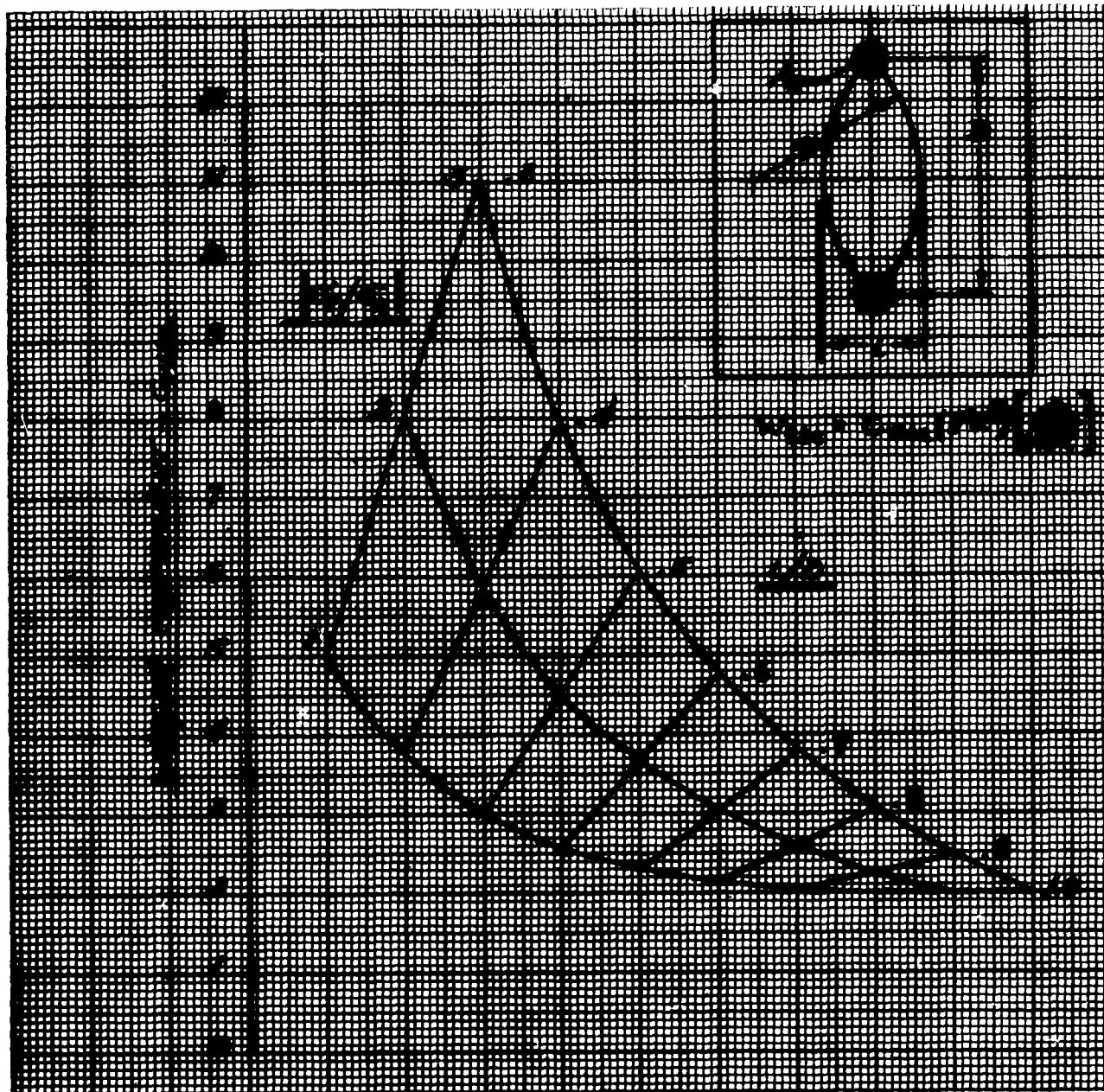
Fig. B12 WEIGHT COEFFICIENTS FOR BICONVEX SPHERICAL CAP VESSELS

APPENDIX C

DETAILS OF ANALYSIS AND EXPERIMENTAL CHECK
OF A CYLINDRICAL TANK BREATHING MODE

INTRODUCTION

This appendix provides the details of analysis of the breath-
ing mode discussed under ELASTIC TANK BREATHING MODE, and describes
the experimental check made to test the breathing mode frequency
equation. While this configuration does not correspond to any
particular one of the positive expulsion devices reviewed in this
report, and since analytical methods for this class of modes are
virtually nonexistent, it was considered the most straight forward
configuration for the illustration of the class of vibrations
under consideration and the study of spray and cavitation possi-
bilities in terms of fluid pressures.

It is felt that further analysis in this area to other tank
shapes and methods of support will lead to a useful body of
analyses techniques and frequency, pressure, spray, and oscil-
latory cavitation criteria for the accurate predictions of the
characteristics and requirements of such liquid filled tanks.

ELASTIC TANK BREATHING MODE ANALYSIS

As indicated in the Section on the ELASTIC TANK BREATHING
MODE, the container analyzed consists of a cylindrical tube (no
end plate) standing on end on a flat frictionless surface. Assum-
ing absolute flatness of both the end of the cylinder and the
support surface, the container may be filled with fluid without
leaking. A fillet of waterproof grease was used around the bottom
of the actual test specimen. The cylinder was left bottomless to
give the simplest most direct possible check between analysis and
experiment showing basic characteristics of a breathing mode.

The mode is assumed to consist of a rising and falling of the
free surface which remains plane, and a corresponding radial con-
traction and expansion or breathing of the cylinder which varies
from zero at the free surface to some maximum value at the base.
Consider first the action of a "slab" of fluid between two parallel
planes a distance S_y apart as indicated in Figure C1.

As the cylinder breathes the wall at y moves radially a
distance ΔR_y and the slab which was S_y thick for an undeflected
cylinder is reduced in thickness by an amount ΔS_y so that the
volume decrease due to ΔS_y is just equal to the increase in
volume brought about by the increase in cylinder radius ΔR_y .
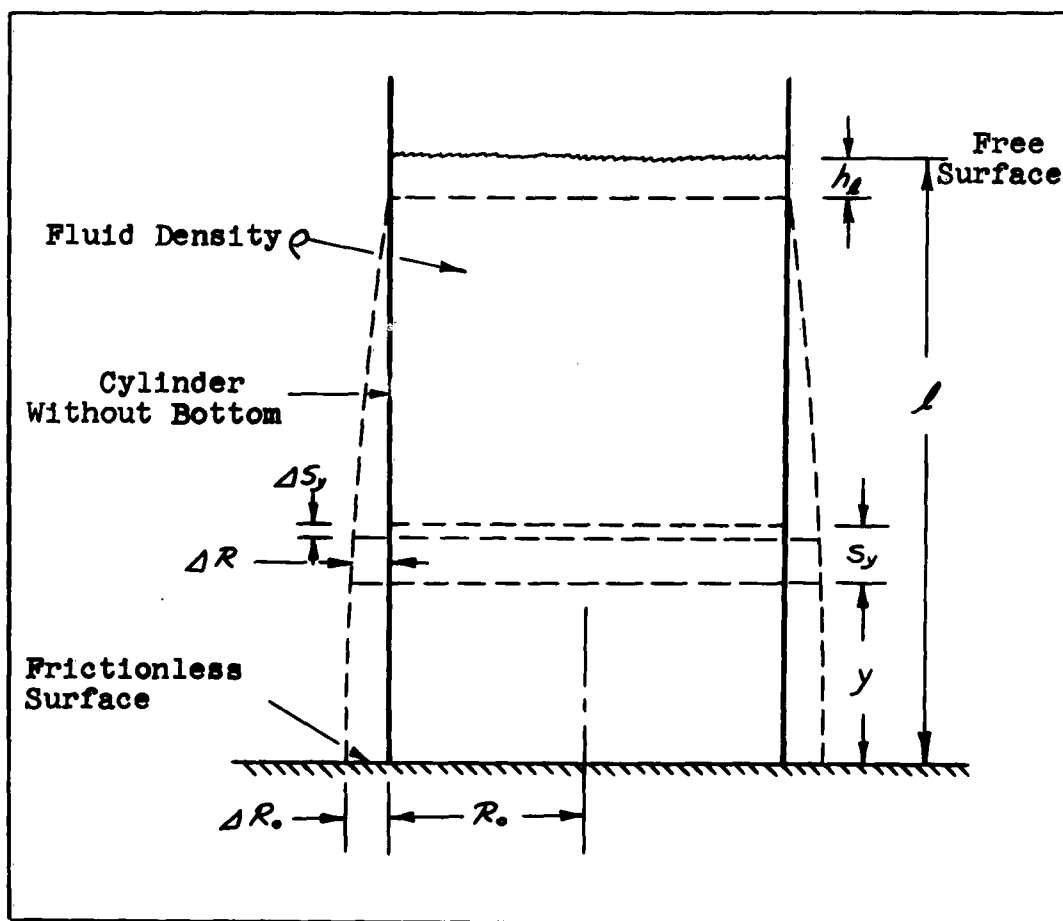
Figure C1. Cylinder Breathing Mode Configuration
For Analysis

Then,

$$\text{Decreased volume} \quad \Delta V_D \approx \pi R_o^2 \Delta S_y \tag{C1}$$

$$\text{Increased volume} \quad \Delta V_I = \pi \left[R_o + \Delta R_y\right]^2 \left[S_y - \Delta S_y\right] - \pi R_o^2 \left[S_y - \Delta S_y\right]$$

$$\Delta V_I = \pi \left[2 \Delta R_y R_o S_y - 2 \Delta R_y R_o \Delta S_y + \Delta R_y^2 S_y - \Delta R_y^2 \Delta S_y\right] \tag{C2}$$

Since the incremental values will be small their products may be considered negligible, therefore

$$\Delta V_I = 2 \pi R_o S_y \Delta R_y \tag{C3}$$

Equating the decrease and increase in volumes yields

$$\pi R_o^2 \Delta S_y = 2 \pi R_o S_y \Delta R_y$$

or

$$\frac{\Delta S_y}{S_y} = \frac{2 \Delta R_y}{R_o} \tag{C4}$$

Assuming $\quad R_o$ = radius at the base of the tank

$\quad\quad\quad\quad \Delta R$ = deflection at the base of the tank

Then, $\quad\quad \Delta R_y$ may be expressed as

$$\Delta R_y = f(y) \Delta R_o \tag{C5}$$

where $\quad\quad f(y)$ = wall mode shape

Assume the depth of the fluid ℓ is divided into n stations thus

$$S_y = \frac{\ell}{n} \tag{C6}$$

Substituting Equations C5 and C6 into C4 yields

$$\Delta S_y = 2 \left(\frac{\ell}{n}\right) f(y) \left(\frac{\Delta R_o}{R_o}\right) \tag{C7}$$

Consequently to determine the vertical motion of the fluid at any station (height) y it is necessary to integrate Equation (C7) from the bottom of the tank to the station y. Thus if h_y is denoted as the half amplitude of oscillation of the "slab" at station y then

$$h_y = \sum_{y_o}^{y} \Delta S_y = 2 \left(\frac{\ell}{n}\right) \left(\frac{\Delta R_o}{R_o}\right) \sum_{y_o}^{y} f(y) \tag{C8}$$

The pressure exerted by the fluid mass m of station y on the station below will be

$$\Delta p_y = \frac{F_y}{A} \tag{C9}$$

where

$$F_y = m \omega^2 h_y = \pi (R_o + \Delta R_y)^2 \left(\frac{\ell}{n}\right) \rho \omega^2 h_y \tag{C10}$$

$$A = \pi (R_o + \Delta R_y)^2 \tag{C11}$$

With the aid of Equations (C10) and (C11), Equation (C9 becomes

$$\Delta p_y = \rho \left(\frac{\ell}{n}\right) \omega^2 h_y \tag{C12}$$

and using Equation (C8),

$$\Delta p_y = 2 \rho \left(\frac{\ell}{n}\right)^2 \left(\frac{\Delta R_o}{R_o}\right) \omega^2 \sum_{y_o}^{y} f(y) \tag{C13}$$

Since the pressure generated at each station will be applied to the station beneath, the total pressure at any station is obtained by integrating (C13) from the liquid surface down to the station in question. Thus

$$p_y = \sum_{y_o}^{y} \Delta p_y \tag{C14}$$

or

$$p_y = 2\rho \left(\frac{\ell}{\pi}\right)^2 \left(\frac{\Delta R_o}{R_o}\right) \omega^2 \sum_y^\ell \left[\sum_{y_o}^y f(y)\right] \tag{C15}$$

To determine the resonant frequency and the associated mode shape consider the pressure effect upon the container. Assuming the container as a series of hoops the hoop stress, S_t , may be written as

$$S_t = \frac{p_y R_o}{t} \tag{C16}$$

The circumference of the tank at station y is ℓ_{cy}, which will

be increased by

$$\Delta \ell_{cy} = \frac{S_t \ell_{cy}}{E} = \frac{p R_o \ell_{cy}}{E t} \tag{C17}$$

where $\ell_c = 2\pi R_y$ (C18)

                t = hoop thickness

                E = modulus of the container

Thus $\Delta \ell_c = 2\pi \Delta R_y$ (C19)

From Equation (C17) and (C18)

$$\Delta \ell_{cy} = 2\pi \frac{R_o^2 p_y}{E t} \tag{C20}$$

Utilizing Equation (C19)

$$2\pi \Delta R_y = 2\pi \frac{R_o^2 p_y}{E t} \tag{C21}$$

and

$$\frac{\Delta R_y}{R_o} = \frac{p_y R_o}{E t} \tag{C22}$$

or

$$p_y = \frac{\Delta R_y}{R_o}\left(\frac{Et}{R_o}\right) \tag{C23}$$

Substituting Equation (C23) into Equation (C15)

$$\frac{\Delta R_y}{\Delta R_o} = 2\rho\left(\frac{\ell}{n}\right)^2\left(\frac{R_o}{Et}\right)\omega^2 \sum_{y}^{\ell}\left[\sum_{y_o}^{y}f(y)\right] \tag{C24}$$

or

$$\frac{\Delta R_y}{\Delta R_o} = A\sum_{y}^{\ell}\left[\sum_{y_o}^{y}f(y)\right] \tag{C25}$$

where

$$A = 2\rho\left(\frac{\ell}{n}\right)^2\left(\frac{R_o}{Et}\right)\omega^2 \tag{C26}$$

But from Equation (C5)

$$\frac{\Delta R_t}{\Delta R_o} = f(y)$$

and from Equation (C25),

$$f(y) = A\sum_{y}^{\ell}\left[\sum_{y_o}^{y}f(y)\right] \tag{C27}$$

The normalized wall deflection mode shape when integrated from bottom to free surface and then from free surface to bottom will then yield the normalized mode shape again but multiplied by a constant, and if an approximate mode shape $f(y)_1$ is assumed at the beginning of the process the derived mode shape $f(y)_2$ will be more nearly correct than the original approximation. An assumed mode shape may thus be iterated to converge on the correct mode shape. This is done in Table CI starting with an assumed straight line mode shape. Three iterations brought convergence to within 0.3 percent.

Writing Equation (C27) for the bottom station where $f(y) = 1.0$ gives

$$1.0 = 2 \left(\frac{\ell}{n}\right)^2 \left(\frac{\rho R_o}{Et}\right) \omega^2 \sum_{y_o}^{\ell} \left[\sum_{y_o}^{y} f(y)\right] \tag{C28}$$

which may be solved for ω^2 giving

$$\omega^2 = \frac{1}{2\left(\frac{\ell}{n}\right)^2 \sum_{y_o}^{\ell}\left[\sum_{y_o}^{y} f(y)\right]} \left(\frac{Et}{\rho R_o}\right) \tag{C29}$$

The summation $\sum_{y_o}^{\ell}\left[\sum_{y_o}^{y} f(y)\right]$ is established from the final iteration of Table CI as 40.6 at station 0 giving

$$\omega^2 = \frac{100}{81.2} \left(\frac{1}{\ell^2}\right)\left(\frac{Et}{\rho R_o}\right) \tag{C30}$$

where $n^2 = 100$ since the cylinder was divided into 10 stations

$$\omega = \frac{1.11}{\ell} \sqrt{\frac{Et}{\rho R_o}} \tag{C31}$$

Writing Equation (C8) for the free surface station $y = \ell$

$$h_\ell = 2 \left(\frac{\ell}{n}\right)\left(\frac{\Delta R_o}{R_o}\right) \sum_{y_o}^{y_\ell} f(y) \tag{C32}$$

From Table CI $n = 10$ and $\sum_{y_o}^{y_\ell} f(y) = 6.348$

giving $\qquad \frac{h_\ell}{\ell} = 1.27 \frac{\Delta R_o}{R_o} \tag{C33}$

Thus the axial displacements of the free surface as a fraction of the fluid depth will be 27 percent larger than the wall breathing amplitude as a fraction of cylinder radius.

Using Equations (C31) and (C33) in Equation (C15) for the pressure at the bottom of the tank

$$p_o = \frac{2(1.23)}{100(1.27)} \left(\frac{h_\ell}{\ell}\right) \left(\frac{Et}{R_o}\right) \sum_{y}^{\ell} \left[\sum_{y_o}^{y} f(y)\right] \tag{C34}$$

Table CI column 10 gives $\quad \sum\limits_{0}^{\ell}\left[\sum\limits_{y_0}^{y} f(y)\right] = 40.6$ (C35)

so that $\quad p_0 = 0.787 \left(\frac{h_\ell}{\ell}\right)\left(\frac{Et}{R_0}\right)$ (C36)

Pressure Considerations

Large oscillating pressures can exist within the fluid in a breathing mode due to the high frequencies of such modes and the large inertia forces provided by the fluid. The total pressure within the fluid a distance y above the tank bottom during a linear oscillation will be:

$$p_y = p_i - p_v + \rho a(\ell - y) + p_{y_{osc}} \sin \omega t$$ (C37)

where $\quad p_i$ = total pressure above fluid

$\qquad p_v$ = fluid vapor pressure

$\qquad \rho$ = fluid density

$\qquad a$ = acceleration of tank

$\qquad \ell$ = depth of fluid

$\qquad p_{y_{osc}}$ = oscillating pressure

$$p_{y_{osc}} = (0.01938)\left(\frac{h_\ell}{\ell}\right)\left(\frac{Et}{R_0}\right)\sum\limits_{y}^{\ell}\left[\sum\limits_{y_0}^{y} f(y)\right]$$

The surface amplitude h_ℓ/ℓ at which cavitation should be expected at the bottom of the tank may be obtained by setting $p_y = 0$ and $y = 0$ in Equation (C18) and solving for h_ℓ/ℓ.

EXPERIMENTAL CHECK ON BREATHING MODE NATURAL FREQUENCY OF A CYLINDRICAL CONTAINER

To verify the existence of this mode and check the frequency formula a plastic cylinder 5.14 inches long and 2.82 inches in diameter was placed on end on a smooth steel plate as indicated in Figure C-2. The cylinder was made watertight by a fillet of waterproof grease around the inside of the container at the bottom. The container was then filled 90 percent full of water and excited
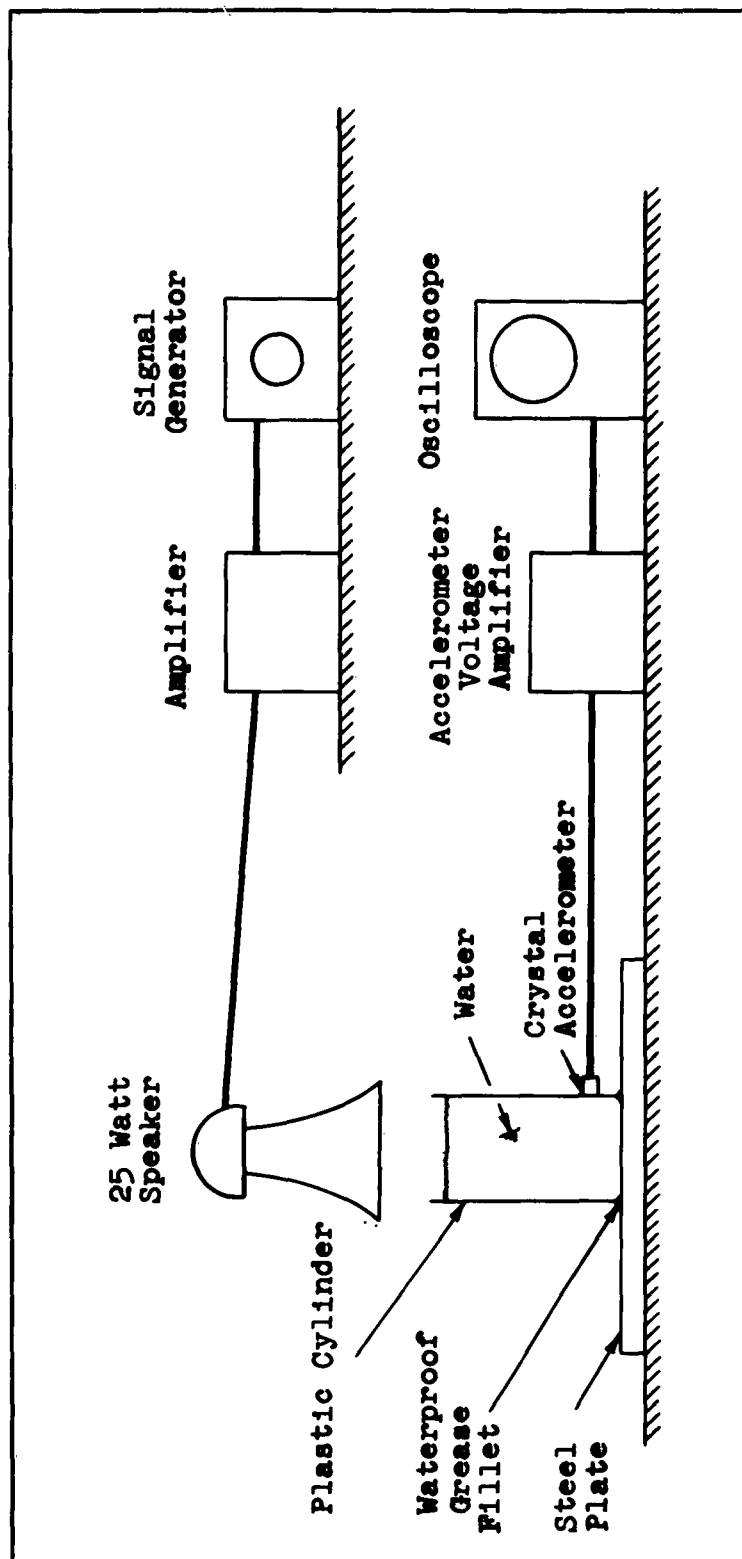
Figure C2. Laboratory Test Set-up for Verification of Cylindrical Tank Breathing Mode

in the breathing mode by a horn speaker of 25 watts capacity placed close to the top of the container. Radial motion of the wall near the bottom was detected by a miniature crystal accelerometer leaning against the cylinder wall with its sensitive axis at an angle of about 30 degrees from the horizontal.

Before using Equation (C6) to predict the breathing frequency it was necessary to evaluate Et, the product of Young's modulus and cylinder wall thickness. This was accomplished by using the cylinder as a compression spring in a single degree of freedom axial vibration mode with a 10 lb. weight on top of the cylinder.

Using the frequency formula

$$\omega_{et} = \sqrt{\frac{k}{M_{10}}} \tag{C38}$$

where   k = the axial spring rate of a rod

$$k = \frac{AE}{l} = \frac{2\pi R_o t E}{l}$$

then

$$Et = \frac{\omega_{et}^2 M_{10} l}{2\pi R_o} = \frac{2\pi f^2 M_{10} l}{R_o}$$

where   f = observed axial frequency = 81 cps

$$M_{10} = 10/386 \ (lbs.sec^2/in)$$

$$l = 5.12 \ in.$$

$$R_o = 1.41 \ in.$$

$$Et = 3870 \ lbs/in$$

Evaluating the breathing mode frequency formula (C31)

$$\omega = \frac{1.11}{l} \sqrt{\frac{Et}{\rho R_o}}$$

$$\omega = \frac{1.11}{(5.12)(0.9)} \sqrt{\frac{3870 \times 10^6}{(93.7)(1.41)}} = 1300$$

or

$$f = \frac{1300}{2\pi} = 207 \ cps.$$

The frequency was observed experimentally at 215 cps.

TABLE CI.   ITERATION OF CYLINDRICAL CONTAINER BREATHING MODE SHAPE

1	2	3	4	5	6	7	8	9	10	11	12
STA	$f(y_1)$	$\Sigma f(y_1)$	$\Sigma\Sigma f(y_1)$	$f(y)_2$	$\Sigma f(y)_2$	$\Sigma\Sigma f(y)_2$	$f(y)_3$	$\Sigma f(y)_3$	$\Sigma\Sigma f(y)_3$	$f(y)_4$	$f(y)_4/f(y)_3$
10	0	4.9875	0	0	6.234	0	0	6.3485			
9	.1	4.8875	4.9875	.1494	6.085	.6234	.1558	6.1927	6.348	.1563	.9968
8	.2	4.6875	9.8750	.296	5.789	12.319	.3080	5.8847	12.541	.3089	.9971
7	.3	4.3875	14.5625	.436	5.353	18.108	.4527	5.4320	18.426	.4538	.9975
6	.4	3.9875	18.9500	.568	4.785	23.461	.5865	4.8455	23.858	.5876	.9981
5	.5	3.4875	22.9375	.688	4.097	28.246	.7062	4.1393	28.703	.7070	.9989
4	.6	2.8875	26.4250	.791	3.306	32.343	.8086	3.3307	32.843	.8089	.9996
3	.7	2.1875	29.3125	.878	2.428	35.649	.8912	2.4395	36.173	.8910	1.0002
2	.8	1.3875	31.5000	.944	1.484	38.077	.9519	1.4876	38.613	.9510	1.0009
1	.9	.4875	32.8875	.986	.498	38.561	.9890	.4986	40.100	.9877	1.0013
0	1.0		33.3750	1.000		40.059	1.000		40.599	1.000	1.0000
		First Iteration			Second Iteration			Third Iteration			Convergence

APPENDIX D

PRELIMINARY DESIGN & TEST CRITERIA
FOR PROPELLANT POSITIVE EXPULSION DEVICES

INTRODUCTION

A criteria of merit in evaluating positive expulsion device concepts is the ability of the configuration to demonstrate repeated expulsions without failure. While it should be the goal of any design to accomplish repeated full expulsions, some compromise to this requirement will probably be necessary. One method of achieving the desired confidence would be for the design to be capable of repeated partial expulsions. On the other hand, certain system configurations are inherently one-shot designs.

Statistical methods can be applied to estimate the reliability of the expulsion device. On previous programs where pliable or plastic materials have been employed in the bladder-expulsion concept, the reliability demonstration was accomplished by repeated cycling and complete expulsion of the full propellant tank load.

This situation is somewhat analogous to liquid and solid rocket engine reliability demonstration methods. Liquid rocket engine reliability is demonstrated by repeated firings of several engines within their life capability. Solid rocket engines being essentially "one-shot" components require a large number of individual rocket firings to demonstrate reliability.

The subject Appendix presents a general and preliminary version of a design and test criteria for propellant positive expulsion devices. This sample criteria is introduced as an example to illustrate the many facets of investigations that are required to establish such a document. The criteria presented is not to be construed as a specification for design but merely as an approach to the preparation of such specifications.

The representative design criteria is based on a survey of several satellite and space probe missions and simplifications have been introduced where possible because of the general nature of the study as compared to the specific applications associated with the survey specifications.

1.0 SCOPE

1.1 Scope

The following preliminary requirements have been established to provide a basis for design and test of propellant positive expulsion devices. A propellant positive expulsion device shall be any device which permits the certain expulsion of designated liquid propellants from their storage containers under "zero gravity" conditions. Consideration shall be given, but not restricted, to positive expulsion devices for use with the following storable and cryogenic propellants.

Storable propellants - N_2O_4, UDMH, H_2O_2, N_2H_4, MON (mixed oxides of nitrogen), "AEROZINE" (50% UDMH, 50% N_2H_4).

Cryogenic propellants - F_2, O_2, H_2

1.2 Classification

Propellant positive expulsion devices shall be of the following general types, classes and sizes:

Type I — Propellants constantly ready for transfer to the engine while the vehicle is under zero-g environment for a period up to 24 hours, for use with earth orbiting systems requiring orbit attainment only.

Type II — Propellants constantly ready for transfer to the engine while the vehicle is under zero-g environment for a period up to 2 weeks, for use with lunar orbit and landing systems, or earth orbiting systems, capable of returning to earth as required.

Type III — Propellants constantly ready for transfer to the engine while the vehicle is under zero-g environment for a period up to 3 years, for use with space probes and lunar or earth orbiting systems requiring engine restart over an extended period of time.

Class A — Rated expulsion life of one cycle with limited ground checkout capability.

Class B — Rated expulsion life of 5.0 cycles.

Class C — Rated expulsion life of 100 cycles.

Size 1   Propellant expulsion volume from 1/10 to 5 cubic
           feet (0.748 gal. to 37.4 gal.)

Size 2   Propellant expulsion volume from 5 cubic feet to
           100 cubic feet (37.4 gal. to 748 gal.)

2.0 APPLICABLE DOCUMENTS

The following shall be used as a guide in establishing design
and test requirements for propellant positive expulsion devices.

MIL-T-5208A (ASG)   Tanks, Removable, Liquid Propellant
                     Rocket Engine, General Specification
                     for

3.0 REQUIREMENTS

3.1 Steady State Accelerations

Limit flight accelerations are specified in Table DI
The propellant tanks shall be full in all cases except for the
"expulsion required" cases applicable to Types II and III. The
tanks shall be half full in this instance.

The limit inertia loads resulting from these accelera-
tions shall be multiplied by 1.50 to obtain ultimate loads. No
evidence of yielding or of excessive deformations shall exist
upon application of limit loads; failure shall not occur under
ultimate loads.

3.2 Shock

Limit shock accelerations for Size 1 expulsion devices
shall be:

>   Longitudinal axis   30 g
>   Lateral axis   20 g   -

Limit shock acceleration for Size 2 expulsion devices
shall be:

>   Longitudinal axis   25 g
>   Lateral axis   15 g

The wave form for these shock loads shall be approxi-
mately a half sine wave of six milliseconds duration and shall
be applied three times in both directions along the three mutually
perpendicular axis. The loads shall be applied at the structural
attachment points; the propellant tank shall be fully loaded and
the expulsion device non-operating.

TABLE DI. LIMIT FLIGHT ACCELERATIONS

| Classification of Expulsion Device | | Acceleration Range (g's) ① | | | |
| | | Expulsion Required | | Expulsion Not Required | |
		Long.	Lateral ②	Long.	Lateral ②
Type I	Size 1 ③	±6	±2	±12	±3
	Size 2	±4	±1	±8	±2
Types II and III	Size 1 ③	±20	±4	±12	±3
	Size 2	±15	±3	±8	±2

① These lateral and longitudinal (vehicle) accelerations shall act in combination (g = 32.2 ft/sec²)

② Lateral accelerations shall be assumed to act in any lateral direction (g = 32.2 ft/sec²)

③ Size 1 tanks may be oriented in any direction with respect to vehicle axes. Size 2 tanks shall have their longitudinal axis aligned with the longitudinal axis of the associated flight vehicle.

Application of the specified shock loads shall not result in loss of utility or structural integrity of the propellant expulsion device or the propellant tank.

3.3 Vibration

Limit vibration amplitudes or accelerations for Size 1 and Size 2 tanks shall be:

Longitudinal and Lateral Axes

5-20 cps at 1/8" single amplitude
20-400 cps at 3.5 g
400-2000 cps at 7.5 g

The excitation shall be applied at the structural attachment points in each of three mutually perpendicular directions for a total time of 45 minutes in each direction. A constant octave band sweep rate shall be employed. The propellant tank shall be fully loaded and the expulsion device nonoperating.

Application of the specified accelerations shall not result in loss of utility or structural integrity of the propellant expulsion device or propellant tank.

3.4 Pressures

Operating pressure shall be specified.as required to assure satisfactory expulsion, and proper thrust chamber or turbine pump inlet pressures. The maximum operating pressure shall correspond to the flow pressure rating of the relief valve employed in a gas pressurization system. If expulsion forces are generated by chemical or mechanical means the estimated upper limit of the associated pressures shall be designated as the maximum operating pressure.

Proof pressure shall correspond to 1.50 times the maximum operating pressure. Burst pressure shall correspond to 2.0 times the maximum operating pressure.

The propellant expulsion device shall be capable of withstanding without leakage or evidence of loss of integrity a differential pressure 1.50 times the largest differential estimated to occur under the maximum operating pressure. A pressure differential of 2.0 times the above shall not cause rupture.

Class B and Class C expulsion devices shall in addition withstand 5 cycles and 100 cycles respectively of normal propellant expulsion at rated pressures without evidence of leakage, or loss of utility or structural integrity. Temperature shall

correspond to those associated with the designated propellants for all pressure tests. Where degradation of the mechanical properties of the expulsion device due to space radiation environments is anticipated, these shall be accounted for in design and test.

3.5 Slosh and Expulsion

The propellant tank and expulsion device unpressurized or pressurized (whichever is more critical) and containing 75% of maximum propellant load shall be capable of withstanding a sinusoidal motion in the lateral direction for 5 minutes for Class A and B tanks, and for 60 minutes for Class C tanks. The sinusoidal motion shall be applied at the frequency which produces the greatest mass motion of propellant. The double amplitude of excitation shall be 3.0 inches.

Following test no evidence of leakage or mechanical damage shall exist. Expulsion of the propellant shall also be accomplished following test.

3.6 Radiation

Exposure to the radiation doses shall not impair the utility or structural integrity of the propellant tank and its expulsion device below levels accounted for in design and test.

3.7 Temperature

Exposure of the propellant expulsion device to temperatures of $+160°F$ and $-65°F$ for a period of 24 hours each shall not impair its utility or structural integrity.

Exposure of the propellant device and fully loaded propellant tank to the maximum and minimum allowable temperatures specified for the associated propellant(s) shall not impair the utility or structural integrity of the expulsion device or the propellant tank.

3.8 Vacuum

The propellant expulsion device and associated propellant tank (assembled) shall not be adversely effected by exposure to ambient pressures as low as 1×10^{-5} to 1×10^{-12} mm of Hg for the following periods of time:

Expulsion Device	Duration of Vacuum Environment (days)
Type I	1
Type II	14
Type III	1095

3.9 Meteoroids

Design to withstand meteoroid impacts shall not be required. It shall be assumed that external protection of the expulsion device will be provided where required. Susceptability to damage shall be nevertheless considered in the qualitative evaluation of the merits of various expulsion devices for Type II and Type III applications.

3.10 Propellant Storage Life

The propellant expulsion device and propellant tank shall not experience loss of utility or structural integrity as a result of chemical or electrolytic action associated with specified propellant(s) for the following periods of time.

Expulsion Device	Propellant Storage Life (days)
Type I	1
Type II	14
Type III	1095

3.11 Reliability

The design expulsion life of Class A expulsion devices shall equal the rated life specified in Paragraph 1.2. The design expulsion life of Class B and C expulsion devices shall equal the rated life specified in Paragraph 1.2 multiplied by a factor of 10.

The reliability of Class A expulsion devices shall be 0.9999 while the reliability of Class B and C devices at their design life shall be 0.999. The failure modes associated with this reliability shall be established according to the characteristics of the expulsion device of interest.

4.0 QUALITY ASSURANCE PROVISIONS

(Note: Only those test requirements are specified which are of direct interest in the present study)

4.1 Material Test

4.1.1 Radiation

4.1.2 Chemical Compatibility

APPENDIX E

FABRICATION TECHNIQUES FOR
BLADDER AND DIAPHRAGM CONSTRUCTION

INTRODUCTION

The incorporation of metals or plastics for the construction of the bladders or diaphragm introduces certain construction problems. Manufacturing is dependent upon materials. It is a growing and changing art, and the processes of the present can be expected to change in the years to come. Metal forming is an example, wherein the explosive forming of the electro-spark method is now utilized for complex re-entrant or closed shapes of sheet construction.

FABRICATION TECHNIQUES

1. Electroforming

Electroforming is a manufacturing technique that merits some consideration. The process is by no means new and has been utilized successfully for many applications by the Bell Aerosystems Company. Several advanges accrue from this electro deposition method of fabrication. The material can be deposited to any desired thickness, uniform or otherwise. Thus, the thickness can be varied to provide the pre-established folding patterns. In addition, the configuration of the shell can be in any arbitrary geometrical shape (including a closed-form) since the mandrel employed in establishing the shape can be dissolved following the electroform process. One advantage is now quite obvious: welding or seams can be eliminated and developed pattern shapes for heads or ends (pie-sections, gores, meridian sections, etc.), as required for sheet metal fabrication are not necessary.

2. Scoring

Scoring metal consists of permanently deforming the metal by stressing it beyond its yield point in a localized and restriced region. Some plastic flow of the metal occurs, but the reduction in the thickness of the foil or sheet is generally negligible. Scoring will result in smooth bends and minimizes tearing of the foil or sheet. As a result, scoring possesses advanges that are applicable to some types of expulsion devices, since it provides controlled bending and deformation.

3. Chemical Milling

Chemical Milling is a process of shaping metals to an exacting tolerance by the chemical removal of metal, or deep etching of parts, rather than by the conventional mechanical milling or machining operations. The amount of metal removed or the depth of etch is controlled by the time of immersion in the etching solution. The location of the unetched or unmilled areas on a given part is controlled by masking or protecting these areas from the action of the etchant solution.

With this process it is possible to produce shell or skin thicknesses below practical machining limits. In addition local reinforcements, that are an integral part of the component, can be readily incorporated, and tapers can be introduced in sheet as well as steps.

Metallic diaphragms or bladders can be designed with tapers, local reinforcements, etc., by this process so that controlled deformation is realized.

4. Metal Spinning

Parts with circular cross sections can be readily made by spinning them from sheet metal. The metal is displaced, perhaps in several steps, by means of pressure until it conforms to the shape of the chuck. For metallic expulsion devices consisting of bladders with spherical or elliptical heads, these heads can be spun. Spinning offers a low tool cost and is economical for small quantities. Since spinning may limit the minimum gage of the material, the spun head can be chem-milled to attain a thinner required gage.

5. Joining Methods

Although fusion welding is a simple approach for expulsion tank construction, there are precautions that must be undertaken to insure reliability. Pin-hole leaks near or in welds cannot be tolerated and inspection test procedures must be established to minimize and eliminate this defect. Segmented metal bladder construction to obtain the necessary contour would require considerable welding length and the use of draw dies, spinnings, explosive forming, etc., can be employed to offset a portion of this welding length.

Ultrasonic welding and electron beam welding should not be overlooked because of its great potential for joining thin sheets and foil-to-plate gages. This technique produces joints of high efficiency without altering the basic properties of the parent

material or the weld zone.

Brazing is another joining procedure that possesses versatility. Brazing can be performed on dissimilar materials and for variable thickness ratios.

6. Stiffened Structures

Use of wires, rods, and strips or edgings could be made an integral part of the expulsion bladder or diaphragm to promote or fix a deformation pattern. The attachment of these reinforcements is accomplished by welding techniques or by brazing. Chemical milling could also be employed to form some of these reinforcement configurations. The incorporation of these types of local stiffenings or restraints is similar to the system employed in "Japanese lanterns", a folding-type of structure.

7. High-Energy-Rate Metal Forming

In this technique, forces are applied at high velocities to form the metal. An explosive shock is transmitted through a liquid or through air to form the metal against a die with almost no springback. This occurs in explosive forming when a piece is squeezed against a die cavity surface by a momentary and uniform pressure much in excess of the flow stress of the material, which induces a permanent set.

CURRENT MATERIALS AND METHODS

1. Seamless Construction

Currently, fabrication of seamless, plastic bladders involves a dispersion spray technique. Resin based dispersions such as Teflon (dispersed in water) or Kel-F (dispersed in solvent) are sprayed onto a metal mandrel e.g. aluminum, dried to remove the liquid vehicle and fused in an oven to a homogeneous film. This technique is very complicated and involves many factors that must be strictly controlled. Briefly, some of the factors are:

a. Mandrel must be smooth, clean, and of proper dimensions to allow for film shrinkage. Sharp contours must be eliminated to minimize localized areas of high stress concentration in film.

b. Absolute cleanliness of raw dispersion, spray equipment, spray room, ovens, personnel, etc. is a must. Contaminants may cause localized stress areas or reactive sites for contained propellants.

c. Spray technique is critical. The dispersions must be sprayed to a given thickness (critical film thickness), dried, and fused. The entire process must be repeated again and again until the proper film thickness is attained. Exceeding the critical film thickness will cause undesirable factors such as orange-peeling or mud-cracking. Dispersion drying conditions and overspraying in hard-to-reach areas may also cause the same undesirable factors.

d. Oven temperature and fusion time must be closely controlled. The sprayed film must be heated high enough and long enough to allow the individual particles to gel and fuse together. Too high a temperature or too long a time may cause degradation of the physical properties of the film. The changes of degradation occurring are more likely as successive spray passes are applied to increase the film thickness.

e. Cooling rate is important. Teflon TFE and Kel-F are crystallizable polymers. The size, amount, and arrangement of crystals determines properties such as stiffness, dimensional stability, flex life, and permeability. Some properties such as thermal resistance, chemical resistance, dielectric properties **and** nonstick characteristics are inherent in the chemical structure of the polymers and relatively independent of crystallinity. Crystallinity is a function of molecular weight and temperature. The number and size of crystalline spherulites formed is controlled by the rate of cooling after oven processing. Rapid cooling allows the formation of very few spherulites. A relatively amorphous, lower density material is formed which has more flexibility but somewhat lower tensile properties. Slow cooling allows the formation of more crystals (higher crystallinity). The higher crystalline material is denser, more rigid (higher flexural modulus) and has higher tensile, lower elongation, and lower permeability than the rapid quench material.

Other crystalline polymers in dispersion form e.g., Kynar (polyvinylidene fluoride) have similar cooling rate characteristics, as described above which would apply when spraying and fusing thin plastic bladders. The degree of control over crystallinity is limited on thicker sections due to the low thermal conductivity of plastics but this rule usually applies to thick sheets or rod stock and not to expulsion bladders.

Teflon FEP dispersion resin does not crystallize as readily as Teflon TFE or Kel-F dispersions. The properties of Teflon FEP film are therefore not particularly influenced by cooling conditions.

Another fabrication technique for seamless positive

expulsion devices (bladder or diaphragms) involves the use of electroformed metals. The metals may be deposited to many configurations but the process is costly, the foil may be porous, and annealing is usually required. Since metals are not as flexible as plastics or elastomers the total number of expulsion cycles may be limited.

2. Seamed Constructions

Many techniques have been developed for fabrication of seamed bladders. Materials such as metals, plastic films, and elastomers have been joined together by welding (heli-arc, electron beam, resistance, hot air), adhesive bonding, vulcanization and heat sealing (hot impulse, dielectric, ultrasonic). Some of the seamed bladder constructions evaluated by aircraft companies included vulcanized silicone rubber for hydrogen peroxide expulsion, adhesive bonded Mylar for liquid hydrogen expulsions and heat sealed Teflon, Kel-F, and polyethylene for fuming nitric acid service.

The main concern in seamed construction is to obtain seams that are as strong as the parent material and are smooth as possible to eliminate localized stress areas and to minimize distortion of the fold pattern.

POTENTIAL MATERIALS AND METHODS

The following list contains potential materials and methods for fabrication of positive expulsion devices. The list is general but contains many possible combinations. Some of the materials of construction or fabrication techniques have been evaluated to a limited extent but since positive expulsion devices are still in their infancy, they should also be considered for future applications. This list is intended to stimulate the reader in thinking of new and novel material combinations and fabrication techniques for positive expulsion devices that are tougher, have lower permeability, have increased radiation and temperature' resistance, have increase propellant resistance, and may be easier to fabricate.

1. Metallized Materials

a. Metallized Teflon

At least three companies claim processes for metallizing Teflon to lower propellant permeability.

b. Metallized plastic textiles and plastic films or combinations of both.

2. Reinforced Teflon

    a. Teflon TFE, Teflon FEP, Teflon TFE/FEP laminate or co-dispersion reinforced with metallic fibers, metallic screen, metallic powders, organic cloth, organic felt (Teflon TFE), inorganic papers, plastic films, plastic or elastromeric coatings.

3. Copolymers

    a. Teflon-elastomer copolymers

    b. Graft copolymers of plastics

4. Elastomer or Plastic Coated Textiles

    a. Neoprene, Buna N, Butyl, Hypalon, Silicone, Viton, Mylar, etc. on textiles such as Nylon, Dacron, Glass, Teflon Cloth.

5. Metals

    a. Electroformed

    b. Clad metals